

THE
LONDON, EDINBURGH, AND DUBLIN
PHILOSOPHICAL MAGAZINE
AND
JOURNAL OF SCIENCE.

[SIXTH SERIES.]

JULY 1925.

- I. *A Method for Increasing the Working Range of an Oscillograph.* By C. E. WYNN-WILLIAMS, M.Sc., University Research Student, University College of North Wales, Bangor*.

[Plate I.]

WITH all types of oscillograph which employ a mechanical moving system as the medium between the quantity to be studied (which actuates the instrument) and the record, a great disadvantage arises from the fact that the usefulness of the instrument is limited by the frequency range over which accurate results are obtainable. The extent of this range depends upon (1) the type of oscillation to be studied, (2) the maximum error permissible, (3) the natural frequency and damping of the instrument. When the oscillograph (which, for the present purpose, is supposed to be a simple mechanical oscillatory system, having only one frequency of vibration, $\frac{n}{2\pi}$, and capable of being made to execute forced oscillations by the quantity to be examined) is adjusted so that the system is just aperiodic (*i. e.* damping factor $k=2n$), thus rendering free oscillation of the system impossible, it can be shown that the amplitude scale (*i. e.* the amplitude of oscillation per unit force) diminishes as the frequency increases. If the natural periodicity of the instrument $=n$, and the amplitude scale for a steady deflexion $=100$, then for an oscillation of periodicity of $0.1n$ the amplitude scale will be 99.3, and for a periodicity of $0.2n$, 96.0, thus

* Communicated by Prof. E. Taylor Jones, D.Sc.

introducing errors of 0.7 per cent. and 4.0 per cent. respectively. As the frequency still further rises, the error increases, until, at the natural frequency of the instrument, it is as large as 50 per cent. Evidently, then, if the nature of the curve makes it desirable for all frequencies to be recorded with uniform amplitude scales, the range of frequencies over which accurate results are obtainable is very small, being, as before mentioned, from 0 to $0.1n$ for errors not exceeding 0.7 per cent., and from 0 to $0.2n$ for a 4.0 per cent. error. With certain curves, however (*i. e.* pure sine waves with or without slight damping), the error is of no account, provided that the amplitude scale for that particular frequency is known.

The difficulty of obtaining true records at high frequencies is evident when it is realized that the frequency of the instrument must be from five to ten times that of the most rapid oscillation to be recorded, and that the natural frequency of most mechanical oscillographs rarely exceeds about 10,000 vibrations per second.

It was thought that some means might be found for compensating the instrument, by reducing the amplitude scale for the lower frequencies, and increasing it for the higher, so that the amplitude scale would tend to vary less with the frequency than in the uncompensated instrument, thus enabling the frequency range to be increased. This might be done by subjecting the instrument to only a fraction of the quantity to be examined, and making this fraction a function of the frequency which would be large at high frequencies and small at low frequencies. The form of function required to secure compensation can best be determined by mathematical analysis. Some indication of the best way of applying the method in practice will also be made evident by this treatment of the problem.

Theory

The equation of motion of the system is

$$\frac{d^2x}{dt^2} + k\frac{dx}{dt} + n^2x = F,$$

where x = displacement, k = damping factor, n = periodicity (undamped), and F = force actually applied to the instrument, per unit of inertia. This may be written as

$$(D^2 + kD + n^2)x = F,$$

where D stands for the operator $\frac{d}{dt}$.

F will, in general, be a periodic function, or a combination of such functions (*i. e.* a Fourier series) such as

$$F = \sum_1^{\infty} F_m \epsilon^{-\mu t} \left\{ \frac{\sin}{\cos} \right\} mpt.$$

For the present purpose, however, it will be assumed that F is only a single undamped oscillation. In this case the equation becomes

$$(D^2 + kD + n^2)x = F_0 \sin pt,$$

the solution of which is

$$x = A\epsilon^{-\frac{k}{2}t} \sin \left(\sqrt{n^2 - \frac{k^2}{4}} t + \alpha \right) + \frac{F_0 \sin pt}{D^2 + kD + n^2}.$$

The first term (the complementary function) is aperiodic, provided that k is not less than $2n$, for which reason k is always made equal to or greater than $2n$ in an instrument of this kind. In any case, the first term tends to zero as t increases. We are then left with a solution,

$$x = \frac{F_0 \sin pt}{D^2 + kD + n^2},$$

which, on expansion, becomes

$$x = \frac{F_0 \sin (pt - \phi)}{\sqrt{(n^2 - p^2)^2 + k^2 p^2}},$$

where

$$\tan \phi = \frac{kp}{n^2 - p^2}.$$

This shows that the amplitude scale

$$\frac{1}{\sqrt{(n^2 - p^2)^2 + k^2 p^2}}$$

is a function of the frequency, and that the phase of the record lags behind that of the force by an angle

$$\phi = \tan^{-1} \frac{kp}{(n^2 - p^2)}.$$

The problem is, therefore, to make (1) the amplitude scale constant, or as nearly constant as possible, so that the amplitude of the record is a true scale representation of the magnitude of the force at all frequencies, and (2) to make the phase angle as nearly equal to zero as possible, so that the various components of the force are recorded in correct phase

relation to one another. This can be done in the following way. So far we have supposed that the instrument is subjected to the whole of the applied force. Suppose, now, that some link is introduced between the force and the instrument (*e. g.* a shunt resistance, potentiometer, or volt-box, etc.) which will tap off a fraction of the force and apply it to the instrument. It is conceivable that the link could be so constructed that the magnitude of the fraction would depend upon the frequency, and that the relative phases of the force and its fraction could be changed. Let this fraction be ρ . Then, if the force to be examined (to which the link is submitted) is equal to A , the fraction which will be passed on to the oscillograph will be ρA . Replacing F by ρA in the expression for x , we get

$$x = \frac{\rho A}{D^2 + kD + n^2}.$$

What is required for perfect compensation is that the expression for x should be of the form $x = \sigma A$, where σ is a constant. Hence, by comparing the two expressions, we see that

$$\frac{\rho A}{D^2 + kD + n^2} = \sigma A.$$

Since σ is a constant, and A a function of p , no matter what form, it is evident that the fraction ρ must be equal to the operator $\sigma(D^2 + kD + n^2)$. The properties of such an operator may be made evident by supposing that A is a single undamped oscillation,

$$A = A_0 \sin pt.$$

Hence

$$\rho A = \rho A_0 \sin pt = \sigma(D^2 + kD + n^2)A_0 \sin pt,$$

which on expanding becomes

$$\rho A = \sigma \sqrt{(n^2 - p^2)^2 + k^2 p^2} A_0 \sin(pt + \phi),$$

where

$$\tan \phi = \frac{kp}{(n^2 - p^2)}.$$

This represents the force F applied to the instrument, so that we now have

$$\begin{aligned} x &= \frac{F}{D^2 + kD + n^2} = \frac{\sigma \sqrt{(n^2 - p^2)^2 + k^2 p^2} A_0 \sin\{(pt + \phi) - \phi\}}{\sqrt{(n^2 - p^2)^2 + k^2 p^2}} \\ &= \sigma A_0 \sin pt. \end{aligned}$$

From this it will be seen that x , the displacement, is a true scale representation of the force at all frequencies, and, further, that the record is in phase with the force, showing that proper compensation has been obtained. This may be explained by saying that the link *multiplies* the amplitude by $\sqrt{(n^2-p^2)^2+k^2p^2}$ and *advances* the phase by an angle ϕ , while the oscillograph *divides* the amplitude by $\sqrt{(n^2-p^2)^2+k^2p^2}$ and *retards* the phase by ϕ , thus giving a constant amplitude scale and zero phase change for all frequencies.

It is not necessary that A should always be of the form $A_0 \sin pt$ for compensation to take place. For, by substituting ρA for F , we get

$$\begin{aligned} x &= \frac{F}{(D^2 + kD + n^2)} = \frac{\rho A}{(D^2 + kD + n^2)} \\ &= \frac{\sigma A (D^2 + kD + n^2)}{(D^2 + kD + n^2)} = \sigma A, \end{aligned}$$

showing that compensation is independent of the form of A . The assumption that $A = A_0 \sin pt$ was made in order that it might be ascertained what properties the link should possess, and so give some indication as to its practical form.

Method of Applying Compensation.

As a specific example, suppose we have an electrostatic oscillograph of small capacity, and satisfying the equation

$$(D^2 + kD + n^2)x = F$$

(F in this case being the potential applied to the instrument), and we require to compensate it. The amplitude x is given by

$$x = \frac{F}{D^2 + kD + n^2}.$$

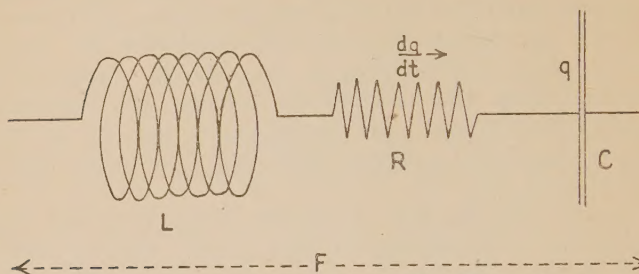
We require it to be of the form $x = \sigma E$, where E = the voltage to be examined. To make this so, F must be of the form

$$F = (D^2 + kD + n^2)E.$$

The problem is then to find a means of tapping off this fraction of the voltage.

Suppose we have a circuit as shown in fig. 1, consisting of an inductance L , a resistance R , and a condenser C , all in

Fig. 1.



series. Let the potential applied to the ends of the circuit be F , and the displaced charge at any moment $= q$, so that the current $= \frac{dq}{dt}$ or Dq . Then

$$F = \left(LD^2 + RD + \frac{1}{C} \right) q.$$

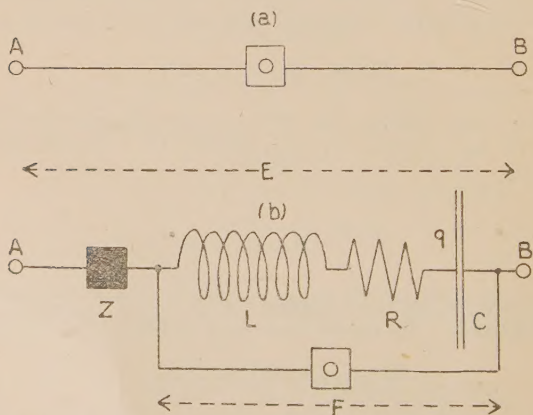
Suppose, now, that L , R , and C be so chosen that

$$\frac{R}{L} = k, \quad \text{and} \quad \frac{1}{LC} = n^2;$$

then

$$F = \left(D^2 + \frac{R}{L} D + \frac{1}{LC} \right) qL \quad \text{or} \quad F = (D^2 + kD + n^2) qL$$

Fig. 2.



Let there be a difference of potential E between the two terminals A and B (fig. 2 (a)), which potential it is required to

examine. Under ordinary circumstances the oscillograph O would be connected as shown. Instead of doing this, however, let the instrument be connected as shown in fig. 2 (b). The terminals A and B are connected by an inductance L, a resistance R, a condenser C, and the apparatus Z (shown by a black square), all in series, while the oscillograph is connected across L, R, and C. The nature of the apparatus Z has to be such that the displacement charge q in the circuit is rendered proportional only to the voltage E (i. e. $q = \sigma E$), and is not a function of p other than a periodic function of the same form as E .

The instrument is now submitted to the back E.M.F. of the combination L, R, and C. Denoting this by F , we get

$$x = \frac{F}{(D^2 + kD + n^2)} = \frac{(D^2 + kD + n^2)qL}{(D^2 + kD + n^2)} = \sigma EL.$$

From this it will be seen that, if the apparatus Z keeps the displacement charge in the circuit proportional only to E , compensation is provided, for x is now proportional to E , no matter what frequency is dealt with.

The next step is to investigate the nature of the required apparatus Z, which, generally, we may consider to have inductance L_1 , resistance R_1 , and capacity C_1 . Writing down the expression for q , we get

$$q = \frac{E}{\left(LD^2 + RD + \frac{1}{C}\right) + \left(L_1D^2 + R_1D + \frac{1}{C_1}\right)}$$

Bearing in mind the fact that L, R, and C have already been determined, and that the presence of the operator D indicates a function of p in the solution, it is evident that it is impossible, by means of such a system, to make q independent of p , but that an approximation to it can be obtained if L_1 and R_1 are both zero and C_1 very small. When L_1 and $R_1 = 0$,

$$q = \frac{E}{LD^2 + RD + \left(\frac{1}{C} + \frac{1}{C_1}\right)}.$$

This indicates that apparatus Z should be a condenser. In practice, however, it has been found necessary to include in the circuit a resistance R_1 , as the whole system must be rendered aperiodic from an electrical point of view, which is done by suitably adjusting the value of R_1 . The inclusion

of this resistance, however, makes q more dependent upon p than it otherwise would be.

The form of compensation given by this arrangement may be seen by writing down the equations for the system :

$$q = \frac{E}{\left\{ LD^2 + (R + R_1)D + \left(\frac{1}{C} + \frac{1}{C_1} \right) \right\}},$$

$$F = \left(LD^2 + RD + \frac{1}{C} \right) q \\ = \frac{\left(LD^2 + RD + \frac{1}{C} \right) E}{\left\{ LD^2 + (R + R_1)D + \left(\frac{1}{C} + \frac{1}{C_1} \right) \right\}},$$

$$x = \frac{F}{(D^2 + kD + n^2)} = \frac{\left(LD^2 + RD + \frac{1}{C} \right) E}{\left\{ LD^2 + (R + R_1)D + \left(\frac{1}{C} + \frac{1}{C_1} \right) \right\}} \\ \times \frac{1}{(D^2 + kD + n^2)}.$$

As it has been arranged that $\frac{R}{L} = k$, and that $\frac{1}{LC} = n^2$, we get

$$x = \frac{E}{\left\{ D^2 + \left(k + \frac{R_1}{L} \right) D + \left(n^2 + \frac{1}{LC_1} \right) \right\}},$$

or, putting

$$\frac{R_1}{L} = k_1 \quad \text{and} \quad \frac{1}{LC_1} = n_1^2$$

to correspond with k and n^2 ,

$$x = \frac{E}{\{ D^2 + (k + k_1)D + (n^2 + n_1^2) \}}.$$

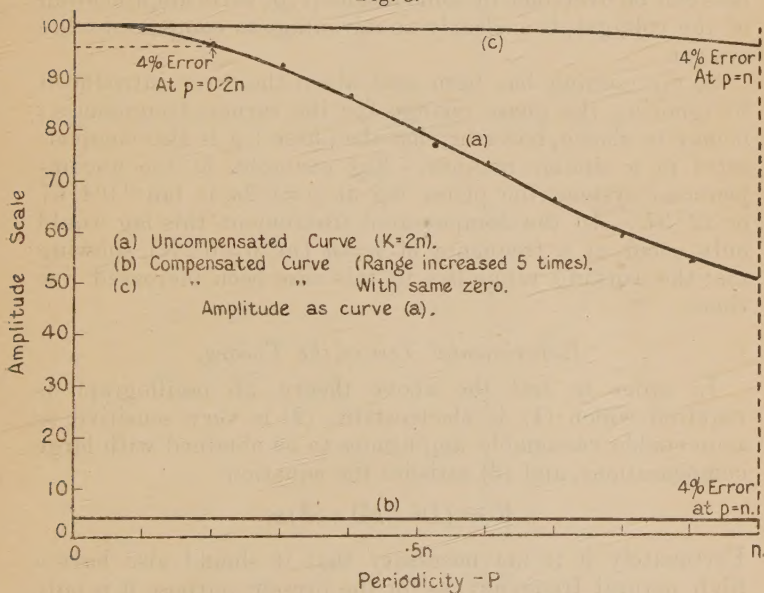
The oscillograph therefore behaves as if it had a periodicity $\sqrt{n^2 + n_1^2}$ instead of n , and a damping factor $k + k_1$ instead of k . We have *virtually increased the natural frequency* of the system, thus giving the instrument a greater working range of frequencies for compound oscillations.

This may be made clearer by the aid of a graph. Assuming the instrument to be just aperiodic ($k = 2n$) and

not compensated, the amplitude scale varies with the frequency as shown by curve (a), fig. 3. Now make $n_1^2 = 24n^2$, so that N , the virtual natural frequency, $= \sqrt{n^2 + 24n^2} = 5n$, and make $k_1 = 8n$, so that K , the virtual damping factor, $= 10n = 5k$. This may be done by making $C_1 = \frac{1}{24}C$ and $R_1 = 4R$; L , R , and C having been previously adjusted so that

$$\frac{R}{L} = k \quad \text{and} \quad \frac{1}{LC} = n^2.$$

Fig. 3.



The amplitude scale will now be the same as that of an oscillograph of periodicity $= 5n$ and damping factor $= 10n$, and will be represented by curve (b), fig. 3. It will be observed that the slope of this latter curve is much more gentle than that of the former, although the amplitude scale for a steady deflexion is much less (*i. e.* in (a) the steady deflexion for unit applied potential is $\frac{1}{n^2}$, while in curve (b) the corresponding deflexion is

$$\frac{1}{n^2 + n_1^2} = \frac{1}{25n^2},$$

a ratio of 25:1). Curve (c) shows the compensated curve (b)

magnified 25 times so as to have the same zero amplitude scale as curve (a) the uncompensated one. It will be observed that curve (a) falls much more rapidly than curves (b) or (c). A 4 per cent. error, for example, would be involved within the range $p=0$ to $p=0.2n$ for curve (a), while the range in which the same error would be incurred in curves (b) and (c) is from 0 to n , or from 0 to $0.2N$. The working range, in this case, has therefore been increased five times. The sensitiveness, however, has been decreased twenty-five times. Hence, provided the decrease in sensitiveness can be overcome by some means (*e.g.* valve amplification of the voltage), it is clearly an advantage to compensate the system.

So far nothing has been said about the error introduced by ignoring the phase change for the various frequencies; it may be shown, however, that the phase lag is also compensated in a similar manner. For example, in the uncompensated system, the phase lag at $p=0.2n$ is $\tan^{-1} 0.4167$ or $22^\circ 37'$. In the compensated instrument this lag would only occur at a frequency of $p=n$ (or $p=0.2N$), showing that the working range has in this case been increased five times.

Experimental Test of the Theory.

In order to test the above theory, an oscillograph is required which (1) is electrostatic, (2) is very sensitive, so as to enable reasonable amplitudes to be obtained with large compensations, and (3) satisfies the equation

$$F = (D^2 + kD + n^2)x.$$

Fortunately it is not necessary that it should also have a high natural frequency, as for the present purpose it is only required to show that a low natural frequency can be virtually raised by compensation. As most electrostatic oscillographs are insensitive at low voltages, it was decided to construct an artificial electrostatic oscillograph by using a current oscillograph in conjunction with a valve.

In fig. 4, O represents a current oscillograph, inserted in the plate circuit of an amplifying valve. This oscillograph is supposed to be sensitive enough to respond to the small changes in the plate current of the valve (of the order of a few milliamperes) caused by any variation of the potential of the grid. In this way a current oscillograph may be made to record potential variations. Two conditions must, however, be observed to obtain true results. (1) The voltage applied to the grid must be such that the plate current in

Fig. 4.

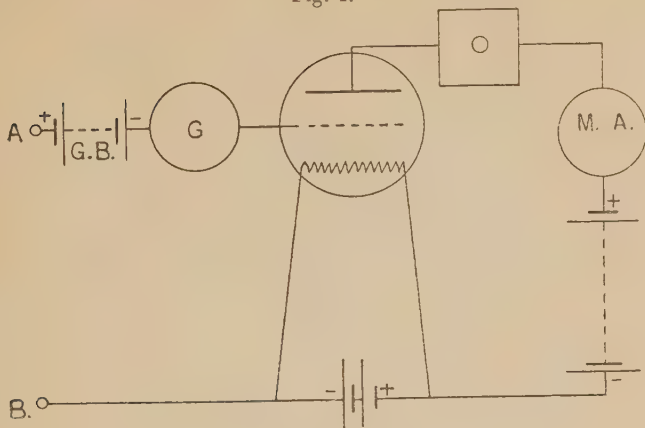
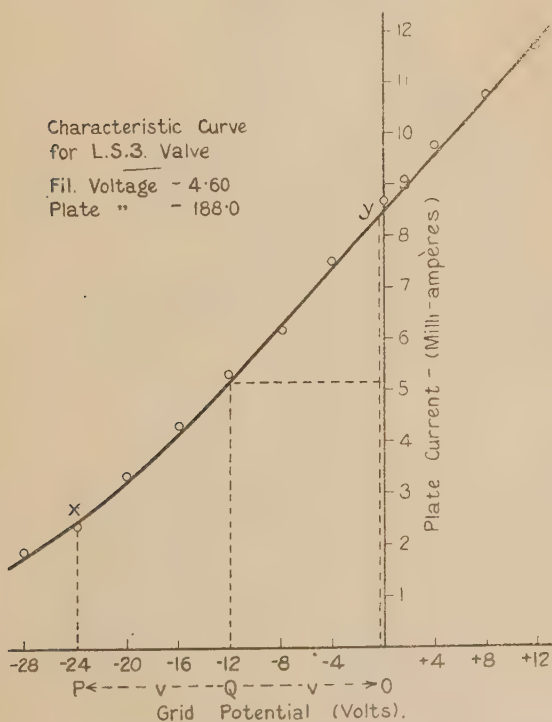


Fig. 5.



the valve is always represented by the straight portion of its characteristic curve (*i. e.* to the right of the point *x* in fig. 5),

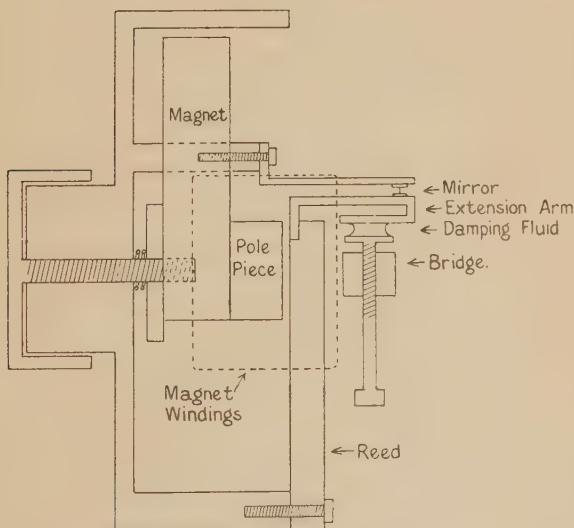
and (2) the grid current must always be zero. Hence it will be observed that the only voltages that can be applied to the grid must lie between zero and the value corresponding to that just above where the plate current curve begins to bend—i. e. from P to O (fig. 5). These are all negative values. The mean working position will be at Q, half-way between P and O. Calling PQ (=QO) r , we see that, by superimposing a steady voltage of $-r$ on the grid by means of the grid battery GB (fig. 4), any voltage oscillation whose peak value does not exceed r will be passed on by the valve and transformed into a similar current oscillation, without distortion, which will be recorded by the current oscill. graph. As the grid current is kept at zero, the "input" side of the valve i. e. the grid and filament terminals) will represent the terminals of a perfectly electrostatic instrument of small capacity—at any rate, so far as concerns any apparatus to which the grid is connected. The sensitiveness of the system will depend upon (1) the slope of the plate current curve, and (2) the sensitiveness of the oscillograph O.

A very convenient, though not ideal, oscillograph was constructed from a Brown's "A" type telephone earpiece*. This was of resistance 4000 ohms, and had a vibrating steel reed attached to a conical diaphragm as an armature. The diaphragm was removed, and to the free end of the reed a thin sheet-brass extension was attached, bent as shown in fig. 6. Between this and a fixed brass plate, a small mirror about 1 mm. square was clamped, the surfaces of both the extension and the plate being covered with thin slips of cork where the mirror was held. This constituted an optical lever which magnified the movement of the free end of the reed. As the distance between the reed and the magnet can be adjusted by means of a screw in this type of telephone, the sensitiveness could be conveniently varied. To supply the necessary damping, a thick brass bridge was attached to the magnet, just under the extension of the reed. Through the centre of this a screw passed, carrying at its upper end a small platform parallel to the extension, and between these two surfaces some viscous liquid was introduced (see fig. 6). It was found necessary to bend the extension back upon itself to prevent the liquid from creeping on to the reed and into the space between the reed and the pole-pieces. The whole was mounted in a universal joint to facilitate the centring of the light-spot.

* The writer is indebted to Mr. W. E. Williams, B.Sc., for this suggestion.

A beam of light from a pinhole, upon which the crater of an arc lamp was focussed, fell on the mirror and, after reflexion, on to a revolving concave mirror, which caused the light-spot to move in a horizontal direction across a photographic plate or a ground-glass screen placed at the distance for correct focus. The oscillograph was so arranged that when working it deflected the beam in a vertical direction. By means of a mirror attached to the prong of a tuning-fork placed near the oscillograph a second spot was made to fall on the screen, just under the first, thus giving a time-scale independent of the velocity of the light-spots across the plate.

Fig. 6.



The valve employed was a Marconi L.S.3, as used for power amplification. In all cases the filament voltage was kept at 4.6 volts and the plate voltage at 188. It was found impracticable to use the ordinary power-mains for the H.T. supply, owing to the presence of a commutator ripple which appeared in the oscillograms. Accordingly four ordinary 60-volt high-tension batteries connected in series were employed, and were found to be quite satisfactory. A milliammeter was inserted in the plate circuit, and a sensitive table galvanometer, G, was connected in series with the grid to indicate the presence of any grid current. It was found that the inclusion of this galvanometer did

not interfere with the working of the apparatus to any observable extent.

The first operation was to standardize the valve and oscillograph. A characteristic curve for the valve was taken in the usual manner, by applying various voltages to the grid and recording the corresponding values of the plate current. This was done with all the apparatus in position. The curve obtained is shown in fig. 5. The curve was taken again after the experiments were concluded, to see if it had altered in the meantime, but it was found not to have changed. From this curve the available voltage range that could be applied to the valve was determined. This extended from just above the lower bend marked x to just short of zero, giving a working range in this case of about 24 volts. The mean potential was therefore -12 volts. This indicated the voltage of the grid battery required, which was then inserted in the circuit.

In order to adjust the oscillograph, the light-spot was allowed to fall on the screen (the revolving mirror being kept stationary) and the adjusting screw altered until, on changing the potential of the grid from zero to -24 volts (thus moving it through its maximum working range), the spot travelled through as great a distance on the screen as possible. This ensured the maximum sensitiveness. To test whether or not the amplitude was a linear function of the grid voltage, the grid was subjected to alternating voltages (frequency about 50 cycles per second) by means of a potentiometer, and the amplitude of vibration of the spot observed for different voltages. The voltage was measured by means of an electrostatic voltmeter. It was found that the displacement of the spot on the screen was not quite symmetrical with respect to its zero position. This was to be expected, since a vibrating reed, acted upon on one side only by a magnetic field, was not a symmetrical arrangement. If, however, the magnet was not brought too close to the reed (*i. e.* if the system was not made quite as sensitive as it might have been), it was found that, although the amplitude was unsymmetrical with regard to the zero position, it was in all cases proportional to the voltage applied to the grid within the limits of experimental error. When a suitable position for the magnet had been found, it was left set in that position during the whole of the subsequent experiments.

The natural frequency of vibration of the reed must be known. This was ascertained in two ways: (1) from the peak of the resonance curve, and (2) by photographing the free oscillations of the reed and measuring the curve.

The first method was approximate only, and served as a check on the second. The amplitude of oscillation was observed while an alternating voltage from an oscillating valve was applied to the grid of the amplifying valve. The frequency of oscillation was raised, and the value found which corresponded to the maximum amplitude of vibration of the spot. This was the resonant frequency of the reed without damping. In the second method a switch actuated by the turn-table of the revolving mirror was arranged suddenly to alter the grid potential at the moment when the spot passed across the photographic plate. This caused the reed to vibrate in its own frequency, and from the oscillogram obtained the natural frequency was determined.

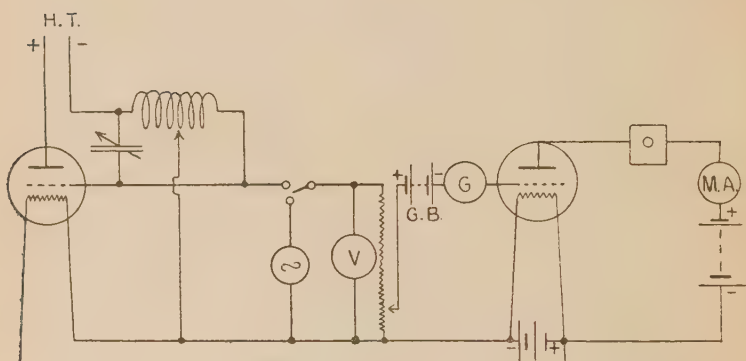
It was necessary to render the system aperiodic. This was done by introducing some viscous fluid between the platform and the extension (see fig. 6). Various fluids were tried—vaseline, castor oil, petroleum, syrup, and a mixture of vaseline and petroleum. The syrup was found to be the most suitable to work with. It was necessary, however, as already explained, to bend the extension back upon itself so as to form a trap for the syrup, to prevent it from creeping. By altering the distance between the platform and the extension the degree of damping could be varied.

The mirror was set revolving and the shape of the curve on the screen was observed (the switch worked by the mirror turn-table as before changing the grid potential suddenly at the moment when the spot passed across the screen), while the damping was varied. With a little care it was found possible to adjust the damping so that there was no trace of free oscillations present. The damping was kept at the minimum value necessary for this so as to ensure operating as near as possible to the curve corresponding to $k=2n$. (Later on, on examining the resonance curve, it was found that k had to be much greater than $2n$ to ensure aperiodicity for this particular instrument.) When the system was aperiodic, the shape of the curve for a sudden change of voltage approximated fairly well to its theoretical value, although the self-inductance of the windings of the magnet caused a slight lag. The lag, no doubt owing to the high resistance of the plate circuit of the valve, was, however, less than was expected.

The system being made aperiodic, an attempt was made to ascertain whether the resonance curve conformed to the theoretical shape of the curve corresponding to $k=2n$. This was done by subjecting the grid to alternating voltages of various frequencies supplied by either an alternator or an

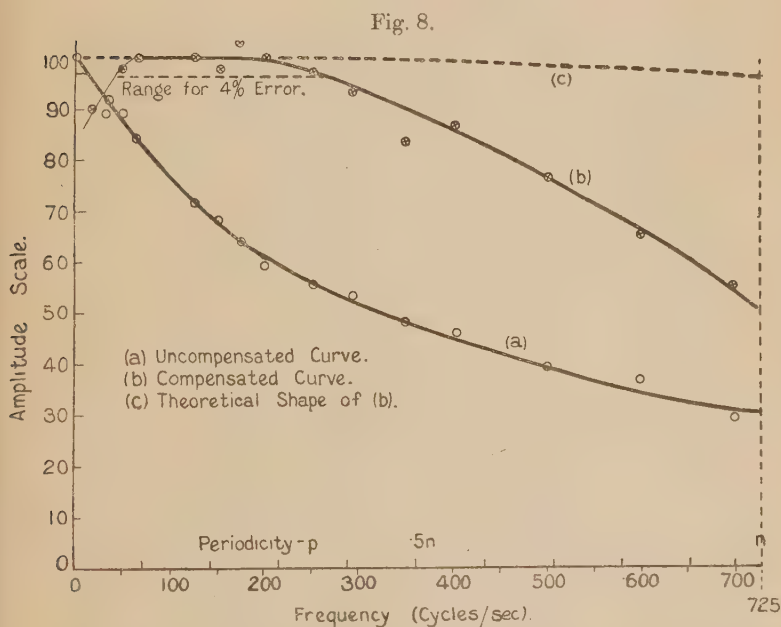
oscillating valve and measuring the amplitude of oscillation of the spot. For frequencies below 100 per second the alternator was used, and above that frequency the valve. In most cases the full voltage was found to be too much for the grid of the amplifying valve, whose working range, as has already been shown, was limited (0 to -24 volts) by the shape of its characteristic curve. A known fraction of the voltage was therefore tapped off by means of a divided megohm. Fig. 7 shows the connexions of the apparatus. The amplitude for steady voltage was found by replacing the alternator by the power-mains and taking readings for equal positive and negative values of potential.

Fig. 7.



On drawing the resonance curves, it was observed (1) that the damping was much greater than that given by $k=2n$, and (2) that a "hump" appeared in the curve at a frequency of about 700–800, although the system was supposed to be aperiodic. After a careful examination of the apparatus it was found that several portions of the telephone were constructed of rather thin material which might possibly have vibrated. Accordingly the whole was dismantled, and packing pieces of thick brass inserted where considered necessary. After reassembling, the preliminary operations of determining the natural frequency and making the system aperiodic had to be repeated. When the new resonance curve was plotted, it was found to be free from "humps," but the damping was still greater than expected. On calculating the values of the damping at various frequencies, by inserting in the formula the values of the amplitude scale read from the graph, it was found that the damping was not

constant, but diminished as the frequency of the applied force increased. This was found to be so in all cases. Although the results were repeated with several damping liquids, and with various adjustments, it was found impossible to obtain a uniformly damped resonance curve, the only conclusion to be drawn from such a result being that the ordinary law of viscosity does not hold under the conditions obtaining in the experiment. For this reason it was decided to assume that the damping was constant over a short range, and to attempt to compensate for this range only, the average value of the damping factor over the range being taken as the value to be inserted in the formula for the determination of R . Fig. 8 (a) shows the resonance curve



dealt with in a particular case. The damping was taken as being equal to $6.60n$. For effecting the compensation, an inductance, two condensers, and two resistances were required. The inductance in this case was part of the secondary winding of a small induction coil from which the core and primary coil had been removed. It had a resistance of 1756 ohms and an inductance of 1.150 henry, as measured by Rayleigh's method. It was necessary to connect this in

series with a condenser, C (see fig. 9), of such a capacity that the two formed an oscillatory circuit of the same frequency as the reed, viz. 725.0. From the formula

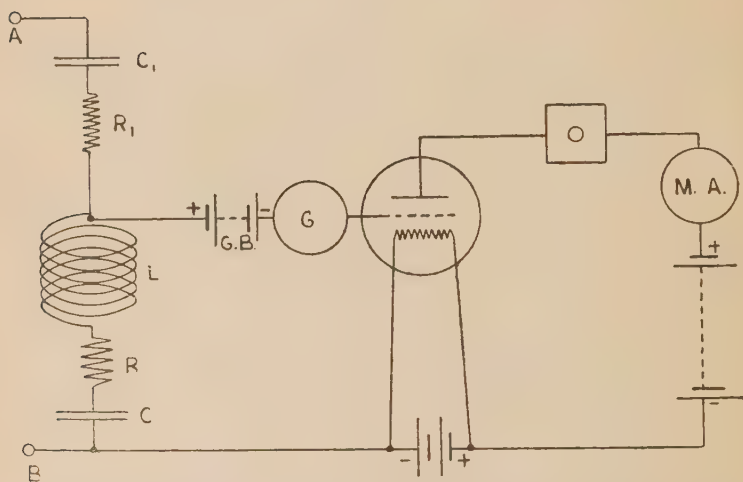
$$T = 2\pi \sqrt{LC} = \frac{1}{F}$$

we find

$$C = \frac{1}{4\pi^2 F^2 L} = \frac{1}{4\pi^2 \times 725^2 \times 1.150} = 0.04191 \text{ mfd.}$$

Accordingly condenser C was adjusted to this value.

Fig. 9.



The total resistance in this part of the circuit (L , R , and C) across which the valve was to be connected had now to be adjusted so that $\frac{R}{L} = k$. From this, taking k as equal to $6.60n$ (the value at the mean position in the range for which the instrument was to be compensated), R was found to be 34,570 ohms. This value included the resistance of the inductance (viz 1756 ohms), so that an additional resistance of 32,814 ohms was required.

It then remained to adjust C_1 and R_1 . In most of the experiments performed, and also in this particular case, it was endeavoured to increase the working range five times, as was done in the theoretical example for which the curves

shown in fig. 3 were drawn. That is, C_1 had to be made equal to $\frac{C}{24}$, or 0.001746 mfd. Condenser C_1 consisted of a large

air dielectric variable condenser having a maximum capacity of 0.0025 mfd. This was calibrated, and the capacity was set to the required value, due allowance being made for the zero error. Lastly, R_1 had to be so adjusted that the whole electrical system was aperiodic. The condition for this was that

$$\frac{R + R_1}{L} = K = 2N \quad \text{or} \quad R + R_1 = 10nL,$$

from which $R + R_1 = 52,390$ ohms. R being equal to 34,570 ohms, R_1 was 17,820 ohms.

This arrangement, when connected up, constituted the required link for effecting compensation. Theoretically the oscillograph should now have behaved as if it had a natural frequency of five times its normal value. On attempting to obtain a resonance curve, however, it was found that several complications were introduced which prevented the full compensation aimed at from being realized, although sufficient evidence was obtained from the results to support the truth of the theory. In all cases the complications were traced to the valve system, and not to the link. Firstly, the valve system, owing to leakage to earth from the grid *via* the cap of the valve etc., was not perfectly electrostatic; and, secondly, it was found practically impossible, when the system was compensated, to ensure that the valve was always operated only on the straight part of the characteristic curve between the lower bend and zero. It will be observed (fig. 9) that, when the system was compensated, the grid of the valve was connected to a point between the two condensers, so that it was insulated from earth on the positive side of the grid battery GB. Consequently the latter, owing to the leakage to earth from the grid side of the battery (which, of course, tended to maintain the grid at zero potential), could not keep the grid at the required mean potential of -12 volts. When an alternating potential was applied to the ends of the link, a fraction of it was passed on to the grid. Suppose that the first half-cycle was in the positive direction. This tended to raise the potential of the grid above its previous value of zero, thus giving rise to a grid current. This current prevented the grid from becoming charged to as high a positive potential as would have been the case had there been no grid current.

In the negative half-cycle the grid current was zero, so that the grid became charged to its full negative value. The mean potential of the grid over the cycle was therefore slightly negative. During succeeding cycles the mean value gradually became more negative until it attained a steady value, at which value it remained as long as the oscillations were maintained. When, however, these ceased, the leakage caused the grid potential to rise to zero once more. This phenomenon is a well-known one, and is made use of in every modern wireless receiver employing a valve detector. In the above system, condenser C functioned as the "grid condenser," and the leakage across the valve cap as the "grid leak." It should be observed that the grid current only flowed while the potential of the grid was actually changing. When the latter was steady the grid current was zero.

An oscillogram illustrating this phenomenon was obtained by photographing the curve traced by the spot at the moment when an alternator (frequency 780.0) was suddenly connected to the link. This curve is shown in fig. 11 (Pl. I.). In this case the change in the mean value of the grid potential was sufficient to carry the working range beyond the bend in the characteristic curve. The mean value of the plate current before connexion was 8.1 milliamps, and after connexion 1.4. On reference to fig. 5 it will be observed that this new value was in the region of the lower bend. If fig. 11 be examined it will be observed that the first few oscillations were recorded with a greater amplitude than those recorded when the grid had taken up its new mean potential. This was accounted for by the movement of the operating range on to the curved portion of the valve characteristic curve, so that a given change of grid potential produced a smaller change in the plate current than when operating on the steep straight portion. This effect will be referred to later. The presence of the small oscillation on the left may be explained by the fact that when the system was compensated the grid was not connected to earth, but to a point between the two condensers which served as a "floating neutral." Any slight capacity effect between condenser C_1 and the alternator, or leakage across the switch terminals, thus altered the potential of this neutral and also of the grid. Theoretically there should have been no oscillation recorded in this section of the curve.

The resonance curve (fig. 8 (b)) was obtained in a similar manner to the method employed when the instrument was uncompensated (*i. e.* measuring the amplitude of oscillation

for voltages at various frequencies). In this case, however, greater care had to be taken owing to the complications involved. Before taking each reading it was necessary to observe whether the mean value of the plate current had fallen below the value corresponding to -12 volts (viz. 5.16 milliamps), and, if so, to raise it slightly by diminishing the voltage applied to the link. In some cases, however, especially at frequencies above about 300 , it was impossible to obtain satisfactory readings if the applied voltage was too low, so that the mean value of the plate current fell below the value corresponding to -12 volts. In these cases, as was expected, the amplitude scale was much less than its theoretical value.

It should be observed that, with this arrangement, it was impossible to obtain the amplitude for a steady deflexion in the manner employed for the uncompensated instrument (viz., by applying a steady potential to the link) owing to the grid current rendering the positive value equal to zero. Accordingly, its theoretical value was calculated from the values of the condensers C and C_1 , and the steady deflexion obtained when uncompensated. The value so obtained was used for reducing the readings at other frequencies to the same scale as for the uncompensated curve.

The compensated curve is shown in fig. 8 (*b*) drawn so as to have the same theoretical zero amplitude scale as curve (*a*). The dotted curve (*c*) is the curve that should have been obtained in this case if the compensation had been perfect. It will be observed that curve (*b*) is flat for a range extending from a frequency of about 60 to about 200 . Over this range, then, the compensation is perfect. Any compound oscillation composed of frequencies between 60 and 200 would therefore be correctly recorded by the instrument. If curve (*a*) be examined it will be observed that the amplitude scale varies considerably over this range (viz., from 84 to 61). Nearer the zero, however, curve (*b*) dips down. This is due to two causes, both of which are peculiar to this apparatus. (1) The damping in the instrument, as has already been explained, is not constant. For low frequencies, it is found that the damping is very much greater than for high ones—a fault no doubt due to the method employed for applying the damping. When the system was compensated, R was calculated from the value of the damping factor at the centre of the desired range. Hence, at low frequencies, R was less than the value necessary to ensure full compensation, so that the system was under-compensated. (2) The combined effect of “grid condenser rectification”

and the leakage to earth is much more marked at low frequencies than at high ones, owing to the fact that the time between two cycles (during which leakage tends to restore the grid to zero potential) is greater. This results in the oscillations of the grid potential not reaching their full value. Hence, the variation in plate current is less than it should have been. Both these effects would tend to lower the amplitude scale, and so help to explain the dip near zero.

Above a frequency of about 200, curve (b) falls as the frequency increases. This is due, as has already been explained, to the change in the mean value of the grid potential being sufficiently great to move the working range to the bend of the characteristic curve.

The curve shown in fig. 8 (b) is a typical one. In all cases, the dip near zero and the fall in amplitude at high frequencies were observed. If the damping of the instrument had been uniform, no doubt the compensated curve would have approximated much better to curve (c) than it does. In any case, if curve (b) be compared with curve (a), fig. 3, which is the best obtainable in any uncompensated instrument, it will be observed that it is a great improvement even on this, and the improvement on curve (a) fig. 8, the best obtainable with this particular instrument, is very marked. The range over which a 4 per cent. error is incurred in curve (b) is from 47 to 250, which, taking the natural frequency as $725\cdot0$, is $0\cdot28n$. In curve (a) fig. 8, the range for this error is from 0 to $14\cdot5$, or $0\cdot02n$, while in curve (a) fig. 3, the best obtainable uncompensated curve, the extent of the range is only $0\cdot2n$.

To illustrate the effect of compensation on the appearance of oscillograms, the curves shown in figs. 12 and 13 (Pl. I.), were taken. Two alternators were connected in series, and arranged so as to give approximately the same R.M.S. voltage. One gave a frequency of 52 per second, and the other about 250. The resulting "mixture" of alternating E.M.F.s was then analysed by the instrument, firstly compensated, and secondly, uncompensated. No change was made in the circuits or alternators etc. during the experiment except to introduce the compensating link. As the whole time of the experiment was only about six minutes, the machines can be assumed to have been running steadily. Fig. 12 (Pl. I.) shows the curve as recorded by the uncompensated instrument, and fig. 13, by the compensated system. In the latter curve, it will be observed that the amplitudes of the two components are much more nearly

equal than in the former, thus showing the great advantage obtained by compensating the system.

These curves have no particular significance beyond illustrating "compensation." The two frequencies (*viz.*, 52 and 250) were employed so as to be at the extreme ends of the compensated range. As one is about five times the other, the curve appears as if it were composed of a fundamental frequency of 52 with a superimposed fifth harmonic of about the same amplitude. The relative phases of the two components are not constant owing to the fact that one frequency is not an exact multiple of the other. While the curves serve as an excellent example of amplitude compensation, for obvious reasons they give no indication of any phase compensation. It is found, however, that the phase lag is compensated in a similar manner to the amplitude. By photographing the oscillogram of an inductor alternator having a frequency of 100, and a pronounced third harmonic, it was found that the relative phases of the fundamental and the harmonic were very different in the two curves.

From the above, it is clear that, in spite of the difficulties of working with this apparatus, an oscillograph can be compensated for amplitude and phase, and that its usefulness is thereby increased. The low frequencies employed in the experiments, it should be observed, were only a matter of convenience for testing the theory, as the compensation should apply equally well to instruments having higher frequencies of vibration. The valve, which was necessary with this type of oscillograph, also introduced several difficulties that prevented the desired results from being fully realized. From the results obtained, however, the conclusion can fairly be drawn that if a perfectly electrostatic oscillograph of small capacity, large sensitiveness, and uniform damping could be obtained, it would be possible considerably to increase its working range by this method of compensation. Apparently the only source of trouble in the experiments was the valve portion of the apparatus. The link gave rise to none.

The experiments are interesting from another point of view. The oscillograph consisted of a telephone receiver, and the frequencies employed lay within the range of human audibility. For perfect reproduction of sound the amplitude of vibration of the diaphragm should be independent of the frequency of vibration, so as to produce sounds of intensities proportional only to the current passing through the coils of the magnet. Possibly, therefore, compensation of the kind

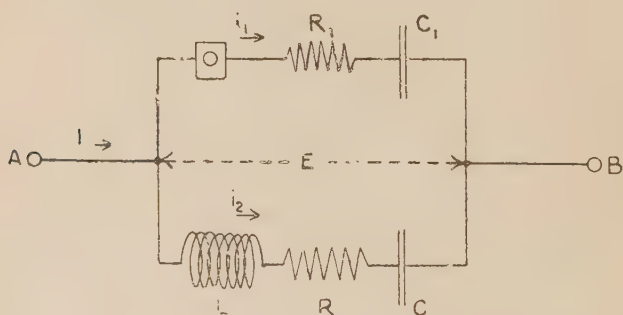
contemplated here might be applied with advantage to ordinary telephone receivers and loud speakers to improve the reproduction of the sound. No experimental work, however, was undertaken in this direction, this being put forward simply as a suggestion.

Application to Current Oscillographs.

So far, potential oscillographs only have been dealt with. It may be shown theoretically, however, that a current oscillograph can also be compensated, although such an instrument could only be used if the impedance of the circuit in which it is inserted were large compared with the impedance of the system including the oscillograph and the compensating link.

In this case, as only a fraction of the current is to be supplied to the oscillograph, the link will have to be some form of a shunt. By an analysis similar to the one used in the case of the potential oscillograph, it may be shown that the required circuit is as shown in fig. 10. The terminals A

Fig. 10.



and B, instead of being connected to the oscillograph, are connected by two circuits in parallel—one containing the oscillograph O, the resistance R_1 , and the condenser C_1 , and the other an inductance L , a resistance R , and a condenser C . The current oscillograph is supposed to have no appreciable inductance or resistance, and to conform to the equation

$$(D^2 + kD + n^2)x = Ai,$$

where A is a constant, and i the current flowing through the instrument. Denoting the main current by I , the branch

currents by i_1 and i_2 , and the back E.M.F. due to the impedance of the system by E , we get :

$$\left(R_1 + \frac{1}{C_1 D}\right) i_1 = \left(LD + R + \frac{1}{CD}\right) i_2 = E,$$

or

$$i_2 = \frac{\left(R_1 D + \frac{1}{C_1}\right)}{\left(LD^2 + RD + \frac{1}{C}\right)} i_1.$$

Now,

$$I = i_1 + i_2 = \frac{\left[LD^2 + (R + R_1)D + \left(\frac{1}{C} + \frac{1}{C_1}\right)\right]}{\left(LD^2 + RD + \frac{1}{C}\right)} i_1,$$

whence

$$i_1 = \frac{\left(LD^2 + RD + \frac{1}{C}\right)}{\left[LD^2 + (R + R_1)D + \left(\frac{1}{C} + \frac{1}{C_1}\right)\right]} I.$$

Since

$$x = \frac{A i_1}{(D^2 + kD + n^2)},$$

we get

$$x = \frac{\left(LD^2 + RD + \frac{1}{C}\right)}{\left[LD^2 + (R + R_1)D + \left(\frac{1}{C} + \frac{1}{C_1}\right)\right]} \times \frac{AI}{(D^2 + kD + n^2)}.$$

As before, making $\frac{1}{LC} = n^2$, and $\frac{R}{L} = k$, and denoting $\frac{1}{LC_1}$ by n_1^2 , and $\frac{R_1}{L}$ by k_1 , we get

$$\begin{aligned} x &= \frac{(D^2 + kD + n^2)}{[D^2 + (k + k_1)D + (n^2 + n_1^2)]} \times \frac{AI}{(D^2 + kD + n^2)} \\ &= \frac{AI}{[D^2 + (k + k_1)D + (n^2 + n_1^2)]}. \end{aligned}$$

The form of this expression is the same as that obtained in the case of a potential oscillograph. The main current I

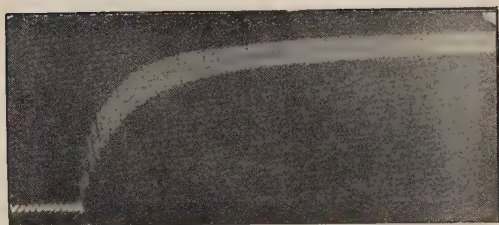
would therefore be recorded by the oscillograph O in the same way as if the terminals A and B had been connected to an oscillograph having a periodicity of $\sqrt{n^2 + n_1^2}$, and damping factor $k + k_1$, so that the oscillograph would be compensated in a similar manner to the potential oscillograph. A difficulty arises, however, in the practical application of this, for it has been assumed that the oscillograph O has no appreciable resistance or inductance. While this is usually so for the oscillograph itself, in the compensated system which replaces the oscillograph the impedance is not negligible.

Conclusion.

The application of this method of increasing the working range of an oscillograph is not confined to electrical instruments, as no assumption as to the nature of the applied force was made in the theory. It should be equally adaptable to any variety of oscillograph (*e. g.*, one used for recording sound waves, etc.), provided that a suitable type of link can be found. The type of link naturally depends upon the function of the particular instrument, and its composition and constants would have to be determined in each case by a mathematical analysis similar to the one shown for the potential oscillograph. It is hoped, however, that the two cases dealt with (*i. e.*, potential and current oscillographs) and the account of the experimental test carried out in the one case, will serve as an interesting introduction to a method for increasing the usefulness of oscillographs, and similar instruments, the operation of which depends upon forced oscillations.

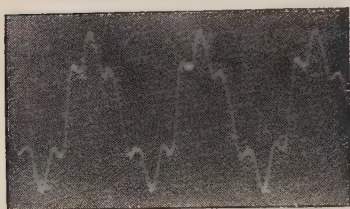
The experimental work in connexion with the above was carried out in the physical laboratories of the University College of North Wales, Bangor, and the writer desires to express his obligation to Dr. Taylor Jones for the interest taken by him in the work, and for suggestions and advice in carrying it out.

FIG. 11.



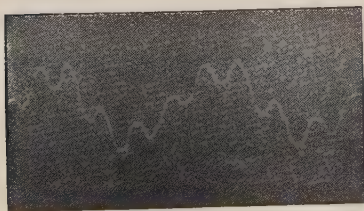
Grid Condenser Rectification Curve.

FIG. 12.



Alternator Voltage (instrument uncompensated).

FIG. 13.



Alternator Voltage (instrument compensated).

II. *The Effect of a Magnetic Field on the Electrical Resistance of Liquid Metals and Alloys.* By E. J. WILLIAMS, M.Sc. (Wales), lately University Research Student, University College of Swansea*.

THE work that has been done on the effect of a magnetic field on the electrical resistance of liquid metals and alloys is briefly reviewed by L. L. Campbell†, and the following is a quotation from the section concerned:—

“Drude and Nernst‡ (1891) observed that the resistance of mercury in a field of 8000 gauss increased about ·2 per cent., whilst that of molten bismuth at 290° C. increased by ·4 per cent. The same year Des Coudres§ called attention to the fact that the apparent increase might be attributed to heating of the metal by the current. The work of Berndt|| (1907) seemed to confirm the contention of Des Coudres. He found that the smaller the tube the less the increase of resistance. In fields from 1000 to 3000 gauss the increase of resistance was not more than ·00004 per cent. for mercury and ·004 per cent. for molten bismuth. Rossi¶ (1911) measured the resistance of mercury and of mercury-bismuth amalgams in tubes of from ·5 mm. to ·7 mm. diameter, in fields from 3350 to 4450 gauss. In both mercury and the amalgam the change of resistance was found to increase with the field, the diameter of the tube, and the concentration of the amalgam. The above subject would seem to deserve further investigation.”

Besides the investigations mentioned here, an extensive series of experiments has been carried out by T. J. Jones** and they are described elsewhere.

Drude and Nernst, and Berndt regarded the effects observed as being due to “electrodynanic” action, and they maintained that there was no true resistance change in liquid metals. Des Coudres regarded the effect as being probably due to heating of the metal by the electric current. On the other hand, Patterson†† (1902) seemed to regard it as a true effect, since he applied to his experimental results a formula developed by Sir J. J. Thomson for a true effect.

* Communicated by Prof. E. J. Evans, D.Sc., Univ. Coll. of Swansea.

† ‘Galvanomagnetic and Thermoelectric Effects’ (1923).

‡ Drude & Nernst, *Wied. Ann.* xlii. (1891).

§ Des Coudres, *Verh. D. Phys.* xxiii. (1907).

|| G. Berndt, *Ann. d. Phys.* xxiii. (1907).

¶ R. Rossi, *Nuov. Cim.* (6) ii. (1911).

** T. J. Jones, *infra*, p. 46.

†† Patterson, *Phil. Mag.* iii. p. 643 (1902).

Recently W. M. Nielson * (1924), who applied a great pressure to the mercury contained in a fine capillary tube in order to eliminate spurious effects caused by mechanical motion of the mercury, has shown that $\frac{\delta r}{r}$ for a field of 16,000 gauss is less than .0003 per cent. The upper limits to $\frac{\delta r}{r}$ for mercury found by Berndt and Nielson do not, however, warrant the general conclusion that metals and alloys in the liquid state exhibit no true magneto-resistance effect. In the first place, these upper limits to the effect in mercury are not appreciably smaller than the actual effect observed in certain solid metals, such as platinum. Moreover, the galvanomagnetic effects for *solid* mercury are abnormally small in comparison with those exhibited by other metals. Fenninger† has found, for instance, that the Hall coefficient for solid mercury is less than .00001, which limit is four times smaller than the Hall coefficient for tin (which, of all other metals, possesses the smallest coefficient), and twenty times smaller than the Hall coefficient for platinum ‡.

It is proposed in this paper, first, to discuss theoretically the effect of a magnetic field upon the resistance of liquid conductors, and then to examine the experimental results in the light of the theory developed. It will be shown that there is evidence for the existence of a true resistance change in certain liquid metals and alloys, and moreover it will be found that the "spurious" effect is itself of considerable interest.

Theoretical Discussion.

It is assumed that the change of resistance of a column of liquid metal, due to the action of a magnetic field, can only arise from the following two effects :—

- (1) A change of resistivity of the metal.
- (2) A change of resistance consequent upon the expenditure of energy required to maintain hydrodynamic currents set up in the liquid by the action of the magnetic field upon the electric current.

* Nielson, Phys. Rev. p. 302 (Feb. 1924).

† Fenninger, Phil. Mag. xxvii. pp. 109-112 (Jan. 1914).

‡ The values taken for tin and platinum are those at room temperatures, but as the Hall coefficient decreases with temperature this only strengthens the argument.

The first takes account of a possible true effect, and the increase of resistance, $\delta_1 r$, due to it bears to the original resistance r a ratio which is independent of the size and shape of the column. It can, therefore, be represented by $A r$, where A is independent of the dimensions of the column.

The second effect will now be considered in detail. In the first place it can be shown that, under the action of the magnetic field, the liquid metal will in general not remain in equilibrium. Let α, β, γ be the components of the magnetic field H , and I_x, I_y, I_z the components of the electric current I , at a point x, y, z in the liquid. Then from Ampère's law the force, P , per unit volume acting upon the liquid at x, y, z has the components $X = \gamma I_y - \beta I_z$, $Y = \alpha I_z - \gamma I_x$, $Z = \beta I_x - \alpha I_y$. If the liquid is to remain at rest, the force P must be derivable from a single-valued potential-function. That will be the case provided the following relations hold at all points in the liquid :

$$\frac{\partial X}{\partial y} - \frac{\partial Y}{\partial x} = 0, \quad \frac{\partial Y}{\partial z} - \frac{\partial Z}{\partial y} = 0, \quad \frac{\partial Z}{\partial x} - \frac{\partial X}{\partial z} = 0. \quad (1)$$

Since the magnetic field and electric current are quite independent, these relations will in general not be satisfied, and the liquid will consequently be set in motion.

In this connexion it should be mentioned that it is possible to have cases in which the equilibrium conditions are satisfied. The simplest and most practical case is that in which the magnetic field and electric current are constant in magnitude

and direction throughout the liquid (when $\frac{\partial}{\partial x} = \frac{\partial}{\partial y} = \frac{\partial}{\partial z}$

$= 0$). An experiment under these conditions was carried out by T. Jones* in his investigation of the effect of the shape and position of the current leads, and his observations are in accordance with these calculations. He found that as the leads were pushed nearer together from a position in which the mercury, contained between them in a cylindrical glass tube, extended outside the magnetic field, to a position in which the mercury was entirely in a uniform field, the resistance change decreased to a hundredth of its first value. The leads did not completely fill the tube so that the electric current was not absolutely uniform, and this probably accounted for the small change still present in the second position. Jones used tubes of diameter of the order of

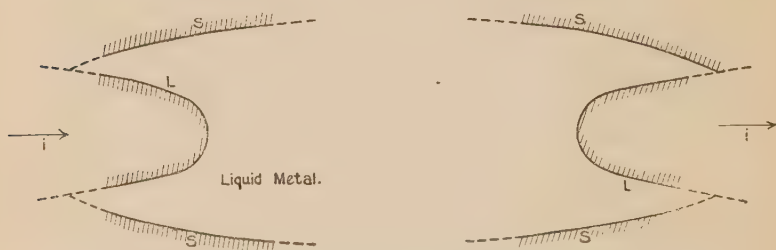
* *Loc. cit.*

·5 cm., and in such cases, as we shall see later, the real effect $\delta_1 r$ is negligible.

In discussing the increase of resistance due to the motion of the liquid, it is necessary to consider a general case since the experiments which have been carried out are not confined to straight cylindrical columns. In some cases bent tubes have been used, and in others leads extending into the liquid in the field, and not filling the tube.

Let the electric current enter the liquid metal from the surfaces L, the liquid being bounded elsewhere by the insulating surfaces S, there being no free surface of the liquid * (see fig. 1).

Fig. 1.



Let i be the total current traversing the liquid, I be the resultant current per unit area at the point x, y, z , and H be the resultant field at x, y, z . The force acting upon the liquid per unit volume at the point x, y, z is then equal to the vector product of H and I (VHI). There is no need to take into account the forces acting upon the liquid initially and under the action of which the liquid was in equilibrium, as it can be shown that they have no effect upon the motion produced. Let p be the increase of pressure at (x, y, z) at time t after the application of the field and current. Then the differential equations of motion of the liquid are :

$$\rho \frac{du}{dt} = X - \frac{\partial p}{\partial x} + \eta \left(\frac{\partial^2 u}{\partial x^2} + \frac{\partial^2 u}{\partial y^2} + \frac{\partial^2 u}{\partial z^2} \right),$$

with similar equations for $\rho \frac{dv}{dt}$ and $\rho \frac{dw}{dt}$, and

$$\frac{\partial u}{\partial x} + \frac{\partial v}{\partial y} + \frac{\partial w}{\partial z} = 0, \quad . \quad . \quad . \text{ equations (2)}$$

* This is satisfied to all intents and purposes in all actual cases, any free surface, which there may be, being far from the affected portion of the liquid.

u, v, w being the components of velocity of the liquid at (x, y, z) , ρ the density of the liquid, and η its viscosity. These equations, together with the boundary conditions, determine the motion produced. The motion will not necessarily reach an absolutely steady state, in which the velocity at a point is the same at all instants. Such a state is not reached in the case of a liquid in turbulent motion. The motion will, however, reach a state in which the velocity at any point, when averaged over a sufficiently large interval of time, is independent of the time. If this velocity be denoted by \bar{u} , then the mean work done by the force "HI" per unit volume, per unit time, at (x, y, z) will be equal to the component of \bar{u} parallel to $\nabla H \times \nabla H$, *i. e.* $\bar{u} \nabla H$, \bar{u} denoting scalar product. The mean total work done per unit time is therefore $\iiint_{\Sigma} \bar{u} \nabla H d\Sigma$, where Σ represents the space occupied by the liquid. This is equal to the mean rate of dissipation of energy due to the motion, and if we denote it by F , and the corresponding increase of resistance by $\delta_2 r$, we evidently have

$$i^2 \cdot \delta_2 r = F = \iiint_{\Sigma} \bar{u} \nabla H d\Sigma,$$

$$\text{or} \quad \delta_2 r = \frac{F}{i^2} = \frac{1}{i^2} \iiint_{\Sigma} \bar{u} \nabla H d\Sigma. \quad . \quad . \quad . \quad (3)$$

In order to obtain the exact value of F^* , it is necessary in the first place to determine \bar{u} —*i. e.*, to solve equations (2). This would be most difficult, and probably impossible. However, much information can be obtained concerning F by means of the method of dimensions. As we have seen, $F = \iiint_{\Sigma} \bar{u} \nabla H d\Sigma$, so that it depends only upon those quantities which affect \bar{u} , H , and Σ . The quantities which can affect \bar{u} are the independent variables, other than time (of which \bar{u} , by its definition, is independent), contained in the differential equations (2), and the corresponding boundary conditions. It follows that F can depend only on H, η, ρ , and Σ .

In most experiments concerned with this problem, the magnetic field is constant over a certain area and then falls off comparatively quickly. No use will be made of this fact here, but it will be assumed that the values of H at

* It has been found as a result of approximate calculations in certain cases (E. J. Williams, Thesis for M.Sc., Wales, 1924) that the increase of resistance, consequent upon the effect under consideration, is of the same order as that of the increase actually observed in those cases.

any two points always bear the same ratio to one another *. The maximum value, denoted by h , will be taken as the standard value. Then the value of H at any point can be expressed in the form $h \times$ (function of coordinates of the point and geometry of the field).

When the liquid is in motion in the magnetic field, induced e.m.f.s are set up. These will produce extra electric currents, which will be superimposed upon the primary current. These induced currents are, however, probably negligible compared with the primary current; for they bear to the latter a ratio which is of the same order as the ratio of the induced back e.m.f. to the primary forward e.m.f., which is in turn equal to the ratio of the increase of resistance, $\delta_2 r$, to the initial resistance r . The latter ratio is generally much less than .01, and it therefore follows that the induced currents are very small compared with the original current, and they will be neglected.

The distribution of the current is then governed by the differential equations $\text{div } I = 0$, $\text{rot } I = 0$, and the boundary conditions, which involve the total current i traversing the liquid, the ratio σ/σ' of the resistivity of the liquid to that of the leads, and the geometry of the boundary. It follows that I can be expressed in the form :

$$I = i \times (\text{function of } \sigma/\sigma') \\ \times (\text{function of } x, y, z \text{ and geometry of boundary}),$$

and the product HI in the form :

$$HI = hi \times (\text{function of } \sigma/\sigma') \\ \times (\text{function of } x, y, z, \text{ geometry of boundary and} \\ \text{geometry of magnetic field}).$$

h and i therefore always appear together as the product " hi ." The dimensions of " hi " are those of $\frac{\text{Force}}{\text{Length}}$, *i.e.* MT^{-2} . The dimensions of the viscosity, η , are $ML^{-1}T^{-1}$, of the density, ρ , ML^{-3} , whilst $\frac{\sigma}{\sigma'}$ is of no dimensions. Geometrically similar systems are considered ;

* The magnetic field is generally furnished by an electromagnet with an iron core. The assumption made would be absolutely correct if the permeability μ of the iron did not vary with the magnetizing force. The permeability μ measures the refractive index of the lines of force at the surface of the iron, and as it is always very large (of the order of 1000) the lines leave the surface almost normally, and the possible variation in μ alters but little the angle which the lines make with the surface on emergence. As a result, the geometry of the field outside remains practically constant.

the similarity applying to the variation of the magnetic field as well as the boundary of the liquid. The dependency upon the configuration of the system is thus nominally reduced to dependency upon its scale, which will be denoted by "s," and is of the dimensions of length.

The dimensions of F are those of $\frac{\text{Energy}}{\text{Time}}$, i.e. ML^2T^{-3} ; and the expression for F, which can only involve hi , η , ρ , s , and $\frac{\sigma}{\sigma'}$, must be of these dimensions also*. A general expression satisfying this dimensional relation is

$$F = B \cdot \frac{h^2 i^2 s}{\eta} \cdot f\left(\frac{\eta^2}{hi s \rho}\right) \cdot \phi\left(\frac{\sigma}{\sigma'}\right),$$

where F and ϕ are any functions whatever, and B a numerical constant. Therefore, from equation (3)

$$\delta_2 r = B \cdot \frac{h^2 s}{\eta} \cdot f\left(\frac{\eta^2}{hi s \rho}\right) \cdot \phi\left(\frac{\sigma}{\sigma'}\right), \quad . \quad . \quad . \quad (4)$$

and the total increase of resistance is given by

$$\delta r = \delta_1 r + \delta_2 r = A \cdot r + B \frac{h^2 s}{\eta} \cdot f\left(\frac{\eta^2}{hi s \rho}\right) \cdot \phi\left(\frac{\sigma}{\sigma'}\right). \quad (5)$$

The application of (5) to particular cases will now be considered.

Case in which the motion of the liquid is steady.

The motion of a liquid is said to be steady when the velocity at any point is the same at all instants. The viscosity of a liquid tends to bring about steady motion, whilst the momentum of the motion has the opposite effect. For these reasons, small linear dimensions and small velocities are favourable to steady motion. The experiments which are pre-eminently included in the case of steady motion are, therefore, those in which the magnetic field, the electric current traversing the liquid, and the dimensions of the column of liquid, are small.

The differential equations governing the steady motion of a liquid are obtained from (2) by putting $\frac{du}{dt} = \frac{dv}{dt} = \frac{dw}{dt} = 0$. It can then be shown that the velocity at any point is

* The dimensions attributed to the various quantities are those which they possess in the differential equations.

proportional to " hi ," and is always in the same direction. It follows that

$$\begin{aligned} \overline{SuVHI} &\propto h^2 i^2, \\ \therefore \delta_2 r &\propto \frac{F}{i^2} \propto \frac{h^2 i^3}{i^2} \propto h^3. \end{aligned}$$

But from (4),

$$\delta_2 r = B \cdot \frac{h^2 s}{\eta} \cdot f\left(\frac{\eta^2}{his\rho}\right) \cdot \phi\left(\frac{\sigma}{\sigma'}\right)$$

$$\therefore f\left(\frac{\eta^2}{his\rho}\right) = \text{constant},$$

so that

$$\delta_2 r = B \cdot \frac{h^2 s}{\eta} \cdot \phi\left(\frac{\sigma}{\sigma'}\right) \quad . \quad . \quad . \quad . \quad . \quad (6)$$

and

$$\delta r = \delta_1 r + \delta_2 r = Ar + B \cdot \frac{h^2 s}{\eta} \cdot \phi\left(\frac{\sigma}{\sigma'}\right). \quad (6a)$$

Berndt *, using a capillary tube of diameter 0.29 mm., containing liquid mercury, failed to observe a change of resistance on the application of a field of 3000 gauss, and from the degree of accuracy attainable in his experiments, concluded that the change, if present, was less than .00004 per cent. This result sets an upper limit to $A = 4 \times 10^{-7}$, for a field of 3000 gauss, the second term in (6a) being essentially positive. Incidentally, with a tube of diameter 0.37 mm., Berndt observed a change of $50 \times 10^{-7} r$, *i. e.* more than 12 times the change in the tube of diameter 0.29 mm. This increase in $\frac{\delta r}{r}$ is attributed to the second term in (6a), *i. e.* to the hydrodynamic effect. The large increase in $\delta_2 r$ was probably due not only to the difference in the diameters of the tubes, but chiefly to the conditions obtaining with the tube of 0.29 mm. diameter being nearer the equilibrium conditions.

W. M. Nielson † (1924) has shown that $\frac{\delta r}{r}$ for mercury for a field of 16,000 gauss is less than 3×10^{-6} , which corresponds to an upper limit to $A = 1 \times 10^{-7}$, for a field of 3000 gauss ‡.

Reference might here be made to the methods adopted in order to eliminate or rather to minimize the spurious effect. In the theory presented here, the spurious effect is represented by $\delta_2 r$. It is seen to be directly proportional to the

* *Loc. cit.*

† *Loc. cit.*

‡ In making this reduction, it is assumed that the true resistance increase is proportional to (field)².

linear dimensions of the system (equation 6), which is in accordance with the result obtained by various observers, that the spurious effect can be diminished by using tubes of finer bore. In addition, however, to using a fine bore tube, Nielson applied a pressure of about 10 atmospheres to the mercury. The effect of such a pressure on the viscosity is small, so that the diminution of $\delta_2 r$ effected by this means was inappreciable. The ideal method seems to be one which ensures that the current and field are uniform throughout the liquid, when, as already shown, the liquid will not be set in motion and therefore $\delta_2 r = 0$.

Having obtained from the experiments of Berndt and Nielson an upper limit to A, we shall consider the results obtained by Rossi*, who used fields of from 3350 to 4450 gauss. With a field of 3350 gauss he observed an increase of resistance of $37 \times 10^{-7} r$, in a capillary tube of diameter 0.7 mm. containing mercury. The value of A for this field (from Nielson's results) is less than 1×10^{-7} , so that at least 97 per cent. of the increase observed by Rossi with pure mercury was due to motion of the mercury, and is represented by $\delta_2 r$.

In the case of steady motion the expression for $\delta_2 r$ is independent of the current "i" (equation 6). Rossi does not mention any dependence of δr upon the current traversing the mercury, and consequently we may assume that the motion in his experiments was steady and equation (6) ought therefore to apply. According to this equation δr is proportional to the square of the field, and an analysis of Rossi's results as given in Table I. shows that this is the case.

TABLE I.

Magnetic Field.	Tube of diameter=0.7 mm.		Tube of diameter=0.5 mm.	
	$\delta r \times 10^7$, in ohms.	$\frac{\delta r}{h^2} \times 10^{14}$.	$\delta r \times 10^7$.	$\frac{\delta r}{h^2} \times 10^{14}$.
3350	69	61	57	51
3640	78	59	66	50
3930	92	60	77	50
4190	104	59	86	49
4450	123	62	104	52

* *Loc. cit.*

Rossi also investigated the effect of a magnetic field upon the resistance of liquid bismuth amalgams. If no true effect was present in these cases also, the values of δr for the amalgams would also be given by *

$$\delta r = \delta_2 r = B \frac{h^2 s}{\eta}$$

This equation applies to geometrically similar systems, and in all probability holds in the case of all experiments carried out with the same tube. The experimental results obtained with a capillary tube of diameter 0.5 mm. are given in Table II. The values of δr calculated on the assumption that it entirely consists of the hydrodynamic effect are also given †. In making the calculations, the viscosity of dilute bismuth amalgams is taken to increase at the rate of 1 per cent. for the addition of 1 per cent. of bismuth by weight to the mercury ‡.

It is seen from this table that there is a more or less consistent increase of δr with the concentration of bismuth. In fact, the mean percentage increases due to the addition of .5 per cent. and 1 per cent. are 10 and 19 respectively, whilst for the saturated bismuth amalgam the increase in δr is 66 per cent. The calculated increase of resistance, $\delta_2 r$, due to the motion of the liquid, however, decreases upon the addition of bismuth, and in order to account for the experimental results it is necessary to assume the existence of a true resistance change in bismuth amalgams. The magnitude of this true effect is given by

$$\delta_1 r = \delta r - \delta_2 r,$$

and its values for the various concentrations and fields are given in Table II. The irregular variation of $\delta_1 r$ with the field is probably due to experimental error. Since $\delta_1 r$ represents a true effect, $\frac{\delta_1 r}{r}$ should be independent of the shape and dimensions of the column of amalgam experimented upon, so that its value for the 0.7 mm. tube should be the same as that for the 0.5 mm. tube. Rossi only used a saturated bismuth amalgam, in addition to mercury, in the 0.7 mm. tube, and a comparison of the results for this

* In Rossi's experiments the leads are sufficiently far removed from the field so as not to introduce any complications, and consequently the term $\phi \left(\frac{\sigma}{\sigma'} \right)$ is a constant and can be included in B.

† The constant B is calculated from the value of δr for pure mercury.

‡ This is the result of an approximate determination by the writer.

TABLE II.

Increase of Resistance, δr .										
Magnetic Field. (gauss).	Pure Mercury (observed).	Amalgam containing .5 % Bi.			Amalgam containing 1 % Bi.			Amalgam saturated at 12° C.		
		δr (obs.).	δ_{gr} (calc.).	$\delta r - \delta_{gr} = \delta_1 r$.	δr (obs.).	δ_{gr} (calc.).	$\delta r - \delta_{gr} = \delta_1 r$.	δr (obs.).	δ_{gr} (calc.).	$\delta r - \delta_{gr} = \delta_1 r$.
3350	57	61	57	4	70	56	14	81	56	25
3640	66	75	66	9	83	65	18	115	64	51
3930	77	86	77	9	95	76	19	133	75	57
4190	86	91	86	5	102	85	17	156	84	72
4450	104	116	103	13	118	103	15	169	101	68

amalgam shows that the mean value of $\frac{\delta_1 r}{r}$ is 32×10^{-7} for the 0.7 mm. tube and $32\frac{1}{2} \times 10^{-7}$ for the 0.5 mm. tube. However, we must not lay too much stress on this experiment, because there is some irregularity amongst the separate values.

If the percentage of bismuth is denoted by p , the mean value of $\frac{\delta_1 r}{r} \cdot \frac{1}{p}$ due to a field of about 4000 gauss is 1.0×10^{-6} , and this can be taken to be the estimated true resistance change in bismuth amalgams. It is of the same order as that observed in solid metals.

The results obtained for a saturated bismuth amalgam at 190°C . seem to indicate that the true effect is much less at this temperature than at room-temperature. This decrease with temperature is also a general characteristic of the true resistance changes observed in solids. Exact calculations cannot be made owing to the lack of data concerning the viscosity of saturated bismuth amalgams at this temperature.

There is also a certain amount of evidence of a true resistance change in the work of Berndt. Since he used tubes of smaller diameter than those used by Rossi, it can be assumed that the motion was steady in his experiments, and therefore that equation (6a) is applicable to his results. It was found that the measure of resistance, δr , in molten bismuth decreased from 1/230 per cent. to 1/400 per cent. on heating the metal from 420°C . to 500°C . The viscosity decreases with the temperature, so that $\delta_2 r$ increases on heating from 420° to 500° . It therefore follows that the bulk of the 1/230 per cent. increase observed at 420°C . is a true effect, which decreases with the temperature.

The existence or non-existence of a true magneto-resistance effect of magnitude comparable with that observed in solids in the case of liquids is of importance to the theory of electrical conductivity. According to some theories the effect should not be exhibited by liquid metals, as they are non-crystalline*. Thus should the evidence, which has been presented here, for the existence of a true effect in bismuth amalgams and molten bismuth be substantiated, these theories would probably have to be abandoned or at any rate considerably modified.

* From evidence provided by work on the vapour pressures and conductivities of amalgams, the added metal in all probability exists in the monatomic state, and therefore an essentially non-crystalline state.

Case in which the motion of the liquid is not steady.

Drude and Nernst* (1891) and independently Jones† (1924) found that, in their experiments, the increase of resistance δr was dependent upon the current “ i ” traversing the liquid. The order of magnitude of δr in these cases is such that the increase is entirely to be ascribed to the hydrodynamic effect, which is represented by $\delta_2 r$. Now in the general expression for $\delta_2 r$, given in equation (4), i only appears in the term $f\left(\frac{\eta^2}{h i s \rho}\right)$. It was found in discussing the first case that if the motion is steady $f\left(\frac{\eta^2}{h i s \rho}\right)$ is constant. The dependency of $\delta_2 r$ upon the current must therefore be attributed to the production of turbulent motion in the liquid. This supposition, and its various other theoretical consequences, will now be considered.

It is well known that, even in the case of rectilinear motion of liquids, the motion becomes turbulent, if the velocity or other quantities concerned reach certain critical values. The type of motion with which we are concerned here is that of a liquid in an enclosed space, and is of necessity “curvilinear.” The curvature of the stream-lines makes the motion much more susceptible to turbulence than rectilinear motion. In support of this statement, the results of certain experiments due to Gibson and Grindley‡ may be mentioned. They found that the value of $\frac{v_c d}{\nu}$, where v_c is the critical velocity, and d and ν the diameter of the pipe and kinematic viscosity of the liquid respectively, in the case of motion through a pipe of diameter .32 cm., wound round a drum of diameter 36 cm., was 130. The value of the same quantity in the case of motion through a straight pipe is about 2000. The average curvature of 18 cm. radius imposed upon the motion in consequence of the curvature of the pipe, therefore, increases the tendency, for turbulence about 15 times. The radius of curvature of the stream-lines, in the motion under consideration here, is of the order of a millimetre. It is impossible to make exact calculations of the velocity, etc.; but as the result of an approximate estimate it has been found that the conditions are such as to make the supposition of turbulence

* *Loc. cit.*

† *Loc. cit.*

‡ Gibson & Grindley, *Proc. Roy. Soc. A*, lxxx. (1908).

quite admissible, especially if due allowance be made for the curvature effect*.

In the case of steady motion the velocity at a given point remains constant in direction, and its magnitude varies directly as the first power of the external forces. We shall assume that in the case of turbulent motion the average velocity \bar{u} is, similarly, constant in direction, but that its magnitude varies as (external forces) y , y being < 1 . Then (using equations (3) and (4)),

$$\delta_2 r = \frac{F}{\bar{v}^2} = \frac{1}{\bar{v}^2} \iint \int_{\Sigma} SuVHI d\Sigma \propto \frac{1}{\bar{v}^2} \cdot (hi)^y \cdot hi \propto h^{1+y} \cdot i^{+1+y}.$$

But

$$\delta_2 r = B \frac{h^2 s}{\eta} \cdot f\left(\frac{\eta^2}{hisp}\right) \cdot \phi\left(\frac{\sigma}{\sigma'}\right);$$

$$\therefore f\left(\frac{\eta^2}{hisp}\right) = \left(\frac{\eta^2}{hisp}\right)^{1-y}.$$

Therefore the increase of resistance, δr , which, as already shown, is entirely represented by $\delta_2 r$, is given by

$$\delta r = \delta_2 r = B \frac{h^{1+y} \cdot s^y}{i^{1-y} \cdot \eta^{2y-1} \cdot \rho^{1-y}} \phi\left(\frac{\sigma}{\sigma'}\right). \quad (7)$$

In those experiments in which the leads extend into the part of the liquid in the field the geometry of the system is complicated, and also $\phi\left(\frac{\sigma}{\sigma'}\right)$ has to be taken into account.

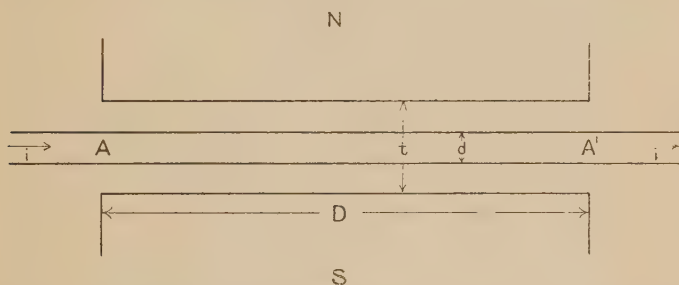
In such cases formula (7) cannot be simplified. However, it can be simplified for cases of straight cylindrical columns with the leads far removed from the field. In the first place, $\phi\left(\frac{\sigma}{\sigma'}\right)$ is a constant and can be included in the constant B . The geometrical configuration of the tube is determined entirely by its diameter d . We shall suppose that the magnetic field is produced by an electromagnet having circular pole-pieces of diameter D , at a distance apart t , and that the tube passes symmetrically between the pole-pieces as shown in fig. 2.

The quantities which affect the geometry of the magnetic field in the neighbourhood of the tube are t , D , and the permeability μ ; and in order to maintain geometrical similarity of the whole system, d/t , D/t , and μ must be kept constant. For reasons already given, the effect of

* An approximate calculation based on certain assumptions is given in an Appendix to the paper.

a possible variation in μ can be neglected. The motion produced in the liquid arises from the variation of HI , and as the variation of the field is practically confined to the ends A and A' the motion will be mostly produced there. The extension of this motion from the ends into the middle of AA' can be neglected, since in all actual cases the distance D is large compared with the diameter d of the tube. It follows that δr is independent of D . The only quantity which need be taken into account is therefore d/t , and s^y in equation (7) can be replaced by $d^y \cdot F(d/t)$.

Fig. 2.



For small variations of d/t , $F(d/t)$ can be replaced by $(d/t)^\beta$, and it can be shown further that $0 < \beta < 1$. Formula (7) then reduces to

$$\delta r = B \cdot \frac{h^{1+y} \cdot d^{\beta+y}}{\eta^{2y-1} \cdot \rho^{1-y} \cdot i^{1-y} \cdot t^\beta} \cdot \cdot \cdot \cdot (7a)$$

An advantage of this case over the more general case represented by (7) is that there are two additional quantities, d and t , with respect to which the variation of δr can be investigated.

Jones* has found that formula (7a) represents the variation of δr with respect to all the quantities concerned, and that formula (7) represents the results of experiments in the more complicated cases with current leads in the field and with bent tubes; the value of y in all cases is, to within experimental error, 0.59. Moreover, in several minor respects, Jones finds his observations to be in accordance with the theory.

δr , represented by formulæ (7) and (7a), is proportional to i^{y-1} . Drude and Nernst observed a variation of δr with the current, the observed δr for mercury decreasing from .271 per cent. for $i = .086$ ampere, to .159 per cent. for $i = 318$ amperes. The corresponding value of y is 0.59, which is the same as the value found by Jones.

* *Loc. cit.*

Some Hydrodynamical Inferences.

The validity of formulæ (7) and (7a) substantiates the theory in general, and in particular justifies the supposition that the motion in the experiments concerned is turbulent. Certain inferences concerning the nature of this turbulent motion will now be made.

In deducing formula (7) it was supposed that the average velocity, \bar{u} , at a given point remains constant in direction as the external forces are varied proportionately : in other words, that the average stream-lines maintain a constant shape. If this is not so, then the dissipation F , $= \iint_{\Sigma} S \bar{u} V H d\Sigma$, is affected in so far as the angle between \bar{u} and VH changes. This effect would certainly be dependent upon the actual configuration of the stream-lines, and as a result the value of γ would be different for cases in which the shape of the boundary of the liquid and the distribution of the external forces are different. However, as has been already stated, γ has the same value in all cases, including those with current leads in or completely out of the field, and with the liquid contained in straight or bent tubes. It can therefore be concluded that in the turbulent motion of a liquid in an enclosed space, maintained by the action of external volume forces, the average stream-lines maintain a constant shape*, and the magnitude of the average velocity, \bar{u} , at any point varies as (the external forces)⁵⁹.

We can calculate from this law of the variation of the velocity the dependency of the resistance to the motion on the velocity. The average resistance to the turbulent motion of the liquid can be resolved into a system of shears, in which the shearing force, S , at any point is tangential to the average stream-line through that point. Since the stream-lines remain unaltered in shape, when the external forces are varied proportionately at all points, it follows that the geometry of the system of shears remains unaltered also. Consequently, since the shears balance the accelerating

* In this respect they resemble the stream-lines of steady motion. However, it is more or less a matter for conjecture whether the actual shape of the former is the same as that of the stream-lines of the steady motion of a liquid produced in the same enclosure by a similar system of forces. If that is the case, then there is a quantity in turbulent motion corresponding to viscosity in steady motion. In the present case the expression for such a quantity would be $K \cdot \bar{u}^{.75} \cdot s^{.75} \cdot \rho^{.75} \cdot \eta^{.25}$, K being a numerical constant depending upon the geometry of the system, \bar{u} the velocity at some standard point, and s a measure of the scale of the system.

effect of the external forces, the shear at any point must vary directly as the external forces. Now the velocities are proportional to (external forces)^{1/59}, so that the shearing forces are proportional to (velocity)^{1/59}, *i. e.* (velocity)^{1/70}. In other words, the "resistance" to the motion is proportional to (velocity)^{1/70}. Osborne Reynolds investigated the turbulent flow of water through straight pipes, and found that the resistance to the motion was proportional to (velocity)^{1/72}. The motion in Reynolds' experiments differs considerably from that which we have been considering here. The average stream-lines in the former are straight, whilst in the latter they have a radius of curvature of the order of a millimetre; also the liquid used by Reynolds was water, whilst in these electrical experiments the liquid generally used has been mercury. In spite of these differences, the laws of variation of resistance with velocity are almost identical in the two cases.

Summary.

The change in the electrical resistance of a liquid conductor due to the action of a magnetic field is attributed to the sum of (1) a true resistance change, (2) a change consequent upon energy expended in maintaining hydrodynamic currents which are shown to be produced in the liquid conductor. An expression for the latter is obtained by means of dimensional analysis.

According to the theory thus developed there is evidence, in the experimental results of Rossi, for the existence of a true resistance change in bismuth amalgams. An analysis of the results shows that a 1 per cent. bismuth amalgam gives a true increase of resistance of '00010 per cent. in a field of 4000 gauss. Further evidence of a true effect in liquid metals is furnished by Berndt's work on molten bismuth, and in this case the estimated true change at 420° is of the order of '002 per cent. for a field of 3000 gauss.

In other cases the hydrodynamic effect certainly predominates, and, in most cases, a true change, if present at all, is negligible.

The variation of δr with the current traversing the liquid metal conductor, an effect which has been observed in certain cases, is explained by supposing that the motion of the liquid in these cases is turbulent. The other theoretical consequences of this supposition are fully substantiated by the experimental work of T. Jones. From the nature of

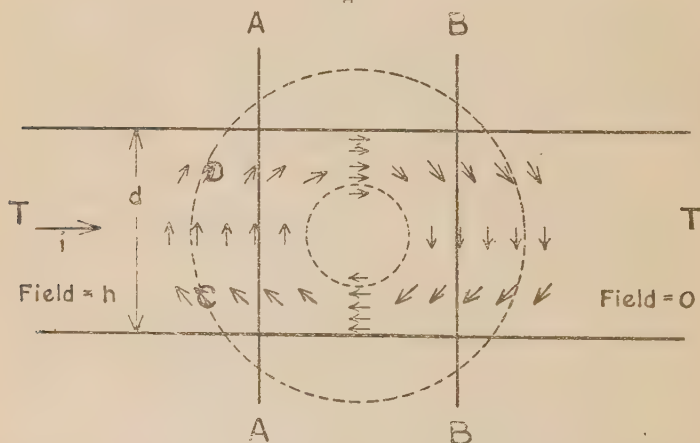
Jones's results it is shown that in the turbulent motion of liquids in an enclosed space due to the action of external volume forces, the average stream-lines maintain a constant shape as these forces are varied proportionately at all points. In this respect the average stream-lines of turbulent motion resemble the stream-lines in steady motion. The resistance to the motion is in all cases proportional to $(\text{velocity})^{1.70}$, and this is in agreement with the law of resistance in turbulent motion, which has been obtained as the result of experiments under very different conditions.

In conclusion, I wish to thank Professor E. J. Evans for his valuable criticism and advice in connexion with this paper.

APPENDIX.

That the velocity acquired under the laws of stream-line motion is greater than the critical velocity, can be deduced on certain assumptions. The calculation, however, only gives the order of magnitude of the velocity.

Fig. 3.



Let TT be a portion of the tube containing mercury, and AB the region where the magnetic field falls off, decreasing from its maximum value at A to a small fraction of that value at B. The volume force HI [which for the sake of argument is supposed to act upwards] is thus a constant " hI " to the left of A, and zero to the right of B. This distribution of volume force produces motion of the liquid somewhat as shown by the arrows in the diagram. In the part CD of the circuit the liquid is acted upon by a

volume force $\frac{h.i.4}{\pi d^2}$ approximately parallel to the direction of the motion, whilst the force parallel to the motion elsewhere is small in comparison and will be neglected. We shall assume the average velocity to be equal to that which would be produced in a straight tube of diameter $d/2$ and of length l equal to that of the circuit marked by the arrows, due to the action of a pressure difference between the ends $= \frac{h.i.4 \times CD}{\pi d^2} = \frac{hi4}{\pi d^2} \times \frac{d}{2}$ approximately. This velocity can be obtained by means of Poiseuille's law, and is equal to $\frac{2hid}{\pi d^2} \times \left(\frac{d}{4}\right)^2 \div 8l\eta$, where η is the viscosity of the liquid. The distance AB in the experiments concerned was about 1 cm., and l can be taken to be equal to $2+d$. The average velocity that would be produced in the case of mercury contained in a tube of diameter $d=0.5$ cm. with a current of 0.5 amp. and a field of 1000 gauss is equal to about 3 cm. per second. The values of the various quantities given above were about the smallest used by Jones in his experiments, so that the case considered is one in which turbulence was least likely. We shall take the velocity necessary to produce turbulence to be that required in the case of motion through a tube of diameter $d/2$, the axial line of the tube being a circle of diameter d . The value in this case is probably higher than in the actual case since uniformity of shape tends to maintain steady motion.

The value of the critical velocity v_c in the case of motion through a curved tube of diameter " a ," whose axis is a circle of diameter " b ," can be shown to be given by

$$v_c = \frac{2000\nu}{a \left\{ 1 + f\left(\frac{a}{b}\right) \right\}} \text{ cm. per sec.,}$$

where ν is the kinematic viscosity of the liquid and the value of $\frac{v_c a}{\nu}$ for a straight tube is taken to be 2000. In the case under consideration, $a=d/2$, $b=d$, and $d=0.5$ cm., so that

$$v_c = 2000\nu / .25 \{ 1 + f(.5) \}.$$

The value of this quantity when the liquid is mercury is given approximately by $\frac{10}{1 + f(.5)}$ cm. per sec.

From the value of the critical velocity for straight tubes it follows that $f(0)=0$, and from Gibson and Grindley's result it follows that $f(0.01)=14$. These values indicate that $f(0.5)$ is probably a large quantity, and therefore that v_c is a small fraction of 10 cm. per second. The calculated velocity is 3 cm. per second, and is therefore according to the discussion above sufficiently large to produce turbulence.

III. *The Electrical Resistance of Mercury in Magnetic Fields.*

By T. J. JONES, M.Sc. (Wales), Research Student, University College, Swansea*.

INTRODUCTION.

THE influence of a magnetic field on the electrical resistance of mercury has been examined by a number of investigators. These have studied the effect observed when the direction of the current in the mercury is perpendicular to the magnetic field, and it is this transverse effect that will be considered in the present paper.

Drude and Nernst† (1891) observed a small increase of resistance in a column of mercury placed in a transverse magnetic field. The change of resistance increased with the field, and for a field of eight kilogauss amounted to 0.2 per cent.

Patterson‡ (1902) obtained an increase of 0.03 per cent. in the resistance of a column of mercury for a field of twenty-five kilogauss.

Berndt§ (1907) noticed that the finer the column of mercury used, the smaller the increase of resistance for a given field; and in a column of diameter 0.29 mm. and a field of three kilogauss the resistance change was only 0.00005 per cent. His work led him to conclude that the observed changes of resistance were to be attributed to what he described as "electrodynanic actions," and that if there were true magneto-resistance effects in mercury they must be exceedingly small compared with those in solid metals.

Berndt's conclusions were supported by the subsequent work of Rossi|| (1911) and of Nielson¶ (1924), both of

* Communicated by Prof. E. J. Evans, D.Sc.

† Drude and Nernst, *Wied. Ann.* p. 568 (1891).

‡ Patterson, *Phil. Mag.* iii. p. 643 (1902).

§ Berndt, *Ann. d. Phys.* xxiii. p. 932 (1907).

|| Rossi, *Nuov. Cimento*, ii. p. 337 (1911).

¶ Nielson, *Phys. Rev.* February 1924.

whom worked on the resistance effects in fine columns. Nielson's investigations showed that the true effect (if any) in mercury must have a value less than 0.0003 per cent. for a field of sixteen kilogauss.

The above is a brief summary of the more important work done in connexion with the phenomenon of the increase of resistance in mercury due to a magnetic field.

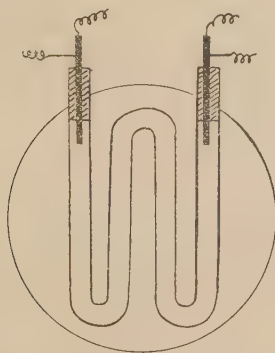
Although it may be said with some certainty, from a consideration of the above works, that the magneto-resistance effect observed in mercury is not a true effect such as is exhibited by solid metals, the nature of the effect seemed to be obscure. In the research described below, therefore, an attempt was made to throw light on the nature of the phenomenon by studying the magneto-resistance effects in fairly wide columns of mercury.

Added interest was given to the work by the development, during its course, of a theoretical investigation* of the magneto-resistance effects in liquid metals.

THE EXPERIMENTAL ARRANGEMENT.

The magnetic fields used in the experiments were obtained with a powerful electromagnet having pole-pieces 8 cm. in diameter, and the fields were measured with a Grassot Flux-meter and exploring coils. With a current of 10 amperes the magnet gave a field of about 10 kilogauss when the poles were placed one centimetre apart, and this value of the field was the largest used in the work.

Fig. 1.

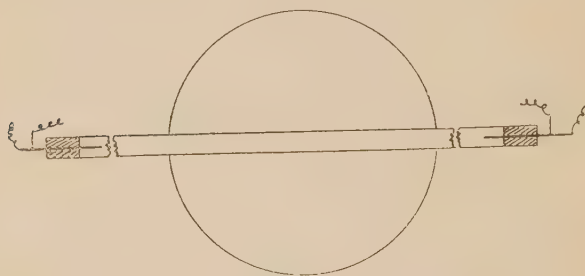


Two forms of glass tubes were used to contain the mercury—bent tubes as in fig. 1 and straight tubes as in

* By E. J. Williams, *suprà*, p. 27.

fig. 2,—the internal diameters varying from 3 to 7 mm. In the figures the circles represent the poles of the magnet, and, neglecting the stray field outside the poles, the magnetic fields act upon the portions of the mercury columns within the circles. The bent tubes enabled a longer column to be placed in the field than in the case of the straight tubes. Hence, if the magneto-resistance effect arose from a change of resistance throughout the column exposed to the field (as is the case with solid metals), then the change of resistance for a given field should be greater in the bent tube than in a straight tube of equal diameter.

Fig. 2.



The current leads into the mercury were of thick platinum wire, and the arrangement of these leads in the tubes is shown in figs. 1 and 2. It will be noticed that in the bent tubes the leads are in the magnetic field; but no correction was necessary for any resistance change which might occur in the leads due to the field, as platinum shows very small magneto-resistance effects.

In order to regulate the temperature of the mercury, a water-bath was at first used to contain the tubes; but later it was found that the bath could be dispensed with without introducing any errors into the work.

The resistance of each mercury column was low (of the order 10^{-2} ohm) and was measured by means of a Kelvin bridge. The bridge enabled a resistance change of a millionth of an ohm (*i.e.*, about 0.01 per cent. of the resistance of a mercury column) to be measured for all the columns.

In measuring the change of resistance for a given field, the following procedure was adopted: (*a*) the bridge was balanced for no field, (*b*) the magnet was excited and the bridge rebalanced, (*c*) the field was cut off and the bridge again balanced. When the reading obtained in (*c*) agreed

with that obtained in (a) the change of resistance given by (b) was recorded.

A complete observation occupied but a few seconds ; and by the above procedure any possible errors in the measurement of the resistance changes due to thermoelectric and Joule heating effects were avoided.

It will be noticed that in this work (for reasons that will be apparent later) it is the actual change of resistance, δR , that is measured and discussed, and not the relative change $\frac{\delta R}{R}$ as is usually the case in work on solid metals.

EXPERIMENTAL RESULTS.

Preliminary experiments showed that the magneto-resistance effect in a column of mercury depended upon the strength of the magnetic field, the strength of the current flowing in the mercury, the diameter of the mercury column, the temperature of the mercury, and upon the distance apart of the poles of the magnet (the magnetic intensity along the axis of the gap between the poles being kept constant).

It was noticed that when the current leads into the mercury were in the magnetic field (*e.g.*, as in fig. 1), a change in the position or shape of the leads had a marked effect on the magnitude of the resistance change.

The following were other phenomena observed. When balancing the bridge with the mercury resistance in the field, it was necessary to allow the bridge current to flow for a few seconds prior to closing the galvanometer circuit, as the resistance change occupied this interval of time in attaining its full value for that particular field. This "lag" effect was found to be due to some cause in the mercury itself and not to any inductive actions in the apparatus. It was also found that even when the "lag" effect was allowed for, the resistance of the mercury column when in the field was not constant but fluctuated very slightly—this fluctuation being manifested by a slight but continual motion of the spot of light about the zero of the galvanometer scale. The greater the change of resistance due to the field, the greater were these fluctuations. However, the magnitude of the fluctuations was always less than 1 per cent. of the corresponding change of resistance.

The following experiments were made to obtain, if possible, a relation between δR and the various factors upon which it depends.

1. *The Variation of δR with the Field.*

The variation of the resistance change with the field was investigated for fields ranging from 2 to 10 kilogauss and the experiments were extended to both types of tubes already described, these having diameters between 3 and 7 mm. Certain definite currents between 0.5 and 5 amperes were passed through the mercury column, and the variations of δR with the field for these currents were recorded.

The change of resistance continued to increase with the field and, up to the highest fields employed, showed no tendency to reach a constant value. It was also found that, within the above limits of the magnetic field, of the current in the mercury, and of the diameter of the mercury column, the relation between the resistance change and the field could be represented (within the limits of experimental error) by the relation

$$\delta R \propto H^{1.58}.$$

The results obtained in a typical case—that of a straight tube of diameter 5 mm.—are collected in Table I., where the first column gives the various fields in gauss, while the other columns give the corresponding resistance changes for the specified currents.

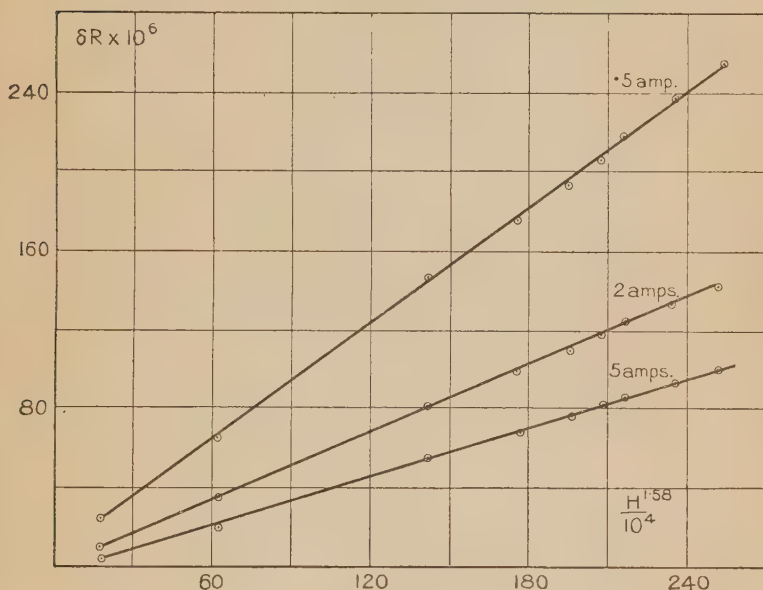
TABLE I.

Field in Gauss.	δR (ohms) $\times 10^6$ for currents ranging from 5 to 0.5 amps.								
H.	5.0.	4.0.	3.0.	2.5.	2.0.	1.5.	1.0.	.7.	.5.
2,000	5	7	8	9	10	12	15	18	23
4,200	18	21	27	30	34	40	50	55	64
7,000	55	62	69	75	82	91	110	127	148
8,000	67	74	83	89	98	111	130	153	176
8,500	77	82	92	98	107	120	145	168	193
8,900	82	88	98	105	116	130	154	181	207
9,100	85	95	104	111	123	137	164	191	219
9,600	93	99	112	122	133	149	178	207	236
10,000	98	108	120	129	142	159	188	218	248

Fig. 3 shows graphically the result of plotting (for certain values of the current in the mercury) the changes of resistance against the field raised to the power 1.58. Similar

curves were obtained for all the tubes, thus indicating that the relation between δR and $H^{1.58}$ is linear.

Fig. 3.



2. The Relation between δR and the Current in the Mercury.

The same experiments as were made in determining the relation between the resistance change and the field, for certain definite currents in the mercury, also sufficed to give the relation between the resistance change and the current.

It was found that the resistance change for a given field was greater the smaller the current in the mercury—the relation between δR and the current being given (within the limits of error) by the equation

$$\delta R \propto i^{-.40}.$$

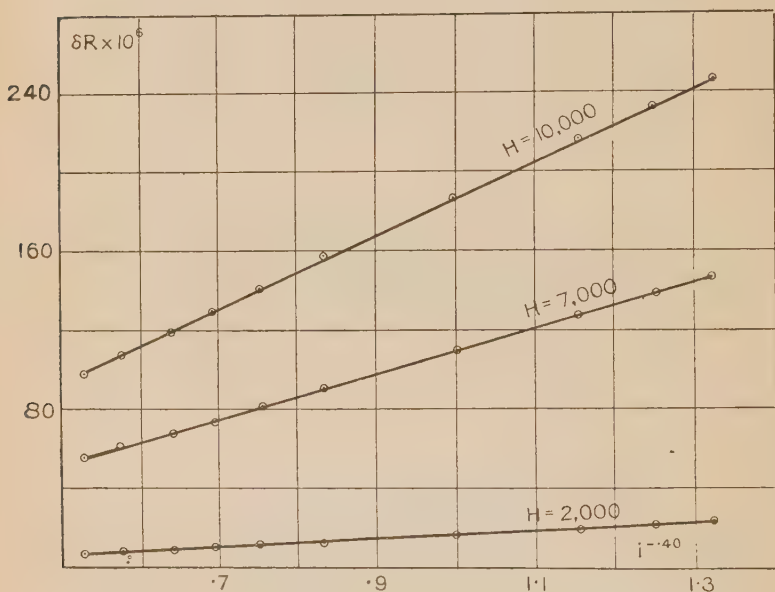
This relation holds within the range of field, current, &c., already given.

Table I. gives (for the tube mentioned above) the resistance changes for different currents between 5 and 0.5 amperes ;

and in fig. 4 the relation between δR and the current raised to the power (minus .40) is shown graphically. Similar curves were obtained for all the tubes.

In connexion with this "current" effect, it is interesting to note that Drude* and Nernst also observed that the change of resistance depended upon the current. Only two values of δR for two different currents are given in their paper, but these values fit in with the above relation.

Fig. 4.



As it is improbable that δR should continue to increase as the current decreases, experiments are being made to investigate (among other things) the relation between δR and the current for small currents. The results already obtained show that for currents of 1/10 ampere, or less, the relation between δR and i is not that given above, but that δR varies inversely as i raised to a power less than -0.40 and which is smaller the smaller i . It is therefore possible that for very small currents the resistance change would be independent of the current in the mercury.

* *Loc. cit.*

3. *The Relation between δR and the Diameter of the Column.*

In studying the dependence of δR on the diameter of the mercury column, the resistance changes in tubes of different diameters under identical experimental conditions were compared. When the current leads into the mercury were in the magnetic field (as in the bent tubes) the position of the leads affected the resistance change to a considerable extent, and hence made it impossible to compare the values of δR for different tubes. This, together with the fact that the resistance changes in the bent tubes were found to be of about the same magnitude as those in straight tubes, caused the bent type of tube to be discarded.

The change of resistance, in straight tubes of different diameters and for a definite field and current in the mercury, are collected in Table II. There is a good agreement in the values of the ratios $\frac{\delta R}{d}$ indicating that the resistance change is proportional to the diameter of the column.

TABLE II.

$\delta R (\times 10^6)$.	Diameter (d).	$\delta R/d (\times 10^6)$.
98	0.68 cm.	144
93	0.64 „	145
74	0.51 „	145
61	0.42 „	145
55	0.38 „	145
45	0.31 „	145

4. *The Relation between δR and the Distance apart of the Poles of the Magnet.*

By varying the current in the magnet, the intensity of the field along the axis of the gap between the poles could be kept constant while the distance apart of the poles was varied. Keeping the intensity constant, in this way, it was found that for tubes with leads in the field only a slight decrease occurred in δR when the poles were moved to a greater distance apart. However, when the leads were out of the influence of the field the distance apart of the poles had a marked effect upon the magnitude of the resistance change. The relation between δR and the distance b between the poles, for a constant field along the axis of the gap and for a constant current in the mercury, was

found to be given within the error of experiment by

$$\delta R \propto \frac{1}{b^{.41}}.$$

Table III. shows the resistance changes in a long straight tube for a magnetic field of 10 kilogauss along the axis of the gap, the distance apart of the poles being varied.

TABLE III.

$\delta R (\times 10^6).$	b (mm.).	$[\delta R \times b^{.41}] \times 10^6.$
93	12	257.6
97	11	258.8
100	10	257.0
105	9	258.4
110	8	258.0
116	7	257.6

It would be well here to point out that the theory of the magneto-resistance effect in mercury, which is discussed later, gives an interpretation of this dependence of δR on the distance apart of the poles. According to the theory $1/b^{.41}$ is a measure of the rate of dying away of the field outside the poles of the magnet; and it can be shown theoretically that the greater this rate of decay of the field the greater is the change of resistance for a given field along the axis of the gap between the poles of the magnet.

5. *The Dependence of δR upon the Position and Shape of the Leads when these were in the Field.*

In the experiments in which the current leads into the mercury were in the magnetic field (*e.g.*, fig. 1) it was noticed that altering the position or shape of the leads had a marked effect on the magnitude of the resistance change.

This "lead" effect was investigated in the following manner. A short tube (diameter 6.4 mm.) was filled with mercury and the platinum wire leads adjusted so that a column of mercury one centimetre long lay between the points of the leads. The tube was then placed in a field of 10 kilogauss and the change of resistance observed was 35×10^{-5} ohm.

A long tube of similar diameter was then filled with mercury and the wire leads placed in the tube so as to be out of the influence of the field. As the diameter of the magnet poles was eight centimetres, a column of mercury eight centimetres long lay in the magnetic field. The change of resistance for the same field and current as before was

now only 10×10^{-5} ohm—a change much smaller than in the short column. These results show that the magneto-resistance changes are independent of the resistance of the column of mercury in the field. They also explain why it is the change of resistance, δR , and not the relative change, $\frac{\delta R}{R}$, that is considered in this work.

Again, when in the short tube mentioned above, thick copper leads which filled the tube were substituted for the wire leads, and the resistance change measured for a column of mercury one centimetre long, it was found that the change of resistance (for the same field and current as before) was only 3×10^{-6} ohm—*i. e.*, less than 1 per cent. of that obtained under similar conditions but with wire point leads.

This result, together with those preceding, seem to indicate that the resistance changes are probably due to some effects occurring in the mercury at those portions where the current enters or leaves the mercury : *i. e.*, at the leads if they are in the field, or, if the leads are not in the field, in those portions of the mercury column near the edges of the poles.

6. The Dependence of δR on the Temperature.

Experiments were made to determine the effect produced on δR by increasing the temperature of the mercury. A long glass tube containing mercury was placed in a copper bath, which in its turn was fixed between the poles of the magnet. The bath was heated by gas flames from underneath and contained first water at the room temperature (17° C.), then boiling water (100° C.), and finally boiling glycerine (290° C.). The resistance changes at these three temperatures (for given fields and current) were measured, and are collected in Table IV. The last two columns show that

TABLE IV.

$\delta R [\times 10^6]$ at 17° C.	$\delta R [\times 10^6]$ at 100° C.	$\delta R [\times 10^6]$ at 290° C.	$\frac{\delta R \text{ at } 100^\circ}{\delta R \text{ at } 17^\circ}$	$\frac{\delta R \text{ at } 290^\circ}{\delta R \text{ at } 17^\circ}$
17	18	19	1.059	1.120
52	55	58	1.060	1.115
74	78	83	1.054	1.112
94	99	106	1.053	1.128
114	120	129	1.053	1.132

on raising the temperature from 17° C. to 100° C. the resistance change increased by about 5.6 per cent., while on heating from 17° C. to 290° C. there was an increase

of 12·5 per cent. However, allowance must be made for the increase in δR due to the increase produced by heating in the diameter of the glass tube. This change of diameter amounted to about 0·4 per cent. on heating from room temperature to that of the boiling glycerine, so that, since δR is proportional to the diameter of the column, the effect of heating from 17° C. to 290° C. is to increase δR by 12·1 per cent., while from 17° C. to 100° C. δR increases by 5·5 per cent.

7. *The Effect of the addition of Cadmium to the Mercury.*

The effect on δR of adding cadmium to the mercury was examined for a 3 per cent. cadmium amalgam. The results for this amalgam, together with those for mercury under similar conditions, are collected in Table V. It is seen that the resistance changes in the amalgam are slightly smaller than those in the mercury—the difference being about 1 per cent. [The change in the resistance of the mercury due to the addition of the cadmium is an increase of about 20 per cent.]

TABLE V.

δR for Mercury.	δR for 3 per cent. amalgam.	$\frac{\delta R \text{ for amalgam}}{\delta R \text{ for mercury}}$
30×10^{-6}	30×10^6	1·00
73 "	72 "	·99
101 "	100 "	·99
121 "	120 "	·99
126 "	125 "	·99

DISCUSSION OF RESULTS.

The experiments described above show that within certain limits the magneto-resistance change at a given temperature in a straight column of mercury with the current leads out of the influence of the field is given by

$$\delta R \propto \frac{H^{1.53} d}{i^{.40} b^{.41}},$$

where H , d , i , and b are respectively the field along the axis of the pole gap, the diameter of the column, the current in the column, and the distance apart of the poles of the magnet.

The experiments also show that the effect in mercury is of a different nature from those exhibited by solid metals; for in

the former the resistance change for a given field is independent of the resistance in the field and is dependent on the current in the mercury, whereas in solid metals the resistance change is proportional to the resistance in the field and is independent of the current in the conductor.

A theoretical investigation of the magneto-resistance effect in liquid metals has been made by E. J. Williams. The increase of resistance of a column of mercury (or any other liquid metal) when in a magnetic field is attributed to the expenditure of energy by the electric current in maintaining mass-motion of the mercury in certain portions of the column, this motion being developed by the electrodynamic action of the magnetic field on the mercury carrying the current.

The motion of the mercury is developed at those portions of the column in the field where the magnetic field is not uniform or where the current-density is not constant. Thus in those tubes in which the leads are in the field, the current-density in the mercury about the leads is not constant so that the motion of the mercury takes place mainly about the leads. In the tubes with leads out of the field the motion is mainly produced in those portions of the column where the current enters and leaves the field—*i. e.*, at the boundaries of the pole-pieces, for at these points the field varies rapidly.

This view of the locality of the motion, and hence of the cause of the resistance change, is consistent with the conclusion arrived at in the experiments that the cause of the change of resistance is not distributed uniformly throughout the column exposed to the field.

The motion of the mercury was experimentally demonstrated by placing one of the current leads so as to just enter the free surface of a mercury column in the magnetic field. The current-density near the surface of the mercury varied considerably, and a vigorous motion of the mercury was observed.

Support for the theory was also provided by the results obtained in the experiments dealing with the effect on δR of the shape of the leads. With thick leads approximately filling the tube—a condition which ensured nearly uniform current-density in the mercury—there was practically no resistance change when the mercury was in a uniform field. The small effect that was observed may be accounted for by a possible slight non-uniformity of the current-density or of the field.

The “lag” effect described in the preliminary experiments is explained as being due to the resistance change

not reaching its full value until the motion of the mercury reaches its full value ; and this might take an appreciable time in consequence of the mass of the mercury.

Two different theoretical relations for the resistance change were obtained by Williams, one relation being based on the assumption that the motion of the mercury was steady, while the other followed from assuming the motion to be turbulent.

On the assumption that the motion of the mercury was turbulent, the following relation was obtained for the change of resistance in a straight column having the leads out of the influence of the field :

$$\delta R \propto \frac{H^{1+\gamma} d^{\beta+\gamma}}{i^{1-\gamma} \eta^{2\gamma-1} \rho^{1-\gamma} b^{\beta}}.$$

In this relation H , d , i , and b have the same significance as before, while η and ρ are respectively the viscosity and density of the mercury. β and γ are numerical constants whose values cannot be determined theoretically—although it is shown that β lies between 0 and 1.

If β and γ be given the values .41 and 1.59 respectively, the above relation becomes

$$\delta R \propto \frac{H^{1.59} d}{i^{.41} b^{.41} \eta^{.18} \rho^{.41}},$$

which agrees well with the relation obtained experimentally when the temperature (and hence η and ρ) is constant.

In order to test the theoretical relation with respect to the dependence of δR upon the viscosity and density of the mercury, it is necessary to vary these quantities. This can be done either by altering the temperature of the mercury or (if it be assumed that the magneto-resistance effect in the amalgam is still mainly due to the motion of the liquid) by dissolving cadmium in the mercury. It should be noted, however, that only small variations of η and ρ can be made, and it is difficult to test accurately the relation between δR and these quantities.

In the experiments on the variation of δR with temperature there was an increase in δR of about 12.1 per cent. when the mercury was heated from 17° C. to 290° C., while from 17° C. to 100° C. δR increased by 5.5 per cent. From known data* on the density and viscosity of mercury at different temperatures, the theoretical change in δR due to a rise of temperature can be calculated from the formula. It is found that δR should increase by 5.5 per cent. from 17° C. to 100° C., and by 11.9 per cent. from 17° C. to

* Kaye and Laby's Tables.

290° C. These calculated results agree within the limits of experimental error with the observed results.

The change in δR produced by a change in the temperature of the mercury can therefore be accounted for by the variation of the density and viscosity of mercury with temperature.

In the experiments with the cadmium amalgam the viscosity and density of the amalgam are different from those of mercury. The theoretical change to be expected in δR , on the assumption that the change is to be accounted for by the alteration of η and ρ , can be calculated as data on the viscosity and density of a 3 per cent. cadmium amalgam are available*.

The required data are:—

η for 3 per cent. amalgam = 1.06 η for pure mercury.

ρ for 3 per cent. amalgam = .98 ρ for pure mercury.

From these values the theoretical change in δR is 0.5 per cent.—a result which is not inconsistent with that obtained in the experiment.

The theoretical relation is thus seen to be in good agreement with the results of experiment.

SUMMARY.

1. The experiments have shown :—

- (a) That for magnetic fields varying from 2 to 10 kilogauss, the magneto-resistance change in a straight column of mercury of diameter about 0.5 cm. when the current in the column lies between 5 and 0.5 amperes, is given by

$$\delta R \propto \frac{H^{1.58} d}{i^{.40} b^{.41}},$$

where H , d , i , and b are respectively the field, the diameter of the column, the current in the column, and the distance apart of the poles of the magnet.

- (b) That the change of resistance is independent of the resistance in the field.
 (c) That the resistance change increases with rise in temperature of the mercury.
 (d) That under the conditions prevailing in the experiments (wide tubes and comparatively large fields and currents) the magneto-resistance effect in mercury is mainly, if not entirely, of a different nature from those exhibited by solid metals.

* *Vide* p. 1043, vol. iv. Mellor's 'Treatise on Chemistry.'

2. The results of the experiments have been examined from the point of view of a theory which attributes the magneto-resistance effects in mercury to the development, under the combined action of the magnetic field and the current, of mass-motion of the mercury in certain portions of the column. This theory has been found to explain all the observed phenomena and to give for the resistance change a relation which is in good agreement with that obtained in the experiments.

In conclusion, I wish to thank Professor E. J. Evans, D.Sc., and Mr. W. Morris Jones, M.A., for their most valuable help and advice in connexion with everything in the present paper.

Further, this Research was made possible by the award of a grant by the Education Committee of the Glamorgan County Council.

IV. *On the Electric Capacity of Certain Solids of Revolution.*
By D. M. WRINCH, M.A. (Oxon.), D.Sc. (Lond.), Lecturer
at Lady Margaret Hall, Oxford*.

Introduction.

THE problems associated with a conducting solid of revolution when it is freely charged with electricity have at present been solved in a few cases only. Beyond the spheroids, few surfaces of revolution have been treated except those which are equipotentials for prescribed sets of electric charges lying entirely within them. In these cases, the set of charges may be replaced by a Green's equivalent stratum in the well-known manner, and the equipotential surface in question may be taken as a conductor carrying the equivalent stratum as a free surface distribution of electricity. The equipotentials associated with further, more complicated, sets of charges may also be investigated and the distribution on the resulting equipotentials may then be deduced.

If, however, it is desired to solve the problems associated with a *given* surface represented by $v=0$ in the transformation of cylindrical coordinates

$$z + ip = \chi(u + iv),$$

z being the axis of figure, it is necessary to satisfy Laplace's

* Communicated by the Author.

equation, which in such cases takes the form

$$\frac{d}{du} \rho \frac{dV}{du} + \frac{d}{dv} \rho \frac{dV}{dv} = 0,$$

throughout the space between the conductor and the sphere at infinity.

Now in the case of the spheroid we have

$$z = (a + a_1) \cos u,$$

$$\rho = (a - a_1) \sin u,$$

given by $v=0$ in the transformation

$$z + i\rho = ae^{i(u+iv)} + a_1e^{-i(u+iv)},$$

and it results that

$$\frac{1}{\rho} \frac{d\rho}{du} = -\cot u$$

and is independent of v , and

$$\frac{1}{\rho} \frac{d\rho}{dv} = -\frac{ae^{-v} + a_1e^v}{ae^{-v} - a_1e^v}$$

and is independent of u . Solutions of Laplace's equation follow, of the form

$$\phi(u) \psi(v),$$

where $\phi(u) \psi(v)$ satisfy the subsidiary equations

$$(d^2/du^2 - \cot u \, d/du - m) \phi(u) = 0,$$

$$\left(\frac{d^2}{dv^2} - \frac{ae^{-v} + a_1e^v}{ae^{-v} - a_1e^v} \frac{d}{dv} + m \right) \psi(v) = 0.$$

But this method of approach to the problem by means of the separation of variables comes to an abrupt end with the spheroid. In general the surface of revolution is represented by the zero v -level in the transformation *

$$z + i\rho = ae^{i(u+iv)} + a_1e^{i\alpha_1 - i(u+iv)} + a_2e^{i\alpha_2 - 2i(u+iv)} + \dots$$

(with certain restrictions on the parameters (α_n, α_n)), and we therefore have the equation in the form

$$\frac{d^2V}{du^2} + P \frac{dV}{du} + \frac{d^2V}{dv^2} + Q \frac{dV}{dv} = 0,$$

* *Vide* a forthcoming paper by the present writer, "Some Boundary Problems of Mathematical Physics," Proc. London Math. Soc.

where

$$P = \frac{[ae^{-v} \cos u - a_1 e^v \cos(\alpha_1 - u) - 2a_1 \cos(\alpha_2 - 2u) - \dots]}{[ae^{-v} \sin u + a_1 e^v \sin(\alpha_1 - u) + \dots]},$$

$$Q = - \frac{[ae^{-v} \sin u - a_1 e^v \sin(\alpha_1 - u) - 2a_1 \sin(\alpha_2 - 2u) \dots]}{[ae^{-v} \sin u + a_1 e^v \sin(\alpha_1 - u) + \dots]},$$

and the possibility of the separation of variables u and v has obviously entirely disappeared in all the cases beyond the spheroid, where it is not the case that

$$a_2 = a_3 \dots = 0.$$

We therefore have to contemplate in these cases solutions in mixed functions, of type $\phi(u, v)$.

Progress in determining such functions associated with the various solids of revolution, which present themselves in orderly array as different choices of the parameters (a_n, α_n) are made, will evidently be increasingly difficult as the coefficients P and Q become more and more complicated. For this reason we select for consideration on this occasion the surfaces which form the zero v -level in the transformation

$$z + ip = a[e^{i(u+iv)} + ke^{-2i(u+iv)}] \quad 0 \leq k \leq \frac{1}{2}.$$

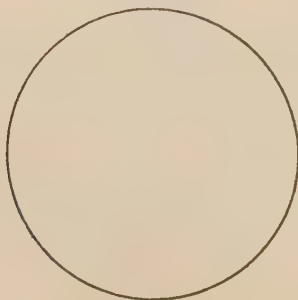
These surfaces have as their generating curves the simple closed nodeless epicycloids of retrograde type,

$$x = a(\cos u + k \cos 2u) \quad 0 \leq k \leq \frac{1}{2}$$

$$y = a(\sin u - k \sin 2u),$$

which range from the circle for $k=0$ to the three-cusped hypocycloid for $k=\frac{1}{2}$, the restriction, $k \leq \frac{1}{2}$, being evidently

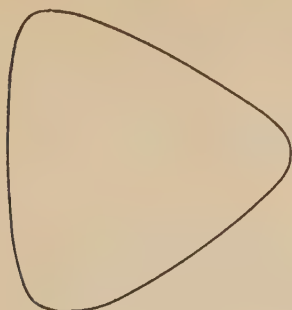
Fig. 1.



$k = 0$

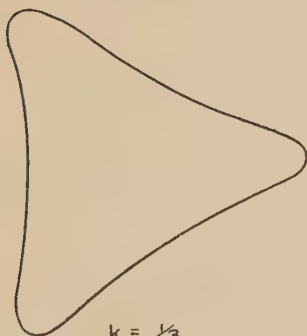
necessary in order that the curves shall not have intersecting branches.

Fig. 2.



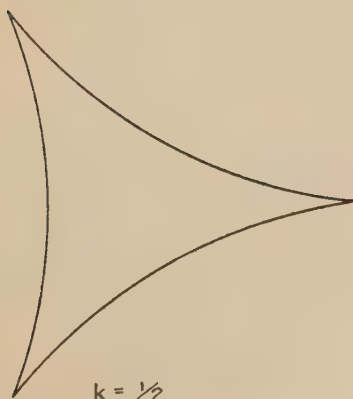
$$k = \frac{1}{5}$$

Fig. 3.



$$k = \frac{1}{3}$$

Fig. 4.



$$k = \frac{1}{2}$$

We are able to obtain an expression for the potential when these conductors are maintained at potential unity in the form

$$V = f_0(u, e^v) + kf_1(u, e^v) + k^2 f_2(u, e^v) + \dots,$$

and as many of the functions f_n as are required can be calculated. The capacity of the conductor can also be obtained in the form

$$C = a({}_1a_0 + {}_1a_2k^2 + {}_1a_4k^4 + \dots).$$

For practical purposes it will, in general, be sufficient to use the approximation given in this paper, namely

$$C = a(1 - \cdot 06857 k^2 - \cdot 00559 k^4),$$

an approximation which is correct to at least 1 in 64, terms in k^6 alone being neglected.

The problem under consideration in this paper is the potential of the solid of revolution given by

$$\begin{aligned} z &= a(\cos u + k \cos 2u) \\ \rho &= a(\sin u - k \sin 2u) \end{aligned} \quad 0 \leq k \leq \frac{1}{2}$$

when it is freely charged to potential unity.

The generating curve is a closed nodeless epicyclic of retrograde type, sometimes also called a hypotrochoid.

Consider the transformation

$$z + i\rho = a(e^{iw} + ke^{-2iw}),$$

with

$$w = u + iv.$$

The surface of the solid is given by $v=0$ and the sphere at infinity by $v=-\infty$. Now the potential V must be equal to unity on $v=0$ and must vanish at $v=-\infty$. Further, for values of v intermediate between zero and $-\infty$, V must be without singularities and satisfy Laplace's equation $\nabla^2 V = 0$. Laplace's equation in the variables z and ρ becomes

$$\frac{d}{du} \rho \frac{dV}{du} + \frac{d}{dv} \rho \frac{dV}{dv} = 0,$$

which may be written

$$\begin{aligned} & (e^{-v} \sin u - ke^{2v} \sin 2u) \left(\frac{d^2 V}{du^2} + \frac{d^2 V}{dv^2} \right) \\ & + (e^{-v} \cos u - 2ke^{2v} \cos 2u) \frac{dV}{du} \\ & - (e^{-v} \sin u + 2ke^{2v} \sin 2u) \frac{dV}{dv} = 0, \end{aligned}$$

or

$$\begin{aligned} & \frac{1}{\sin u} \frac{d}{du} \sin u \frac{dV}{du} + \frac{d^2 V}{dv^2} - \frac{dV}{dv} \\ & = ke^{3v} \left(\frac{1}{\sin u} \frac{d}{du} \sin 2u \frac{dV}{du} + 2 \cos u \right) \left(\frac{d^2 V}{dv^2} + 2 \frac{dV}{dv} \right). \end{aligned}$$

Using the coordinates μ and η given by

$$\mu = \cos u,$$

$$\eta = e^v,$$

as will from time to time be convenient, we have the equation in the form

$$\begin{aligned} & \frac{d}{d\mu} (1 - \mu^2) \frac{dV}{d\mu} + \eta^2 \frac{d^2 V}{d\eta^2} \\ & = k \left(2\eta^3 \frac{d}{d\mu} \mu (1 - \mu^2) \frac{dV}{d\mu} + 2\mu\eta^2 \frac{d}{d\eta} \eta^3 \frac{dV}{d\eta} \right). \end{aligned}$$

In terms of η , the surface of the conductor is given by $\eta=1$ and the sphere at infinity by $\eta=0$.

Introducing operators given by

$$\begin{aligned} D & \equiv \frac{d}{d\mu} (1 - \mu^2) \frac{d}{d\mu} + \eta^2 \frac{d^2}{d\eta^2}, \\ E & \equiv 2\eta^3 \frac{d}{d\mu} \mu (1 - \mu^2) \frac{d}{d\mu} + 2\mu\eta^3 \frac{d}{d\eta} \eta^3 \frac{d}{d\eta}, \end{aligned}$$

the equation for V may be written in the form

$$D \cdot V = kE \cdot V.$$

Now the degenerate case $k=0$ represents the sphere and the equation for V then reduces to

$$D \cdot V = 0.$$

This equation has the solutions

$$\sum_0^{\infty} P_n(\mu)(a_n \eta^{n+1} + b_n \eta^{-n}),$$

and, in particular, solutions evanescent on the sphere at infinity are given by

$$\sum_0^{\infty} a_n P_n(\mu) \eta^{n+1}.$$

Now, in this degenerate case, we have

$$V = P_0 \eta = \eta$$

when the sphere is freely charged to potential unity. The general case under consideration in this paper may evidently therefore be treated by assuming for V the form

$$V = f_0(\mu, \eta) + k f_1(\mu, \eta) + k^2 f_2(\mu, \eta) + \dots$$

with

$$f_0(\mu, \eta) = \eta.$$

By allowing only positive powers of η in the various functions f_n , we at once ensure that V shall be evanescent at infinity.

The form assumed for V will be satisfactory, so far as the satisfying of Laplace's equation is concerned, provided that

$$D \cdot f_{n+1} = E \cdot f_n,$$

and if we are able in addition to select for the functions f_n functions which vanish on $\eta=1$, the conditions of the problem are satisfied, the restriction, to positive powers of η only, having already ensured that V is evanescent at infinity.

We consider first the equation for f_1 , namely

$$D \cdot f_1 = E \cdot f_0 = 6\eta^4 P_1.$$

A particular integral is given by

$$\frac{3}{5} P_1(\mu) \eta^4,$$

and the complementary function—which is evidently shared by all the f_n functions—is

$$\sum a_n P_n(\mu) \eta^{n+1}.$$

Thus a solution which vanishes on $\eta=1$ is obtained in the form

$$f_1(\mu, \eta) = \frac{3}{5} P_1(\mu) (\eta^4 - \eta^2).$$

We therefore have

$$V = \eta + \frac{3}{5} k P_1(\mu) (\eta^4 - \eta^2),$$

terms in k^2 being neglected.

The equation for f_2 in the same way is given by

$$D.f_2 = \frac{3}{5} E(P_1(\eta^4 - \eta^2)),$$

and it will be worth while to consider at once the effect of the operator E on products of P_n functions and powers of η . We have

$$\begin{aligned} E.P_n(\mu)\eta^s &= 2\eta^{s+3} \left\{ \frac{d}{d\mu} \mu(1-\mu^2) \frac{dP_n}{d\mu} + \mu s(s+2)P_n \right\} \\ &= 2\eta^{s+3} \left\{ (1-\mu^2) \frac{dP_n}{d\mu} - \mu n(n+1)P_n + \mu s(s+2)P_n \right\} \\ &= 2\eta^{s+3} \left\{ nP_{n-1} - nP_n - \mu n(n+1)P_n + \mu s(s+2)P_n \right\} \\ &= 2\eta^{s+3} \left\{ nP_{n-1} + (s-n)(s+n+2)\mu P_n \right\} \\ &= 2\eta^{s+3} \left\{ nP_{n-1} + \frac{(s-n)(s+n+2)}{2n+1} [(n+1)P_{n+1} + nP_{n+1}] \right\} \\ &= \frac{2}{2n+1} \eta^{s+3} \left\{ n(s-n+1)(s+n+1)P_{n-1} + (n+1)(s-n)(s+n+2)P_{n+1} \right\} \end{aligned}$$

Now consider the effect of the operator D on a similar product. We have

$$\begin{aligned} D.P_\nu(\mu)\eta^\sigma &= [\sigma(\sigma-1) - \nu(\nu+1)] P_\nu \mu^\sigma \\ &= (\sigma+\nu)(\sigma-\nu-1) P_\nu \mu^\sigma. \end{aligned}$$

Thus if $f_r(\mu, \eta)$ is of the form

$$f_r(\mu, \eta) = \sum b_{n,s} P_n(\mu)\eta^s,$$

it follows that

$$\begin{aligned} D.f_{r+1}(\mu, \eta) &= E.f_r(\mu, \eta) \\ &= \sum \frac{2\eta^{s+3}}{2n+1} b_{n,s} \{ n(s-n+1)(s+n+1)P_{n-1} + (n+1)(s-n)(s+n+2)P_{n+1} \}, \end{aligned}$$

and we have at once a particular integral for f_{r+1} in the form

$$\begin{aligned} \sum \frac{2\eta^{s+3}}{2n+1} b_{n,s} \left\{ \frac{n(s-n+1)(s+n+1)}{(s-n+3)(s+n+2)} P_{n-1} + \frac{(n+1)(s-n)(s+n+2)}{(s-n+1)(s+n+4)} P_{n+1} \right\}. \end{aligned}$$

With the help of the complementary function we then

obtain a solution which vanishes on $\eta=1$ in the form

$$f_{r+1}(\mu, \eta) = \sum \frac{2}{2n+1} b_{n,s} \left\{ \frac{n(s-n+1)(s+n+1)}{(s-n+3)(s+n+2)} (\eta^{s+3} - \eta^n) \right. \\ \left. + \frac{(n+1)(s-n)(s+n+2)}{(s-n+1)(s+n+4)} (\eta^{s+3} - \eta^{n+2}) \right\}.$$

These results make it possible to write down the various functions f_n one at a time. The types of terms which occur in the functions $f_0, f_1 \dots$ are as follows:—

$$f_0(\mu, \eta) = {}_1a_0\eta P_0,$$

$$f_1(\mu, \eta) = P_1({}_4a_1\eta^4 + {}_2a_1\eta^2),$$

$$f_2(\mu, \eta) = P_0({}_7a_2\eta^7 + {}_5a_2\eta^5 + {}_1a_2\eta) + P_2({}_7b_2\eta^7 + {}_5b_2\eta^5 + {}_3b_2\eta^3),$$

$$f_3(\mu, \eta) = P_1({}_{10}a_3\eta^{10} + {}_8a_3\eta^8 + {}_6a_3\eta^6 + {}_4a_3\eta^4 + {}_2a_3\eta^2) \\ + P_3({}_{10}b_3\eta^{10} + {}_8b_3\eta^8 + {}_6b_3\eta^6 + {}_4b_3\eta^4),$$

$$f_4(\mu, \eta) = P_0({}_{13}a_4\eta^{13} + {}_{11}a_4\eta^{11} + {}_9a_4\eta^9 + {}_7a_4\eta^7 + {}_5a_4\eta^5 + {}_1a_4\eta) \\ + P_2(\dots) + P_4(\dots).$$

The surface density of electrification, σ , at any point u on the conductor is given in the form

$$4\pi\sigma = -\frac{\partial V}{\partial v} \bigg/ \left| \frac{ds}{du} \right| = -\eta \frac{\partial V}{\partial \eta} \bigg/ \left| \frac{ds}{du} \right|,$$

where ds is the element of arc of the generating curve, so that

$$(ds/du)^2 = a^2 \{ \sin u + 2k \sin 2u \}^2 + (\cos u - 2k \cos 2u)^2 \\ = a^2 (1 - 4k \cos 3u + 4k^2).$$

Thus

$$4\pi\sigma = - \left\{ \eta \frac{\partial}{\partial \eta} (f_0(\mu, \eta) + kf_1(\mu, \eta) + \dots) \right\}_{\eta=1} \bigg/ \left| \frac{ds}{du} \right|,$$

where $\cos u = \mu$.

To find the capacity of the conductor we have to obtain the total charge E on the conductor. Now as $r \rightarrow \infty$, $V \rightarrow E/r$. But

$$r^2 = \frac{a^2}{\eta^2} + a^2 \eta k \cos 3u + \frac{1}{4}a^2\eta^4,$$

so that

$$r = \frac{a}{\eta} + \text{terms in } \eta, \eta^2 \dots$$

Thus

$$E/a = \lim_{\eta \rightarrow 0} V/\eta \\ = {}_1a_0 + {}_1a_2k^2 + {}_1a_4k^4 + \dots$$

Since the conductor is maintained at unit potential the capacity is given by E itself, so that

$$C = a\{ {}_1a_0 + {}_1a_2k^2 + {}_1a_4k^4 + {}_1a_6k^6 + \dots \}.$$

Since k ranges between unity and one-half, it will be sufficient for practical purposes to use the approximation

$$C = a({}_1a_0 + {}_1a_2k^2 + {}_1a_4k^4),$$

which neglects terms in k^6 and so gives an accuracy of at least 1 in 64. In the case of curves of cross-section which approximate more nearly to the sphere, the accuracy of this approximation will be considerably greater.

To find the coefficients necessary for this evaluation we proceed as follows. We already have

$${}_1a_0 = 1, \quad {}_4a_1 = \frac{3}{5}, \quad {}_2a_1 = -\frac{3}{5}.$$

Then in view of the derivation of terms in each f_n function from terms given in the preceding function f_{n-1} , we have the following relations:—

$$\text{I. } {}_{13}a_4 = \frac{1}{13} \cdot \frac{2}{3} \cdot {}_{10}a_3,$$

$${}_{11}a_4 = \frac{8}{11} \cdot \frac{2}{3} \cdot {}_8a_3,$$

$${}_9a_4 = \frac{6}{9} \cdot \frac{2}{3} \cdot {}_6a_3,$$

$${}_7a_4 = \frac{4}{7} \cdot \frac{2}{3} \cdot {}_4a_3,$$

$${}_5a_4 = \frac{2}{5} \cdot \frac{2}{3} \cdot {}_2a_3,$$

$$-{}_1a_4 = {}_{13}a_4 + {}_{11}a_4 + {}_9a_4 + {}_7a_4 + {}_5a_4.$$

$$\text{II. } {}_{10}a_3 = \frac{7}{8} \cdot \frac{9}{11} \cdot \frac{2}{1} \cdot {}_7a_2 + \frac{6}{8} \cdot \frac{1}{11} \cdot \frac{4}{5} \cdot {}_7b_2,$$

$${}_8a_3 = \frac{5}{6} \cdot \frac{7}{9} \cdot \frac{2}{1} \cdot {}_5a_2 + \frac{4}{6} \cdot \frac{8}{9} \cdot \frac{4}{5} \cdot {}_5b_2,$$

$${}_6a_3 = \frac{2}{4} \cdot \frac{6}{7} \cdot \frac{4}{5} \cdot {}_3b_2,$$

$${}_4a_3 = \frac{1}{2} \cdot \frac{3}{5} \cdot \frac{2}{1} \cdot {}_1a_2,$$

$$-{}_2a_3 = {}_{10}a_3 + {}_8a_3 + {}_6a_3 + {}_4a_3.$$

$$\text{III. } {}_7a_2 = \frac{4}{7} \cdot \frac{2}{3} \cdot {}_4a_1,$$

$${}_5a_2 = \frac{2}{5} \cdot \frac{2}{3} \cdot {}_2a_1,$$

$$-{}_1a_2 = {}_7a_2 + {}_5a_2,$$

$${}_7b_2 = \frac{3}{4} \cdot \frac{7}{9} \cdot \frac{4}{5} \cdot {}_4a_1,$$

$${}_5b_2 = \frac{1}{2} \cdot \frac{5}{7} \cdot \frac{4}{5} \cdot {}_2a_1,$$

$$-{}_3b_2 = {}_7b_2 + {}_5b_2.$$

Then after reduction we obtain the results

$${}_1a_2 = -12/175 = -\cdot 06857,$$

$${}_1a_{4/4}a_1 = -(16 \times 563320) / (25 \times 35^2 \times 9 \times 13 \times 27) \\ = -\cdot 09316 ;$$

$$\therefore {}_1a_4 = -\cdot 00559.$$

Thus

$$C = a(1 - \cdot 06857 k^2 - \cdot 00559 k^4),$$

terms in k^6 being neglected.

It is further possible to solve the problem of these conductors in a uniform field of force, or any other electric field, by application of the type of analysis which has been developed in this paper.

Summary.

The problem associated with a conducting solid of revolution when it is freely charged with electricity, which have at present been solved only for the spheroid and a few isolated cases, are discussed in this paper for solids whose generating curves are certain closed nodeless epicycloids of retrograde type with equation

$$z = a(\cos u + k \cos 2u) \\ \rho = a(\sin u - k \sin 2u), \quad 0 \leq k \leq \frac{1}{2}$$

which range from the circle, for $k=0$, to the three-cusped hypocycloid, for $k=\frac{1}{2}$. The potential when such a solid is freely charged is expressed in *mixed* functions in the form

$$V = f_0(u, e^v) + k f_1(u, e^v) + k^2 f_2(u, e^v) \dots,$$

the coordinates u and v being specified by the transformation

$$z + i\rho = a(e^{iw} + k e^{-2iw})$$

with

$$w = u + iv,$$

and the capacity of the conductor results in the form

$$C = a\{{}_1a_0 + {}_1a_2 k^2 + {}_1a_4 k^4 + \dots\}.$$

The approximation given in this paper, viz.

$$C = a\{1 - \cdot 06857 k^2 - \cdot 00559 k^4\},$$

is correct to at least 1 in 64.

V. *On Transient Electric Phenomena in a Non-Inductive Circuit.* By J. A. WILCKEN, B.Sc., Ph.D., Lecturer in Electrical Engineering at Armstrong College, Newcastle-upon-Tyne*.

IT is known that the discussion of the electric phenomena in a so-called non-inductive circuit, containing capacity and resistance only, with rigorous exclusion of inductance, leads to the inconsistency of an instantaneous rise of current, from zero to a finite value, on closing the switch†, and it would thus appear that the observed transients can only be accounted for by the presence of a certain amount of inductance which, however small, appreciably affects the current and voltage for a very short time after closing or opening the circuit, though without any measurable influence under steady conditions, such as obtain in a system supplied with continuous current. Obviously, the influence of even a very small inductance becomes farther enhanced in the case of alternating currents, through the frequency-factor.

Mathematically, the problem turns on the integration of the differential equation

$$e = L \frac{di}{dt} + ri + \frac{1}{C} \int i dt \quad . \quad . \quad . \quad (1)$$

in the case of L being small. For the sake of physical interpretation, however, the magnitude of L must be compared with other quantities of the same dimensions. In the usual notation, we have,

L , inductance	—	dimension	$[l]$
r , resistance	—	„	$[lt^{-1}]$
C , capacity	—	„	$[l^{-1}t^2]$,

and the smallness of the inductance may thus be adequately expressed in terms of the numerical fraction L/r^2C .

We consider first the case of a constant impressed electromotive force e , $de/dt=0$, and derive the equation

$$L \frac{d^2i}{dt^2} + r \frac{di}{dt} + i/C = 0, \quad . \quad . \quad . \quad (2)$$

* Communicated by the Author.

† Steinmetz, 'Transient Electric Phenomena,' p. 55, McGraw-Hill, 1920.

the general solution of which can be written in the usual exponential form,

$$i = A\epsilon^{a_1 t} + B\epsilon^{a_2 t}, \quad . \quad . \quad . \quad . \quad . \quad (3)$$

α_1 and α_2 being the roots of the quadratic

$$L\alpha^2 + r\alpha + 1/C = 0. \quad . \quad . \quad . \quad . \quad (4)$$

The potential difference at the condenser terminals is now obtained from (1),

$$e_1 = e - ri - L \frac{di}{dt}, \quad . \quad . \quad . \quad . \quad (5)$$

and the initial conditions,

$$\left. \begin{aligned} i|_{t=0} &= i_0, \\ e_1|_{t=0} &= e_0, \end{aligned} \right\} . \quad . \quad . \quad . \quad . \quad (6)$$

determine the constants of integration,

$$\left. \begin{aligned} A &= \{e - e_0 - (r + \alpha_2 L)i_0\} / (\alpha_1 - \alpha_2)L, \\ B &= -\{e - e_0 - (r + \alpha_1 L)i_0\} / (\alpha_1 - \alpha_2)L. \end{aligned} \right\} . \quad . \quad (7)$$

As the fraction L/r^2C decreases indefinitely, the root

$$\alpha_1 = (-r + \sqrt{r^2 - 4L/C})/2L$$

assumes the indeterminate form $0/0$, and the general solution ceases to have any meaning. Steinmetz gives special attention to this case (*l. c.*), but, through a somewhat careless omission of small quantities, arrives at an expression,

$$i = (1/r) \{ (e - e_0)\epsilon^{-t/rC} - (e - e_0 - ri_0)\epsilon^{-rt/L} \}, \quad . \quad (8)$$

which, on substitution in the left-hand side of equation (2), gives

$$\{ (L/r^2C)(e - e_0)\epsilon^{-t/rC} - (e - e_0 - ri_0)\epsilon^{-rt/L} \} / rC,$$

a quantity which is not negligible for all values of t unless both L/r^2C and $e - e_0 - ri_0$ are very small. The deductions obtained are therefore not to be trusted without a more careful scrutiny, and in this investigation a slightly different method has been adopted, leading to conclusions at variance with Steinmetz's results, especially for very small time-intervals.

When L/r^2C is a small number, squares of which may be neglected, the finite root of equation (4) is approached by taking

$$\alpha = -1/rC,$$

a farther approximation being

$$\alpha = -1/rC - L/r^3C^2 \text{ etc.}$$

We confine the discussion to the first approximation, and take

$$i = u \in {}^{\text{at}}$$

u being a function of t subject to

$$L \frac{d^2 u}{dt^2} + (r + 2\alpha I_1) \frac{du}{dt} = 0;$$

$$\therefore u = A e^{(-r/L - 2\alpha)t} + B, \quad (9)$$

and so, $i = A e^{(1/rC - r/L)t} + B e^{-t/rC}, \dots \dots \dots (10)$

$$e_1 = e - (L/rC) A e^{(1/rC - r/L)t} - (r - L/rC) B e^{-t/rC}. \quad (11)$$

Writing $\eta = L/r^2C$, the boundary conditions (6) give,

$$\begin{aligned} A &= \{-(e-e_0)/r + (1-\eta)i_0\}/(1-2\eta), \\ B &= \{(e-e_0)/r - \eta i_0\}/(1-2\eta), \end{aligned} \quad (12)$$

and thus finally, neglecting higher powers of η ,

$$i = \{ (1 + \eta) i_0 - (1 + 2\eta) (e - e_0) / r \} \epsilon^{(1 - 1/\eta)t/rC} - \{ \eta i_0 - (1 + 2\eta) (e - e_0) / r \} \epsilon^{-t/rC}, \quad (13)$$

$$e_1 = e(1 - \epsilon^{-t/rC}) + \eta(e - e_0 - ri_0)(\epsilon^{(1-1/\eta)t/rC} - \epsilon^{-t/rC}). \quad (14)$$

If the circuit is initially dead, $i_0=0$, $e_0=0$, the values become

$$\dot{i} = (1 + 2\eta)(e/r)(\epsilon^{-t/rC} - \epsilon^{(1-1/\eta)t/rC}), \quad . \quad . \quad (15)$$

$$e_1 = e(1 - \epsilon^{-t/rC}) + \eta e(\epsilon^{(1-1/\eta)t/rC} - \epsilon^{-t/rC}). \quad (16)$$

For comparison, the curves representing the growth of current and potential on charging a condenser to 1000 volts are shown in figs. 1 and 2, for an initially dead circuit with the constants $r=200$ ohms, $C=10^{-5}$ farad, and $L=4 \times 10^{-3}$ henry, giving $\eta=0.01$.

Our equations (15) and (16) become

$$i = 5.1 (\epsilon^{-500t} - \epsilon^{-49500t}), \quad . \quad . \quad . \quad (17)$$

$$e_1 = 1000(1 - e^{-500t}) - 10i/5.1, \dots \quad (18)$$

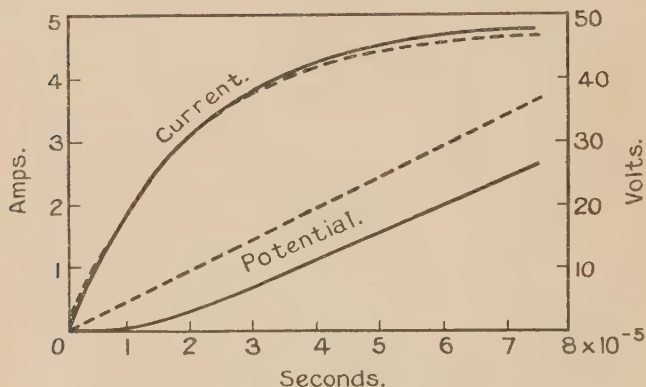
whereas Steinmetz's formulæ would give

$$\dot{i} = 5(\epsilon^{-500t} - \epsilon^{-50000t}), \quad . \quad . \quad . \quad . \quad . \quad (19)$$

$$e_1 = 1000(1 - e^{-500t}). \quad . \quad . \quad . \quad . \quad . \quad (20)$$

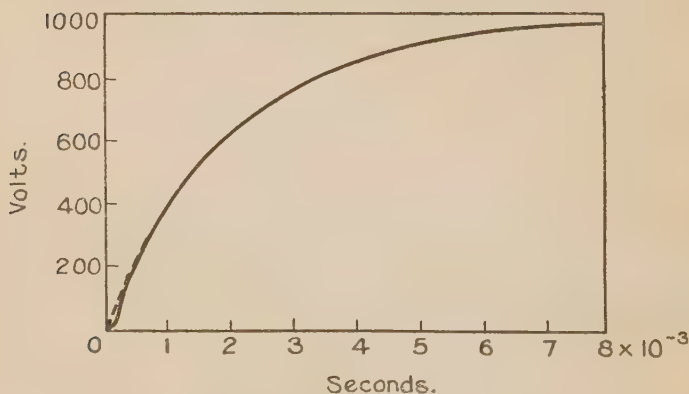
Dotted lines represent the results obtained from equations (19) and (20), while full lines connect values deduced from (17) and (18). A portion of the potential curves is also shown in fig. 1 in order to bring out more clearly the different character of the two results during the first five hundred-thousandths of a second.

Fig. 1.



The growth of current and potential in a non-inductive circuit.

Fig. 2.



The growth of potential in a non-inductive circuit.

It is seen from these diagrams that, as far as the current-values are concerned, the more accurate formula (17) gives somewhat higher values—about 2 per cent.—than (19) except at the very beginning. The current rises rapidly, attaining to 90 per cent. of its final value within five hundred-thousandths of a second.

According to Steinmetz, the growth of potential is nearly linear for the first two-hundred thousandths of a second, but the more accurate formula (18) shows an entirely different mode of building up, the rise being very slow at first and then gradually increasing to a nearly constant slope from about the third hundred-thousandth of a second. The later portions of the two curves are nearly identical and in both cases the potential reaches 90 per cent. of its final value within five thousandths of a second.

The more gradual rise in potential is worth noting, for various reasons. Theoretically, it is interesting to observe the continuity not only of e itself, but also of its gradient de/dt , at the transition point $t=0$. Practically, the results are important in connexion with the effect of a unidirectional surge, on an overhead transmission line, caused by a lightning discharge suddenly raising the potential at one point of the line and giving rise to a single pulse of high voltage. The first portion of our potential curve in fig. 1 shows that the wave-front of such an impulse is gradually rising and so arrives without shock, whereas Steinmetz's result implies an abrupt rise of the wave-front, a condition which evidently increases the danger considerably.

VI. *Reverberation Equations for Two Adjacent Rooms connected by an Incompletely Soundproof Partition.* By A. H. DAVIS, D.Sc. (*From the National Physical Laboratory**)

THE subject of this paper is closely related to a method of measuring the transmission of sound through a partition of a given material. In such a test the partition is built between two otherwise soundproof chambers. In one of the rooms, which is large and reverberant, an organ-pipe is sounded and after a time is suddenly stopped. Note is made of the length of time for which the residual sound is audible both in the source room and in that separated from it by the test partition.

W. C. Sabine † and P. E. Sabine ‡ working on these lines have determined the difference in intensity in two such rooms when different thicknesses of various partitions were used. The present paper, on the basis of a reverberation hypothesis, investigates the manner in which the general

* Communicated by the Author.

† W. C. Sabine, 'Collected Papers,' p. 237 (1922).

‡ P. E. Sabine, *Phys. Rev.* xxi. p. 480 (1923). 'Am. Architect,' July 28, 1920; Sept. 23, 1921; July 4, 1923.

duration of audibility in the two rooms in such a test may depend upon the circumstances of the experiment and the transmission factor for the partition.

The decay of sound in a single room has been considered by W. C. Sabine* and by Jäger†. More recently Eckhardt‡ has published a treatment due to Buckingham. In all cases it is recognized that a sound suffers some two or three hundred reflexions before it finally dies away, and in consequence, by random arrangement, the sound energy rapidly becomes uniformly distributed throughout the enclosure. Interference phenomena are ignored, and so results are valid only to the extent to which this is justifiable.

Buckingham assumes that the sound energy is divided up into a large number of equal parts, and that in the steady state these energy units are uniformly distributed throughout the room, both with regard to position and direction of motion. Each is assumed to move with the velocity v of sound. He shows that if the intensity of sound in the room be I (*i.e.* I energy units per unit volume) the number reaching any element of boundary surface dS in unit time is $\frac{1}{4}v.dS.I$. Of this energy a fraction will be absorbed or transmitted and the remainder reflected back into the room.

Using this result, we may readily derive differential equations governing the general intensity of sound in two adjacent rooms connected by an imperfectly soundproof partition when a source is sounded in one of them.

Let W represent the area of the test partition; k the (unknown) fraction of incident energy which is transmitted through the partition on incidence; V, V_1 the volumes of the source and test rooms respectively; S, S_1 the respective total areas of exposed surface (including the partition area); a, a_1 the mean § fractions of incident energy which are lost by the room at each reflexion through absorption or through transmission elsewhere; E the energy emission from the source in unit time.

Then, on the basis of the above reverberation theory,

* W. C. Sabine, 'Collected Papers,' p. 3 (1922).

† Jäger, *Akad. Wiss. Wien, Ber.* 120. p. 613 (1911). See 'Science Abstracts,' p. 17 (1912).

‡ Eckhardt, *Frank. Inst. J.* 195. p. 799 (1923).

§ If in the room there are surfaces S', S'', S''' etc. having respectively coefficients a', a'', a''' etc., then $aS = a'S' + a''S'' + a'''S''' + \dots$ We may note here that for highly absorbent surfaces or highly transmissive openings, with dimensions which are small compared with the wavelength of the sound, effective areas may differ somewhat from actual values owing to diffraction effects (*cf.* P. E. Sabine, *Phys. Rev.* xix. p. 402, 1922).

if the intensities in the two rooms be I and I_1 respectively, the diminution of energy in the source room due to its total surface S is $\frac{1}{4}vaSI$ units per second; the energy received in the second room in unit time by transmission through the partition area W is $\frac{1}{4}vkWI$; the energy transmitted back to the source room from the second room in unit time is $\frac{1}{4}vkWI_1$; the rate of diminution of energy in the second room is $\frac{1}{4}va_1S_1I_1$. Consequently, the following differential equations represent the energy growth in the rooms at any instant.

$$\text{Source Room} \quad V \frac{dI}{dt} + \frac{vaS}{4} I = E + \frac{vkW}{4} I_1, \quad . \quad . \quad . \quad (1)$$

$$\text{Second Room} \quad V_1 \frac{dI_1}{dt} + \frac{va_1S_1}{4} I_1 = \frac{vkW}{4} I. \quad . \quad . \quad . \quad (2)$$

Condition attained in steady state under constant emission E .

From the above equations we find that when the conditions become steady (i. e., $dI/dt = 0 = dI_1/dt$) the intensities have maximum values given by

$$I_{\max.} = \frac{4E}{vaS \left(1 - \frac{k^2 W^2}{aSa_1S_1} \right)}, \quad . \quad . \quad . \quad (3)$$

$$I_{1\max.} = I_{\max.} \left(\frac{kW}{a_1S_1} \right). \quad . \quad . \quad . \quad (4)$$

Emission stopped after steady state has been reached.

If through prolonged use of the source E the intensity has reached the steady values given in (3) and (4), and if the source is then suddenly stopped, the subsequent decay of sound (with $E=0$) is given by the following solutions of the differential equations (1) and (2), viz. :—

$$I = I_{\max.} \left\{ \frac{1 - \frac{4V_1\lambda_1}{va_1S_1}}{1 - \frac{\lambda_1}{\lambda_2}} e^{-\lambda_1 t} + \frac{1 - \frac{4V_1\lambda_2}{va_1S_1}}{1 - \frac{\lambda_2}{\lambda_1}} e^{-\lambda_2 t} \right\}, \quad . \quad (5)^*$$

$$I_1 = I_{1\max.} \left\{ \frac{1}{1 - \frac{\lambda_1}{\lambda_2}} e^{-\lambda_1 t} - \frac{1}{\frac{\lambda_2}{\lambda_1} - 1} e^{-\lambda_2 t} \right\}, \quad . \quad . \quad (6)$$

* If (5) and (6) be written $I = AI_{\max.}$ and $I_1 = A_1 I_{1\max.}$ respectively, then the solution of equations (1) and (2) corresponding to uniform sound emission beginning at zero time is

$$I = I_{\max.} (1 - A) \text{ and } I_1 = I_{1\max.} (1 - A_1).$$

78 Dr. Davis on *Reverberation Equations for Two Adjacent*
 where

$$\lambda_1 = \frac{v}{8} \left(\frac{aS}{V} + \frac{a_1S_1}{V_1} \right) - \frac{v}{8} \sqrt{\left(\frac{a_1S_1}{V_1} - \frac{aS}{V} \right)^2 + \frac{4k^2W^2}{VV_1}}, \quad (7)$$

$$\lambda_2 = \frac{v}{8} \left(\frac{aS}{V} + \frac{a_1S_1}{V_1} \right) + \frac{v}{8} \sqrt{\left(\frac{a_1S_1}{V_1} - \frac{aS}{V} \right)^2 + \frac{4k^2W^2}{VV_1}}. \quad (8)$$

These expressions give the general conditions under which reverberant sound dies away in the two rooms when the source is stopped. It remains to ascertain the conditions to be fulfilled in the design of the chambers in order that simpler relations may be obtained.

Conditions for Simpler Formulæ.

(i.) The expressions (7) and (8) defining λ_1 and λ_2 are much simplified if k^2W^2/VV_1 be small compared with $(aS/V - a_1S_1/V_1)^2$.

Since, as we shall see later, V should be larger than V_1 , and a_1S_1/V_1 should be several times as great as aS/V , the above condition would be satisfied if, in addition, kW were sufficiently small compared with a_1S_1 .

With the condition fulfilled we have the great simplification

$$\lambda_1 = \frac{vaS}{4V}, \quad . \quad . \quad . \quad . \quad . \quad . \quad (9)$$

$$\lambda_2 = \frac{va_1S_1}{4V_1}, \quad . \quad . \quad . \quad . \quad . \quad . \quad (10)$$

and equation (5) reduces to $I = I_{\max} e^{-\lambda_1 t}$.

(ii.) Within the brackets of (6) the term remaining in $e^{-\lambda_2 t}$ rapidly becomes negligible compared with that in $e^{-\lambda_1 t}$ provided λ_2 be several times as great as λ_1 , *i.e.* if the absorbing power per unit volume for the second chamber (a_1S_1/V_1) be sufficiently great compared with that (aS/V) for the source room. Even a moderate ratio of say 2 or 3 may be sufficient in suitable cases. To this end the second room should be smaller than the first (since area per unit volume is greater for small rooms) and its surface should be more absorbent.

Possibly it is unnecessary to simplify further, but if λ_2 be as much as fifty times as great as λ_1 , then the coefficient of $e^{-\lambda_1 t}$ within the brackets of (6) differs from unity by only 2 per cent., an amount which would not be perceptible in ordinary reverberation work. The higher absorptive power necessary for this would be advantageous in damping any tendency for the room to act as a resonator.

Simplified Formulæ.

With all the conditions fulfilled, the residual intensities in the rooms rapidly attain the values

$$I = I_{\max.} e^{-vaSt/4V}, \quad . \quad . \quad . \quad . \quad . \quad (11)$$

$$I_1 = I_{1\max.} e^{-vaSt/4V}, \quad . \quad . \quad . \quad . \quad . \quad (12)$$

where

$$\frac{I_{\max.}}{I_{1\max.}} = \frac{a_1 S_1}{k W}. \quad . \quad . \quad . \quad . \quad . \quad (13)$$

The quantity $(I_{\max.}/I_{1\max.})$ may be called the reduction factor for the partition, under the conditions considered.

If now T and T_1 be respectively the times which elapse in the two rooms before the reverberant sound dies away from its initial maximum value to the threshold of audibility, we have

$$I_{\max.} e^{-vaST/4V} = I_{\min. \text{ aud.}} = I_{1\max.} e^{-vaST_1/4V}, \quad . \quad . \quad (14)$$

whence

$$\log \left(\frac{a_1 S_1}{k W} \right) = \frac{vaS}{4V} (T - T_1), \quad . \quad . \quad . \quad (15)$$

a simple equation involving k .

The factor $\frac{vaS}{4V}$ determining the rate of decay of the sound can be obtained from a preliminary calibration of the room. For this the duration of reverberation would be determined first with a source of intensity E , and then with another of intensity nE : the difference in duration is the time taken for n -fold decay of sound in the room, and is a measure of $vaS/4V$.

The simplified formulæ given above will not generally apply to the case (presumably $k=1$) of an uncovered aperture, owing to conditions which have been introduced in the analysis. However, on extrapolating a curve of experimental results to which the formulæ apply—say, for a series of diminishing thicknesses of porous non-resonant material—it is towards the value $a_1 S_1/W_1$ that the reduction factor tends as the condition of an uncovered aperture is approached, and not towards unity as might be conjectured at first glance. It is interesting, therefore, that P. E. Sabine*, working with various musical notes, found a reduction factor of about $2\frac{1}{2}$ to be indicated on an average for zero thickness of felt. While he suggests that this result may be due to surface phenomena in transmission by

* P. E. Sabine, 'Am. Architect,' Sept. 28, 1921.

felt, the above analysis indicates that, apart from such a cause, factors greater than unity may arise from the circumstances of the experiment.

Audibility at special points in the second room.

In some conditions the above equations for reverberant sound may not represent the sound actually heard at a given point in the second room. For instance, if the room were very large and completely absorbent, there would be no general reverberation within it, but an ear situated close to the partition would detect transmitted sound. An estimate may be made of the intensity in this case. According to the above considerations, the energy transmitted in unit time through unit area of the partition would be $\frac{1}{4}kvI$, which, in a simple progressive wave, corresponds to an intensity of $\frac{1}{4}kI$ energy units per unit volume. With the sound in the source room decaying exponentially according to equation (11), the intensity of the entrant sound just near the partition would be

$$I_e = \frac{1}{4}kI_{\max.} e^{-vaSt/4V}, \dots \dots \dots (16)$$

a quantity which differs from the reverberant sound of equation (12) in the ratio $\frac{1}{4} : W/a_1S_1$.

Consequently, in some circumstances, it may depend upon the position of the hearer whether (12) or (16) more nearly represents the audibility observed in the second room. However, if the chamber be suitably designed, both entrant and reverberant sound should die away at the same rate as that in the source room, and reduction factors obtained should bear a simple relation to k . The actual relation in a given case should be the subject of experiment.

Summary.

The subject of the paper is related to a method of measuring the transmission of sound through partitions. Equations have been derived for the decay of reverberant sound in each of two chambers connected by an incompletely soundproof partition, when a source in one of the chambers is suddenly stopped. While in general the relations are complicated, they are considerably simplified if the receiving chamber has adequate absorbing power compared with the transmitting power of the partition, and if it is sufficiently less reverberant than the source room.

March 1925.

VII. *The Theory of the "Schrot-effect."*By NORMAN CAMPBELL, *Sc.D.**

SUMMARY.—Attention is drawn to a general proposition relating the fluctuations in any fortuitous phenomenon and those in an instrument by which it is observed. Use of it would avoid the elaborate calculations upon which the study of the schrot effect has been based hitherto, and enable the observations to be interpreted much more directly in terms of measurements.

The results obtained by Hull and Williams with secondary emission are discussed; it is shown that conclusions other than those that they draw are not excluded.

1. **I**N the course of a study of the discontinuity of photoelectric emission †, a general proposition was established which is valid in the study of discontinuous processes of any other kind, and, in particular, in the study of Schottky's ‡ "schrot" effect, or the discontinuity of thermionic emission. It was shown that if $\overline{x^2}$ is the mean square deviation from the average of the number of events occurring in unit time; if

$$\theta = f(t) \quad . \quad . \quad . \quad . \quad . \quad . \quad (1)$$

gives the reading of an indicating instrument at time t after the occurrence of one of these events at $t=0$, this event being followed by no others; and if $\overline{\theta^2}$ is the mean square deviation of θ from its mean, when the events are occurring in their normal fortuitous succession, then

$$\overline{\theta^2} = \overline{x^2} \int_0^\infty f^2(t) dt. \quad . \quad . \quad . \quad . \quad . \quad (2)$$

The only limitations imposed upon the function f are that $f(\infty)$ should be zero, and that the effects of successive events on the instrument should be strictly additive.

Fürth § has, in effect, used this proposition to calculate the schrot effect, when the observing instrument is assumed to be an ideal damped harmonic oscillator attached to

* Communicated by the Author.

† N. R. Campbell, *Proc. Camb. Phil. Soc.* xv. pp. 117, 310, 513 (1909-1910).

‡ W. Schottky, *Ann. d. Phys.* lvii. p. 541 (1918).

§ R. Fürth, *Phys. Zeit.* xxiii. p. 354 (1922).

amplifiers giving the same amplification for all kinds of disturbances. He attempted no formal proof of it; and Fry *, in his discussion of all attempts to calculate the schrot effect, dismisses it summarily as based on a mere analogy. I would urge, on the contrary, that it is the only formula yet offered which is based by unexceptionable logic on physical assumptions that can be disentangled from the argument and discussed separately.

The most important of these assumptions is that the effects of isolated electrons on the observing system are strictly additive, even when their passages through it are separated by intervals comparable with its period. Fry insists on the importance of this assumption, and, indeed, it is almost obvious that no observing instrument can measure truly the schrot effect, which depends on the isolation of the electrons, unless it is true. And yet it might well be doubted; it might be thought, for example, that when a single isolated electron passed through a system, there could be no quantity such as self-induction †. Schottky's treatment of the problem by means of Fourier analysis conceals the assumption; it is very difficult to discover at what point of the argument it is introduced. It may be urged, therefore, that the only evidence in favour of the result that Schottky reached by exceedingly involved analysis is that it is the same as that reached by Fürth, on the basis of (2), by the simplest algebra.

2. Hull and Williams ‡ object to Fürth's formula that it does not cover the case of their apparatus, because they find that the amplification is not entirely independent of the frequency of a harmonic disturbance. Their contention is, of course, true; but their method of avoiding the difficulty is open to grave objection. They revert to Schottky's Fourier analysis, but introduce an empirically determined amplification factor, varying with the frequency of the components. It is never satisfactory to introduce an empirical correction into a theory which does not show explicitly the need for it; there is always the danger of assuming in the theory propositions which are effectively denied in making the correction. This danger is present here. The variation of the amplification factor may well be due to a variation of the inductances and capacities with the frequency. But if the inductances and capacities in the amplifiers vary with the frequency, is it certain that those in the oscillating circuit, excited by the

* T. C. Fry, Journ. Frank. Inst. cxcix. p. 203 (1925).

† Cf. N. R. Campbell, 'Modern Electrical Theory,' 2nd ed. p. 129.

‡ A. W. Hull and N. H. Williams, Phys. Rev. xxv. p. 148 (1925).

thermionic discontinuities, are independent of the frequency, as the theory assumes? There is no doubt that their formula is very nearly right; the correction is small, and it must be in the right direction. But when they claim that their method might give a value for the electronic charge more accurate than that obtainable by any other method, they appear to forget that their greater experimental accuracy is set off by greater theoretical uncertainty.

It may be worth while, therefore, to point out that all this difficult and obscure calculation could be avoided, ideally if not actually, by a direct experimental determination of $\int_0^\infty j'^2(t)$ in (2). For this purpose, a known charge Q_1 , so small that it lies within the additive range, is passed from cathode to anode of the thermionic tube in a time short compared with the period of the oscillating circuit; the total charge Q_2 passing through the rectifier in consequence is measured. If the rectifier obeys accurately the "square law,"

$$Q_2 = \int_0^\infty I dt = \int_0^\infty \alpha V^2 dt, \quad (3)$$

where I is the current through the rectifier associated with a voltage V across its terminals. Q_2 should be proportional to Q_1^2 ; if it proves to be so, and if we identify θ in (2) with V , we shall have

$$\bar{V}^2 = \bar{x}^2 \cdot \frac{\epsilon^2}{Q_1^2} \int_0^\infty V^2 dt. \quad (4)$$

But

$$x^2 = i_0 / \epsilon, \quad (5)$$

where i_0 is the mean thermionic current. Hence, if \bar{I} is the mean current through the rectifier,

$$I = \alpha \bar{V}^2 = \frac{i_0}{\epsilon} \cdot \frac{\epsilon^2}{Q_1^2} \cdot Q_2, \quad (6)$$

or

$$\epsilon = \frac{\bar{I}}{i_0} \cdot \frac{Q_1^2}{Q_2}. \quad (7)$$

If, as in Hull and Williams's experiments, the frequency of the oscillating circuit is of the order of one million, there would be great difficulty in securing the passage of Q_1 in a time short compared with the period; but if low-frequency circuits were used, there would be no difficulty. The problem

of determining \bar{I} can then be solved simply enough by taking a sufficient number of readings, if necessary by a recording instrument, and averaging them arithmetically.

3. However, the experiment would hardly be worth the labour expended on it. It is unlikely that the accuracy of Millikan's determination of ϵ could be approached; and, on the other hand, the work of Hull and Williams and others has established that the quantities observed are measures of the thermionic fluctuations, although the unit of measurement may be slightly uncertain. The value of such experiments will probably lie now in comparative, and not absolute, measures of the schrot effect, such as those already made on the effect of the space-charge and of secondary emission.

But it may not always be easy to interpret the results. Thus Hull and Williams, having shown that the fluctuations from their insulated plate are the sum of those due to the primary and secondary electrons, conclude that the emission of the secondaries is entirely "independent" of the primaries. By this they seem to mean that the emission of a secondary must be entirely uncorrelated with that of the primary, and may occur at any instant after the incidence of the primary. But that conclusion is not really established so far by their experiments. There might be fluctuations even if the emission of the secondary was simultaneous with the incidence of the primary or always followed it at an interval short compared with the period of the oscillating circuit. For it is consonant with what is known of secondary emission to suppose that the number of secondaries emitted by the incidence of a single primary varies about a mean; the fluctuations of this number would produce a schrot effect.

The problem is very similar to one discussed in connexion with photoelectric emission*. Let the mean number of secondaries emitted by one primary be ω , and let η represent the variations of the number about this mean. Then if N is the mean number of primaries striking the plate per unit time, and ξ the variation of this number from the mean during a very short time τ , then the gain of electrons by the plate during τ is

$$(N\tau + \xi) - (N\tau + \xi)(\omega + \eta), \quad . \quad . \quad . \quad (8)$$

and the value of $\overline{x^2}$ in (2) is given by

$$\overline{x^2} = N\{(1 - \omega)^2 + \eta^2\}. \quad . \quad . \quad . \quad . \quad (9)$$

* Campbell, *loc. cit.* p. 314.

Here it is assumed that the emission of the secondaries is simultaneous with the incidence of the primary ; if emission and incidence are independent in Hull and Williams's sense, then in place of (8) we have

$$(N\tau + \xi_1) - (N\tau + \xi_2)(\omega + \eta), \quad . \quad . \quad . \quad (10)$$

ξ_1 and ξ_2 being independent with the same mean values, and in place of (9)

$$\overline{x^2} = N\{1 + \omega^2 + \overline{\eta^2}\}. \quad . \quad . \quad . \quad (11)$$

In this calculation it is assumed that, within any interval τ , however short, a primary is as likely to be incident at any one instant as at any other. If the fluctuations of the primaries are partly suppressed by a space-charge, and electrons tend to follow each other at regular intervals, the argument breaks down. At the other extreme, when the intervals are perfectly regular, it is easy to show that in place of (9) we have

$$\overline{x^2} = N\overline{\eta^2}, \quad . \quad . \quad . \quad . \quad (12)$$

and in place of (11)

$$\overline{x^2} = N(\omega^2 + \overline{\eta^2}). \quad . \quad . \quad . \quad . \quad (13)$$

The intermediate case, which is that of Hull and Williams, when the regularity is partial, cannot be treated accurately without a precise knowledge of the form of regularity ; but it seems reasonable on all accounts to assume that if the regularity introduced by the space-charge is such as to reduce the fluctuations in the primaries in the ratio β , then we shall have in place of (9)

$$\overline{x^2} = N\{\beta(1 - \omega)^2 + \overline{\eta^2}\}, \quad . \quad . \quad . \quad (14)$$

and in place of (11)

$$\overline{x^2} = N\{\beta + \omega^2 + \overline{\eta^2}\}. \quad . \quad . \quad . \quad (15)$$

In Hull and Williams's experiments ω was 1 ; their experimental result was

$$\overline{x^2} = N\{\beta + \omega^2\}.$$

If that result is general for all values of ω —that is to say, for all ratios of primary to secondary current, and therefore for all energies of the primaries,—then their conclusion truly follows, and with it the conclusion that $\overline{\eta^2} = 0$. But it is so surprising to find that, while there is complete temporal independence between emission and incidence, the number of secondaries emitted by each primary is not subject to

appreciable variations, that it is to be hoped that they will extend their observations over a wider range. A single experiment, in which $\omega = 1$, cannot distinguish between (14) with $\overline{\eta^2}$ fortuitously equal to $1 + \beta$ and (15) with $\eta^2 = 0$; or, further, between either of these alternatives and some relation intermediate between (14) and (15) with some intermediate value η^2 , corresponding to partial but not complete temporal independence.

VIII. *A Study of the Electrolytic Interrupter.* By J. A. CROWTHER, *Sc.D., F.Inst.P., Professor of Physics, University College, Reading*, and R. J. STEPHENSON, *B.Sc.**

[Plate II.]

Introduction.

THE Wehnelt electrolytic interrupter is from a mechanical point of view one of the simplest interrupters for use with an induction coil, and still provides one of the most effective methods of producing continuous interruptions of really large currents. It consists essentially of a metal wire (usually platinum) projecting through a small hole in a non-conducting cylinder into an electrolytic solution. This "point," as it is called, serves as the anode; the cathode is a large plate of lead or some other indifferent metal dipping in the same solution. Sulphuric acid at its maximum conductivity is the electrolyte usually employed, but similar effects are produced in other electrolytes, and ammonium phosphate is now often used as it does not evolve noxious fumes. If the current to be interrupted is very large, three or more points connected in parallel and dipping into the same vessel can be employed.

The principal characteristics of the break in use are as follows:—(a) The interruptions of the current are very sharp. This is shown by introducing an oscillograph into the current circuit (see Pl. II. fig. 6a). The sharpness of the breaks is quite comparable with that of a mechanical interrupter. (b) The interruptions are very regular. The break when working normally emits a note, which, though hardly to be described as musical, is of very definite and perfectly recognizable pitch. The pitch of the note depends on the length of point exposed, on the supply voltage, and

* Communicated by the Authors.

on the resistance and self-induction of the circuit, and in certain conditions is very sensitive to quite small changes in resistance and induction. (c) The point, when the break is working, is covered with a bluish glow. Examination with a revolving mirror showed that this glow was actually intermittent. In order to determine at what part of the current cycle this glow occurred, an image of the point was focussed upon a falling photographic plate upon which a current oscillograph in series with the break registered its deflexions. The resulting photograph (Pl. II. fig. 1) shows that the luminosity corresponds to the break in the current, and apparently takes place at the moment when the current is about to be re-made. The sharpness of the image of the point indicates that the flash is practically instantaneous. There is no perceptible drawing-out of the image, although the plate was falling with an average speed of 1 metre per second. (d) Finally, when two or more points are connected in parallel, interruption takes place simultaneously at all the points, and no particular care in adjustment is required to produce this effect.

The behaviour of the break is generally ascribed to the temporary formation of a non-conducting layer round the point by the collection of the gas bubbles which are produced there by the electrolysis. It seemed to us, however, that some further phenomenon must be involved to account both for the extreme sharpness and the regularity of the interruptions. Experiments were therefore made to investigate the action of the break in more detail. After a considerable number of oscillograms, both of the current through the break and of the potential difference across it, had been taken and examined, a clue to the action was finally discovered in the nature of the current-voltage curves for conduction through an unsymmetrical electrolytic cell, such as the Wehnelt break supplies. It will be convenient to discuss these curves before dealing with the oscillograms.

Current-voltage Curves for conduction through an Electrolyte with a Point Anode.

The apparatus employed was of the simplest. The wire forming the anode protruded through a hole in the bottom of a pyrex glass tube which was drawn down to fit it as closely as possible. This dipped into a beaker containing the electrolyte, and a plate of lead dipping in the same beaker formed the negative pole. This simple arrangement performed all the functions of a Wehnelt interrupter when the circuit included a suitable inductance. In the experi-

ments described in this section, however, as the effect of resistance only was to be investigated the circuit was non-inductive, the voltage being supplied by a large battery of accumulators. The current was measured by an ammeter in series with the break, and the voltage by a high-resistance voltmeter connected across its terminals.

Fig. 2.

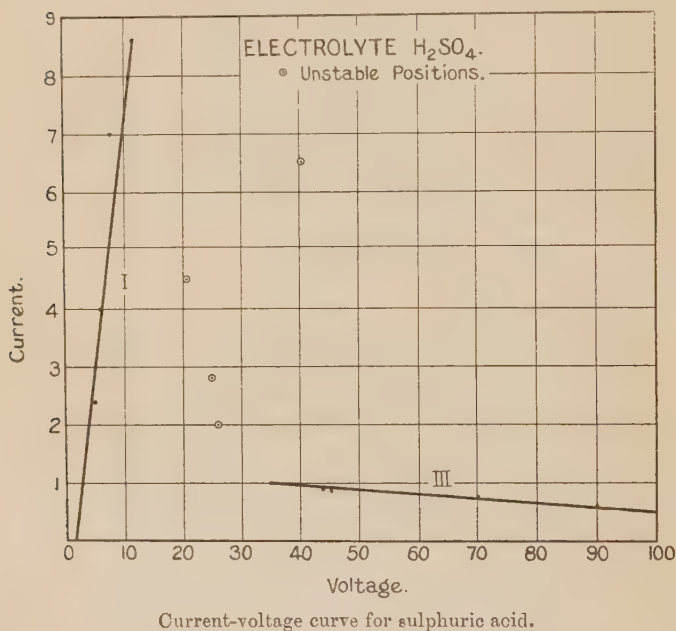


Fig. 2 is typical of the kind of results obtained. It was obtained using a platinum point 1.0 cm. in length and $\frac{1}{2}$ mm. in diameter in dilute sulphuric acid of S.G. 1.20. It will be seen that the curve falls into three sections. In the first part of the curve we have the normal relation between current and voltage for an electrolytic conductor. The current begins to flow when the applied voltage exceeds the polarization E.M.F. and increases linearly with the voltage until the voltage across the break is 12.5 volts. The corresponding current in this particular instance was 8.7 amperes, and this was the maximum current which could be passed through this particular system. If the voltage was increased beyond this point the average current, as measured by the ammeter, became smaller. At the same

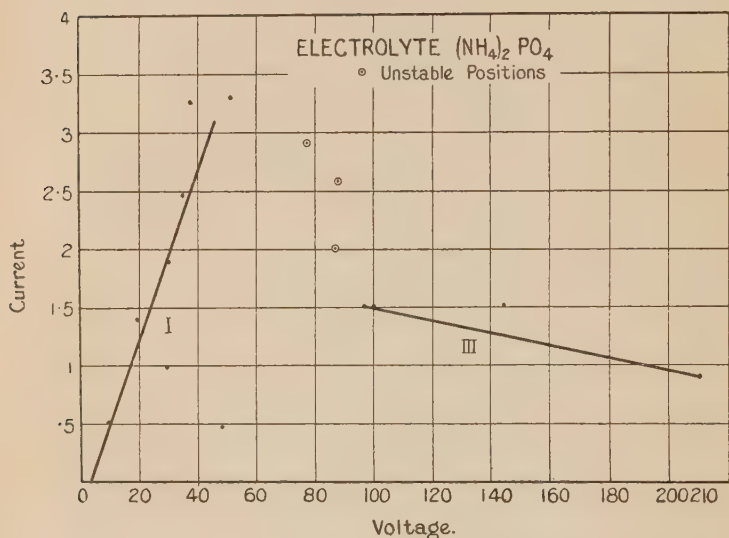
time, both the voltmeter and ammeter began to show very considerable fluctuations, which made accurate readings impossible. This stage lasted until the applied voltage was rather more than 30 volts, when conditions again became steady, the current for a P.D. of 35 volts being 1.0 ampere. If the voltage was now still further increased, the current became progressively smaller and decreased almost linearly with increase in voltage. This is indicated by the straight line between 35 and 100 volts on the graph. It may be mentioned that the point was usually non-luminous throughout this range of voltages.

A repetition of the experiments with the same electrolyte, but with different anode points, gave exactly similar graphs. It was found that for the same electrolyte the critical voltage at which the change in the graph occurred (12.5 volts in the case of sulphuric acid) remained the same. Thus doubling the length of the point or doubling its diameter gave in each case a graph showing a discontinuity at exactly the same voltage. The corresponding current at this voltage, however, increased with the area of wire exposed, and was found to be directly proportional to it. Hence we may also express the results of these experiments by saying that the current ceased to be proportional to the P.D. when the current density at the point reached a value which was a constant for a given electrolyte. For sulphuric acid of the strength named, its value was about 45 amperes per sq. cm. Reasons will be given later which suggest that the P.D. is the more fundamental factor.

Analogous results were obtained with a number of other electrolytes, including sodium hydrate, sodium chloride, sodium sulphate, hydriodic acid, and ammonium phosphate. The critical voltage differed with the electrolyte. For sodium hydrate it was 24 volts, and for ammonium phosphate somewhere in the neighbourhood of 45 volts. It appeared to vary slightly with the strength of the solution. The phenomena for ammonium phosphate were not quite so well marked as for the other electrolytes used. The intermediate stage extended over a longer range of voltages, and the final stage in which the current decreased regularly with increase in voltage did not become established for potential differences less than 90 volts. The conductivity of the break in this stage was also greater than when sulphuric acid was employed, although the normal conductivity in the first stage was much smaller. A current-voltage curve for ammonium phosphate is shown in fig. 3. It will be seen that it does not differ essentially from that for sulphuric acid.

Experiments made with points of other metals, including iron, nickel, and lead, gave precisely similar results. The critical voltage appeared to be slightly less with these elements than with platinum (11 volts in dilute sulphuric

Fig. 3.



Current-voltage curve for ammonium phosphate.

acid as against 12.5), but the phenomena were otherwise the same. Unfortunately, all these metals disintegrate rapidly in use, and they cannot, therefore, be used as substitutes for platinum in the Wehnelt break.

Phenomena at the Point.

An examination of the point during the experiments just described revealed very interesting changes in the method of evolution of gas in the different stages into which the conduction falls. In the normal stage the gas was given off from all parts of the point in bubbles of moderate size, such as generally attend the evolution of gas by electrolysis. Pl. II. fig. 4*a* is a photograph of the point in this stage. The actual appearance to the eye is that of a rapid stream of bubbles rising rapidly to the surface, but as the time of exposure was $1/200$ of a second, only a few of these bubbles appear in the photograph. On increasing the voltage so as

to bring in the third stage, the appearance of the point was entirely altered. Instead of leaving the wire in bubbles, the gas evolved seemed to cling to it tenaciously, gradually working its way upwards until it reached the glass sheath, where it collected into a single bubble of considerable size, which broke away from time to time. This is indicated by the photograph in Pl. II. fig. 4*b*. The way in which the little bulges to be seen in the photograph gradually worked their way up the wire was very characteristic, and conveyed strongly the impression that the gas was forcing its way up inside a tightly-fitting elastic skin enclosing the wire. This impression may be quite erroneous as an explanation of the effect, but it is certainly a very close description of it.

In the intermediate stage the gas was evolved partly in the form of the bubbles characteristic of the first stage, and partly in the form of large bubbles from the point characteristic of the third stage. The most striking feature of this stage, however, was the formation of large numbers of very minute bubbles which were shot off from the point with considerable velocities, so that, in a short time, the whole of the liquid became quite milky in appearance. The bubbles were so minute that this milkiness took some minutes to clear.

The second stage thus appears to be a series of rapid alternations between the first and third stages. The transition could actually be watched in the case of ammonium phosphate when the applied voltage was just below that required to ensure permanence for the third stage. The silvery film on the point would break down every now and then, its dissolution being signalized by a spurt of very minute bubbles and a simultaneous kick of the ammeter needle. This suggestion is amply confirmed by oscillographic records of the current in the three stages. Pl. II. fig. 5*a* (with ammonium phosphate in the interrupter) was taken with an applied voltage of 42 volts (just below the critical voltage for the electrolyte), while Pl. II. fig. 5*b* shows the same circuit with the P.D. across the break increased to 46 volts. The fluctuations, shown in the latter oscillogram, were found to increase in amplitude and frequency as the voltage was further increased, until finally, at sufficiently high voltages, the current again became steady at a much lower value.

It may be mentioned in passing that, with sulphuric acid as the electrolyte, the gas given off during the transition stage was strongly ozonized; the large bubbles emitted during the third stage smelt strongly of oxides of sulphur, and at high voltage were sometimes filled with white fumes.

Application of the Results to the Action of the Interrupter.

The current-voltage graphs described in a previous section were obtained by adjusting the voltage in circuit to the required value by altering the number of accumulators employed. The voltage across the break can also be adjusted by having a variable resistance in series with the break. The actual P.D. across the break is then the difference between the applied voltage and the product of the external resistance into the current. Suppose now we apply 100 volts to a circuit containing a variable resistance and the Wehnelt break, the current-voltage curve for which is indicated in fig. 2. Starting with a high resistance and consequently a small voltage across the break, we can, by gradually reducing the resistance, describe the first portion of the curve. As soon, however, as the P.D. across the break exceeds 12.5 volts the current begins to fluctuate, owing to momentary passages into the third stage. As the current falls, the drop of potential in the external resistance becomes less and the voltage across the break becomes greater. This greater voltage still further reduces the current, owing to the nature of the graph. The system is thus unstable, and jumps across the intermediate stage to the third stage. The voltmeter thus moves, with a jump, from the critical voltage to a voltage only slightly less than the full voltage in the circuit. This is very easily verified by experiment.

If, now, inductance is included in the circuit instead of resistance, a somewhat similar state of affairs is produced. When the voltage across the break has risen to a value greater than the critical value, fluctuations in the current begin. As the current begins to fall, an E.M.F. is induced in the circuit, producing a rapid increase in the applied voltage across the interrupter, and thus throwing it into the third or highly resistant stage. The current thus falls with great rapidity from its maximum value (8.7 amperes in the case illustrated in fig. 2) to the value corresponding to this higher voltage. If the inductance is very small, the induced voltage may not be sufficient to throw the system into the third or highly resistant stage, and the effect will simply be to emphasize the fluctuations in the current. This is shown by the oscillogram in Pl. II. fig. 5c, where the conditions were identical with those for Pl. II. fig. 5b, except that a small inductance (0.1 millihenry) was included in the circuit without altering the total resistance.

If the self inductance is larger, the induced E.M.F. will be sufficient to throw the system into the highly resistant stage, and the current will fall rapidly to half an ampere or less. This rapid change in current will produce a still higher induced E.M.F. in the circuit, an E.M.F., in fact, sufficiently high to spark through the resistant layer and destroy it.

The cycle of operations in the Wehnelt break is thus as follows :—When the circuit is made, the voltage across the break gradually rises until, after a time depending on the time constant of the circuit, it reaches a value exceeding the critical value. The current then begins to fall rapidly, and an induced E.M.F. is produced which rapidly attains the sparking voltage, while the current falls to a small value. A discharge then takes place across the resistant layer, thus destroying it and bringing the system back to the normal stage. The current then begins to rise again, and the cycle is repeated indefinitely. The luminous discharge thus takes place during the break, as indicated in Pl. II. fig. 1, and its function is to restore the system to its conducting phase.

It will be seen that the principal characteristics of the interrupter become immediately explicable on this view of the phenomenon. The sharpness of the interruptions is due to the sudden change in resistance of the break when the conduction passes from one phase to the other. The regularity of the interruptions is also explained, since the time which it takes for the voltage across the break to rise to a definite value will be determined by the applied voltage and the time constant for the circuit, *i.e.* by its resistance and self inductance (and possibly its capacity), and will be a constant for a given circuit. The simultaneous working of two or more points in parallel is also accounted for, since the potentials of all the points must be the same, and all will reach the critical condition at the same time.

Evidence from the Oscillographic Records of Current and Voltage.

The theory suggested in the previous section was amply corroborated by oscillographic records made of the behaviour of the interrupter under varied working conditions. Oscillograms of the current through the break were made by a simple high-frequency-current oscillograph of the Duddell type connected across the terminals of a low resistance in series with the break. Those of the P.D. across the break

were obtained by connecting the same current oscillograph across the terminals of the break through a high resistance (2000 ohms and upwards). The inductances placed in series with the break were the various layers of the primary of a large induction coil. The secondary of the induction coil was removed during these experiments, in order to avoid the complications which might arise owing to the reaction of the secondary circuit on the primary. These reactions probably play an important part in determining the efficiency of the interrupter as part of an X-ray outfit, and we hope to investigate this part of the problem later. In discussing the theory of the interrupter itself, it seemed desirable to keep the conditions of the circuit as simple as possible.

Typical oscillograms of current and voltage are reproduced in Pl. II. fig. 6*a* & *b*. The sudden fall in current and the corresponding rise in the P.D. are clearly shown. The maximum potential reached is far too high to be recorded on the scale of Pl. II. fig. 6*b*. By increasing the resistance in circuit with the potential oscillograph to 10,000 ohms, the complete potential curve could be obtained, and an example is reproduced in Pl. II. fig. 6*c*. The peak potential as calculated from the calibration curves for the oscillograph was 600 volts in this particular case, and in general varied between 400 and 600 volts. These values are of the order of the minimum sparking voltage in oxygen, and direct experiment showed that a luminous discharge was actually produced at the point when a steady P.D. of 420 volts was applied directly across the interrupter in the absence of self induction.

The hypothesis that the interruption in the current occurs when the P.D. across the break reaches a definite value, which depends only on the electrolyte, can be verified directly from the potential oscillograms. A series of such oscillograms was taken in which all the conditions in the circuit were varied except the electrolyte. Experiments were made with applied voltages varying from 68 volts to 210 volts, with and without external resistance in circuit; with a variety of self inductances; and with points of various lengths and diameters. The critical breaking voltage to be measured was taken as that corresponding to the point on the potential graph where the voltage takes a sharp upward turn, and this discontinuity was generally sufficiently marked to be measured with reasonable accuracy. This voltage was found to be, within the limits of experimental error, quite independent of the changes made in the circuit. With

sulphuric acid of S.G. 1.20 as the electrolyte, all the measurements lay between 24 volts and 26 volts, and these slight variations appeared to be quite accidental.

A comparison with the current-voltage graph for the electrolyte suggests that this voltage marks the point at which the third stage of conduction sets in. This, we suggest, is what might be expected, as the irregular transitions which characterize what we have called the intermediate stage usually take some little time before they manifest themselves (see Pl. II. fig. 5), and with a rapidly rising voltage, such as we have in these experiments, the probability that such an interchange will occur before the voltage has reached that at which the third stage is definitely established is very small.

The conduction, until the moment of break, is in the normal stage, and the peak value of the current, as read from the oscillograms, is much higher than the maximum steady current which can be sent through the break. In fact it corresponds to the value of the current which would be obtained by producing the first straight portion of the current-voltage curve for the interrupter to the measured breaking voltage. This explains an observation which often puzzled us in the earlier stages of the work, that the average current through the break as measured by an ammeter was very materially increased when self induction was introduced into the circuit. By instantaneous measurements, therefore, it appears possible to prolong each of the straight portions of the current-voltage curve to a common voltage, about 25 volts for sulphuric acid, where the real discontinuity occurs, both phases being unstable for a certain range of voltages on each side of this point.

It is possible, however, to produce interruptions in the current when the voltage across the interrupter only slightly exceeds what we have called in the earlier sections of the paper the critical voltage. The production of such interruptions has already been discussed. They are very slow and comparatively irregular. Oscillograms show that in these cases the current rises to a maximum and then remains practically steady. The P.D., however, gradually increases until the usual breaking voltage is reached, when an interruption takes place. This gradual increase in voltage may be due to a gradual increase in resistance of the electrolyte near the point, owing to the rapid removal of the ions by the current. The value of the current at break for these slow interruptions is always appreciably smaller

than for the rapid interruptions obtained with the higher voltages. It is for this reason that we have suggested that the P.D. rather than the current density is the more fundamental factor in determining the break.

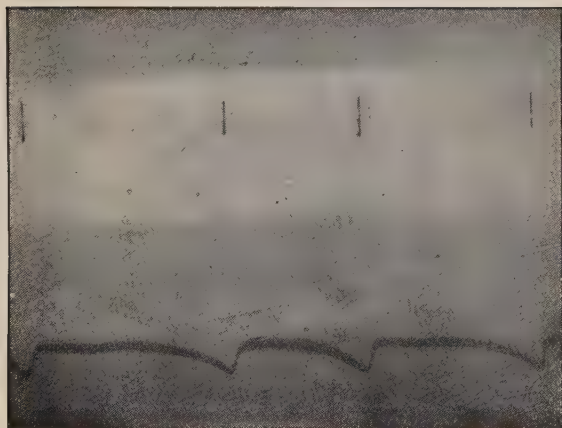
Conclusion.

In the absence of any theory to account for the high resistance developed at the point, we have judged it desirable to record our experimental results without any adjustments or corrections. It may be pointed out that the voltages measured were those across the terminals of the interrupter, whereas in all probability the deciding factor is the fall of potential between the point anode and some point in the electrolyte close to it. Since there is always some current flowing in the interrupter, this will be less than the P.D. between the terminals by the P.D. required to drive this current through the remainder of the electrolyte, which in turn depends on its specific resistance. It is possible that the observed differences between different electrolytes and, in particular, the differences observed between different solutions of the same electrolyte may be due in part to this cause. The fact that the critical voltage increased with the resistance of the electrolyte gives some support to this suggestion.

Until further evidence has been accumulated, it does not seem desirable to advance any suggestions as to the cause of the sudden increase of resistance which occurs when the critical voltage is passed, and which accounts for the action of the Wehnelt interrupter. It is natural to postulate the formation of a highly resistant layer at the anode, and the tightly-clinging gas layer which is so characteristic of this high-resistance stage of the conduction presents itself as a very obvious explanation. The change in the mode of emission of the gas has, however, itself to be accounted for. It is hoped that further experiments may throw some light on this interesting problem.

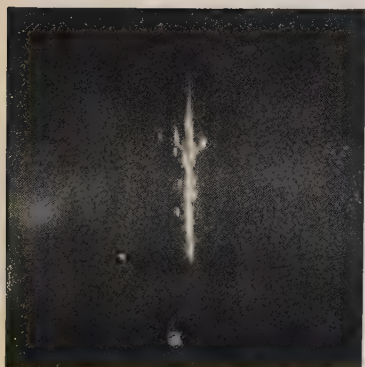
University College,
Reading,
March 18th, 1925.

FIG. 1.



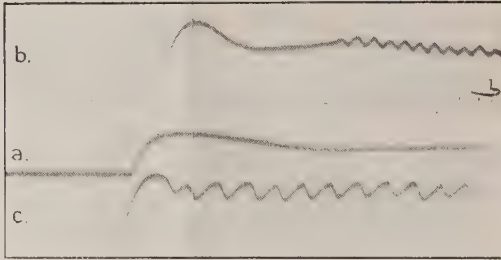
Showing coincidence between luminosity at the point (above)
and interruption of the current.

FIG. 4.



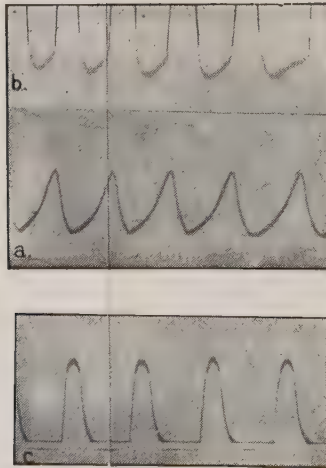
Appearance of point : *a* during normal stage ; *b* during
highly resistant stage.

FIG. 5.



Oscillograms of current through break. *a*, below critical voltage. *b*, just above critical voltage. *c*, as in *b* with $\frac{1}{10}$ m.h. self-induction.

FIG. 6.



Oscillograms of normal interruptions. *a*, current graph. *b*, potential graph (through 2000 ohms). *c*, potential graph (through 10,000 ohms).

IX. *On an Experimental Verification of Castigliano's Principle of Least Work and of a Theorem relating to the Torsion of a Tubular Framework.* By Professor A. J. SUTTON PIPPARD, M.B.E., D.Sc., University College, Cardiff, and J. F. BAKER, B.A.*

THE mathematical proof of the "Principle of Least Work" was given in Castigliano's original treatise†, and recently Mr. R. V. Southwell has demonstrated the physical basis of the theory‡.

During the past year the present authors have carried out experimental work upon the properties of certain braced frameworks, and in the course of these experiments very satisfactory verification of the Principle was obtained. Although the truth of the Principle has been established by the work cited, the importance of the method and its wide range of application makes experimental evidence of some interest and value, more particularly since very little experimental work of any kind upon braced frameworks appears to have been published.

In addition to the verification of Castigliano's Principle, experiments were made to check a theorem relating to the stress distribution in a tubular framework subjected to torsion. This theorem, due originally to Batho§, has recently been obtained independently by Southwell|| in an investigation of the case of tubular frameworks with redundant bracing members. The work upon which the authors were engaged was of a more comprehensive character than outlined above, and is fully described elsewhere¶, but since much of it was of a specialized interest, only those experiments bearing on the two theorems mentioned are included here.

The framework upon which the experiments were conducted was a space frame in the form of a braced hexagonal tube consisting of six longitudinal members divided into a number of equal bays by transverse frames in the form of regular hexagons: the panels thus formed by the transverse strut members and the longitudinal members were braced across both diagonals (figs. 1 and 2).

* Communicated by Mr. R. V. Southwell, M.A.

† 'Elastic Stresses in Structures'—English translation by E. S. Andrews, 1919.

‡ Phil. Mag. Jan. 1923.

§ 'Engineering,' Oct. 15, 1915, p. 398.

|| Aeronautical Research Committee, R. & M. 791.

¶ Aeronautical Research Committee, R. & M. 948.

The theoretical stress analysis for such a framework supported at one end and loaded at the other has been fully worked out * upon the following assumptions:—

(1) The framework was assumed to be pin-jointed throughout.

(2) The transverse framework to which the load was applied was assumed to be rigid in its own plane but free to warp out of that plane.

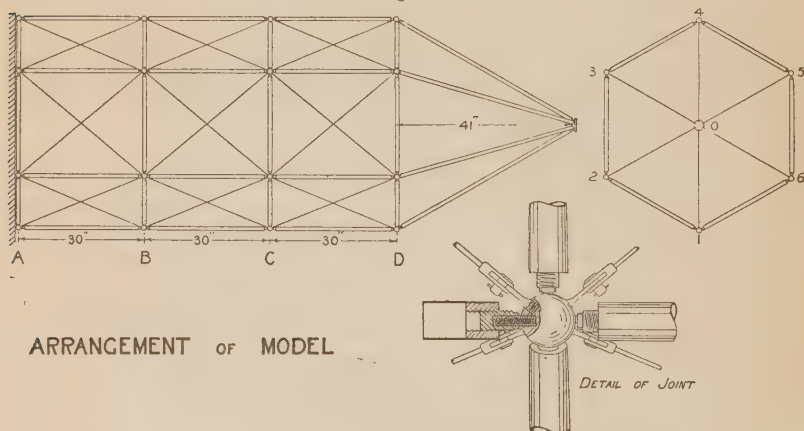
(3) All members were assumed capable of resisting either tensile or compressive forces.

(4) All longitudinal members were assumed to be of the same size except the bottom or "keel" member which could be made any desired area.

DESCRIPTION OF STRUCTURE.

The leading dimensions of the experimental structure and some details of its construction are shown in fig. 1. The

Fig. 1.



ARRANGEMENT OF MODEL

framework was 3 bays in length, each bay being 30 inches long; the side of the hexagon was 25 inches. Since the theoretical analysis had been based on the assumption that the structure was pin-jointed throughout, an attempt was made to design a suitable joint of this type. The difficulties in this will be apparent, and although several designs were made it was found that even in the best of them the friction on the bearing surfaces would have been considerable, and would

* Aeronautical Research Committee, R. & M. 800, Appendix V.

in fact have introduced a fixing factor of an incalculable amount. The attempt to obtain true pin or ball ends was therefore abandoned, and a suggestion made by Mr. R. V. Southwell was examined: this suggestion was that the members of the structure should be attached to the joints by short dowels or pins, which would be of sufficient cross sectional area to transmit the direct loads in the members, but so short that no tendency to buckle would occur. The necessary strength was given by dowels of small diameter and flexural rigidity: consequently the amount of bending which could be transmitted by them was small, and moreover could be calculated if necessary and allowed for as a correcting factor.

Tests were carried out upon struts with ball ends and with ends fixed by dowels, and the results were such as to justify the latter method of construction. The transverse and longitudinal members of the structure were made of steel tube $\frac{7}{8}$ in. outside diameter and .028 in. thick. All cross bracing members were 4 B.A. swaged rods, ability to resist compression being obtained by initially tensioning these rods to such an extent that they remained operative under the maximum loads imposed. Provision was made for replacing the keel member by solid steel bars $\frac{7}{8}$ in. diameter, since it was desired to carry out experiments upon the effect of varying the size of this member. The nose-piece of tubes in the form of a regular pyramid, seen in the photograph of the structure (fig. 2), was provided for a special experiment not described in the present paper.

The structure was attached to wall-plates by dowels of the same size as used in the joints, and was loaded at the free end by means of a beam weighing machine, one pan of which was replaced by a special hook fastened to the top joint of the structure, a turn-buckle being inserted between the beam and the joint for adjustment.

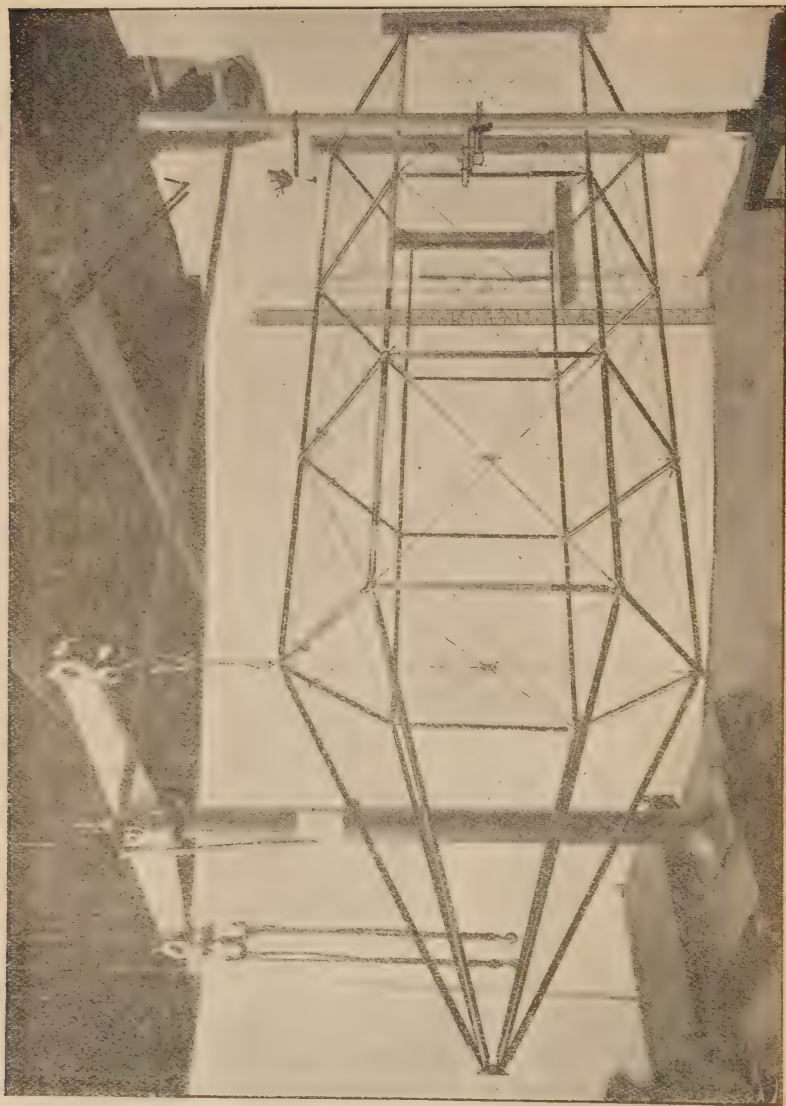
MEASUREMENT OF STRAINS.

Means for measuring the strains in all the members of the structure to a high degree of accuracy were essential, and for this purpose none of the standard types of extensometer were suitable, either on the score of weight or expense; in consequence, a special instrument had to be designed, and this was done in collaboration with the Cambridge Instrument Company Limited.

Gauges made of thin aluminium, corrugated for the sake of stiffness, were attached to each member of the structure

100 Prof. Pippard and Mr. Baker on an *Experimental*
by a hardened steel knife-edge and small setscrew ; at the
end of the gauge was a small circle of glass marked on the

Fig. 2.

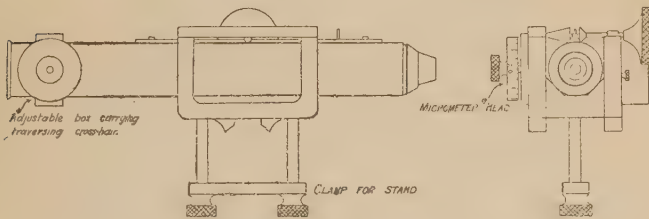


under side with two fine cross-lines. The glass was held in
contact with the member by small indiarubber bands. A
fine line was scratched on the surface of the member by

means of a Gillette safety-razor blade, to coincide as nearly as possible with the line on the glass. This was effected by the use of a special marking-off gauge. The distance between the scratches on the member and the glass was measured by a special microscope, and the alteration in this distance under different conditions of loading gave the strain. The gauges were 15 inches between the point of attachment to the member and the line on the glass.

The microscope used is shown diagrammatically in fig. 3. The optical arrangement is standard and needs no special description. The eyepiece is provided with a traversing cross-hair operated by a micrometer head. This cross-hair was first brought into coincidence with the line on the glass and then traversed until it coincided with the scratch on the

Fig. 3.



MICROMETER MICROSCOPE

member. The readings of the micrometer head were noted in each case, and the difference gave the distance between the scratches.

The same procedure was followed after the structure had been loaded, and the difference between the distances before and after loading was the strain produced by the external load system. The movement of the traversing cross-hair as measured by a standard grid was $1/17780$ inch per division on the micrometer head, but actual calibration curves were used to reduce the micrometer-head readings to loads in the member, as will be described later.

The objective of the microscope was $2/3$ inch, this being the smallest with which reasonable illumination could be obtained under the conditions in which the instrument was to be used. Illumination was obtained from a small 6 volt lamp carried on the end of the microscope; this ensured that the light was always in the same relative position to the scratches which were being viewed through the microscope, and thus error due to variation of the angle from which the light fell was avoided. Since the microscope had to be used on

all members of the structure in turn it was carried on a steel tubular stand, 2 inches diameter, mounted on a heavy tripod base. This stand was 7 feet high, and the microscope could be attached to any part of it. A tubular extension arm at right angles to the vertical post enabled the instrument to be placed in position for measurements upon the top and bottom members of the framework. The instrument on its stand but without the extension arm is shown on the right of fig. 2, which also shows the gauges in position upon the structure, ready for observation.

By calibrating a tube and a rod under controlled conditions of loading, it was found that with a 15-inch gauge length, one division of the micrometer head was a measure of the strain produced by a load of 7.84 lb. on the tube, and of 1.02 lb. on the rod.

THE CONDUCT OF EXPERIMENTS.

The structure having been erected and trued up, the wires were tensioned so that they could operate as struts. The magnitude of these initial tensions was immaterial as long as they were sufficient to ensure effective strut action under the maximum load to be imposed. An initial load was first placed on the scale-pan and the readings of the gauges taken. The desired increment of load was then applied and the readings again taken. The difference was then reduced to loads by the use of the calibration figures. It was originally intended to mount gauges on all members of the structure and take readings on each in turn for one condition of loading; then to add load and once more take all readings. It was found, however, much more satisfactory to keep the microscope in position for one member and to complete the two readings for it. This meant considerably more labour in loading and unloading than the other method, but was more accurate and reliable.

Having obtained a complete set of readings for the framework, certain checks were applied as follows:—

(i.) In the case of symmetrical loading the strain of the corresponding members on the two sides of the structure should be the same.

(ii.) The vertical components of the force in the members across any section should give the total vertical shear at that section. Thus in the centre of each bay the total of the vertical components of the loads in the cross bracing wires should give the shear across that bay.

(iii.) The forces in the members at each joint should give static balance.

After the first set of readings had been taken it was found that the errors, as indicated by the out of balance forces at several joints, were of a serious character, and repeat readings were made with no better result. Further investigation indicated that the probable source of error was due to some of the strut members bending slightly, so that the resultant strain due to direct compression and bending stress was being measured and not the direct compression alone. Since the members were circular in section this trouble was overcome by taking readings of strain at the opposite ends of any diameter: the average then gave the strain due to direct compression stress alone. When this was done results were very much better and within the limits of experimental accuracy, and the method was therefore always adopted in measuring strains of tube members in later experiments.

EXPERIMENTAL ERRORS.

The main sources of possible error in obtaining experimental results are three in number, viz. :—

- (i.) Errors due to the limitations of the method of measurement.
- (ii.) Errors due to the variation in the sizes of the members of the structure.
- (iii.) Errors in reading the instrument.

(i.) *Errors due to the limitations of the method.*

As already stated, one division of the micrometer head of the microscope corresponds to $1/17780$ inch, and the magnification required entailed very delicate manipulation of the micrometer head if exact coincidence was to be obtained between the lines on the glass and on the member, and that on the traversing eyepiece. This, however, was principally a matter of practice, and after some experience it was found to be a comparatively simple matter to obtain satisfactory results, and observations could be repeated to within about one division of the micrometer head, which is therefore assumed to be the limit of experimental accuracy. This will be seen on reference to the calibration figures to correspond to ± 8 pounds on the standard tube members and ± 1 pound on the wires. The small error on the wires makes the results obtained for these members particularly reliable and useful. Another difficulty arose from vibration of the laboratory, and it was found impossible to take readings if

plant were running in certain parts of the buildings, or if a heavy vehicle were passing outside. Such disturbances were, however, only occasional, and usually this trouble was not sufficiently serious to cause any prolonged interruption of the work.

(ii.) *Errors due to the variation in the size of the members.*

The structure was made of aircraft materials in which great care is taken to ensure uniformity of quality and dimensions. Tolerances, however, are unavoidable, and in the case of the tubes the variation in thickness allowed by specification amounts to 7 per cent., and due to this cause the error in the readings of any tubular member may be $\pm 3\frac{1}{2}$ per cent., while the corresponding error in the wires may be the same.

(iii.) *Errors in reading.*

Errors in reading the instrument were eliminated as far as possible by taking at least three measurements on each member. Even with this precaution, however, it was found that occasionally a wrong value for the strain was obtained, but this could always be detected by an application of the checks previously mentioned. Having obtained a complete set of readings for the structure, the out of balance force at each joint was expressed as components along three mutually perpendicular axes. If this out of balance force were serious, check readings were made in order to trace the error, but in the majority of cases the errors were within the limits of experimental accuracy. These errors were then distributed among the members of the structure at the joint concerned as far as was possible. This was of necessity a somewhat arbitrary matter, and the general method was to neglect the wires, since the area of these was only 1/10 of that of the tube members. The out of balance force was then distributed between the tube members. It was found that the corrections thus applied were always very small and never exceeded the amount by which the reading might have been in error due to the causes enumerated above.

EXPERIMENTAL RESULTS.

In identifying the various members of the structure the following system has been adopted, and is shown on fig. 1. Each transverse frame is distinguished by a letter beginning at the fixed or wall end with A. Each joint in the transverse is numbered, beginning at the bottom with 1 and

following round the frame in a clockwise direction viewed from the free end. The middle joint in a transverse frame is 0. Thus each joint in the structure is denoted by a letter and a numeral suffix, *e. g.* A₄, B₃, etc. A positive sign is used to denote a tensile load and a negative to denote a compressive load.

PART I.

Experiments on the framework subjected to a constant shear and uniformly varying bending moment for comparison with the theoretical results obtained by an application of the Principle of Least Work.

Experiment 1.

All longitudinal members 7/8 in. O.D. \times .028 in.

End bulkhead radially braced with 4 B.A. rods.

No bulkhead bracing in remaining transverse frames.

Single load of 400 lb. applied at end bulkhead joint D₄.

The two sides of the structure gave practically exact agreement, differences being only of the order of experimental errors. The shears were also satisfactory, and under these circumstances the strains in the wires only were measured for comparison with the theoretical values. The results are given in Table I., which also gives the theoretical values.

TABLE I.

Member.	Load as measured. lb.	Calculated load. lb.	Difference. lb.
A ₄ B ₅	- 75.5	- 70.8	+ 4.7
A ₅ B ₄	35.5	27.2	+ 8.3
A ₅ B ₆	-103.7	-106.0	- 2.3
A ₆ B ₅	103.5	106.0	- 2.5
A ₆ B ₁	- 26.75	- 27.2	- 0.5
A ₁ B ₆	69.9	70.8	- 0.9
B ₄ C ₅	- 70.5	- 62.0	+ 8.5
B ₅ C ₄	38.5	36.0	+ 2.5
B ₅ C ₆	-103.5	-106.0	- 2.5
B ₆ C ₅	103.0	106.0	- 3.0
B ₆ C ₁	- 40.6	- 36.0	+ 4.6
B ₁ C ₆	61.8	62.0	- 0.2
C ₄ D ₅	- 59.6	- 53.3	+ 6.3
C ₅ D ₄	57.4	44.6	+12.8
C ₅ D ₆	-102.8	-106.0	- 3.2
C ₆ D ₅	102.3	106.0	- 3.7
C ₆ D ₁	- 44.6	- 44.6	0
C ₁ D ₆	50.0	53.3	- 3.3

It will be seen that there are appreciable differences

between the measured and theoretical loads in the members, the characteristic being that the loads in the wires of the top panels, that is C_4D_5 , C_5D_4 , etc., are larger than calculated, while the loads of the remaining wires are smaller.

This is the result which would be expected if the end bulkhead were distorting in its own plane, and it was therefore decided to substitute much heavier bracing in the end bulkhead in place of the 4 B.A. wires used in this experiment, in order to approximate more nearly to the conditions of rigidity assumed in the mathematical investigation.

Experiment 2.

All longitudinal members $7/8$ in. O.D. $\times .028$ in.

End bulkhead radially braced with $5/8$ in. diameter solid steel rods.

No bulkhead bracing in other transverse frames.

Single load of 400 lb. applied at end bulkhead joint D_4 .

The radial members in the end bulkhead, which had previously been 4 B.A. swaged rods, were replaced by $5/8$ inch diameter steel rods, each rod being provided with a turn-buckle for tightening up. It was considered that this gave as close approximation to a rigid bulkhead as could be conveniently obtained, and should afford clear evidence as to whether the discrepancy between the measured and theoretical loads found in the previous experiment were due to the elastic deformation of the bulkhead in its own plane, or to other causes. Agreement between the two sides of the structure was excellent as well as the results obtained for shear, and a comparison of the measured and theoretical values of the loads in all cross bracing members is given in Table II. One side only of the structure is given, the loads being the average of the two sides in each case.

It will be seen that good agreement between the measured and the calculated loads was obtained throughout the structure. In only one case does the difference exceed 2 pounds.

Comparing these results with those of Table I., it is clear that the elasticity of the end bulkhead is an appreciable factor in the distribution of loads in the members of the structure.

TABLE II.

Member.	Measured load. lb.	Calculated load. lb.	Difference. lb.
A ₄ B ₅	- 72.8	- 70.8	+2.0
A ₅ B ₄	27.5	27.2	+0.3
A ₅ B ₆	-106.5	-106.0	+0.5
A ₆ B ₅	104.5	106.0	-1.5
A ₆ B ₁	- 27.1	- 27.2	-0.1
A ₁ B ₅	68.4	70.8	-2.4
B ₄ C ₅	- 63.5	- 62.0	+1.5
B ₅ C ₄	36.7	36.0	+0.7
B ₅ C ₃	-105.0	-106.0	-1.0
B ₆ C ₅	107.6	106.0	+1.6
B ₆ C ₁	- 35.7	- 36.0	-0.3
B ₁ C ₆	63.2	62.0	+1.2
C ₄ D ₅	- 52.0	- 53.3	-1.3
C ₅ D ₄	45.8	44.6	+0.8
C ₅ D ₆	-105.5	-106.0	-0.5
C ₆ D ₅	105.0	106.0	-1.0
C ₆ D ₁	- 43.8	- 44.6	-0.8
C ₁ D ₆	53.1	53.3	-0.2

Experiment 3.

Keel members A₄B₄C₄D₄ 7/8 in. diameter solid steel bars.

Other longitudinal members 7/8 in. O.D. \times .028 in.

End bulkhead radially braced with 4 B.A. swaged rods.

Remaining bulkheads unbraced.

Single load of 400 lb. applied at joint D₄.

In this experiment the keel member, which had hitherto been the same size as the other longitudinal members, was made of solid steel bar 7/8 inch diameter, attached to the joints by dowels in the same manner as the other tubular members. In this case the loads in all the members were measured, and not only those in the wires. Good agreement was obtained between the two sides of the structure. The shears were practically exact, and the corrections necessary to give static balance at the joints were in all cases less than the equivalent of one division of the micrometer head (Table III.).

This case was analysed theoretically, and it will be seen that the agreement between calculation and experiment is very good. In view of the closeness of this agreement, it was considered unnecessary to repeat the experiment with a stiffer end bulkhead. It will be clear from a consideration of the earlier results that such alteration would tend still further to reduce the errors between measured and calculated loads. Owing to the size of the keel member, which was

approximately ten times the area of any other longitudinal, the strains in that member were too small to be measured satisfactorily, and the figures given in brackets have been deduced from consideration of static balance at the joints.

TABLE III.

Member.	Measured load. lb.	Correction for balance. lb.	Corrected reading. lb.	Calculated load. lb.	Difference. lb.
A ₁ B ₁	330.0	3.2	333.2	337.8	-4.6
A ₂ B ₂	180.5	-1.0	179.5	177.3	+2.2
A ₃ B ₃	-119.6	3.9	-115.7	-116.4	-0.7
A ₄ B ₄	—	—	(-510.0)	-506.8	+3.2
A ₁ B ₂	67.9	—	67.9	67.6	+0.3
A ₂ B ₁	-27.5	—	-27.5	-28.0	-0.5
A ₂ B ₃	102.5	—	102.5	100.8	+1.7
A ₃ B ₂	-96.4	—	-96.4	-96.2	+0.2
A ₃ B ₄	60.1	—	60.1	60.4	-0.3
A ₄ B ₃	-74.4	—	-74.4	-74.0	+0.4
B ₁ B ₂	-17.6	-4.0	-21.6	-20.0	+1.6
B ₂ B ₃	-3.9	1.2	-2.7	-2.5	+0.2
B ₃ B ₄	7.8	0.8	8.6	7.0	+1.6
B ₁ C ₁	204.0	-6.4	197.6	202.4	-4.8
B ₂ C ₂	109.1	0.9	110.0	106.4	+3.6
B ₃ C ₃	-66.8	-0.9	-67.7	-69.6	+1.9
B ₄ C ₄	—	—	(-306.0)	-304.0	+2.0
B ₁ C ₂	60.7	—	60.7	59.6	+1.1
B ₂ C ₁	-36.7	—	-36.7	-36.0	+0.7
B ₂ C ₃	98.5	—	98.5	99.8	-1.3
B ₃ C ₂	-97.4	—	-97.4	-96.8	+0.6
B ₃ C ₄	63.1	—	63.1	63.0	+0.1
B ₄ C ₃	-72.7	—	-72.7	-71.2	+1.5
C ₁ C ₂	-7.8	-2.0	-9.8	-10.0	-0.2
C ₂ C ₃	-3.9	4.0	0.1	-1.2	+1.3
C ₃ C ₄	3.9	-0.5	3.4	3.5	-0.1
C ₁ D ₁	70.6	-5.5	65.1	67.2	-2.1
C ₂ D ₂	35.3	2.7	38.0	35.2	+2.8
C ₃ D ₃	-19.6	-4.1	-23.7	-23.2	+0.5
C ₄ D ₄	—	—	(-104.0)	-101.2	+2.8
C ₁ D ₂	49.5	—	49.5	51.8	-2.3
C ₂ D ₁	-42.3	—	-42.3	-43.8	-1.5
C ₂ D ₃	99.2	—	99.2	98.8	+0.4
C ₃ D ₂	-98.9	—	-98.9	-98.0	+0.9
C ₃ D ₄	67.6	—	67.6	66.0	+1.6
C ₄ D ₃	-68.4	—	-68.4	-68.6	-0.2
D ₁ D ₂	-35.3	-2.0	37.3	-37.0	+0.3
D ₂ D ₃	58.9	-0.5	58.4	59.0	-0.6
D ₃ D ₄	161.0	4.0	165.0	166.0	-1.0
D ₀ D ₁	65.3	—	65.3	—	—
D ₀ D ₂	3.5	—	3.5	—	—
D ₀ D ₃	-122.0	—	-122.0	—	—
D ₀ D ₄	191.8	—	191.8	—	—

The members D₀D₁, D₀D₂, D₀D₃, and D₀D₄ are the radial wires in the end bulkhead, and since these are considered to

be rigid in the theoretical analysis no separate values can be calculated. The analysis does, however, permit certain differences to be obtained, and these are given in Table III. *a*, together with the measured differences.

TABLE III *a*.

Difference.	Measured value. lb.	Calculated value. lb.	Difference. lb.
$D_0D_2-D_0D_4$	-188.3	-187.6	+0.7
$D_0D_1-D_0D_4$	-126.2	-126.5	-0.3

PART II.

Experiments on the framework subjected to a pure torque.

The theoretical analysis for the stresses in a redundantly braced tube when subjected to a pure torque * indicates that the panel bracing members alone are brought into operation, and no stresses are put into the longitudinal members or transverse struts.

In the theoretical investigation it is assumed that the external loading is applied in the particular manner which prevents any distortion of the transverse frame, and also that the structure is pin-jointed throughout. Transverse frames which were plane before loading are then shown to remain plane in the strained condition of the structure.

The following experiments were carried out to determine the degree of accuracy obtained in an actual structure compared with calculations based on the above analysis, and also to discover the effect of varying the elasticity of the bulkhead bracing in the transverse to which the torque was applied when the external loading, although giving a resultant pure torque, was not applied to the joints as hypothecated in the analysis.

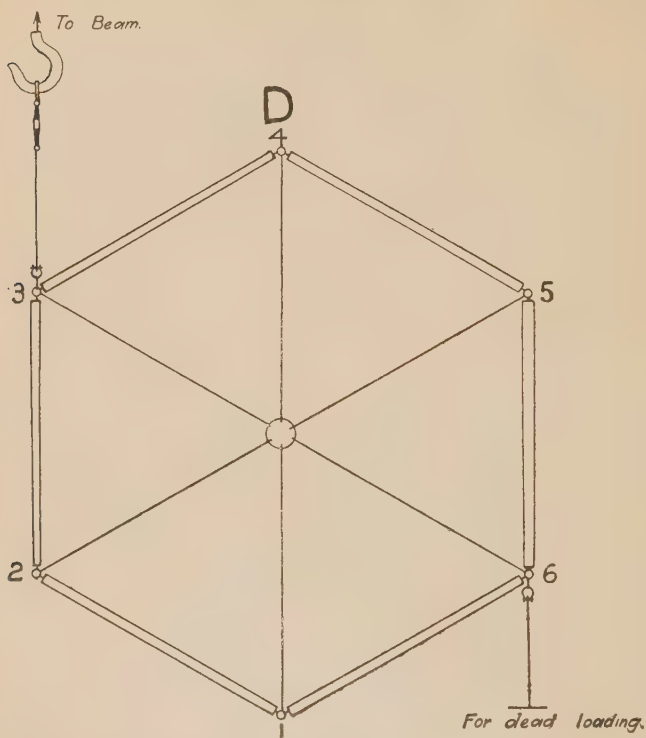
The structure used was the hexagonal frame already described, fitted with a solid 7/8 inch diameter steel keel member and no pyramidal nose-piece.

The torque was applied by loads at the joints D_3 and D_6 , into which special swivel hooks were screwed. An upward load was applied at D_3 by means of the weighing balance used in the shearing-force experiments, and weights were

* Aeronautical Research Committee, R & M 791.—Southwell.

hung from D_6 (fig. 4). An initial load was applied to D_8 equal to the weight of the scale-pan which was transmitted to D_3 .

Fig. 4.



The methods adopted in the experiments were exactly as described in the earlier work.

The increment of load in each case was 280 lb. upward at D_3 , and 280 lb. downwards at D_6 , giving a torque of 12124 inch-lb.

Experiment 4.

End bulkhead radially braced with $5/8$ in. diameter solid steel rods.

Other bulkheads unbraced.

This experiment reproduces as nearly as possible the theoretical conditions, since the approximately rigid bulkhead bracing serves to distribute the torque in a manner corresponding to that required by the analysis.

The theoretical load in each of the panel wires is 72·8 lb., and the closeness of the experimental results to this will be seen from Table IV., which gives the measured loads in all these members.

There are small departures from the theoretical figures, but these balance each other as will be seen from the average load in the wires of each bay.

In bay AB. Average load=72·54 lb.

In bay BC. Average load=73·58 lb.

In bay CD. Average load=72·38 lb.

TABLE IV.

Member.	Measured load. lb.	Member.	Measured load. lb.
A ₁ B ₂	74·5	A ₄ B ₅	71·5
A ₂ B ₁	-71·5	A ₅ B ₄	-72·5
A ₂ B ₃	74·5	A ₅ B ₃	72·5
A ₃ B ₂	-70·5	A ₆ B ₅	-71·5
A ₃ B ₄	72·5	A ₆ B ₁	73·5
A ₄ B ₃	-72·0	A ₁ B ₆	-73·5
B ₁ C ₂	74·5	B ₄ C ₅	71·5
B ₂ C ₁	-73·5	B ₅ C ₄	-72·5
B ₂ C ₃	72·5	B ₅ C ₃	73·5
B ₃ C ₂	-74·5	B ₆ C ₅	-74·5
B ₃ C ₄	75·5	B ₆ C ₁	73·5
B ₄ C ₃	-73·5	B ₁ C ₆	-73·5
C ₁ D ₂	73·5	C ₄ D ₅	74·5
C ₂ D ₁	-70·5	C ₅ D ₄	-71·0
C ₂ D ₃	70·5	C ₅ D ₃	71·5
C ₃ D ₂	-73·5	C ₆ D ₅	-71·5
C ₃ D ₄	71·0	C ₆ D ₁	74·0
C ₄ D ₃	-73·5	C ₁ D ₆	-73·5

Experiment 5.

End bulkhead radially braced with 4 B.A. swaged rods.

Other bulkheads unbraced.

In this experiment the elasticity of the transverse bracing was modified, but, as will be seen from the results in Table V., the measured loads were of the same degree of accuracy as with the nearly rigid bracing of the two previous experiments.

In bay AB. Average load=72·92 lb.

In bay BC. Average load=72·83 lb.

In bay CD. Average load=73·04 lb.

TABLE V.

Member.	Measured load. lb.	Member.	Measured load. lb.
A_1B_2	71.5	A_4B_5	73.5
A_2B_1	-73.5	A_5B_4	-72.0
A_2B_3	72.0	A_5B_6	73.0
A_4B_2	-74.5	A_0B_5	-73.5
A_2B_4	71.0	A_6B_1	73.5
A_4B_3	-75.5	A_1B_6	-71.5
B_1C_2	74.5	B_4C_5	74.5
B_2C_1	-71.0	B_5C_4	-73.5
B_2C_3	74.5	B_5C_5	71.5
B_2C_2	-73.5	B_5C_5	-74.5
B_3C_4	71.5	B_6C_1	71.5
B_1C_3	-73.0	B_1C_3	-70.5
C_1D_2	74.5	C_4D_5	73.0
C_2D_1	-70.5	C_5D_4	-72.5
C_2D_3	75.5	C_5D_6	74.5
C_3D_2	-71.5	C_6D_5	-73.5
C_3D_4	71.5	C_6D_1	73.5
C_4D_3	-74.5	C_1D_6	-71.5
D_0D_4	10.2	D_0D_5	-81.6
D_0D_6	104.5		

X. *The Motion of an Air Bubble rising in Water.* By
OTOGORÔ MIYAGI, *Professor of Hydraulics and Hydraulic
Engineering in the Tôhoku Imperial University, Sendai,
Japan* *.

[Plate III.]

ABSTRACT.

Air bubbles of various sizes moving up in still water are carefully treated experimentally and then theoretically. Their terminal velocities are determined in relation to their sizes, and the changes of their shapes during their motion are investigated.

The mass of water carried up with a moving bubble and the resistance to its motion are determined, and the most probable equation of motion is proposed. It is also proved that there are two different kinds of motion of a bubble in water exactly analogous to the stream-line and the turbulent flows of a viscous fluid, which passes from the one to the other distinctly at the critical radius of the bubble.

* Communicated by the Author.

1. INTRODUCTORY.

AIR bubbles are formed in water naturally or artificially. As in a water-turbine or a pump, atmospheric air naturally mixed with water expands to form large bubbles in the space where the pressure is very low, as in the draught- or suction-tube, which destroy the effective action of the machine. As in an air-lift pump, air is purposely admitted in the water deep in a well to make it form bubbles rising in the eduction pipe, and their sizes and forms affect greatly the action of the pump.

The forces acting on an air bubble rising in water may be classed as the surface tension, the upward force due to buoyancy, and the resistance to motion offered by the surrounding water.

The surface tension acts to keep the bubble spherical as the most stable form, while the resistance makes it deform in a flattened shape, and, owing to the result that it moves up with the minimum resistance acted upon, it shows some peculiar outline as to its form and passage.

The smaller the bubble, the larger the effect of surface tension to keep it spherical becomes in comparison with the resistance, the more it resembles a true spherical shape and the more stable it is. When the bubble is large, the effect of the surface tension is small compared with the resistance, and it displays some peculiarly flattened outline, which is very unstable, changing its shape momentarily with some oscillating features.

A very small bubble, therefore, may be regarded approximately as a sphere, and, with some suitable assumptions, its motion may be treated mathematically; but for a large bubble as is common in practical cases the simple mathematical treatments cannot by any means be applied in order to solve even approximately its motion in water.

The present object is, for an air bubble of a practical size, to study its motion in water from accurate experiments and to find the law of resistance connected with mathematical considerations. For very small bubbles up to the radius of 0.0385 cm. valuable experiments have already been carried on by Mr. H. S. Allen*, which will be referred to later on.

* *Phil. Mag.*, Sept. and Nov. 1900.

II. DESCRIPTION OF THE EXPERIMENTAL APPARATUS.

The apparatus consisted of an experiment vessel, a recording drum, a flash-light apparatus, and a tuning-fork.

The experiment vessel was made of two rectangular flat glass plates about 13 cm. in width and 30 cm. in height, set vertically and secured firmly by a metal holder about 2.4 cm. apart to form a transparent rectangular box to retain water, in which an air bubble was made to rise.

The recording drum was a cylindrical drum of 20 cm. in diameter and 26 cm. in height, made of aluminium casting, which was caused to rotate by an electric motor. This drum was set vertically and rotated horizontally with a bromide paper to be used in an ordinary photographic process wrapped round it. A stationary cylindrical case of about 22 cm. in diameter made of copper plate was set concentric to enclose the drum to protect the bromide paper against any light. A vertical window extending about the whole length of this case in the form of a narrow slit was made in it, the width of which was made adjustable by a sliding door in contact with the window, through which the bromide paper was exposed to the flash-light.

The flash-light apparatus consisted of a 500 candle-power incandescent lamp encased in a wooden box and a rotating disk. The disk was made of a wooden plate of 45 cm. in radius, and it had eight radial slots each of 2 cm. in width and 25 cm. in radial length uniformly spaced. This was placed about 60 cm. in front of the box to rotate in a vertical plane with a horizontal shaft by an electric motor. On the front face of the box there was made a vertical slot of 3 cm. in width and 25 cm. in length, through which the light from the incandescent lamp was projected on the face of the disk, which was so placed that at the moment that the slot on the disk came in line with that on the box a flash of light was passed through the disk to project it on the bromide paper through the vertical window mentioned above.

The tuning-fork was used to record accurately the velocity of rotation of the recording drum. It was one of a frequency of 82 vibrations per sec. A small mirror was put on its edge by which the light from a point-light was reflected on the bromide paper. The point-light was encased in a box furnished with a small hole fitted with a convex lens to lead the light through it, and a second convex lens was placed in front of the hole by means of which the point-light image was focussed on the bromide paper to get a fine wave-line on

it, by which the time of rotation of the recording drum was accurately recorded.

Figs. 1 and 2 show diagrammatically the elevation and the plan respectively of the experimental apparatus. The adjustable window in the stationary protecting case set concentric with the recording drum was set in line with the incandescent lamp, and the experiment vessel was placed immediately in front of it. The tuning-fork was so

Fig. 1.

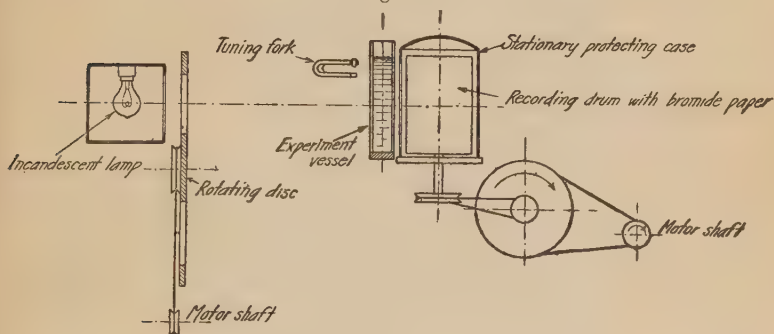
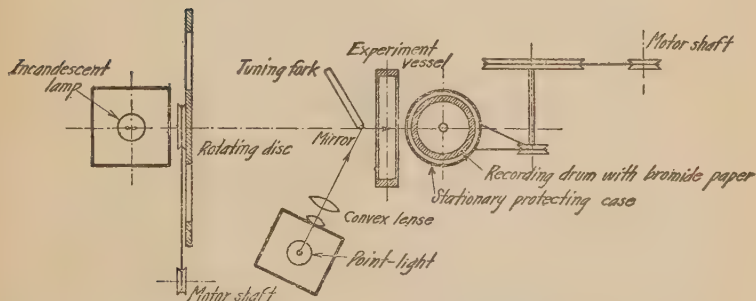


Fig. 2.



placed in front of this vessel that the point-light image was projected on the bromide paper through the water space.

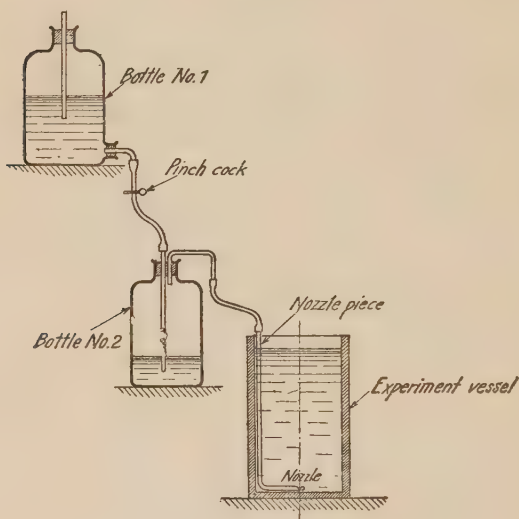
The experiment vessel was placed as near as possible to the recording drum, while the flash-light apparatus was set far away from it in order to get an approximately horizontally projected shadow of the air bubble on the bromide paper. Actually the distance from the bromide paper to the centre line of the experiment vessel was about 2.3 cm., and that to the incandescent lamp was about 156 cm., so that the error deviating from the horizontal projection was almost negligible.

All the above apparatus were set up in a dark room.

III. METHOD OF MAKING A BUBBLE.

Fig. 3 is a diagrammatic view showing the method of making a bubble in the experiment vessel. The bottles No. 1 and No. 2 were set at different levels, and they were connected

Fig. 3.



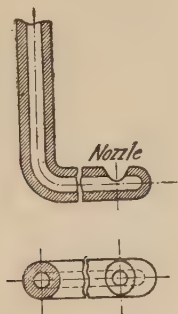
by an india-rubber tubing fitted with a pinch-cock by which the formation of the bubble at the nozzle was regulated at will.

The nozzle-piece was made of a fine glass tube bent at right angles, closed at the end, and it was connected to bottle No. 2 by an india-rubber tubing as shown in fig. 3. Near the closed end of this nozzle-piece a nozzle was made, which was formed by grinding off cylindrically by a bar with emery-powder so as to open a sharp-edged mouth, the elevation and the plan of which are shown in fig. 4. The sizes of bubbles being dependent on the sizes of the nozzle, several nozzle-pieces of different diameters with different sizes of nozzles were made.

The nozzle-piece was sunk into the water in the experiment vessel, as shown in fig. 3, setting the nozzle at the centre of the vessel near its bottom. Special care was paid in this case in order to set the edge of the nozzle symmetrically

about the vertical axis, which was absolutely necessary to get a symmetrical bubble free from initial disturbance.

Fig. 4.



Such a bubble would rise initially vertically upwards, otherwise it would rise in an inclined direction with an initial impulsive disturbance which had a great influence on its motion.

IV. MEASUREMENT OF THE SIZES OF BUBBLES.

On opening the pinch-cock slightly the water in the nozzle-piece would be first expelled slowly from the nozzle by the pressure of the air and then the air would appear at the nozzle which gradually grew large and finally separated from it as a free bubble.

On watching the formation of the bubble carefully, adjusting the pinch-cock so that the bubble was formed as slowly and steadily as possible, it was observed that its convex top gradually swelled from a hemisphere to a sphere just at the moment of leaving the nozzle. A microscope with a measuring scale inside was set horizontal to observe this action and to measure the diameters of such spherical bubbles just at the moment of their leaving the nozzle.

Bubbles successively formed from a given nozzle leaving the pinchcock untouched being observed to be the same in all respects, the experiment was made on a bubble which was formed a little after the one the diameter of which was measured.

V. METHOD OF CONDUCTING EXPERIMENT.

The speeds of the electric motors to drive the recording drum and the rotating disk were adjusted previously to suit the experiment. These speeds had to be in a good relation with the amount of the opening of the adjustable window made on the stationary protecting case to get fine successive photographs of a bubble on the bromide paper.

The water in the experiment vessel was saturated with air previous to the experiment causing air bubbles to rise in it for a long time, in order to avoid the absorption of air from the bubble in the course of the experiment.

Now, for conducting an experiment, a bromide paper was secured firmly around the recording drum with cramps arranged to it, and the protecting case was put on it with adjustable window closed. The pinch-cock was adjusted to give off successive bubbles very slowly in the water in the experiment vessel, and the diameter of one of them was measured accurately by the measuring microscope, the process being made under a red or ordinary incandescent lamp as the case might be. The temperature of the water was read on the thermometer inserted in the experiment vessel.

The adjustable window was then opened to the amount previously adjusted, the electric motors were started and the tuning-fork was set in action. The 500 candle-power incandescent and the point-light lamps were now lighted at as nearly the same time as possible, and they were put out after the recording drum had made about a complete rotation.

The protecting case was then removed, the bromide paper was taken off, and the only thing remaining was to develop this bromide paper. This was done in the same room after each experiment was performed.

VI. EXPERIMENTAL RESULTS.

Terminal Velocity with which a Bubble rises vertically upwards.—Figs. 1 to 5 (Pl. III.) show some of the photographic pictures taken by developing the bromide paper as above mentioned with a reduced scale. (The complete sheet of a bromide paper contains usually one or more than one of such pictures arranged in series by successive bubbles which rise almost periodically one after the other. Here we have shown one of them taken out of each sheet.) Each of them shows the successive shapes and positions of a bubble distributing between the successive photographs of the nozzle used and one continuous vibration curve of the tuning-fork.

The shadows of the nozzle and the bubble obviously being projected at the same time by one flash, the successive photographs of the nozzle and the corresponding photographs of the bubble will be easily pointed out on a given picture. The number of vibrations of the tuning-fork between any two consecutive photographs of the nozzle being directly counted on it, the time occupied by the bubble to move from one position to the next can be easily determined, and the vertical distance between any two consecutive photographs of the bubble divided by this time will be the mean vertical velocity at that position.

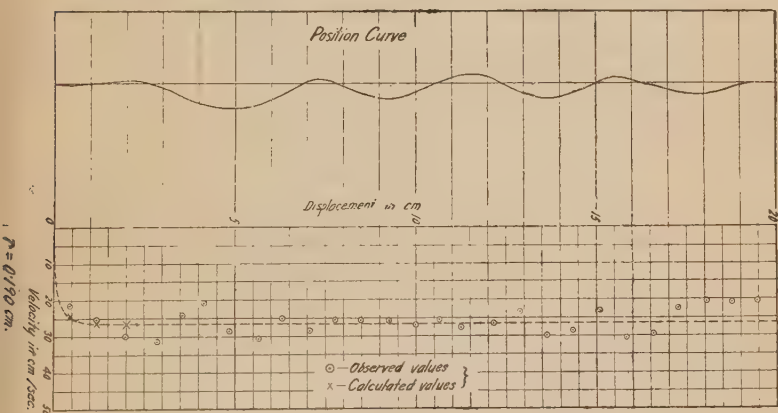


Fig. 5.

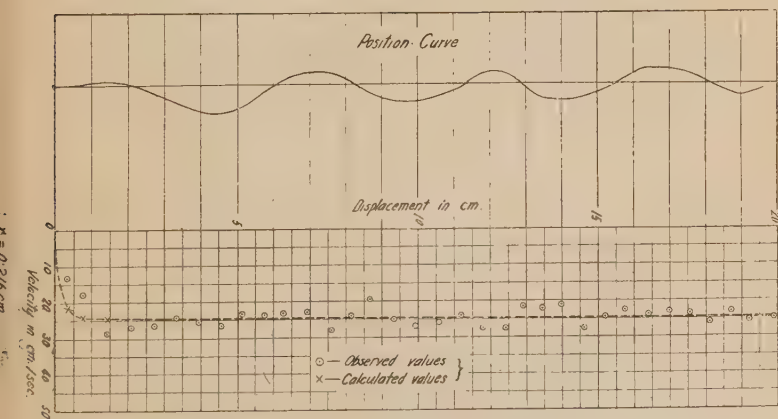


Fig. 6.

Such velocities were calculated at every position of the bubble on each picture, and they are plotted on a squared paper against the displacement or the height of the bubble above the nozzle to show diagrammatically the velocities of

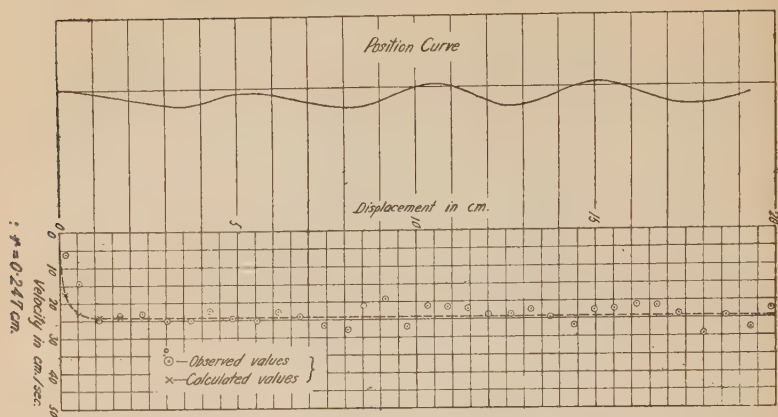


Fig. 7.

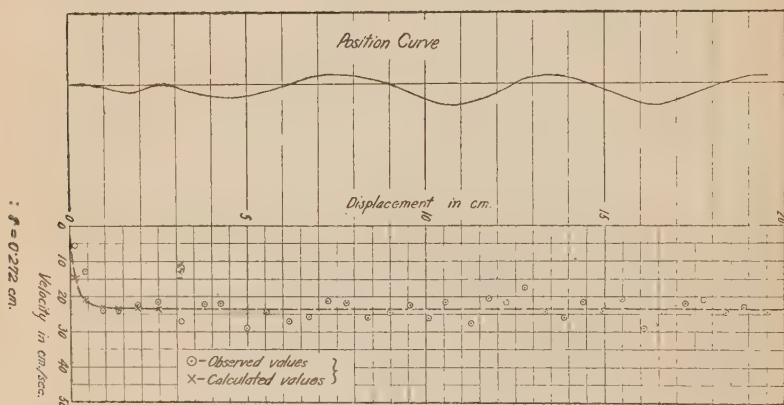


Fig. 8.

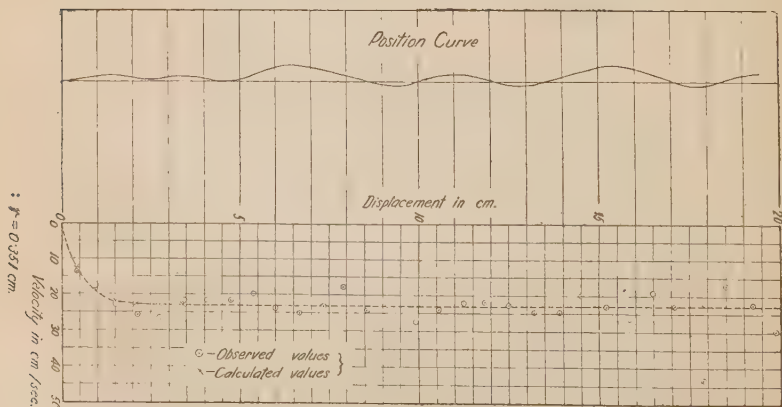


Fig. 9.

the bubble with respect to its positions. Figs. 5 to 9 show some of such diagrams, the averaging curve being drawn on each of them, and we can see from these curves that all the bubbles attain their constant terminal velocities almost as soon as they have left the nozzle.

As the effect of the depth of water on the size of the bubble in the present experiment was negligibly small and was assumed to be unchanged during its passage, the above fact shows that for a bubble of a given size there is always a fixed velocity of rise. Table I. gives the experimental results showing the relation between the sizes of bubbles and their terminal velocities.

Fig. 10.

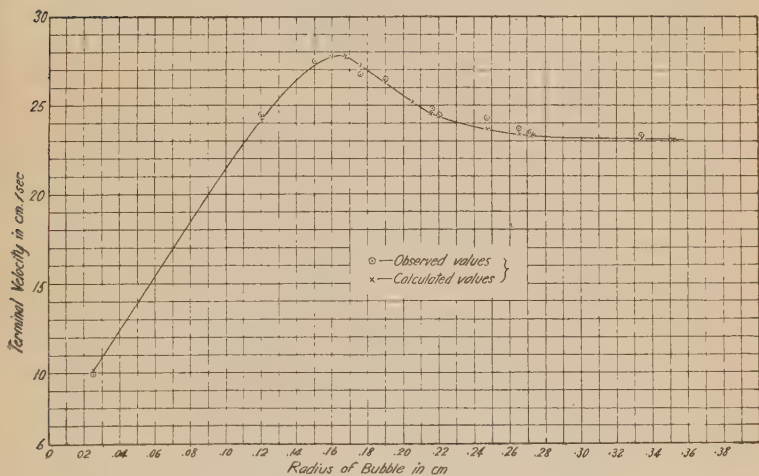


Fig. 10 shows the above results by a curve, on which the points with circular marks are those plotted in accordance with the experiments, and those with cross marks are those calculated from the formula deduced by the writer to be explained later on.

For very small bubbles, as up to the radius of 0.0385 cm. Mr. Allen gave a straight-line relation between their radii and velocities, and according to the present experiment, with reference to fig. 10, his conclusion may be acknowledged to extend approximately to one of the radius of about 0.12 cm. without appreciable error, although we have no experimental results of bubbles of the sizes lying between the radii of

0.025 cm. and 0.12 cm. to prove the statement owing to the difficulty of making such small bubbles.

For larger bubbles than the radius of about 0.12 cm. the velocities increase in a less ratio than proportional with their radii showing some curvature in the curve, and soon after there occurs a maximum velocity of about 27.8 cm. per sec. corresponding to a bubble of the radius of about 0.165 cm. Then the curve falls and tends to be directed horizontally, showing that the velocity decreases contrary to the radius and tends to a final constant velocity of about 23.1 cm. per sec. for bubbles larger than a radius of about 0.33 cm.

The above results are of course dependent on the temperature of the water which has an influence on the viscous resistance to the motion of bubbles, but under the range of temperature experienced by the present experiments, the temperature effect on the viscosity of the water being negligibly small, they can be taken as correct for water at an average of 18° C.

We may infer from the above phenomena that when the bubble is very small the buoyancy increases in the same proportion as the resistance showing the velocity increasing proportionally with its size, and there is a limit of proportionality, after which the resistance comes to act with an increasing proportion to its buoyancy, and at the end of which the velocity shows its maximum value. Then the velocity decreases contrary to its size owing to the rapidly increasing resistance, which tends gradually to the state of counterbalancing of the resistance with the buoyancy, showing a final constant velocity irrespective of its size.

When the bubble is very small it is considered to assume nearly a stable spherical shape, as already mentioned, and its velocity curve is shown by the straight ascending part in fig. 10. When the bubble is sufficiently large its shape deviates greatly from the sphere which is exposed to the greater proportional resistance, and its velocity curve is shown by the descending part in fig. 10. When the bubble is very large it becomes very unstable, subjected to the greater resistance and buoyancy, and its velocity is shown by the straight horizontal part in fig. 10. Such a large bubble has a tendency to divide into smaller ones.

Course of a Bubble.—If a bubble should rise on a vertical straight course, the centre of its photograph in figs. 1 to 5 (Pl. III.) would have to be in the vertical line drawn at the centre of the corresponding photograph of the nozzle in all its positions. In order to test this, vertical lines were drawn at

the centres of the successive photographs of the nozzle on each photographic picture as shown in figs. 1 to 5 (Pl. III.) and it was found that the photographs of a bubble did not lie on such lines, some being on the right and others being on the left, indicating that the course of the bubble was never a vertical line. It loiters about that line, dashing in every direction, tracing a course like a helix round it, as observed from the top of the experiment vessel looking down into the water.

To see such a course, the successive positions of the centre of a bubble were plotted about a vertical line, and we obtained the diagram as shown on the left-hand space in figs. 5 to 9, by which it can be easily understood how it loiters about the line as it ascends through the water. This, of course, shows its projection on a vertical plane parallel to the face of the experiment vessel, and supposing such a course to be shown also on a vertical plane perpendicular to the above, the course traced in space can be imagined to be a kind of helix.

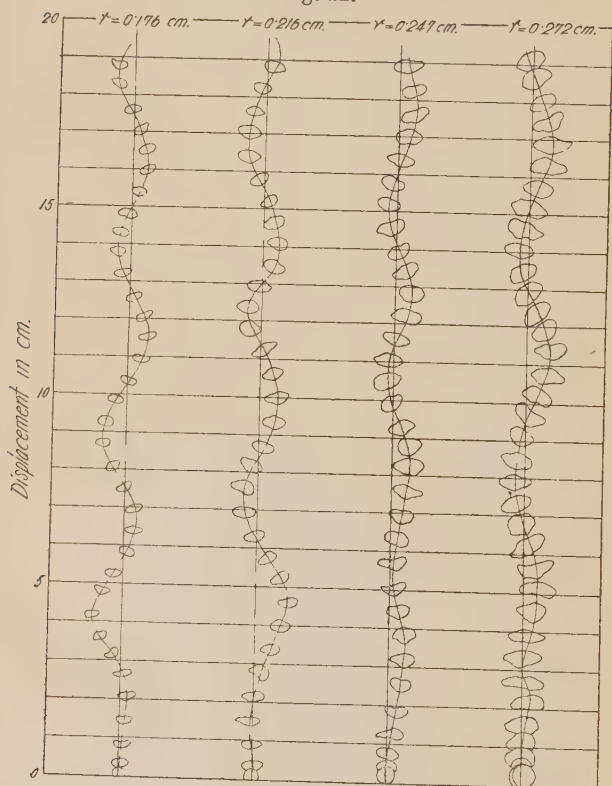
Variation of the Shape of a Bubble in its Course.—If a bubble always kept a regular symmetrical shape in all respects about the vertical line through its centre of gravity, its course would be a vertical line. The shape, however, is never symmetrical owing to the very slight initial disturbance which by no means can be avoided as a practical problem, and it traces a course as explained above about the vertical line.

The deviation of its course from a vertical line thus being due to its deformation from symmetry, there must be a certain relation between the change in its shape and the position in its course. For the purpose of testing this, with some comparatively large bubbles in order to see it clearly, the outline shapes of each of the bubbles were carefully traced and put on the corresponding positions plotted about a vertical line as shown in fig. 11, by which we can see, at a glance, that there are certain regular changes of shape along their courses, and after a close observation we can find that the major axis of any bubble is always perpendicular to its course, that is, it moves always with its flattened face directed ahead, the reason of which can be explained as follows :—

Fig. 12 is a diagrammatical sketch showing the successive changes of the shape of a bubble along its upward course, assuming the motion to occur in a two-dimensional space. Suppose a bubble at the position A to dash or to move in the

inclined direction AB to the vertical XY, acted upon by some practically unavoidable initial disturbance, then the resistance acting upon the front face of the bubble retards its motion, and makes it flat in the direction AB and pause for a while at the position B. The course will now change in the

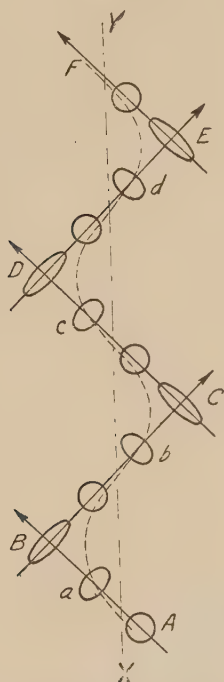
Fig. 11.



direction BC by the action of gliding, due to its buoyancy, at first accelerating and then retarding, changing its shape from B to C with the flattened face directed towards BC, and it pauses again at the position C. Then its course will change in the direction CD and then in the direction DE, alternately repeating a similar movement, showing a resultant zig-zag passage like ABCDEF about the vertical XY.

The above is the result of the two-dimensional motion. In a three-dimensional space, however, the bubble does not go so far as such positions as B, C, D, E where it pauses for a while, but it continues its motion round the vertical XY, but it continues its motion round the vertical XY,

Fig. 12.



keeping its shape flattened in the direction of motion by the head resistance as shown at *a*, *b*, *c*, *d*, etc. The course of the bubble, therefore, is a helix round the vertical as shown with a broken line, and it keeps its major axis always perpendicular to this course.

VII. THEORETICAL INVESTIGATION.

Comparison of Stokes' and Allen's Conclusions.—From the measurement of terminal velocities of small bubbles Mr. Allen* has given his conclusions that the terminal velocity acquired by a small bubble ascending through a viscous fluid is the same as that which would be acquired by a solid

* Phil. Mag., Sept. and Nov. 1900.

sphere, and that when the motion is very slow the velocity of a bubble agrees with that deduced from theoretical considerations by Stokes, and for greater velocities he has given his own formula. His experiments, however, were limited to very small bubbles up to a radius of 0.0385 cm. As for the motion of a solid sphere in a viscous fluid there are many authorities, such as G. Stokes, R. S. Woodward, H. S. Allen here mentioned and others, but there are few who have treated air bubbles of practical sizes, a subject most useful from the practical point of view.

The formula introduced by Stokes is as follows :—

$$v = \frac{2}{9} g r^2 \frac{\rho - \sigma}{\eta} \frac{\beta r + 3\eta}{\beta r + 2\eta},$$

where v = constant velocity (terminal velocity),

r = radius of the sphere,

η = viscosity of the liquid,

β = coefficient of the sliding friction,

ρ = density of the liquid,

and σ = density of the sphere.

Under the assumption that there is no slipping on the surface of the sphere assuming a capillary flow, β is infinity, and writing $\eta = \mu\rho$, so that μ is the kinematic coefficient of viscosity, we shall have

$$v = \frac{2}{9} g r^2 \frac{\rho - \sigma}{\mu\rho}^*, \quad . \quad . \quad . \quad . \quad . \quad (1)$$

which shows that the terminal velocity varies as the square of the radius of the sphere, the velocity curve against the radius being a parabola.

For greater velocities exceeding a definite critical value, Allen has deduced the formula :

$$v = \frac{1}{2} \left(\frac{\rho - \sigma}{\rho} g \right)^{\frac{2}{3}} \frac{r - \frac{2}{5} \bar{r}}{\mu^{\frac{1}{3}}},$$

where \bar{r} is the value of r which makes $vr = \mu$, so that when β is infinity it gives such a value as is expressed by

$$\bar{r}^3 = \frac{9\mu^2\rho}{2g(\rho - \sigma)}.$$

Allen's formula will be, therefore,

$$v = \frac{1}{2} \left(\frac{\rho - \sigma}{\rho} g \right)^{\frac{2}{3}} \left\{ \frac{r}{\mu^{\frac{1}{3}}} - \frac{2}{5} \left[\frac{9\mu\rho}{2g(\rho - \sigma)} \right]^{\frac{1}{3}} \right\}, \quad . \quad . \quad (2)$$

and this shows that the terminal velocity varies linearly as the radius of the bubble.

* Whetham, Phil. Trans. 1890, and Allen, Phil. Mag., Sept. and Nov. 1900.

Table II. gives the velocites of air bubbles moving upwards in water calculated from the above formulæ and the corre-

TABLE I.

Temperature, Deg. C.	14	18	26	18.8	23.7	12	14	12	15	21	18	23	21
Radius of Bubble, cm.025	.12	.15	.176	.19	.205	.216	.22	.247	.265	.272	.334	.351
Velocity of Bubble, cm./sec.	9.85	24.5	27.5	26.75	26.5	25.5	24.85	24.5	24.3	23.75	23.5	23.35	23.0

TABLE II.

Temperature, Deg. C.	14	18	26	18.8	12
Radius of Bubble, cm.025	.12	.15	.176	.205
Velocity in cm./sec. (observed)	9.85	24.5	27.5	26.75	25.5
Velocity in cm./sec. (calculated from Stokes' formula)	11.55	295.0	542.7	548.3	734.2
Velocity in cm./sec. (calculated from Allen's formula)	4.63	26.2	34.95	39.02	42.8

TABLE III.

Radius of Bubble, cm.025	.12	.15	.176	.19	.205	.216	.22	.247	.265	.272	.334	.351
Velocity, cm./sec.	9.85	24.5	27.5	26.75	26.5	25.5	24.85	24.5	24.3	23.75	23.5	23.35	23.0
Value of $\phi^{1/2}$0257	.1087	.1353	.1779	.2002	.2378	.2574	.2694	.321	.368	.3866	.5295	.5791

sponding actual ones measured from the experiments. From this table we can at once observe that Stokes' parabolic

formula is applicable only when the bubble is very small, and that, for the larger ones, Allen's linear formula holds somewhat approximately.

Both of these formulæ, however, show that the velocity increases without limit as the size of the bubble increases, which seems questionable from a mere common-sense point of view, and how could the existence of a maximum velocity be expected from them as shown by a curve in fig. 10? It is naturally misleading to compare a bubble with a solid sphere, and any formula deduced from the analogy of a solid sphere cannot be applied to a bubble except in the case of very small ones. The shape of a bubble is never spherical; it changes momentarily throughout its course. It is not so simple that it may be compared with a solid and be represented by a simple formula obtained from the mere analogy of a solid.

Equation of Motion.—For considering the equation of motion of an air-bubble in water the following assumptions will be made :—

- (1) The volume of the bubble is constant during its motion.
- (2) The bubble moves up along a vertical straight course.

The depth of water in the experiment vessel used in the present experiment being about 25 cm. and the change of volume at the surface being only 0.02 or 1/50 time of volume at the bottom, the first assumption will be justified without any sensible error. The second assumption differs somewhat from the actual motion, but it may to some extent be justified.

From a close inspection of a moving bubble we found that there always remained an upward current of water which moves after the bubble, and the larger the bubble the larger the mass of the upward current was. This is an indication that a bubble does not perfectly slip in its motion, but it carries with it a certain mass of surrounding water depending on its size.

On this consideration, and with the assumption that the resistance to motion varies as the square of the velocity, as is usual in treating of the motion of a body in a viscous fluid, we have assumed the following equation of motion, taking the axis of z upwards to be positive :—

$$\left(\sigma V + \frac{1}{k} \rho V\right) \frac{d^2 z}{dt^2} = g(\rho - \sigma)V - \phi \left(\frac{dz}{dt}\right)^2, \dots (3)$$

where σ = density of the air,
 ρ = density of the water,
 V = volume of the bubble,
 ϕ = coefficient of resistance depending on the size of the bubble,
 and k = coefficient depending also on the size of the bubble.

In this equation, $\frac{1}{k} \rho V$ is the mass of water carried up with the bubble under the assumption that it is $1/k$ times of the mass of water displaced by it and $g(\rho - \sigma)V$ is the buoyancy.

Under standard pressure and at the average temperature of 18°C , σ is as small as 0.0012 in C.G.S. units, which is negligible in comparison with ρ , and the mass of water carried up by the bubble seems to be so great that the mass of air in it is also negligible. The above equation then may be written in the form :—

$$\frac{1}{k} \rho V \frac{d^2 z}{dt^2} = g \rho V - \phi \left(\frac{dz}{dt} \right)^2$$

or
$$\frac{d^2 z}{dt^2} = kg - \frac{k\phi}{\rho V} \left(\frac{dz}{dt} \right)^2 \dots \dots \dots (4)$$

Putting
$$\frac{dz}{dt} = \xi \text{ and } \frac{k\phi}{\rho V} = A,$$

it gives
$$\frac{d\xi}{dt} = kg - A\xi^2,$$

or
$$dt = \frac{d\xi}{kg - A\xi^2};$$

and integrating we obtain

$$t = \frac{1}{2\sqrt{kgA}} \log \frac{\sqrt{kg} + \xi \sqrt{A}}{\sqrt{kg} - \xi \sqrt{A}} + C.$$

At the beginning of the motion when $t=0$, the velocity of the bubble ξ is zero, so that the integration constant C in the above equation is zero. Hence we have :—

$$t = \frac{1}{2\sqrt{kgA}} \log \frac{\sqrt{kg} + \xi \sqrt{A}}{\sqrt{kg} - \xi \sqrt{A}}$$

or
$$\exp(2t \sqrt{kgA}) = \frac{\sqrt{kg} + \xi \sqrt{A}}{\sqrt{kg} - \xi \sqrt{A}},$$

from which solving for ξ we get

$$\xi = \sqrt{\frac{kg}{A}} \left[1 - \frac{2}{1 + \exp(2t\sqrt{kgA})} \right],$$

or
$$\frac{dz}{dt} = \sqrt{\frac{g\rho V}{\phi}} \left[1 - \frac{2}{1 + \exp\left(2kt\sqrt{\frac{g\phi}{\rho V}}\right)} \right] \quad (5)$$

This is the expression for the velocity of the bubble with respect to the time.

Again integrating the above equation we get

$$z = \sqrt{\frac{g\rho V}{\phi}} \left\{ t - 2t + \frac{1}{k\sqrt{\frac{g\phi}{\rho V}}} \times \log \left[1 + \exp\left(2kt\sqrt{\frac{g\phi}{\rho V}}\right) \right] \right\} + C.$$

Taking the origin at the centre of the nozzle where the motion starts, we have $z=0$ when $t=0$, and the integration constant C in the above equation is

$$C = -\sqrt{\frac{g\rho V}{\phi}} \cdot \frac{1}{k\sqrt{\frac{g\phi}{\rho V}}} \log 2,$$

and we have

$$z = -\sqrt{\frac{g\rho V}{\phi}} t + \frac{\rho V}{k\phi} \log \frac{1 + \exp\left(2kt\sqrt{\frac{g\phi}{\rho V}}\right)}{2} \quad (6)$$

This is the equation expressing the relation between the position and the time of a bubble.

As the terminal velocity is a constant velocity, as already said, it must be such that it is independent of t , and with reference to (5), if v be the terminal velocity, it must be

$$v = \sqrt{\frac{g\rho V}{\phi}}, \quad (7)$$

and the corresponding expression for z will be

$$z = z_1 + \sqrt{\frac{g\rho V}{\phi}} (t - t_1), \quad (8)$$

z_1 being the displacement at time t_1 after the terminal velocity is passed.

If r be the radius of the bubble measured just at the moment of its leaving the nozzle, when its shape is a sphere, its volume V will be equal to $\frac{4}{3}\pi r^3$, and we have by (7) :

$$\phi^{1/2} = \frac{\sqrt{g\rho V}}{v} = \sqrt{\frac{4}{3}\pi g\rho} \frac{r^{3/2}}{v},$$

which in C.G.S. units gives

$$\phi^{1/2} = 64 \cdot 10 \frac{r^{3/2}}{v} \quad \text{or} \quad \phi = 4110 \frac{r^3}{v^2}. \quad . \quad . \quad (9)$$

The resistance to motion of a bubble with a terminal velocity will be, therefore,

$$\text{Resistance} = \phi v^2 = 4110 r^3, \quad . \quad . \quad . \quad (10)$$

that is, the resistance is proportional to the cube of its radius or to its volume, and not to its projected area as often may be expected.

Table III. shows the value of $\phi^{1/2}$ calculated from the above equation with r and v obtained from the present experiment, and fig. 13 shows diagrammatically the relation between r and $\phi^{1/2}$, by which it can be seen how the value of $\phi^{1/2}$ increases with respect to the radius.

Equations (5) and (6) are applicable only before the terminal velocity is reached, and in that case, if z_0 be the displacement at time t_0 , (6) will give

$$z_0 + \sqrt{\frac{g\rho V}{\phi}} t_0 = \frac{\rho V}{k\phi} \log \frac{1 + \exp\left(2kt_0 \sqrt{\frac{g\phi}{\rho V}}\right)}{2},$$

or putting

$$\left(z_0 + \sqrt{\frac{g\rho V}{\phi}} t_0\right) \frac{\phi}{\rho V} = P, \quad \text{and} \quad \sqrt{\frac{g\phi}{\rho V}} t_0 = Q,$$

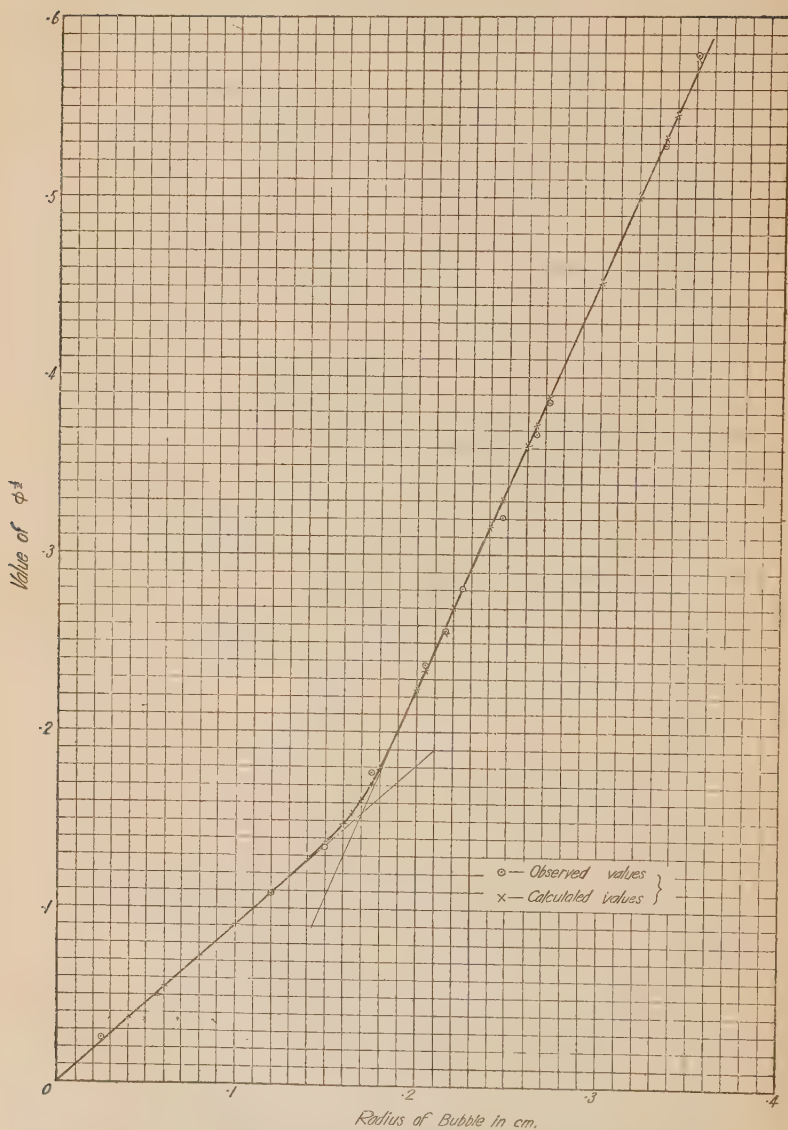
we have

$$kP = \log \frac{1 + \exp(2kQ)}{2}$$

$$\text{or} \quad 2 \exp(kP) = 1 + \exp(2kQ) \quad . \quad . \quad . \quad (11)$$

The experimental coefficient k can be determined by solving this equation, which can be accomplished most conveniently by graphical means, and in order to do this the first thing will be to calculate the values of P and Q . The values of $\phi^{1/2}$ in the expression of P and Q are given in Table III., and the question is what values are to be given

Fig. 13.



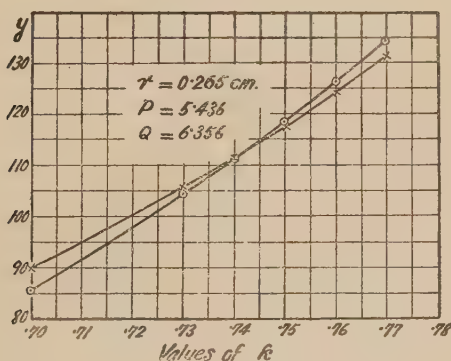
for z_0 and t_0 . Strictly speaking, all the values of z_0 and t_0 must satisfy (11), if we take them in the course of time before the terminal velocity is reached. Actually, however, the bubble attains its terminal velocity almost as soon as it

has left the nozzle, and the "critical position," that is, the position at which the terminal velocity is first attained, is very near to the nozzle, and it is difficult to find the correct values for z_0 and t_0 . Here we have taken the middle point of the displacement to the critical position for z_0 and corresponding time for t_0 measured on the averaging curves, some of which are shown in figs. 5 to 9, to get rid as much as possible of the errors. The values of P and Q calculated by such procedure are given in Table IV.

How the calculated results with such values of P and Q coincide closely with the actual results can be seen in figs. 5 to 9, in which the points with circular marks are those plotted in accordance with the experiments, and those with cross marks are those calculated from (5) and (6).

The graphical solution of (11) is made by plotting two curves $y=2\exp(k\rho)$ and $y=1+\exp(2kQ)$ for various values of k with given values of P and Q . The value of k read at the intersection of these curves is the value of k to be found which satisfies (11). Figs. 14 and 15 show only two of such

Fig. 14.



solutions applied as examples to the bubbles of the radii of 0.265 cm. and 0.351 cm. In Table V. the values in the third column give the values of k obtained by such graphical solutions.

In the fourth column in Table V. the values of kr^2 are given, by which we can see at a glance that kr^2 is approximately constant, irrespective of the size of the bubbles, the mean value of it being 0.054. We have, therefore,

$$kr^2 = \text{constant} = 0.054 \dots \dots (12)$$

Fig. 15.

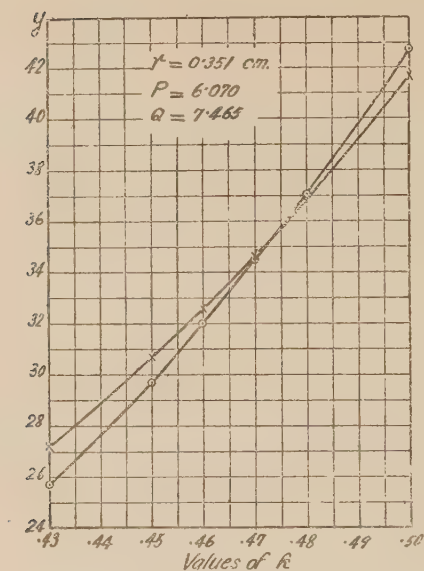


TABLE IV.

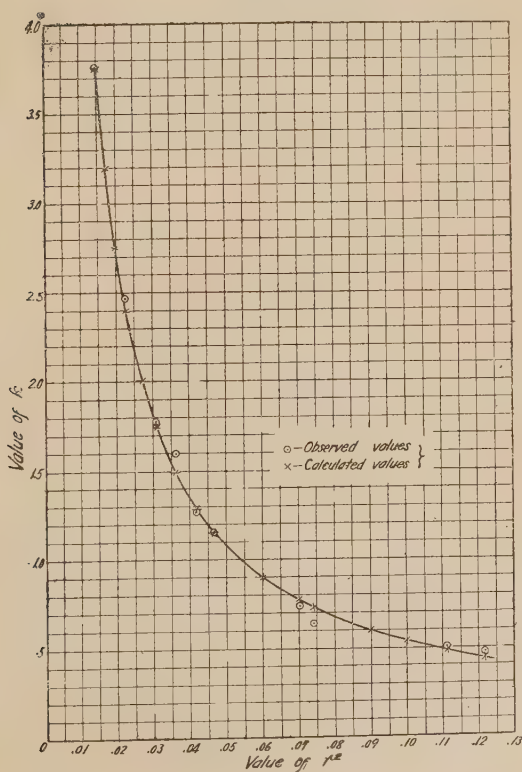
Radius of Bubble. cm.	z_0 . cm.	t_0 . sec.	Value of P.	Value of Q.
.12	1.25	.0556	4.267	4.451
.15	1.35	.0570	3.779	4.060
.176	1.35	.0611	4.088	4.478
.19	1.33	.0618	4.140	4.567
.205	1.33	.0663	4.553	5.096
.216	1.30	.0673	4.718	5.310
.265	1.30	.0770	5.436	6.356
.272	1.34	.0824	5.813	6.871
.334	1.30	.0872	5.996	7.320
.351	1.262	.0876	6.070	7.465

The last column in Table V. shows the values of k calculated from this equation, and fig. 16 shows the points plotted according to the third and the last columns in Table V., by which their close coincidence can be seen.

TABLE V.

Radius of Bubble, r cm.	Value of r^2 .	Value of k (observed).	Value of kr^2 .	Value of k (calculated).
·12	·0144	3·76	·05414	3·75
·15	·0255	2·47	·05558	2·40
·176	·0310	1·78	·05514	1·74
·19	·0361	1·60	·05776	1·50
·205	·0420	1·27	·05337	1·285
·216	·0467	1·165	·05435	1·16
·265	·0702	·74	·05197	·7695
·272	·0740	·64	·04735	·730
·334	·1116	·505	·05634	·785
·351	·1232	·47	·05790	·439

Fig. 16.



The physical meaning of $kr^2 = \text{constant}$ is that the percentage mass of water carried up with a bubble is proportional to the square of its radius or to its surface area.

Terminal Velocity.—Referring to fig. 13 we may see that the points of $\phi^{1/2}$ plotted against r are distributed approximately on the two kinds of straight lines intersecting at the point of about $r = 0.17$ cm. and $\phi^{1/2} = 0.154$. This indicates that there are two kinds of motion of bubbles which are governed by the different proportional resistance, and the resistance almost suddenly increases to a larger proportion at the "critical radius," which is the radius of the bubble at which the above two straight lines intersect. According to the present experiment the critical radius is, therefore, about 0.17 cm.

From the analogy of the stream-line and turbulent motions of the flow of fluid which are distinguished by the critical velocity, we may conclude that in the case of a moving bubble a kind of turbulent motion suddenly takes place in the space surrounding the bubble, when the bubble is equal to the critical radius, and that it makes its shape and passage unstable to make it display a greater rate of resistance. This fact can be clearly understood by examining the shapes and passages of the bubble in the photographs. It follows, therefore, that the velocity will be a maximum for a bubble of critical radius.

According to the method of least squares the equations of the above two straight lines are :

$$\phi^{1/2} = 0.9055 r$$

and

$$\phi^{1/2} = 2.305 r - 0.2374,$$

the inclinations to the axis of r being $42^\circ 10'$ and $66^\circ 33'$ respectively, and the coordinates of the point of intersection being $r = 0.17$ and $\phi^{1/2} = 0.154$.

With reference to fig. 10 we cannot discover any discontinuity on the curve of v against r . It follows, therefore, that on the curve of $\phi^{1/2}$ against r there must not be a perfect discontinuity. Hence, in fig. 13, it is proper to see the curve as one continuous curve instead of seeing it as the combination of two straight lines. On this consideration and also for mathematical convenience, we have assumed it to be a hyperbola of the second order which has these straight lines as its asymptotes. Then, with these asymptotes as the oblique coordinate axes X and Y , the equation of the hyperbola has been found to be

$$XY = 0.000108,$$

from which the following formula has been deduced :

$$\phi + (0.236 - 3.2r)\phi^{1/2} + (2.07r^2 - 0.211r - 0.000282) = 0 \quad (13)$$

and solving $\phi^{1/2}$ from this we have

$$\phi^{1/2} = 1.6r - 0.118 + \sqrt{0.49r^2 - 0.167r + 0.0142}. \quad (14)$$

Table VI. shows the values of $\phi^{1/2}$ calculated from this formula against their observed ones given in Table III., and fig. 13 shows these plotted on a diagram, by which their close coincidence can be seen.

With calculated values of $\phi^{1/2}$ the terminal velocities can be determined by (9). In order to obtain a formula for the terminal velocity, substitute $\phi^{1/2}$ given in (9) in (13), then the following will result :

$$(2.07r^2 - 0.211r - 0.000282)v^2 + (15.1 - 205r)r^{3/2}v + 4110r^3 = 0 \quad (15)$$

The terminal velocity of a bubble whose radius is r can be solved from this quadratic equation. Table VII. shows those calculated against their observed ones given in Table I. and those plotted on a diagram are shown in fig. 10, by which it can also be seen how they coincide closely.

From our formulæ deduced above we can find the following facts :—

(1) When the bubble is so small that Stokes' formula may be applied, the terms containing r in (14) become negligible and $\phi^{1/2}$ becomes constant. It follows that when the bubble is very small the terminal velocity v varies as $r^{3/2}$ as is obvious from (9). This does not agree with Stokes' formula (1), but as the present experiment was not carried out on such small bubbles, owing to the difficulty of making them, our formulæ cannot be compared with Stokes' to find how the former is approximated to the latter.

(2) When the bubble is smaller than about 0.04 cm. in radius as Mr. Allen treated in his experiment, the first term in the right-hand side of (14) is negligible in comparison with the second, and the term with r^2 in the square-root sign is also negligible in comparison with the accompanying two terms. It follows, therefore, that in this case $\phi^{1/2}$ varies according to the square root of r , other terms being all constant values, and that the terminal velocity varies linearly as the radius, as is evident from (9). Hence our formula is perfectly coincident with Allen's formula (2), so that the former may be considered to include the latter, which may be considered to be only a special case of the former.

TABLE VI.

Radius r cm.....	.025	.04	.06	.08	.1	.12	.14	.15	.16	.165	.176	.18	.19	.2
Value of $\phi^{1/2}$ (observed)0257	—	—	—	—	.1087	—	.1353	—	—	.1779	—	.2002	—
Value of $\phi^{1/2}$ (calculated)...	.0237	.0372	.0553	.0734	.0915	.1096	.128	.136	.148	.1546	.1725	.18	.202	.224
Radius r cm.205	.216	.22	.24	.247	.26	.265	.272	.28	.3	.32	.334	.351	
Value of $\phi^{1/2}$ (observed)2378	.2574	.2694	—	.321	—	.368	.3866	—	—	—	.5295	.5791	
Value of $\phi^{1/2}$ (calculated)...	.2357	.261	.2698	.3156	.331	.361	.3729	.389	.406	.453	.499	.531	.5766	

TABLE VII.

Radius of Bubble, cm.025	.12	.15	.176	.19	.205	.216	.22	.247	.265	.272	.334	.351
Velocity, cm./sec. (observed)...	9.85	24.5	27.5	26.75	26.5	25.5	24.85	24.5	24.3	23.75	23.5	23.35	23.0
Velocity, cm./sec. (calculated)	10.68	24.25	27.37	27.26	26.27	25.22	24.57	24.48	23.72	23.44	23.36	23.37	23.1

(3) When the size of the bubble lies between about 0.17 cm. and 0.25 cm. in radius, the value with the square-root sign in (14) becomes negligible compared with the others,

and it follows that $\phi^{1/2}$ varies linearly as r . Hence we find from (9) that in this case the terminal velocity varies as the square root of the radius, the curve of v against r being a parabola as seen in fig. 10.

VIII. BOUNDARY EFFECT OF THE EXPERIMENT VESSEL.

In order to get as fine and sharp photographs of the bubbles as possible, in the above experiments we used a comparatively thin experiment vessel which might give a certain boundary effect to the motion of the bubbles, especially for large bubbles.

To test this, we carried some experiments with a larger experiment vessel of the cross-section of about 15.6 cm. into 10.95 cm., set the shorter side parallel to the flash-light direction, and about 48.5 cm. high with water about 23 cm. deep.

The photographs of the bubbles were not so sharp and fine as those obtained with the thin experiment vessel, and the size of the bubbles, especially of the small ones, could not be measured so accurately as in the thin one. The results obtained, therefore, did not have much value in treating its equation of motion, but we ascertained after experiments with six different sizes of bubbles that the terminal velocities were about 4 per cent. greater for all the bubbles of practical sizes.

IX. SUMMARY.

As the result of the present experiments we have arrived at the following conclusions:—

(1) When an air bubble rises from rest in still water it attains a constant terminal velocity almost as soon as it has started. (The critical position at which the terminal velocity is attained is about 3 to 4 cm. high above the air-nozzle.)

(2) The terminal velocity is maximum for a bubble whose radius is equal to the critical radius. (The critical radius is about 0.165 cm. and its terminal velocity is about 27.8 cm. per sec.)

(3) For bubbles smaller than the critical radius the terminal velocities increase approximately linearly with their sizes.

(4) For bubbles larger than the critical radius the terminal velocities decrease nearly parabolic with the sizes, and

tend to be constant irrespective of their sizes. (The constant velocity is about 23 cm. per sec.)

(5) The rate of resistance almost suddenly increases at the critical radius, and the shape and the course of the bubble become unstable at it.

(6) The bubble traces a kind of a helical course on its upward motion and it displays a flattened outline, the major axis of which lies perpendicular to its course.

(7) The ratio of the mass of water carried up with a passing bubble to that displaced by it is proportional to the square of its radius or to its surface area.

(8) The resistance to motion of a bubble is proportional to the cube of its radius or to its volume.

(9) The following equation of motion agrees closely with the practical case, with the axis of z upwardly directed.

$$\frac{1}{k} \rho V \frac{d^2 z}{dt^2} = g \rho V - \phi \left(\frac{dz}{dt} \right)^2,$$

where ρ = density of the water,

V = volume of the bubble,

ϕ = coefficient of resistance depending on the size of the bubble,

and k = coefficient depending also on the size of the bubble.

The values of ϕ and k should be calculated from the following empirical formulæ :—

$$\phi = (1.6r - 0.118 + \sqrt{0.49r^2 - 0.167r + 0.0142})^2,$$

$$\text{and } k = \frac{0.054}{r^2},$$

r being the radius of the bubble as measured just at the moment of its leaving the nozzle when it shows a spherical outline. All are expressed in C.G.S. units.

(10) The terminal velocity v in cm. per sec. of a bubble the radius of which is r cm. is determined by solving the following quadratic equation :

$$(2.07r^2 - 0.211r - 0.000282)v^2 + (15.1 - 205r)r^{3/2}v + 4110r^3 = 0.$$

(11) The above results contain the very slight boundary effect of the experiment vessel by which the terminal velocity in a widely open space is about 4 per cent. greater than that obtained above.

Sendai, Japan.

July 8, 1924.

FIG. 1.



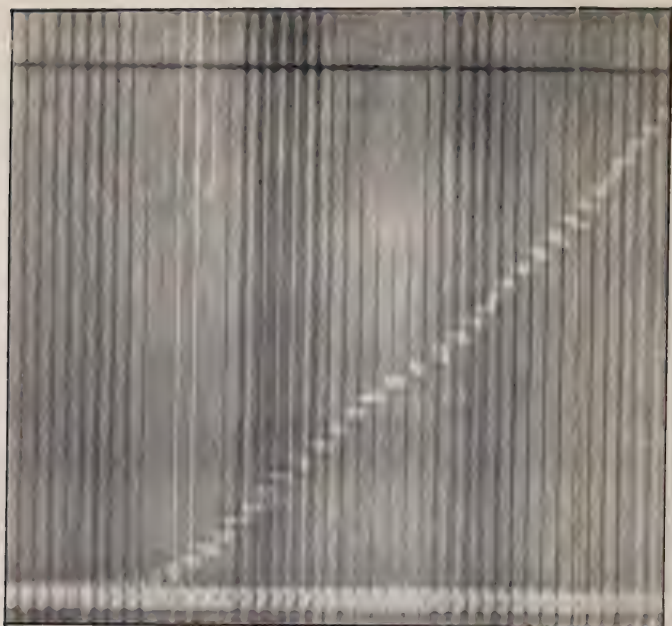
Bubble of radius 0.351 cm. About $\frac{1}{3}$ of actual size.

FIG. 2.



Bubble of radius 0.334 cm. About $\frac{1}{3}$ of actual size.

FIG. 3.



Bubble of radius 0.272 cm. About $\frac{1}{3}$ of actual size.

FIG. 4.



Bubble of radius 0.247 cm. About $\frac{1}{3}$ of actual size.

FIG. 5.



Bubble of radius 0.025 cm. About $\frac{1}{3}$ of actual size.

XI. *On a Method of Calculating the Vapour Pressure of a Solution with a Simple Solvent and a Non-Volatile Solute.*
By SASI BHUSHAN MALI*.

IN the theoretical calculation of the constant of integration of the vapour pressure formula for a substance from kinetic considerations, Stern† makes use of a simple mechanical model. He assumes that inside the body of the substance there are points P, such that they attract the molecules with forces proportional to the distance r of the individual molecules from each of the points in question. The work done by a molecule in freeing itself from the influence of such a point is, according to Stern, the latent heat of evaporation of that molecule. The forces of attraction due to the points P which operate on the molecule are of such a nature that they vanish beyond a certain distance s from the points P, which are supposed to be surrounded by spherical spheres of influence. Within the sphere of influence the molecules (or rather atoms) vibrate as monochromatic resonators, while in the rest of the space surrounding these spheres of influence they fly about like ordinary gas molecules. Hence, the potential energy of the individual molecules at every point in space is fixed. Here, Stern makes use of Boltzmann's law of logarithmic distribution to determine the ratio of the density of the molecules inside the spheres of influence, and also in the free space intervening between these spheres, and he makes the further important assumption that inside each sphere of influence there is only one vibrating atom. The vapour pressure of the substance can now be uniquely determined if we remember that, according to Stern's model, there are as many attracting centres P in a substance as there are atoms in the substance.

The working model of Stern essentially resembles the known model of matter in the crystalline state as revealed by X-ray work, for in crystals the atoms are vibrating about positions of rest. And in fact Stern's value for the integration constant actually coincides with those found by Sackur‡ and Tetrode§ for monatomic vapours. This is especially noteworthy in view of the fact that some physicists of the

* Communicated by Prof. W. A. Jenkins, M.Sc., I.E.S.

† Stern, *Physik. Zeitschr.* xiv. p. 629 (1913). Also Nernst's 'Theoretischen und experimentellen Grundlagen des neuen Wärmesatze,' 1918 edition, p. 138.

‡ Sackur, *Ann. d. Phys.* xl. p. 67 (1913).

§ Tetrode, *Ann. d. Phys.* xxxviii. p. 434; xxxix. p. 255 (1912).

present day * are inclined to believe that matter in the liquid state possesses an unstable crystalline structure.

Stern has determined the vapour pressure formula for simple condensed systems. It appears that with very simple modifications his assumptions can be utilized to find the vapour pressure formula for a dilute solution with a non-volatile solute, especially when the solvent is monatomic both in the liquid and in the vapour state. A solution consists of a certain distribution of solvent molecules with a rarer distribution of solute molecules superimposed upon the former. On account of the mutual attraction of the solute molecules and the surrounding solvent molecules, the distribution of the solvent molecules just around a solute molecule will be somewhat different from the distribution at points further away from the solute molecules.

And owing to the presence of the solute molecules the general distribution of the solvent molecules at points beyond the immediate influence of the solute molecules will be somewhat different from that in the pure solvent, and this even though the amount of solvent in a certain volume may remain the same in the pure state as well as in the state of solution. We shall now make use of Stern's reasoning in order to develop a vapour pressure formula for the solution. If, in the pure state, n_0 and ϕ_0 respectively denote the molecular density and the potential energy of a molecule in free space, and if n_r and ϕ_r denote the same quantities at a point inside a sphere of influence whose distance from the corresponding equilibrium point P is r , then, according to Boltzmann's law,

$$n_r/n_0 = e^{-\frac{\phi_r}{kT}} / e^{-\frac{\phi_0}{kT}}.$$

In the corresponding case of the solution the value of n_r remains unchanged, since the volume of the solvent molecule is supposed to be unaffected by the presence of the solute molecule. The value of ϕ_0 is, however, increased by an amount proportional to the number of solute molecules in unit volume of the solution, and the molecular latent heat in free space of the solution may be expressed as $\phi_0 + cn$ †,

* Debye and Scherrer, *Nachr. Kgl. Ges. Wiss. Göttingen*, 1916; Eastman, J. A. C. S. xlv. p. 917 (1924).

† ϕ_0 is the latent heat of evaporation of a solvent molecule from the pure solvent, and $\phi_0 + cn$ is that of the same molecule from the solution. Hence, cn is the heat of dilution of the solution, and is defined by Sackur (Sackur's 'Thermo-chemistry and Thermo-dynamics,' 1917 ed. p. 228) as "the amount of heat evolved when a large volume of the liquid is diluted by the addition of one molecule of the solvent."

where c is a constant and n is the number of solute molecules in one c.c. of the solution. We do not know in what way n_0 and ϕ_r will change in the case of the solution, but we can at once determine their product by the application of Boltzmann's law of distribution. Thus, in the case of the solution

$$n_r = n_0 e^{-\frac{\phi_r}{kT}} \cdot e^{\frac{\phi_0 + cn}{kT}}.$$

But, since there is only one molecule (or atom) in the sphere of influence,

$$1 = \int_0^s n_r \cdot 4\pi r^2 dr = n_0 e^{\frac{\phi_0 + cn}{kT}} \cdot 4\pi \int_0^s e^{-\frac{\phi_r}{kT}} r^2 dr.$$

The force acting on the molecule vibrating inside the sphere of influence is represented by the equation

$$m \frac{d^2 r}{dt^2} + a^2 r = 0.$$

The potential energy ϕ_r of a vibrating molecule when at a distance r from an attracting centre P is equal to $\frac{a^2 r^2}{2}$, and the potential energy $\phi_0 + cn$ in free space is equal to $\frac{a^2 s^2}{2} + cn$. Thus, we find

$$\int_0^s e^{-\frac{\phi_r}{kT}} r^2 dr = \int_0^s e^{-\frac{a^2 r^2}{2kT}} r^2 dr.$$

To simplify the right-hand side of the equation we may put

$$\frac{a^2 r^2}{2kT} = x^2, \quad \text{and} \quad \frac{a^2 s^2}{2kT} = x_0^2.$$

Then,

$$\int_0^s e^{-\frac{a^2 r^2}{2kT}} r^2 dr = \left(\frac{kT}{a^2/2} \right)^{3/2} \int_0^{x_0} e^{-x^2} x^2 dx.$$

If λ_0 denotes the latent heat of evaporation of the solvent when the solute is absent, $x_0^2 = \frac{\lambda_0}{RT}$, and this must be a large number compared with unity, for $\frac{\lambda_0}{T}$ represents the Trouton constant, and its value is of the order of 21 at the boiling

point of normal liquids and has higher values at temperatures lower than the boiling points*, whereas R has the value 2. Hence, $e^{-x_0^2}$ must be a very small quantity.

Thus, in the integration of the equation $\int_0^{x_0} e^{-x^2} x^2 dx$ we

may, without appreciable error, take the upper limit of the integration to be ∞ instead of x_0 . Integrating the equation in this way, according to Nernst's "Rekursion Formel," Stern shows that

$$\int_0^{x_0} e^{-x^2} x^2 dx = \frac{\sqrt{\pi}}{4}.$$

In this way we finally get

$$1 = n_0 e^{\frac{\phi_0 + cn}{kT}} \cdot \pi^{3/2} \left(\frac{kT}{a^2/2} \right)^{3/2},$$

$$\text{or} \quad n_0 = e^{-\frac{\phi_0 + cn}{kT}} \cdot \left(\frac{a^2/2}{\pi kT} \right)^{3/2}.$$

Substituting $m(2\pi\nu)^2$ for a^2

$$n_0 = e^{-\frac{\phi_0 + cn}{kT}} \cdot \left(\frac{2\pi m\nu^2}{kT} \right)^{3/2}.$$

Now, in a dilute solution, we may suppose that most of the solvent molecules are distributed at points beyond the influence of the solute molecules and have a distribution of n_0 molecules per unit volume. Hence, in the case of a dilute solution, we may put

$$p = n_0 kT = e^{-\frac{\phi_0 + cn}{kT}} \cdot \frac{(2\pi m\nu^2)^{3/2}}{(kT)^{1/2}},$$

$$\text{or} \quad \ln p = \frac{\phi_0 + cn}{kT} - 0.5 \ln T + \ln \frac{(2\pi m)^{3/2} \nu^3}{k^{1/2}}.$$

If λ_0' denotes the latent heat of evaporation of a gram mol. of the solvent from the solution

$$\ln p = -\frac{\lambda_0'}{kT} - 0.5 \ln T + \ln \frac{(2\pi m)^{3/2} \nu^3}{k^{1/2}}. \quad \dots, \quad (1)$$

Also, for the pure solvent, Stern has shown that

$$\ln p_0 = -\frac{\lambda_0}{kT} - 0.5 \ln T + \ln \frac{(2\pi m)^{3/2} \nu^3}{k^{1/2}}. \quad \dots \quad (2)$$

* Mali, Phil. Mag. xlv. p. 94 (1923).

We thus find that the vapour pressure formulæ for the pure solvent and the solution with a non-volatile solute differ only in the terms containing the latent heat of evaporation, but are otherwise identical. And specially we notice that the constant of integration comes out as identical in both the cases. This is as is to be expected, for the constant of integration, as explained by Nernst, depends upon the nature of the evaporating molecules and is independent of the nature of the condensed system.

There are certain consequences to be derived from these results. From equations (1) and (2)

$$\ln \frac{p_0}{p} = \frac{cn}{kT},$$

and since p_0 and p are approximately equal,

$$\ln \frac{p_0}{p} = \frac{p_0 - p}{p} = \frac{p_0 - p}{p_0} \text{ approximately.}$$

Thus, the lowering of the vapour pressure of the solution is proportional to the concentration of the solute. Again, from thermodynamics,

$$\frac{p_0 - p}{p_0} = \frac{\lambda_0 dT}{RT_0^2},$$

where dT is the raising of the boiling point corresponding to the lowering of the pressure by the amount $p_0 - p$. Combining these two equations, we find that

$$Ncn = \frac{\lambda_0 dT}{T} \text{ approximately.}$$

Or, Heat of dilution of the solution = Heat of evaporation $\times \frac{dT}{T}$, where dT is the difference in boiling points of the original and the dilute solutions.

The present arguments may not be strictly accurate in the case of metals, for the metals are monatomic in the vapour state, yet from surface tension data they are found to be associated in the liquid state (Siedentopf, *Wied. Ann.* lxi. p. 265 (1897). These arguments will be strictly true in the case of a hypothetical liquid which is monatomic both in the liquid and in the vapour state.

Finally, I have to record my thanks to Prof. W. A. Jenkins for the kind interest he took in the work during the course of its progress.

Department of Physics,
University of Dacca.

Sept. 7, 1924.

XII. *The Temperature Dependency of the Molecular Heats of Gases, especially of Ammonia, Methane, and Hydrogen, at Low Temperatures.* By FRANKLIN A. GIACOMINI, M.A., Ph.D.*

[Abridged Report.]

SINCE the discovery of the extraordinarily rapid fall of C_v for hydrogen down to the value of a monatomic gas at low temperatures (first observed by Eucken), physicists have been endeavouring to explain this phenomenon (which seems to stand in marked opposition to the deductions of the Equipartition of Energy Theorem) chiefly by means of the Quantum Theory †. None of the attempts made thus far, however, have been successful, and until a greater body of empirical evidence has been obtained with regard to the behaviour of the molecular heats of gases at low temperatures, little hope can be entertained of making any positive progress in this direction ‡. The work outlined in this paper was undertaken for the purpose of providing additional data concerning the relation of the energy-content of gas molecules to the temperature,—particularly in that temperature-domain in which the value of the said energy-content sinks beneath that value which the molecule must have when considered as perfectly rigid and as having three degrees of freedom of rotation (decrease in the rotational energy of the molecule).

* Communicated by Prof. J. R. Partington.

† It is of interest to note that, previous to Eucken's observations, Nernst had predicted the rapid fall of C_v for H_2 with decreasing temperatures as a necessary consequence of his thermo-dynamical theorem by applying the Quantum Theory to gases; Eucken's experiments were subsequently made to test the correctness of this deduction of Nernst.

‡ Among the many theoretical attempts made, which (in addition to the theories of Planck-Einstein and of Nernst-Lindemann, both of which had previously been developed for the purpose of accounting for the decrease of the vibrational energies of the atoms in solids, by diminishing temperature) have been built up for the sole purpose of explaining the decrease of the rotational energies of gas molecules by falling temperature, may be mentioned the following:—Planck, *Berichte d. deutsch. Phys. Gesellsch.* li. p. 285 (1915), which is founded on the assumption of coherent degrees of freedom of the molecules; S. Rotszayn, *Ann. d. Phys.* lvii. p. 81 (1918), which assumes incoherent degrees of freedom between the molecules; and in addition to these:—

E. Holm, *Ann. d. Phys.* xlii. p. 1311 (1913); Ehrenfest, *Verhandl. d. deutsch. Phys. Gesellsch.* xv. p. 451 (1913); A. Einstein und O. Stern, *Ann. d. Phys.* xl. p. 551 (1913); v. Wyssenhof, *Ann. d. Phys.* li. p. 285 (1916); F. Reiche, *Ann. d. Phys.* lviii. p. 657 (1919); G. W. Todd, *Phil. Mag.* xl. p. 357 (1920) (based on the Classical Theory).

By so doing a system of data is obtained for the study of the molecular energies which is reduced to its utmost simplicity. The plan of the work decided upon, therefore, involved the following objectives:—

(1) The determining upon and the examining of all such gases (chiefly those having small molecular moments of inertia) which in addition to hydrogen might, in all probability, still show an experimentally establishable decrease in their molecular energy-content, C_v , by falling temperatures, below the C_v -values corresponding to rigid molecules (decrease in the rotational energy of the molecule).

(2) The determining, as far as possible, of the specific-heat-temperature curves (C_v -T-Curves) for these gases.

As a prerequisite to the attaining of this end there was necessary:—

(3) The developing of a method by means of which the molecular energy-content, C_v , can be *directly* obtained, *i. e.* determined, as far as possible, without the use of any assumptions or hypotheses concerning either the ratio of the specific heats, C_p/C_v , at the temperatures in question or the other thermodynamical corrections usually necessary to reduce the observed values of C_v to their true values at low temperatures.

The method used, however, requires that the gas under investigation be as nearly as possible in the ideal state (measurements at small gas pressures, see below). This follows, first, as a consequence of the fact that, in the measurements, the coefficient of pressure-increase of the gas $(dp/dT)_v$, is assumed to be approximately that of an ideal gas and to be practically independent of the temperature, *i. e.*, that $(d^2p/dT^2)_v=0$ (*vide* Principle of the Method, below); and, secondly, from the desirability of avoiding, as far as possible, the corrections needed to reduce the obtained values of C_v to the values C_v would have if the gas were in the ideal state, *i. e.*, for $p=0$. This second condition is also fulfilled when $(d^2p/dT^2)_v=0$, as is evident from the general thermodynamical relation

$$(dC_v/dv)_T = T \cdot (d^2p/dT^2)_v.$$

No claims are made for the applicability of this method to measurements of precision on the absolute values of C_v . The scope of the method is essentially the enabling of qualitatively accurate determinations of the relative values of C_v for the same gas over a large range of temperature (downward) and of the relative values of C_v for various gases at the same temperature and pressure.

Principle of the Method.

The method, which was adopted as the result of a suggestion of Professor Nernst, to whom I here wish to express my sincere thanks, depends on the principle, first enunciated by Nernst, concerning the determinability of the molecular heat of a gas at constant volume,—even when the heat increment added to a given volume of the gas is not uniformly distributed throughout the gas but is isolated in heat-zones or clouds in the interior of the containing-vessel (avoidance of heat-conduction directly to the walls of the containing-vessel). The comparison-measurements of C_v are obtained by determining with a very sensitive membrane-galvanometer the pressure rise which immediately follows upon the transmission of a small inductive electrical impulse through a diminutive constantan foil placed towards the centre of the vessel (*vide* Apparatus). This method of determining C_v was first tried out by Voller *. He limited his trials, however, to room temperature and atmospheric pressure. No investigation was then (or has since been) made concerning the validity of this principle of determining C_v ; nor concerning the conditions that must be fulfilled if the principle be at all allowable in order to obtain reliable results.

The first matter to be settled in these researches was, accordingly, (*a*) to examine whether, or to what extent, the above described principle of determining C_v is permissible—for this principle presupposes a non-uniform temperature distribution in the gas-filling of the heating-chamber which is alone sufficient to preclude any *prima facie* assumption concerning the determinability of C_v by this principle,—and (*b*), if permissible, the establishing of the conditions under which the principle can be applied in order that reliable results may be obtainable; *i.e.*, so that C_v , and not some polytropic specific heat lying somewhere between C_p and C_v , be obtained. This question was settled:—

(1) Through an experimental investigation of what was going on in the interior of the heating-chamber immediately succeeding the induction-impulse in the heating-foil. This included the direct observation of the development and evolution of the heat-clouds in the heating-chamber (gas made visible by smoke particles); the measurement of the time required for the foil to give off its heat; the determination of the temperature attained by the foil during an

* Voller, Berlin Dissertation, 1908.

induction-impulse ; and, most important of all, the determining of the pressure-increase curves for various gases by various heat charges and under various initial conditions of pressure, etc. (see fig. 2) ; and

(2) Through the theoretical considerations suggested by Dr. K. Bennewitz, of the University of Berlin, concerning the thermodynamical stages gone through in the gas-filling in the interior of the heating-chamber during and immediately after the inductive impulse in the heating-foil. The fundamental idea underlying the theory of Bennewitz is this : it considers what actually takes place in the heating-chamber as identical with the following two idealized stages : (1) an isochoric heating of a small volume of the gas immediately surrounding the heating-foil, and (2) the adiabatic expansion of this volume and the adiabatic compression of the remaining part of the volume of the heating-chamber (a fuller account will be given in another paper).

As the result of the above-mentioned experimental and theoretical investigations, the conditions were ascertained which must be fulfilled in order that C_v may actually be determined. Among other things, in order to obtain reliable results, the most important condition that must be fulfilled is given by the expression

$$\left[\frac{RQ}{V_0 C_v P_0} \right]^2 < < 1$$

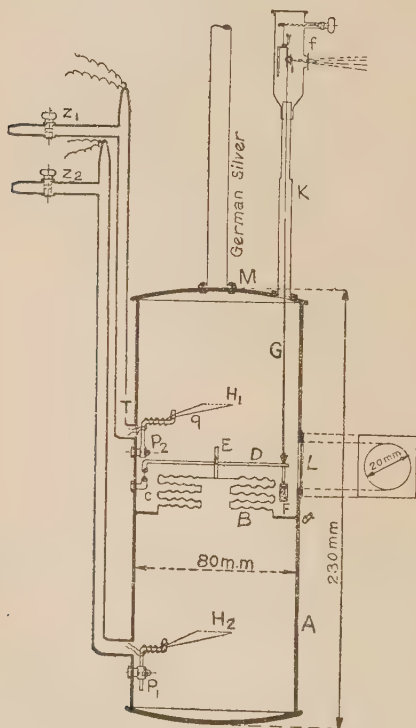
(where Q designates the heat-charge given off by the induction-impulse ; V_0 , the volume of the heating-chamber ; P_0 , the initial pressure in the heating-chamber ; C_v , the molecular heat ; and R , the universal gas-constant, all expressed in absolute units). The above condition demands that for given values of V_0 and of P_0 the smallest possible value of Q be used. The expression shows, moreover, that the smaller P_0 is taken the more unfavourable the experimental conditions become ; *i. e.*, the greater are the demands made on the experimental efficiency of the apparatus.

Apparatus.

The apparatus finally used (fig. 1) consisted essentially of a cylindrical metallic vessel of about 8 cm. diameter and 20 cm. height. This could easily be dipped into a Dewar vessel. The cylinder was divided into two chambers, a

higher and a lower one. In the lower chamber (heating-chamber) of about 600 c.c. capacity there was placed the heating-foil of constantan, a metal with a negligibly small temperature coefficient of electrical conductivity. Platinum is, on account of its great temperature coefficient, not suited to comparison-measurements of C_v for various gases, or for the same gas at various temperatures. This is chiefly a

Fig. 1.



Double-heating chamber apparatus.

consequence of the discrepancies in the magnitudes of k , η^* , and C_v (*i. e.*, in the heat-receiving capacity) in the two gases being compared, which causes unequal temperature variations and, therefore, unequal inductive charges in the heating-foil in the respective gas-fillings of the heating-chamber. In the higher chamber (manometer chamber) of about 300 c.c.

* k =coefficient of thermal conductivity of the gas, η =coefficient of internal friction of the gas.

capacity was built the membrane manometer (B) with its connexions to the very sensitive deflexion mirror above, which was suspended on a cocoon fibre. The nature and magnitude of the manometer deflexions were usually observed directly by means of a telescope and scale. In the figure shown here (double-heating-chamber apparatus), the manometer chamber is of the same capacity as the lower one, and is also equipped with a heating-foil (H_1) by means of which this chamber can likewise be used as a heating-chamber simultaneously with the lower one: differential or zero deflexion method of procedure (rejected later as unsatisfactory, see below). A complete description of the apparatus will be given in another paper.

Measurements.

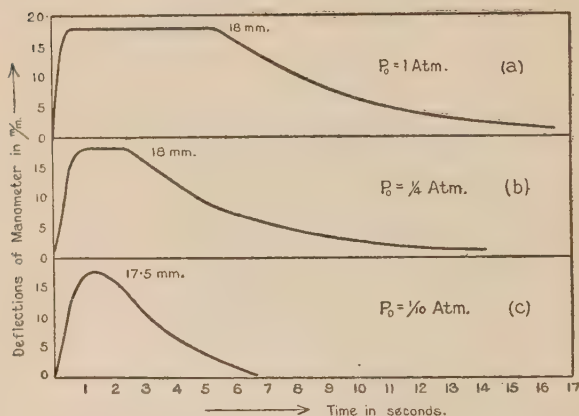
On account of the great difficulty in determining the absolute values of the heat charges, Q , developed by each induction-impulse, the measurements were limited to determining the relative magnitudes of the pressure-increments Δp (of the magnitude of about 0.0894 g./cm.^2) produced by inductive impulses of invariable magnitude in the several gases compared with that brought about in a standard gas, viz., air. The relative value, of C_v for the different gases in terms of the C_v -value for air should hereby be obtained (comparison-measurements). The value of $4.979 \text{ cal./mol. } ^\circ\text{T}$, determined by Scheel and Heuse, was taken as the standard C_v -value for air at 291° abs. and atmospheric pressure. The relative pressure-increments were obtained by observing the relative magnitudes of the maximum manometer deflexions for the various gases under the above conditions (the corresponding mean value of ΔT in the air was 0.025° C.). *It is very important to state here that comparisons of the maxima of the deflexions were made only when each deflexion-maximum remained at a constant and invariable value for an extended interval of time, sometimes lasting for seconds (fig. 2).* That these long-enduring pressure maxima were not spurious ones is shown by the fact that, within broad limits, the same maxima were obtained by gas-fillings (of the same gas) at different densities. A special study was made of these pressure maxima (of incredibly long duration). This will be treated of in another paper.

For the purpose of additional orientation concerning the reliability of the results obtained, a determination of the

absolute value of C_v for air was attempted*. The trials showed that, although approximately correct values of C_v were obtained, the method must be further perfected before satisfactory measurements of this nature can be hoped for.

Preliminary experiments by means of a double-heating-chamber apparatus (mentioned above) were made. By this differential procedure inductive impulses are sent simultaneously into both chambers. The trials were, however, on account of the differences in phase in the pressure rise in the

Fig. 2.



The above curves (fig. 2) show the Time-Pressure-increase relations for a CO_2 -gas-filling at room temperature ($T = 291^\circ$) and at the indicated initial pressures, P_0 , of 1, $\frac{1}{4}$, and $\frac{1}{10}$ Atmospheres.

The magnitudes of the maxima of the deflexions remain unchanged down to almost $\frac{1}{10}$ of an atmosphere initial pressure. This fact insures us that the maxima obtained are not spurious. The duration of the maxima, however, diminishes with the decrease of the initial pressures, P_0 , in the heating-chamber.

One mm. deflexion in the above curves is equivalent to about 0.0036 g./cm.^2 pressure increment.

(two) gases being compared (caused chiefly by the discrepancies in the values of k and η of the respective gases), given up as unreliable; therefore the first-mentioned single-heating-chamber apparatus — with successive fillings of different gases — was used in the final measurements.

* Here the determination of the magnitude of the heat-charge Q was necessary.

The number of mols of the various gases in the heating-chamber at each gas-filling was kept practically equal by introducing the pure gas into the chamber at relatively low pressures and at room temperatures. The experiments revealed, however, that the actual number of mols of gas in the heating-chamber had very little effect on the maximum of the pressure-increments (and correspondingly deduced, values of C_v) caused by a given induction-charge; for, within broad limits of variation of the initial pressure, the maxima of the manometer deflexions remained unchanged*; or at least the variations in the pressure-increments were too small to be observable. Only for great diminutions of the initial pressure did the pressure-increments begin to decrease. This was attributed chiefly to imperfections in the apparatus, or rather to the fact that the experimental limits of the apparatus were overstepped; for the smaller the initial pressure, P_0 , of the gas the greater the demands made on the efficiency of the apparatus become. All this is to be seen from the pressure-increment curves for various initial pressures spoken of above.

Two sources of error of fundamental importance, which had to be corrected for, were the following:—(a) the influence of the initial gas pressure in the manometer chamber on the magnitude of the manometer deflexion—which varies according to the values of the initial pressures in the manometer chamber (the initial pressures in the manometer and heating-chambers must, of course, always be kept alike to avoid strains on the manometer and to keep it in its neutral zero-position); and (b) the work performed on the membrane-manometer itself and on the gas in the manometer chamber, which becomes slightly compressed during each manometer deflexion. For an unfavourably designed apparatus (b) can become very great. In the final experiments carried out here (b) was negligibly small (less than $\frac{1}{2}$ per mille of the measured quantity, apparatus No. 3). The effect of (a), however, had to be eliminated whenever measurements were made at various initial pressures P_0 (at times amounting to 5 per cent., apparatus No. 3).

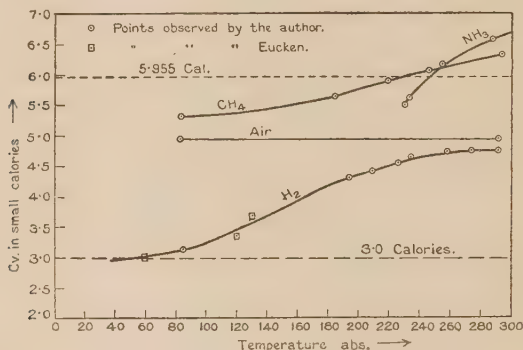
The C_v -T-Curves obtained (fig. 3) show that the molecular heats of CH_4 and NH_3 sink with falling temperature below the values corresponding to rigid molecules (decrease in the energy of rotation of the molecule). With the exception of H_2 (observed by Eucken), these are the only gases for which

* It can also be shown theoretically that this should be expected.

this property has yet been directly observed*. For CH_4 the value of C_v sank to a value of 5.30 cal./mol. T at a temperature $T=83^\circ$ abs.; for NH_3 , to a value of 5.55 cal. at $T=229^\circ$ abs.

A few of the numerical results heretofore obtained by this method as a first contribution to the establishment of the C_v -T-Curves are shown in the table below (the author hopes soon to be able to complete the curves).

Fig. 3.



General view of the C_v -T-Curves for H_2 , NH_3 , CH_4 and air (see table).

The observations made on H_2 , which were made primarily as a practical test of the applicability of the method at low temperatures, are in excellent agreement with those made by Eucken. The C_v values obtained in the neighbourhood of 200° abs. are also in harmony with the observations of Scheel at 197° abs.

The remarkably rapid fall of the C_v -T-Curve for NH_3 is noteworthy†.

* Since the observations described in this paper were made (discontinued January 1922), a paper by R. W. Millar (Journ. Amer. Chem. Soc. xlv. S. 874-881 (1923), No. 4) has appeared, which—by means of the steady flow method, measurements of C_p —qualitatively corroborates the observations made here on the decrease of C_v for CH_4 below the values corresponding to a rigid molecule having three degrees of freedom of rotation. Millar's measurements extended only down to a temperature of 142° abs.

† A number of theoretical considerations, which arose out of the results of the measurements of C_v for NH_3 and CH_4 , led to the conclusion that at small pressures an observable and rapid fall of C_v with decreasing temperature would probably be observable also for a few other gases not yet investigated, such as PH_3 and AsH_3 . These gases are presumably of the same molecular structure as NH_3 ; and according to the latest measurements of Rankine and Smith on the viscosities of these gases should have molecules with small diameters.

TABLE.

Gas.	T.	P.	C_v cal./mol. T.	Remarks.
NH ₃ .	288	1/10 Atm.	6.65	{ Nernst : 6.61. Partington : 6.7.
	253	"	6.25	
	243	"	6.05	
	231	"	5.60	
	229	"	5.55	
	193	20 mm. Hg.	16.5	{ Polymerization or Condensation, ab- normal C_v value.
CH ₄ .	278	1 Atm.	6.41	
	222	3/4 "	5.89	
	180	2/3 "	5.68 ₅	
	83	60 mm. Hg.	5.30 ¹	
	83	250 "	18.00	{ Polymerization or Condensation.
H ₂ .	291	760 mm. Hg.	4.847	
	273	715 "	4.80	Eucken : 4.84.
	258	680 "	4.76	
	234	614 "	4.68	
	227	595 "	4.65	
	224	590 "	4.57	
	211	550 "	4.52	
	208	545 "	4.48	
	83	220 "	3.196	Eucken : 3.19.
C ₂ H ₄ .	286	1 Atm.	8.14	{ Scheel and Heuse : 8.19.
CO ₂ .	291	1 Atm.	6.81	" " 6.86.
	291	1/2 "	6.81 ₂	
Air.	291	1 Atm.	4.979	{ Standard value taken from Scheel and Heuse.
	273	1 "	4.979	
	243	1 "	4.979	
	233	1 "	4.96	
	83	1/3 "	4.95	

Miscellaneous Remarks.

The following remarks deal chiefly with some of the difficulties encountered in manipulating the apparatus. A few suggestions are also appended, indicating the general lines along which these difficulties may be eliminated and the method further developed and perfected for future measurements.

(a) Difficulties : the chief difficulty met with in completing a series of measurements was that of keeping in order the delicately suspended deflecting-mirror, which served as a member of the optically magnifying system necessary to accurately and expeditiously indicate the minute displacements of the membrane-manometer (the details, figures, etc., of the mirror-suspension will be given later in a longer paper); the fragile nature of the magnifying system (enabling accurate and rapid measurements of pressure-increments of the order of magnitude of $7 \cdot 10^{-4}$ g./cm.²) made frequent breakdowns unavoidable—derangements often occurring near the end of a series of measurements, necessitating the discarding of all the readings thereby obtained. Another difficulty met with was that of keeping the manometer in its true zero-position and free from disturbing vibrations during a comparison-measurement. These disturbances were of two types:—first, rapid oscillations due to vibrations in the building (tramway-cars, etc.); and, second, gradual displacements of the manometer, to and fro, due to slight temperature discrepancies between the heating-chamber and the manometer chamber.

(b) Improvements : the lines along which the method may be experimentally improved are, to a great degree, already implicitly indicated in the above-mentioned difficulties. This demands the developing of an equally sensitive but at the same time less easily derangeable means of measuring the pressure-increments following the inductive impulses in the heating-chamber. The positive direction, therefore, in which the method is to be perfected is (as will be shown in the general theory of the method, which will be treated of in the paper mentioned above) in making accurate and rapid measurements of pressure-increments of a still smaller order of magnitude possible than were obtainable by the apparatus described in this paper.

The experimental part of this investigation was carried out in the Physico-Chemical Laboratories of the University of Berlin, and was finished in January 1922.

Sterling, Colorado, U.S.A.

XIII. *Electric and Magnetic Spectroscopy.*By Professor W. ARKADIEW, *Moscow* *.

THE velocity of very long waves in dielectrics depends on the dielectric coefficient ϵ_{∞} , which can be defined by electrostatic measurements taking in consideration the increase of the capacity of a condenser, and on the magnetic permeability μ_{∞} , which can be measured by a magnetometer. If the electromagnetic wave is very short, its electric and magnetic fields alternate so rapidly that the electric and magnetic particles fail to undergo any displacement and no electric or magnetic polarization can arise in a body of any influence on the velocity of the wave; there is no friction that produces a considerable absorption of waves of medium length. Therefore, the absorption of short waves is very small, and their velocity in matter does not differ from the velocity in vacuum; such are the X-rays, which hardly suffer any absorption; all bodies are transparent to X-rays, their velocity in matter is the same as the velocity in vacuum: the refractive index n of X-rays is equal to 1. This is because in the high-frequency electric fields of the X-ray waves the electrons and ions have not sufficient time for any perceptible displacement†. The vibrations of X-rays are outside the domain of electric qualities of matter in the region where the dielectric coefficient is equal to 1.

In the central part of the spectrum, where the frequency of the electromagnetic waves is equal or nearly so to the natural frequency of the electric centres, we have the region of vast variations of the refractive index n and of the dielectric coefficient ϵ , the *region of electric dispersion* and of strong absorption of rays, and the *region of electric absorption*. Here dielectric bodies obtain the so-called *electric conductivity of polarization* designated by σ .

The values of ϵ and σ , in the case of oscillating centres of a uniform group, are defined by the equations:

$$\epsilon = 1 + (\epsilon_{\infty} - 1) \frac{1 - \nu^2}{\theta^2 \nu^2 + (1 - \nu^2)^2} \text{ and } \sigma = \frac{\epsilon_{\infty} - 1}{2T_0} \frac{\theta \nu^2}{\theta^2 \nu^2 + (1 - \nu^2)^2}, \quad (1)$$

where T_0 is the natural period of the centre, ν the relative frequency, equal to T_0/T ; T is the period of the wave, and θ the coefficient of friction. (The vibrations become aperiodic when $\theta=2$.)

* Communicated by the Author.

† A. H. Compton, *Phil. Mag.* xlv. p. 1121 (1923).

The refractive index n and the coefficient of absorption k are determined by the following known expressions :

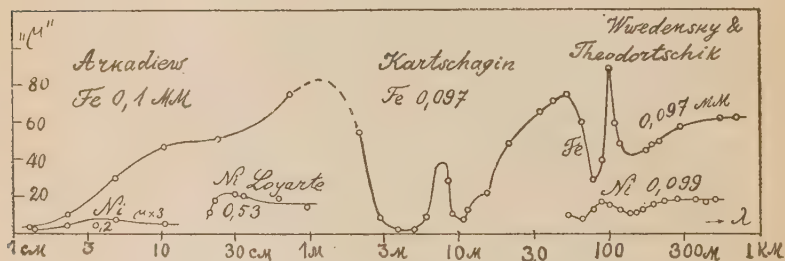
$$2n^2 = \sqrt{\epsilon^2 + \sigma'^2} + \epsilon \quad \text{and} \quad 2k^2 = \sqrt{\epsilon^2 + \sigma'^2} - \epsilon, \quad (2)$$

where $\sigma' = 2\sigma T$.

The magnetic properties of bodies are distinctly expressed in constant and slowly changing fields, where the magnetic permeability amounts to hundreds and thousands of units. On the other hand, in the waves of light and in the long infra-red waves, the magnetic properties of all bodies are equal and their magnetic permeability μ is equal to that of vacuum, *i. e.* $= 1$.

Therefore, the thermal waves have the same relation to magnetic centres as the X-rays to electric centres. This shows, that somewhere in the intermediate region, between the thermal oscillations and the slow electric vibrations, must be the *disappearance of the magnetic behaviour*, accompanied by *magnetic absorption* of the passing rays and by strong alterations of the magnetic permeability. This critical region

Fig. 1.



The magnetic spectra of iron and nickel wire for electromagnetic vibrations between 1 cm. and 1 km. wave-length.

occupies a very considerable part of the spectrum, at least from the length of waves of 1 cm. up to 1 km., as was shown by the investigations of Arkadiew*, Kartschagin†, Wwedensky and Theodortschik‡, Gans and Loyarte§, and Nikitin||.

All along this line we find strong variations of the magnetic permeability (fig. 1) in weak fields.

* *Phys. Zeitschr.* xiv. p. 561 (1913); xxii. p. 511 (1921).

† *Ann. d. Physik*, lxvii. p. 325 (1922).

‡ *Ann. d. Physik*, lxviii. p. 429 (1921). *Physik. Zeitschr.* xxiv. p. 216 (1923).

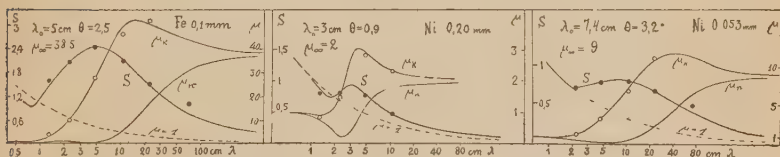
§ *Ann. d. Physik*, lxiv. p. 209 (1921); lxvi. p. 429 (1921).

|| *Zeitschr. f. Physik*, xxix. p. 288 (1924).

In the case of the very shortest waves this critical region was investigated in 1913, when there was found a big drop of the permeability in short Hertz waves: at $\lambda=72.7$ cm., $\mu \cong 100$; at $\lambda=10.63$ cm., $\mu \cong 30$; and at $\lambda=1.14$, $\mu=3.7$.

In this region iron and nickel show a strong absorption of electromagnetic waves, as can be seen in fig. 2, where the black dots show the values of S found in the experiments that are proportional to the coefficient of absorption k' of various waves in iron and nickel. They are represented as ordinates and the wave-lengths in vacuum as abscissæ.

Fig. 2.



The bands of magnetic absorption in iron and nickel wires and their apparent permeability μ_k and μ_n .

The material and the diameter of the wires are denoted on the diagram. In the same diagram are shown the proper wave-lengths λ_0 of the elementary magnets lying in this region, and the friction θ .

Within this region of absorption the magnetic permeability is subject to variation. In one case it even comes down to the value of 0.80.

Assuming that the elementary magnets in ferromagnetic metals under the influence of weak fields rotate under the same laws of viscous-elastic motion as are generally adopted for displacement of electric centres in dielectric bodies, we get for the permeability μ and magnetic conductivity ρ the following formula :

$$\mu = 1 + (\mu_{\infty} - 1) \frac{1 - \nu^2}{\theta^2 \nu^2 + (1 - \nu^2)^2} \text{ and } \rho = \frac{\mu_{\infty} - 1}{2T_c} \frac{\theta \nu^2}{\theta^2 \nu^2 + (1 - \nu^2)^2}. \quad (3)$$

Four coefficients of the matter, ϵ , σ , μ , and ρ lead to the following form of the Maxwell equation :

$$\begin{aligned} \frac{\epsilon}{c} \frac{\partial E}{\partial t} + \frac{4\pi\sigma}{c} E &= \text{curl } H \\ -\frac{\mu}{c} \frac{\partial H}{\partial t} - \frac{4\pi\rho}{c} H &= \text{curl } E. \end{aligned}$$

These equations give the values of the coefficient of refraction

and of absorption * defined by the following expressions :

$$\left. \begin{aligned} 2n^2 &= \sigma'(\sqrt{\mu^2 + \rho'^2} - \rho') = \sigma' \mu_n, \\ 2k^2 &= \sigma'(\sqrt{\mu^2 + \rho'^2} + \rho') = \sigma' \mu_k, \end{aligned} \right\} \quad \dots \quad (4)$$

where $\rho' = 2\rho T$.

The coefficient of absorption k' , which defines the decrease of the amplitude of the wave along the distance x according to the formula $e^{-k'x}$, is $2\pi k/\lambda = 2\pi \sqrt{\frac{\sigma}{c}} \cdot \sqrt{\frac{\mu_k}{\lambda}}$. The

coefficient S , shown in the figure, is $\sqrt{\frac{\mu_k}{\lambda}}$. The lines show the theoretical course of the values μ_k and μ_n . The blank circles represent the values μ_k , calculated from the absorption of the waves in ferromagnetic wires †. The coincidence of the theoretical values with those derived from the experiments is fully satisfactory.

On the basis of the already existing experimental materials such determinations could be performed with wires of different diameters. Knowing the intensity of magnetization up to saturation I_∞ and the density of matter δ , it is possible, supposing that the oscillating elementary magnets are only of one type, to calculate their radius a according to the following formula:

$$a = I_\infty T_0 \sqrt{\frac{5}{3\pi\delta(\mu_\infty - 1)}} \text{ cm.}$$

These values for wires of different diameters together with other quantities are given in the following table:—

	NICKEL.			IRON.						
	Arkadiew.		Gans.	Arkadiew.						
	2R mm....	0.053	0.20	0.54	0.05	0.10	0.20	0.30	0.40	0.50
λ_0 cm. ...	7.4	3.0	24.3	5.9	5.0	3.55	3.0	2.5	2.3	
μ_∞	9.0	2.0	12.0	35.0	38.5	27.5	22.2	18.7	14.5	
θ	3.2	0.90	1.3	2.0	2.5	2.0	1.7	1.7	1.6	
$10^{-10} \cdot \rho_{\max}$	0.50	0.55	0.5224	4.3	4.5	5.7	6.3	6.3	5.5	
$10^8 \cdot \alpha$ cm.	1.12	1.28	3.11	1.49	1.20	1.01	0.96	0.87	0.92	

* The general expressions for n and κ are $2n^2 = \sqrt{(\epsilon^2 + \sigma'^2)(\mu^2 + \rho'^2)} + \epsilon\mu - \sigma'\rho'$ and $2\kappa^2 = \sqrt{(\epsilon^2 + \sigma'^2)(\mu^2 + \rho'^2)} - \epsilon\mu + \sigma'\rho'$; from these equations we get (2) and (4) as special cases. W. Arkadiew, *Physik. Zeitschr.* xiv. p. 928 (1913); *Ann. d. Physik*, lxxv. p. 643 (1921).

† W. Arkadiew, *Ann. d. Physik*, lviii. p. 105 (1919).

We see that, notwithstanding the great inconstancy of the values λ_0 , μ_∞ , and θ , the values ρ_{\max} , i. e. ρ near $\nu=1$ and α show a certain stability.

The instability of the magnetic spectra and their dependence on the properties of the material for the wire, especially on its diameter (fig. 1), is connected with the known unsteadiness of the ferromagnetic qualities in general. Their natural period T_0 depends upon the directing internal field which keeps the elementary magnets in their natural state of equilibrium, and defines the value of permeability μ_∞ in weak fields. It would better answer the purpose to analyse the magnetic spectra of iron magnetized by strong constant external field.

From the above-mentioned formulæ (2) and (4) we see that n and k in the case of electric and magnetic dispersion are defined by the binoms :

$$r + \alpha, \quad r - \alpha, \\ \mu_k = r + \beta', \quad \mu_n = r - \beta',$$

where α replaces ϵ and μ , β' replaces σ' and ρ' , and $r = \sqrt{\alpha^2 + \beta'^2}$.

The researches on the course of the values $r \pm \alpha$ are the object of the theory of electric dispersion and absorption and, as a special case, the ordinary optic dispersion; the study of the course of the values $r \pm \beta'$ forms the object of the theory of magnetic dispersion and absorption.

Lately the binoms μ_k and μ_n have been the subject of electrotechnical researches, where by means of them the theoretic analysis of electromagnetic processes has been accomplished, by which it has been shown that the absorption of energy in iron is due not only to the damping friction θ of the rotating elementary magnets, but also to other causes, as hysteresis and eddy currents (Uller *, Truxa †, Tonks ‡, Gans §).

The researches on the quantities $\mu = \sqrt{\mu_k \cdot \mu_n}$, $2\rho' = \mu_k - \mu_n$, ρ , μ , and μ_n in their dependence on the wave-lengths λ , for various ferromagnetic metals and their combinations, i. e. their *passive magnetic spectra*, form the object of *passive magnetic spectroscopy* ||. The difference between this and

* *Verh. d. Deutsch. Phys. Ges.* iv. p. 31 (1923).

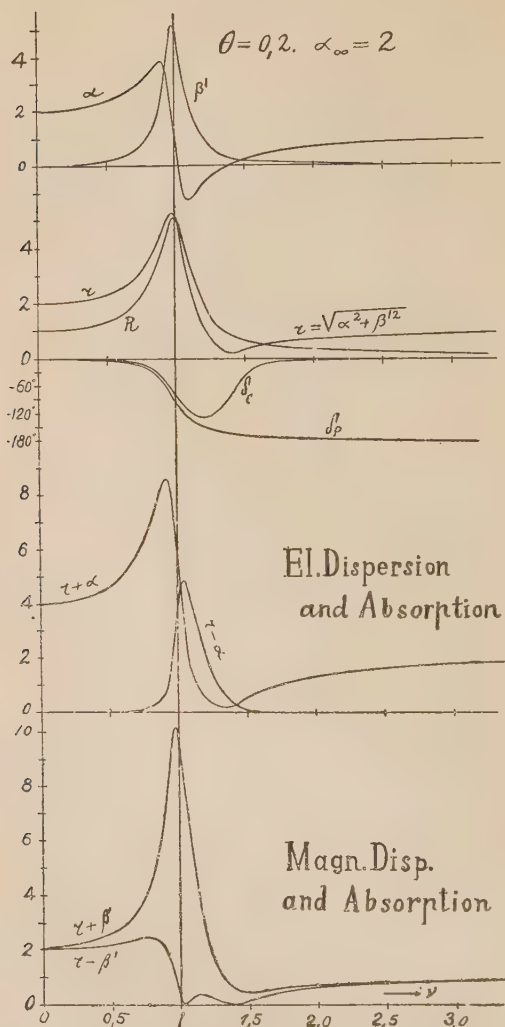
† *Archiv für Electrot.* xii. p. 354 (1923).

‡ *Phys. Rev.* xxiii. p. 221 (1924).

§ *Phys. Zeitschr.* xxiv. p. 232 (1923).

|| This subject is treated in the monograph "Magnetic Spectroscopy" by W. Arkadiew: No. 4 of Transactions of the State Electrical Research Institute, Moscow, 1924 (in Russian, with the abstract in English). Also No. 6 of Transactions "Researches in Electromagnetism," edited by Arkadiew, and *Zeitschrift f. Physik*, xxvii. p. 37 (1924); xxviii. p. 11 (1924).

Fig. 3.



R =resonance of electric and magnetic centres.

δ_p =the retardation of their phase and the phase of the polarization against the phase of the field.

δ_c =the retardation of the phase of induction.

r =the value $\sqrt{a^2 + \beta'^2}$; the coefficient of refraction n in dielectric bodies is determined by $2n^2 = r + a$; the coefficient of absorption k in them by $2k^2 = r - a$; the coefficient of apparent permeability $\mu_k = r + \beta'$ and $\mu_n = r - \beta'$.

the old *passive electric spectroscopy* is that the former investigates the influence on matter of the *electric vector* of the electromagnetic wave, and the latter, of the *magnetic vector* of the same wave. We find that both these branches of the general electromagnetic spectroscopy have equal rights.

Magnetic spectroscopy forms the special object of study in the Moscow Magnetic Laboratory.

I. University and State Electrical
Research Institute,
Moscow, 7 June, 1924.

XIV. *A Physical Interpretation of Bohr's Stationary States.*
By G. P. THOMSON, M.A., Professor of Natural Philosophy
in the University of Aberdeen and Fellow of Corpus Christi
College, Cambridge.*

MONSIEUR L. DE BROGLIE has shown in a paper in this Magazine † that the stationary states of an electron can be regarded as determined by the condition that the orbital motion of an electron can only be stable if the length of the path is such as to be in tune with the "phase wave" which M. de Broglie supposes to accompany the electron.

A similar result, in the case of the hydrogen atom, can be obtained, without the necessity of postulating waves with a velocity greater than that of light, by the development of the model proposed by Sir J. J. Thomson ‡ to explain the existence of bundles of energy in radiation.

Suppose the electron to be attached to the nucleus by a tube of force which is to be regarded, not as on the classical theory as spreading out to fill all space, but as forming a connexion of limited, though possibly varying cross-section between the two charges. Suppose, as on the classical theory, that the tension of the tube provides the attraction between the electron and the nucleus, and that the tube possesses energy and therefore mass. It will thus be able to transmit waves, and the condition that will be taken as determining the possible states is that the vibrations in this tube shall be in tune with the period of the orbit. Only when this is the case can the motion be strictly periodic, for there will always be in practice some slight external effects to produce disturbances.

* Communicated by the Author.

† Phil. Mag. xlvii. p. 446.

‡ Phil. Mag. xlvii. p. 737.

The condition required is that

$$\int^T V dt / \lambda = n, \text{ an integer,}$$

where the integral is taken over a complete period of the orbit, V is the velocity of the waves and λ is the wavelength. Making the supposition that the waves with which we have to deal are the transverse vibrations of a stretched string, λ is $2r/m$, where m is an integer and r the length of the tube, so the condition will be satisfied for *all* modes of vibration if

$$\int^T V dt / 2r = n.$$

For an elliptic orbit of eccentricity ϵ , semi-latus rectum l and for which $r^2 \theta = p$, the condition becomes

$$n = \int_0^\pi V l d\theta / p (1 + \epsilon \cos \theta),$$

and if V is taken as a constant a simple integration gives

$$n = V \pi l / p \sqrt{1 - \epsilon^2}.$$

Substituting for p, l, ϵ in terms of the axes this becomes

$$n = V \pi \sqrt{am}/e \quad \text{or} \quad a = n^2 e^2 / V^2 \pi^2 m,$$

where a is the semi-major axis, m the mass of the electron, and $\pm e$ the charges on nucleus and electron. This reduces to Bohr's condition

$$a = n^2 h^2 / 4 \pi^2 e^2 m$$

$$\text{if} \quad V = 2e^2/h.$$

The value of V thus found is not equal to the velocity of light, with which waves would travel on a free tube of force on the classical theory. The proposal is to account for the failure of the classical theory by ascribing different properties to the tube of force according as to whether it is fixed only at one end and radiates into space, or forms a bond between an electron and a nucleus. If in the latter case the velocity of waves along it is taken to be $2eE/h$ where E is the charge on the nucleus, a simple extension of the above accounts also for the stationary states of ionized helium, and gives approximately the energy of the K ring of electrons. On this view the non-dimensional quantity hc/eE is a measure of the extent to which such a "bound" tube of force departs from the condition of the free tube.

Aberdeen,
March 14.

XV. *The Spectrum of Sodium at Low Voltages.* By F. H. NEWMAN, D.Sc., A.R.C.S., Professor of Physics in the University College of the South-West of England, Exeter*.

[Plate IV.]

1. INTRODUCTION.

ALTHOUGH the theory of the atom, as developed by Bohr, Sommerfeld, Rubinowicz, etc., has not reached that state which gives a complete representation of spectra other than those of hydrogen and helium, yet it yields a general indication of the structure. Considering the case of the sodium atom, the 1σ ring represents the outermost stable orbit and the innermost unstable orbit of the normal atom, and all the principal series doublets, $1\sigma - m\pi$, are emitted when the valency electrons in various atoms fall from one of the π rings to the 1σ orbit, the series converging at 1σ . The first subordinate series lines are produced by electrons falling from the $m\delta$ rings to the 1π ring, and the second subordinate series when the electrons are transferred from the $m\sigma$ to the 1π rings. Interorbital motions, other than those mentioned, give rise to the fundamental series and various combination lines, although in such interorbital motions the selection principle allows only those transitions in which the azimuthal quantum number changes by unity. The azimuthal quantum numbers of the $m\sigma$, $m\pi$, $m\delta$, and $m\phi$ orbits are, respectively, 1, 2, 3, and 4, so that interorbital transitions from the $m\pi$ to the $m\sigma$ or the $m\delta$ levels are possible, but transitions from the $m\sigma$ to the $m\delta$ orbits are precluded. It is true that in some cases lines are observed which represent interorbital movements where the change in azimuthal quantum number is according to Sommerfeld 2 units, such, for example, as the pair $\lambda 4642.2$, 4641.6 in the potassium spectrum, but the excitation of this pair is explained by the incipient Stark effect. This doublet, and the corresponding one in the sodium spectrum, are excited also in low-voltage arcs when the electron density is great. In this case the excitation is caused, apparently, by the interaction of atomic fields of neighbouring positive ions and electrons. Such atomic fields are probably many times greater than the intensity of the applied external electric force.

The electron is displaced from the 1σ ring to the next

* Communicated by the Author.

outer orbit—the 1π ring—whenever the sodium atom receives energy, either by bombardment or by the absorption of radiation, equivalent to 2.1 volts, and the valency electron being now in a temporary orbit falls to the 1σ ring and, in so doing, gives up the quantum of energy received during its ejection from the 1σ ring as a quantum of radiation $h\nu$ with the emission of the D lines. When energy equal to, or greater than, 5.12 volts is communicated to the atom the valency electron is displaced from its normal orbit and leaves the atom and, in returning, may occupy temporarily any one of the stationary orbits, the dimensions of which are large compared with the X-ray orbits, before it reaches the 1σ ring. The many electrons returning in the different atoms will do so by various different steps and the many-line spectrum results, the intensities of the different lines representing to some approximation the chances of the corresponding interorbital transitions.

The atom also absorbs radiation of frequency corresponding to a $1\sigma - m\pi$ change and accordingly the electron is displaced to any of the $m\pi$ rings. Rayleigh* has observed that the sodium line $\lambda 3303$, incident on sodium vapour, excites the D lines and $\lambda 3303$, so that electrons within the 2π orbit may fall directly to the 1σ orbit, or they may pass, directly or indirectly, to the 1π orbit and thence to the normal orbit 1σ . Absorption and fluorescence phenomena indicate that the electron can be displaced directly from its normal orbit to any of the π rings but not to others. It is to be expected, therefore, that similar displacements would be produced by electronic bombardment. Until recently experimental confirmation of this latter expectation was not available, although Franck and Einsporn†, who used a “photo-electric” method, had shown that the photo-electric current in mercury vapour increased suddenly as the critical energy for each of the known orbits was attained. In spite of this electron displacement to these orbits spectroscopy gave no evidence of the successive emission, line by line, all the results obtained indicating the existence of a single line spectrum at resonance potential, and an abrupt transition to the entire arc spectrum as the energy of the bombarding electrons increased to the ionization potential.

Following a suggestion made by Birge, and utilized by Foote and Meggers‡, a graphical representation of the

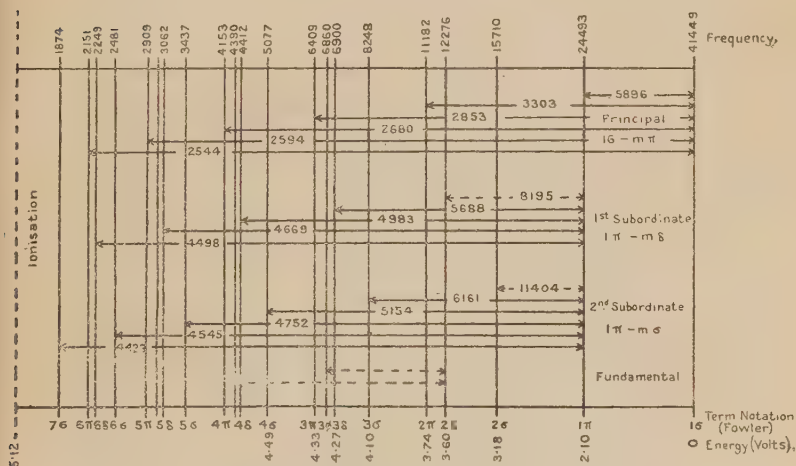
* See Strutt, Proc. Roy. Soc. A, vol. xevi. p. 272 (1919).

† *Zeits. f. Phys.* 2. i. p. 18 (1920).

‡ Phil. Mag. xl. p. 80 (1920).

energy levels in the sodium atom is shown in fig. 1. Regarding the lines as representing the non-radiating orbits, the nucleus is supposed situated away to the right of the diagram, and the actual sodium lines correspond to the transition of electrons from orbits on the left to orbits on the right. The π orbits are really double but their separation is too small to be represented, and in the diagram only that orbit corresponding to the higher energy level has been shown. The lines really represent portions of the elliptical or ring orbits about the nucleus, 1σ being the outermost stable orbit of the valency electron. The first doublet of the principal

Fig. 1.



Graphical representation of sodium atom.

series is produced by the electron falling from the 1π to the 1σ orbit, the line of longer wave-length— λ 5896—having a frequency equal to the difference of the frequencies characterizing these orbits, viz. 41449–24493. The second doublet of the principal series is emitted when the electron falls from the 2π orbit to the 1σ orbit, etc. The first line of the first subordinate series is represented by an electron falling from the 2δ ring to the 1π ring, and the other lines of this series correspond to ejections from the $m\delta$ orbits to the 1π orbit. The falls from the $m\sigma$ orbits to the ring represented by 1π yield the second subordinate lines; falls from the ϕ orbits to the 2δ orbit give the fundamental series lines, and the various combination lines can be considered in the same way. All horizontal lines extending

between the orbits indicate emission lines produced by energy falls between these orbits. The dotted lines represent emission lines in the infra-red.

The energy level of any particular orbit can also be expressed in terms of the potential difference through which an electron must fall in order to accumulate kinetic energy equivalent to the quantum of radiation corresponding to this energy. The potential difference V is given by the quantum relation $Ve = h\nu$, where e is the unit of charge, h is Planck's constant, and ν the frequency. For example, in order to displace the valency electron from the 1σ orbit to the 1π orbit the energy of the bombarding electron must be equal to that which it would possess by falling through 2.1 volts—the resonance potential of sodium vapour,—and the displaced electron, being then in a temporary orbit, falls back to the 1σ orbit giving up the quantum of energy eV , received at the collision, as a quantum of radiation energy $h\nu$ of frequency ν . In a similar manner, bombardment with electrons of energy corresponding to 3.74 volts should eject the valency electron to the 2π orbit. Theoretically, an electron of this energy should be capable of ejecting the valency electron to the 1σ , 2σ , or 2δ orbit, for such ejections require energy less than 3.74 volts. If sodium atoms are bombarded with electrons possessing this energy, the lines $\lambda 5896, 5890$; $\lambda 8195, 8183$; $\lambda 11404, 11382$; and $\lambda 3303, 3302$ should be emitted by interorbital transfers permitted by the quantum theory. In a similar manner, by increasing the energy of the bombarding electrons to values below the ionization potential the other lines in the various series should be excited, until when the energy has reached 5.12 volts the entire arc spectrum of sodium should appear.

Recently Eldridge*, using a three-electrode discharge tube in which electrons emitted from an incandescent cathode were accelerated by a potential between the grid and cathode and entered a force-free space between the grid and plate, has obtained such a line-by-line emission with mercury vapour as the impacting energy increased to those values sufficient to eject the electrons to their proper orbits, and he has stated that the previous failure to observe this step-by-step emission is explained by the space charge effect lowering the impacting energy except at the immediate surface of the anode. Formerly, spectroscopic investigation of mercury vapour bombarded with electrons of energy less than the ionization potential—10.4 volts—had shown the

* Phys. Rev. xxiii. p. 685 (1924).

lines $1S-1p_2$ and $1S-1P$ only, but Eldridge has photographed the line $1S-1p_2$ at 7 volts, 4 additional lines due to electrons returning from the $2S$ or $1s$ levels at 8.4 volts, 8 additional lines at 8.9 volts, and 16 more lines at 9.9 volts, in full agreement with the theory and with the photoelectric experiments of Franck and Einsporn.

Hughes and Hagenow*, employing a large equipotential source of electrons by fitting a nickel cylinder over an alundum tube, heated internally by a tungsten spiral, showed definitely that lines in the principal series of caesium appear in the order, and within 0.1 volt, of the potential required by the theory. They found the first and second subordinate series lines more difficult to observe, but these lines did appear below the ionization potential of caesium vapour, viz. 3.9 volts.

From a study of fig. 1 it is evident why only the principal lines show absorption. The valency electron, lying normally in the 1σ orbit, can be displaced directly to one of the $m\pi$ orbits, the necessary energy for such a displacement being provided by the energy quanta abstracted from the incident light and resulting in light absorption of corresponding frequency.

Foote, Meggers, and Mohler†, who studied the excitation of the sodium spectrum, employed a grid mounted extremely close to a tungsten hot-wire cathode and in metallic contact with a concentric hollow cylinder of relatively large diameter. By regulating the temperature a vapour pressure was obtained for which relatively few electronic-atomic collisions occurred over the short accelerating field between the grid and cathode. The majority of the electrons passed into the force-free space between the grid and the plate and had, at the instant of collision, a velocity corresponding to the impressed field. These experimenters found that only the single line spectrum, consisting of the D lines, was excited above the resonance potential and below the ionization potential. With potential differences above the latter the entire arc spectrum appeared. An interesting feature was the excitation of $\lambda 3427$ which has the notation $\nu=1\sigma-2\delta$. This line represents an interorbital transfer where the change in the azimuthal quantum number is 2 units, and apparently contradicts the Bohr principle of selection as applied by Sommerfeld to spectra of non-hydrogenic type, but, as explained previously, the appearance of the line is

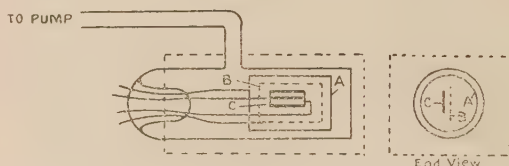
* Phys. Rev. xxiv. p. 229 (1924).

† Astrophys. Jour. lv. p. 145 (1922).

accounted for, probably, by the electric forces between neighbouring electrons and positive ions.

It was decided to repeat the work of these investigators with sodium vapour, minimizing the space charge effect within the discharge tube. It should then be possible to bring out the lines, step-by-step, in accordance with the theory. The apparatus employed is shown diagrammatically in fig. 2.

Fig. 2.



2. EXPERIMENTS.

The discharge tube—about 1 cm. in diameter—was of quartz and had a quartz plate cemented at one end. The source of the electrons was a tungsten filament cathode C consisting of three tungsten wires arranged in parallel, each wire being 1.2 cm. long. By using three tungsten wires in this way a good supply of electrons was obtained without raising the filament to very bright incandescence. The nickel gauze grid B, placed not more than about 1.5 mm. away from the cathode, was in electrical contact with the nickel cylinder A which completely surrounded the cathode and made the interior of the tube a constant potential region. The electrons, accelerated by a potential difference applied between the negative end of the cathode and the grid, entered the constant potential space between A and B. The whole tube, which contained a small quantity of sodium metal, was enclosed within an electric furnace the interior of which was maintained at 350° C. At this temperature the vapour pressure of sodium, although not known with any great degree of accuracy, is certainly below 0.1 mm. of mercury*. The electron currents used were about 2 milliamperes.

In consequence of the space charge effects it was necessary to focus on the slit of the quartz spectrograph light coming from the immediate neighbourhood of the grid, and throughout the period that spectroscopic observations were

* See Hackspill, *Comptes Rendus*, cliv. p. 877 (1912).

being made the discharge tube was connected to a Cenco-Hyvac oil pump which, running continuously, insured that the residual gas pressure was maintained well below 0.01 mm. of mercury. If the tube was not continuously exhausted in this manner, the gas pressure rose to such a value that no luminosity appeared between the grid and the plate even with accelerating voltages exceeding the ionization potential of sodium vapour. The spectrograms at different accelerating voltages were photographed on special rapid panchromatic plates.

The potential difference, as measured between the cathode and grid, does not give necessarily the energy of the electrons at the instant that they pass through the grid. There are other factors which influence their kinetic energy such as contact potential, fall of potential along the lead-in wires and along the filament, and the initial velocity of the electrons emitted from the cathode. At dull red heat about 3 per cent. of these electrons have an initial velocity corresponding to 0.5 volt. The discrepancy between the apparent and true values of the electron energy can be determined and allowed for by measuring the ionization potential. The experimental value was 4.7 volts, and as the calculated value is 5.1 volts, the correction to be applied is 0.4 volt. This correction has been made in all the measurements quoted.

As the accelerating voltage was raised to 2.2 volts a yellow glow appeared in close proximity to the grid and plate. Increasing the voltage still further the colour of the radiation changed to greenish-yellow and extended a short distance from the electrodes, until at 5.2 volts the whole of the space between the grid and plate was filled with the glow. From the appearance of the tube it is evident that the space charge lowers the effective potential except in the immediate neighbourhood of the electrodes. The various spectrum lines which appeared at different voltages are given in Table I.

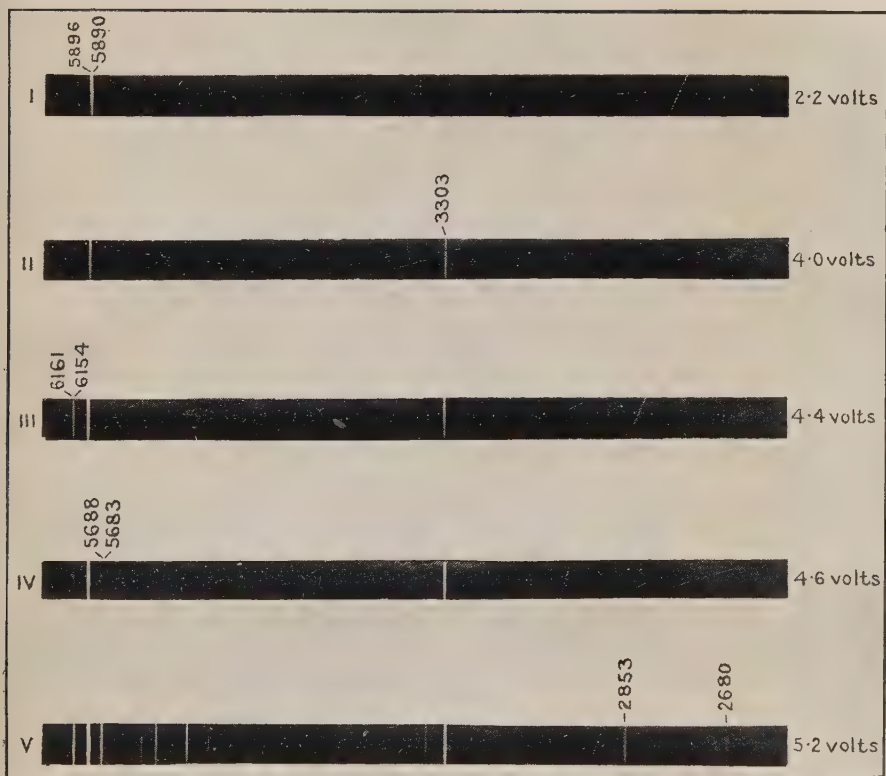
The spectrograms obtained with different excitation voltages are shown in Plate IV. In the first one the doublet λ 5896, λ 5890 appears at 2.2 volts. The energy of the electrons is sufficient to displace the valency electron to the 1π orbit. At 3.18 volts the doublet λ 11404, λ 11382 should be additional to the D lines, but it is far beyond the range of the plate. Similarly at 3.6 volts λ 8195, λ 8183 should appear, but this doublet also is outside the range of the plate, so that at 3.74 volts the only lines on the plate should be λ 5896, λ 5890, λ 3303, and λ 3302. The second spectrogram at 4.0 volts shows these lines and no others.

TABLE I.

Series.	Wave-length.	Excitation voltage.	
		Experimental.	Calculated.
$1\sigma-1\pi$	λ 5890 λ 5896	2.2 volts.	2.10 volts.
$1\pi-2\sigma$	λ 11382 λ 11404	—	3.18
$1\pi-2\delta$	λ 8183 λ 8195	—	3.60
$1\sigma-2\pi$	λ 3302 λ 3303	4.0	3.74
$1\pi-3\sigma$	λ 6154 λ 6161	4.4	4.10
$1\pi-3\delta$	λ 5683 λ 5688	4.6	4.27
$1\sigma-3\pi$	λ 2853	—	4.33
Complete arc spectrum		5.2	5.12

In a similar manner λ 6161, λ 6154 should be the next lines to appear, and spectrogram No. III. contains these additional lines at 4.4 volts. The doublet λ 5688, λ 5683 made its appearance at 4.6 volts (spectrogram No. IV.), but with the exposures employed no further lines were excited until the voltage reached 5.2 volts, when ionization set in (spectrogram No. V.). It is difficult to differentiate between the excitation of lines within the range 4.6–5.2 volts, for the number of collisions resulting in excitation is probably small at the actual critical voltage but increases as the latter is exceeded.

The results indicate that the valency electron within the sodium atom is displaced to different orbits by inelastic impacts with bombarding electrons possessing the requisite energy, and line-by-line excitation is possible. The line λ 3127 photographed by Foote, Meggers, and Mohler at the ionization potential was not observed in the present experiments, but the electron currents employed were very small compared with those used by the previous investigators, and it is only in the presence of strong electrostatic fields, either external or internal, that this line becomes prominent.



The Spectrum of Sodium at Low Voltages.

3. SUMMARY.

On the basis of Bohr's theory of atomic structure it is shown that the normal operation of an arc below ionization should result in the excitation of a line-by-line spectrum corresponding to changes of orbit involving less energy than the ionizing potential. Previous attempts to obtain such an emission with sodium vapour have failed. In the present work a three-electrode discharge tube was used, and the electrons emitted from a heated tungsten wire cathode were accelerated by a potential difference applied between the grid and cathode. Photographic observations showed the development of the spectrum in the order of the potential predicted by theory. At 2.2 volts λ 5896, 5890 only appear. At 4.0 volts the lines λ 3303, 3302 are excited, and the lines λ 6161, 6154 and λ 5688, 5683 are emitted at 4.4 and 4.6 volts respectively, in agreement with theory.

The cost of the quartz spectrograph, used in the experiments described above, has been defrayed by a Government grant, through the Royal Society, for which the author wishes to express his sincere thanks.

XVI. *Some Remarks on the Fulcher Hydrogen Bands.*

By G. H. DIEKE *.

SEVERAL papers have appeared recently which deal with the regularities in the secondary spectrum of hydrogen discovered by Fulcher † in 1912. Most of them give interpretations of these regularities which agree in principle with the one given first by Lenz ‡, but which differ in details from it and among themselves. M. Kiuti § connects the branches in the red and green part of the spectrum by a Q-branch discovered by him. Quite recently W. E. Curtis ||, making use of an investigation of A. S. Allen ¶, gives a critical revision of the numeration of the band-lines, and offers an explanation of the connexion between the different branches.

In an earlier paper ** the author showed that there is

* Communicated by Prof. P. Ehrenfest.

† G. S. Fulcher, *Phys. Zs.* xiii. p. 1137 (1912); *Astroph. Journ.* xxxvii. p. 60 (1913).

‡ W. Lenz, *Verh. d. Phys. Ges.* xxi. p. 632 (1919).

§ M. Kiuti, *Proc. Phys.-Math. Soc. Japan*, (3) v. p. 9 (1923).

|| W. E. Curtis, *Proc. Roy. Soc. A*, cvii. p. 570 (1925).

¶ A. S. Allen, *Proc. Roy. Soc. A*, cvi. p. 69 (1924).

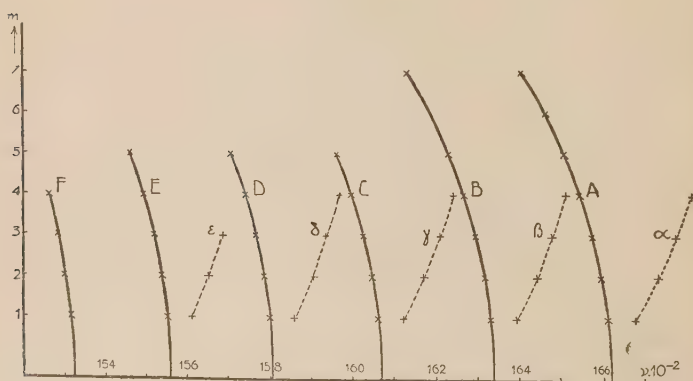
** G. H. Dieke, *Proc. Roy. Acad. Amsterdam*, xxvii. p. 490 (1924).

another possibility of explaining the regularities which gives quite different results regarding the structure of the molecule which emits the bands. Therefore it seems desirable to give a comparison between the two different possibilities.

For brevity's sake we shall call the interpretation of the bands accepted by Lenz, Kiuti, Allen, and Curtis "Interpretation A" (or simply "A") and the one proposed by the author "Interpretation B," and shall refer for "A" mainly to the paper of Curtis as being the most recent one and containing the most details.

1. The lines in one band (m variable, n_1 and n_2 constant)*, as well as the corresponding lines of the bands in one group (n_1 variable, $\Delta n = n_1 - n_2$, and m constant), follow Deslandres's law. Owing to the small moment of inertia of the hydrogen molecule, the spacing of the lines in one band will be of the same order of magnitude as the spacing of the bands in one group. Therefore, if a parabolic series is given, one cannot immediately see from the relations between the wave-numbers alone whether the variable is m or n .

Fig. 1.



In fig. 1 the regularities in the red are represented graphically. The lines on a horizontal, which are represented by the same sign (\times or $+$), form a "Fulcher band" (called here, as in Curtis's paper, *horizontal series*), and the lines connected by the curves the extension of the Fulcher triplets (*vertical series*). For simplicity, in the beginning we shall leave out of consideration the lines connected by the dotted curves.

* m is the rotational, n the oscillation-quantum number.

Now the two assumptions interpret the regularities in a different manner:—

“A” says the horizontal series form a band, whereas “B” considers the vertical series as branches of a band. The different vertical series are considered by “B” as different bands of a group ($n_1 - n_2 = \text{constant}$). The same was done by Curtis with respect to the different horizontal series. The numerical relationships as expressed by Deslandres’s law cannot help us to decide between the two assumptions, as they are consistent with both.

But the lines of a vertical series can be represented exactly by

$$\nu = A - Cm'^2 - Dm'^4 \quad (m' = 1.5; 2.5, \dots), \quad (1)$$

in which the term Dm'^4 is only a small correcting term. If we accept “A,” the existence of the relation (1) must be attributed to chance or, as this is not very likely, to a property of the molecule which is still unknown and which is found in no other band-spectrum. This difficulty does not exist if we take assumption “B,” for according to it the vertical series are interpreted as Q-branches, and (1) is the theoretical formula for them.

2. The *structure of one band* is not one familiar to us from other band-spectra. If we take interpretation “A,” only a P- and P'-branch exist, for Kiuti’s assumption that the bands in the green form R-branches leads to serious difficulties, and has therefore been abandoned also by Allen and Curtis. The existence of a P-branch without a Q- or R-branch belonging to it ought not to be considered as a serious difficulty; but the connexion between the P- and P'-branches is not the same here as in the helium bands, where it can be understood theoretically. If the interpretation “B” is accepted, thus far only a Q- and an R-branch could be identified. But it is very probable that several other lines belong to the same bands, and form perhaps a P-branch. There is, however, no sufficient criterion which would allow us to decide whether a certain arrangement is right or not. For the same reason the arrangement of the lines in the positive branches (the dotted ones in fig. 1) can be considered only as provisional. Only further experimental investigation can give sufficient certainty.

3. *Intensity of the Lines.*—We expect that in the hydrogen bands, owing to the small moment of inertia of the carrier, the first or second line will have the maximum

intensity at ordinary temperatures, and that the intensities of the following lines will diminish very rapidly, so that each band only contains a few lines. However, we can predict nothing about the intensities of the different bands of one group.

In our case the distribution of intensities is a normal one in the horizontal series, whereas in the vertical series the even lines are much weaker than would be expected from the intensities of the neighbouring odd lines. It seems very difficult to give an explanation of these alternating intensities on the basis of assumption "A." If, however, we accept the interpretation "B," we are led to the conclusion that each vertical series consists in reality of two different series, a strong one and a weak one. Then the odd lines belong to the transitions $m - \frac{1}{4} \rightarrow m - \frac{1}{4}$, and the even lines to $m + \frac{1}{4} \rightarrow m + \frac{1}{4}$, and formula (1) must be written (if we neglect the correcting term Dm'^4)

$$\left. \begin{aligned} \nu &= A - 4C(m - \tfrac{1}{4})^2 && \text{odd lines} \\ & && m = 1, 2, 3 \\ \nu &= A - 4C(m + \tfrac{1}{4})^2 && \text{even lines} \end{aligned} \right\} \quad (2)$$

With the half-quantum interpretation (formula (1)) it could not be understood why the line corresponding to the transition $0.5 \rightarrow 0.5$ is absent. With quarter effective quantum numbers no such line (which would here be due to the transition $0.25 \rightarrow 0.25$) can exist because, according to a general rule of Bohr, one is the smallest possible value of m . A strong support for this conception is that recently exactly the same intensity anomalies have been found in the negative nitrogen bands*, and the author† was able to show that one does not come to any contradiction if one considers the weak lines as forming one branch and the strong lines as forming another one. It is further remarkable that quarter effective quantum numbers have been found to exist in almost all bands which must be attributed to pure elements.

4. *Variation of the Intensities with Temperature.*—Goos‡ measured the intensities of the red Fulcher triplets accurately at three different temperatures, and McLennan and Shrum§ observed the many-lined spectrum at the temperature

* M. Fassbender, *Zs. f. Phys.* xxx. p. 73 (1924); see also R. Mecke, xviii. *Phys. Zs.* xxv. p. 597 (1924).

† G. H. Dieke, *Zs. f. Phys.* xxxi. p. 326 (1925).

‡ F. Goos, *Zs. f. Phys.* xxxi. p. 229 (1925).

§ J. C. McLennan and G. M. Shrum, *Trans. Roy. Soc. Canada*, (3) p. 177 (1924).

of liquid hydrogen. In the following tables the results of these authors are given. In Table I. the lines are arranged according to interpretation "A" and in Table II. according to "B." The first column gives the author's notation, the

TABLE I.

	$\lambda \text{Å.}$	M.	W.	T=19°.	T=87°.		T=295°.		T=495°.	
					2.5.	29.	2.0.	17.	1.4.	$18\rho/\rho_0 10^4$.
A (1)	6018.29	10	9	++	100	100	100	100	100	100
B (1)	6121.76	10	10	++	128	109	108	100	113	100
C (1)	6224.81	9	10	++	125	114	101	94	105	92
D (1)	6327.07	8	8	++	88	85	71	57	72	57
E (1)	6428.10	5	2	++	24	32	23	31	23	26
A (3)	6031.80	10	5	=	100	100	100	100	100	100
B (3)	6135.34	8	6	=	135	144	105	105	106	94
C (3)	6238.39	8	6	=	74	67	77	60	90	66
D (3)	6340.57	6	2	—	—	33	40	29	51	37

TABLE II.

	$\lambda \text{Å.}$	M.	W.	T=19°.	T=87°.		T=295°.		T=495°.	
					2.5.	29.	2.0.	17.	1.4.	$18\rho/\rho_0 10^4$.
A (1)	6018.29	10	9	++	100	100	100	100	100	100
A (2)	23.74	7	4		16	19	27	34	34	41
A (3)	31.80	10	5	=	23	36	43	62	73	106
B (1)	6121.76	10	10	++	100	100	100	100	100	100
B (2)	27.40	9	2		16	20	37	38	49	53
B (3)	35.34	8	6	=	24	48	42	65	68	100
C (1)	6224.81	9	10	++	100	100	100	100	100	100
C (2)	30.23	7	2		13	13	29	31	33	39
C (3)	38.39	8	8	=	14	31	33	39	63	76
D (1)	6227.07	8	8	++	100	100	100	100	100	100
D (2)	32.46	5	1		—	16	24	30	44	46
D (3)	40.57	6	2	—	—	14	24	32	51	68

second one the wave-lengths according to Merton and Barratt*, and the following two the intensities as observed by Merton and Barratt (M) and Watson (W)†. The fifth column

* T. R. Merton and S. Barratt, Phil. Trans. A, ccxxii. p. 369 (1922).

† H. E. Watson, Proc. Roy. Soc. A, lxxxii. p. 189 (1909).

contains the observations of McLennan and Shrum, and the following ones the measurements of Goos at the given temperatures and densities (ρ). ++ means that the line is strongly enhanced at $T=19^\circ$, - resp., and = that it is weakened, resp. strongly weakened. Goos's measurements are multiplied by such a factor that the first line in every band has the intensity 100.

With increasing temperatures the lines which belong to higher m must be enhanced, and they must be weakened at low temperatures. This behaviour of band-lines with variations of temperature has been confirmed experimentally in all cases where it could be investigated.

If the Tables I. and II. are compared, we see that there is practically no influence of temperature upon the intensity distribution in the horizontal series. (The small irregular differences must be attributed to secondary effects.) Table II., however, shows definitely that the vertical series have the behaviour of the intensities which is postulated by the theory if they are interpreted according to assumption "B." It shows also that increased pressure has the same effect as increased temperature in accordance with what we expect. Goos measured only the first three lines of each band. That the higher members also behave in the right way may be seen from Kiuti's photographs of the spectrum of the hydrogen arc*. In accordance with the higher temperature of the arc, the first lines are much weakened and the higher ones enhanced, so that the fifth line is much stronger than the first one. The sixth line, which is recorded by Merton and Barratt as appearing only with the admixture of helium, has in the arc the same intensity as the first line. For a more detailed discussion of the variation of the intensity distribution with temperature the reader is referred to another paper by the writer†.

It seems that it will be very difficult, if not impossible, to account for this behaviour of the lines on the basis of assumption "A," and therefore" it is a very strong support for assumption "B."

5. *Moment of Inertia.*—Interpretation "A" gives a reasonable value for the moment of inertia (Curtis found $0.186 \cdot 10^{-40}$ for the final state of the first band). The value which was given in the author's paper (assumption "B") is $0.82 \cdot 10^{-40}$; but this value depends on the interpretation of the positive branches, which, as was already mentioned above, is still

* *Loc. cit.*

† G. H. Dieke, *Zs. f. Phys.* xxxii. p. 180 (1925).

very uncertain. The intensity anomalies suggest that the value must be changed by a factor $\frac{1}{2}$ or $\frac{1}{4}$, but, as recent examples have shown, a secure value for the moment of inertia can only be derived from a band if its structure is *completely* known. Therefore it seems rather premature just now to discuss the various possibilities. Attention must, however, be drawn to the fact that the model of the H_2^+ -ion as calculated by Pauli* and Niessen† has a much larger moment of inertia ($7.13 \cdot 10^{-40}$). The only thing which can be predicted about the moment of inertia of an *excited* H_2^+ -molecule is that its value will lie between that of the normal molecule (as derived from specific heat data) and that of the H_2^+ -ion. Although the model of Pauli and Niessen could not be verified quantitatively, a large value for an excited molecule is not unlikely. Therefore the writer cannot agree with Richardson and Tanaka's conclusion‡ that the carrier of the band discovered by these authors must be H_3 only because of its large moment of inertia ($0.624 \cdot 10^{-40}$ and $0.480 \cdot 10^{-40}$).

6. The existing data do not yet allow us to decide with certainty how the three groups are connected. It seems, however, impossible that all the three groups are due to *one* electronic transition, but not unlikely that they must be attributed to three different electronic transitions.

If in a molecule the electric momentum has no component, or a constant one along the line joining the nuclei, according to Bohr's correspondence principle there is no possibility that a simultaneous change of the electronic configuration and the oscillation occurs. Therefore to such an electronic transition belongs only the group $\Delta n = 0$. It is possible that the bands which we have considered represent such a case. A further investigation of the bands will surely give certainty also regarding this point.

Leiden, Instituut voor theoretische Natuurkunde,
April 1925.

* W. Pauli, jun. *Ann. d. Phys.* lxxviii. p. 177 (1922).

† K. F. Niessen, *Arch. Néerl.* 1923; *Ann. d. Phys.* lxx. p. 124 (1923).

‡ O. W. Richardson and T. Tanaka, *Proc. Roy. Soc. A*, cvi. p. 640 (1924).

For the earth's attraction $\mu = ga^2$, where a is the earth's radius; also h , the constant angular momentum about S , is seen from the circumstances of projection to be $av \sin \phi$. Hence (1) becomes

$$\frac{d^2u}{d\theta^2} + u = \frac{1}{2H \sin^2 \phi}, \quad \dots \dots (2)$$

where H is written for $v^2/2g$.

The energy equation connecting the velocity V at any distance r with the major axis $2a$ of the orbit of the particle is

$$V^2 = \mu \left(\frac{2}{r} - \frac{1}{a} \right). \quad \dots \dots (3)$$

Inserting the condition that $V = v$ when $r = \frac{1}{u} = a$, we get

$$a = \frac{ga^2}{2ga - v^2} = \frac{a^2}{2(a - H)}. \quad \dots \dots (4)$$

The first integral of (1) is

$$\frac{1}{2} \left\{ \left(\frac{du}{d\theta} \right)^2 + u^2 \right\} = \frac{u}{2H \sin^2 \phi} + C, \quad \dots \dots (5)$$

where the value of the constant C is determined from the condition that $r d\theta/dr = \tan \phi$ when $r = a$. Thus we find that $C = -\frac{\text{cosec}^2 \phi}{2a^2 H} (a - H)$. Hence (5) becomes

$$\left(\frac{du}{d\theta} \right)^2 = \frac{u}{H} \text{cosec}^2 \phi - \frac{a - H}{a^2 H} \text{cosec}^2 \phi - u^2, \quad \dots \dots (6)$$

which may be written

$$\left(\frac{du}{d\theta} \right)^2 = \frac{\text{cosec}^4 \phi}{4H^4} - \frac{a - H}{a^2 H} \text{cosec}^2 \phi - \left(u - \frac{\text{cosec}^2 \phi}{2H} \right)^2. \quad (6')$$

The apsidal distances are given by the values of u for which $\frac{du}{d\theta} = 0$.

Thus for the discussion of the highest point attained by the particle above the earth's surface we require the smaller root u_1 of the quadratic obtained by putting the right-hand side of (6') = 0.

Thus

$$u_1 = \frac{\text{cosec}^2 \phi}{2H} - \frac{\text{cosec}^2 \phi}{2H} \sqrt{1 - 4 \frac{H}{a} \left(1 - \frac{H}{a} \right) \sin^2 \phi}. \quad (7)$$

In the figure $SA' = \frac{1}{u_1}$,

$$\text{i. e. } SA' = \frac{a}{2} \frac{1 + \sqrt{1 - 4 \frac{H}{a} \left(1 - \frac{H}{a}\right) \sin^2 \phi}}{1 - \frac{H}{a}} \quad \dots \quad (8)$$

If e is the eccentricity of the elliptic path,

$$SA' = a(1+e) = \frac{a}{2 \left(1 - \frac{H}{a}\right)} (1+e) \text{ from (4).}$$

Hence

$$e = \sqrt{1 - 4 \frac{H}{a} \left(1 - \frac{H}{a}\right) \sin^2 \phi} \quad \dots \quad (9)$$

When this expression for e is developed in powers of H/a not above the third, we find on putting $H = v^2/2g$,

$$e = 1 - \frac{v^2}{ga} \sin^2 \phi + \frac{v^4}{2g^2 a^2} \sin^2 \phi \cos^2 \phi + \frac{v^6}{2g^3 a^3} \sin^4 \phi \cos^2 \phi + \dots \quad (10)$$

The greatest height attained is $SA' - a$.

From (8) we obtain after reduction and expansion

$$SA' - a = H \cos^2 \phi \left\{ 1 + \frac{H}{a} (1 + \sin^2 \phi) + \frac{H^2}{a^2} (1 + \sin^2 \phi + 2 \sin^4 \phi) + \dots \right\}.$$

Calling this height H' , putting $H = v^2/2g$, and writing θ for the angle which the direction of projection makes with the horizontal through P, we obtain, corresponding to a result of elementary dynamics:

$$H' = \frac{v^2 \sin^2 \theta}{2g} \left\{ 1 + \frac{v^2}{2ga} (1 + \cos^2 \theta) + \frac{v^4}{4g^2 a^2} (1 + \cos^2 \theta + 2 \cos^4 \theta) + \dots \right\}. \quad (11)$$

Note that $2ga$ is the square of the "velocity from infinity," so that the assumption made in the ordinary elementary case is that squares and higher powers of $(v^2/2ga)$ are to be neglected.

If e. g. v is of the order of 3000 f./s., (11) would become

$$H' = \frac{v^2 \sin^2 \theta}{2g} \left\{ 1 + \cdot 0066 (1 + \cos^2 \theta) + \cdot 000044 (1 + \cos^2 \theta + 2 \cos^4 \theta) + \dots \right\}. \quad (12)$$

Reverting again to the figure,

$$S'A' = \alpha(1-e) = \frac{a^2(1-e)}{2(a-H)},$$

and if this be developed in powers of v^2/ga we get

$$S'A' = \frac{v^2 \cos^2 \theta}{2g} \left\{ 1 + \frac{v^2}{2ga} \cos^2 \theta + \frac{v^4 \cos^2 \theta}{4g^2 a^2} (1 - 2 \sin^2 \theta) \dots \right\}. \quad (13)$$

If all but the first term of this last expansion be neglected, we get that the distance from the nearer focus to the highest point is $v^2 \cos^2 \theta / 2g$. Now in the case of the slowly moving projectile the equation of the path referred to tangent and normal through the vertex is $x^2 = \frac{2v^2 \cos^2 \theta}{g} y$, i. e. the "parameter" of the parabola is $\frac{2v^2 \cos^2 \theta}{g}$.

The results (10) and (13) show that when a particle is projected from a point on the earth's surface the path is really an ellipse, but that when the speed of projection is relatively small the part of the ellipse above the earth's surface is not much different from a parabola. Only if gravity were constant would the path be an exact parabola.

Reverting to (6'), this equation gives on integration

$$\theta - \alpha = \cos^{-1} \left[\frac{2aHu - a \operatorname{cosec}^2 \phi}{a \operatorname{cosec}^2 \phi \sqrt{1 - \frac{4H}{a} \left(1 - \frac{H}{a}\right) \sin^2 \phi}} \right] \quad (14)$$

in terms of the original data H and ϕ , or using the value of e already obtained,

$$2Hu \sin^2 \phi = 1 + e \cos (\theta - \alpha). \quad (15)$$

Now from the triangle SPS' ,

$$SP = a, \quad PS' = 2\alpha - a = \frac{aH}{a-H},$$

$$\text{and} \quad \frac{\sin \theta_0}{\frac{aH}{a-H}} = \frac{\sin 2\phi}{a^2 e};$$

$$\therefore \sin \theta_0 = \frac{H}{ae} \sin 2\phi.$$

From (9) we get

$$a^2 e^2 = a^2 - 4Ha \left(1 - \frac{H}{a}\right) \sin^2 \phi, \quad \dots \quad (16)$$

so that $a^2 e^2 - 4H^2 \sin^2 \phi \cos^2 \phi = (a - 2H \sin^2 \phi)^2$.

Hence we have

$$\cos \theta_0 = \sqrt{1 - \frac{H^2}{a^2 e^2} \sin^2 2\phi} = -\frac{a - 2H \sin^2 \phi}{ae}, \quad \dots \quad (17)$$

since $\theta_0 > \frac{\pi}{2}$.

Hence to find the constant α in (15) we have $\theta = \theta_0$ when $u = \frac{1}{a}$.

The final form of the equation of the orbit then becomes

$$2Hu \sin^2 \phi = 1 + e \cos \theta. \quad \dots \quad (18)$$

For the time of flight,

$$h = r^2 \frac{d\theta}{dt} = \frac{4H^2 \sin^4 \phi}{(1 + e \cos \theta)^2} \cdot \frac{d\theta}{dt}.$$

The time taken for the particle to encounter the earth's surface again is therefore given by

$$hT = 8H^2 \sin^4 \phi \int_{\theta_0}^{\pi} \frac{d\theta}{(1 + e \cos \theta)^2}.$$

This integral can be evaluated by the substitution $u = \tan \theta/2$ or by putting

$$\cos \lambda = \frac{\cos \theta + e}{1 + e \cos \theta}.$$

Using the latter method we get

$$hT = \frac{8H^2 \sin^4 \phi}{(1 - e^2)^{3/2}} \int_{\lambda_0}^{\pi} (1 - e \cos \lambda) d\lambda,$$

where

$$\cos \lambda_0 = -\frac{a(1 - e^2) - 2H \sin^2 \phi}{2He \sin^2 \phi}.$$

Performing the integration, we get finally

$$hT = \frac{8H^2 \sin^4 \phi}{(1 - e^2)^{3/2}} \left[\tan^{-1} \left\{ \frac{2H \sqrt{1 - e^2} \sin \phi \cos \phi}{a(1 - e^2) - 2H \sin^2 \phi} \right\} + \sqrt{1 - e^2} \cot \phi \right]. \quad \dots \quad (19)$$

To test the accuracy of this result we apply it to obtain

the result of one of the examples proposed in Gray's 'Dynamics' (Ex. 15, p. 302). The question reads: "A particle is projected from the earth's surface so as to describe a portion of an ellipse whose major axis is 1.5 times the earth's radius. If the direction of projection makes an angle of 30° with the vertical, prove that the time of flight is $\frac{3}{4}\sqrt{\frac{3a}{g}}\left\{\tan^{-1}\sqrt{6} + \sqrt{\frac{2}{3}}\right\}$."

In this case

$$v^2 = \frac{2}{3}ga, \quad e = \frac{\sqrt{7}}{3}, \quad \phi = \frac{\pi}{6},$$

so that the formula of (19) gives in the present case

$$T = \frac{2\left(\frac{2}{3}ga\right)^{3/2}\left(\frac{1}{8}\right)}{g^2a\left(1-\frac{7}{9}\right)^{3/2}}\left[\tan^{-1}\left\{\frac{\frac{2}{3}ga \cdot \frac{1}{2} \cdot \frac{\sqrt{3}}{2} \cdot \frac{\sqrt{2}}{3}}{\frac{2}{9}ga - \frac{1}{6}ga}\right\} + \frac{\sqrt{2}}{3}\sqrt{\frac{2}{3}}\right],$$

and this readily gives the result required.

We next proceed to develop the expression for T in powers of v^2/ga , i. e. to give the time of flight explicitly in terms of the initial data v and ϕ .

We rewrite (19) first as

$$T = \frac{2v^3 \sin^3 \phi}{g^2a(1-e^2)^{3/2}}\left[\tan^{-1}\left\{\frac{v^2 \sin \phi \cos \phi \sqrt{1-e^2}}{ga(1-e^2) - v^2 \sin^2 \phi}\right\} + \sqrt{1-e^2} \cdot \cot \phi\right]. \quad (19')$$

From (9) we get

$$1-e^2 = 4\frac{H}{a_1}\sin^2 \phi(a-H);$$

$$\therefore \frac{2v^3 \sin^3 \phi}{g^2a(1-e^2)^{3/2}} = \frac{1}{\sqrt{2}}\sqrt{\frac{a}{g}}\left\{1 + \frac{3}{2}\frac{H}{a} + \frac{15}{8}\frac{H^2}{a^2} + \frac{35}{16}\frac{H^3}{a^3} + \dots\right\}. \quad (20)$$

Similarly $\tan^{-1}\left\{\frac{v^2 \sin \phi \cos \phi \sqrt{1-e^2}}{ga(1-e^2) - v^2 \sin^2 \phi}\right\}$ becomes on expansion in powers of H ,

$$2 \cos \phi \sqrt{\frac{H}{a}}\left\{1 + \frac{H}{a}\left(\frac{3}{2} + \frac{4}{3}\cos^3 \phi\right) + \frac{H^2}{a^2}\left(\frac{23}{8} - 6\cos^3 \phi\right) \dots\right\}. \quad (21)$$

Also

$$\sqrt{1-e^2} \cot \phi = 2\sqrt{\frac{H}{a}}\left\{1 - \frac{1}{2} \cdot \frac{H}{a} - \frac{1}{8}\frac{H^2}{a^2} \dots\right\}. \quad (22)$$

Adding (21) and (22) and multiplying by the expansion on the right of (20), we get finally

$$T = \sqrt{\frac{2H}{g}} \cos \phi \left\{ 2 + \frac{H}{a} \left(\frac{5}{2} - \frac{4}{3} \cos^3 \phi \right) + \frac{H^2}{a^2} \left(\frac{49}{8} - 8 \cos^3 \phi \right) \dots \right\};$$

or in terms of v and θ ,

$$T = \frac{v \sin \theta}{g} \left\{ 2 + \frac{v^2}{2ga} \left(\frac{5}{2} - \frac{4}{3} \sin^3 \theta \right) + \frac{v^4}{4g^2 a^2} \left(\frac{49}{8} - 8 \sin^3 \theta \right) \dots \right\} \dots \quad (23)$$

Where $\frac{v^2}{2ga}$ is neglected, this result reduces to

$$T = \frac{2v \sin \theta}{g}.$$

If v is 3000 f./sec.,

$$T = \frac{2v \sin \theta}{g} \left\{ 1 + .0033 \left(\frac{5}{2} - \frac{4}{3} \sin^3 \theta \right) + .000022 \left(\frac{49}{8} - 8 \sin^3 \theta \right) + \dots \right\}.$$

We next wish to find the range on the horizontal plane through the point of projection.

The equation of the orbit referred to rectangular axes through C is

$$\frac{x^2}{\alpha^2} + \frac{y^2}{\beta^2} = 1, \quad \text{where} \quad \beta^2 = \alpha^2(1 - e^2). \quad \dots \quad (24)$$

The equation of the chord PR which is at right angles to SP and is the range required is

$$\frac{x - a \cos \theta_0}{-\sin \theta_0} = \frac{y - a \sin \theta_0}{\cos \theta_0} = \rho, \quad \dots \quad (25)$$

where ρ is the distance of (x, y) from P measured along PR. (24) and (25) give

$$\frac{(a \cos \theta_0 - \rho \sin \theta_0)^2}{\alpha^2} + \frac{(a \sin \theta_0 + \rho \cos \theta_0)^2}{\beta^2} = 1,$$

whence

$$PR = \rho = -\frac{2ae^2 \cos \theta_0 \sin \theta_0}{1 - e^2 \sin^2 \theta_0}.$$

Inserting the values of $\cos \theta_0$ and $\sin \theta_0$ previously determined and expanding as before, we obtain

$$PR = \frac{v^2 \sin 2\theta}{g} \left\{ 1 - \frac{v^2}{ga} \cos^2 \theta + \frac{v^4}{4g^2 a^2} \sin^2 2\theta + \dots \right\}. \quad (26)$$

This reduces to $v^2 \sin 2\theta/g$ when the velocity is relatively small.

If $v = 3000$ f./sec.,

$$PR = \frac{v^2 \sin 2\theta}{g} \{ 1 - 0.0132 \cos^2 \theta + 0.000044 \sin^2 2\theta + \dots \}.$$

Next compare this with the arc intercepted on the meridian, viz.

$$2a\theta_0 = 2a \sin^{-1} \left(\frac{H}{ae} \sin 2\phi \right).$$

On expansion we get

$$\text{arc} = \frac{v^2 \sin 2\theta}{g} \left\{ 1 + \frac{v^2}{ga} \cos^2 \theta + \frac{v^4}{24g^2 a^2} \sin^2 2\theta + \dots \right\}, \quad (27)$$

agreeing with the distance along the chord PR to a first approximation.

For a speed of 3000 f./sec. the difference between the chord and the arc on the meridian is $\frac{0.0264v^2 \sin 2\theta \cos^2 \theta}{g}$, the maximum value of which is about $0.0005 \cdot v^2 =$ about $\frac{9}{10}$ mile in a range of approximately 46 miles.

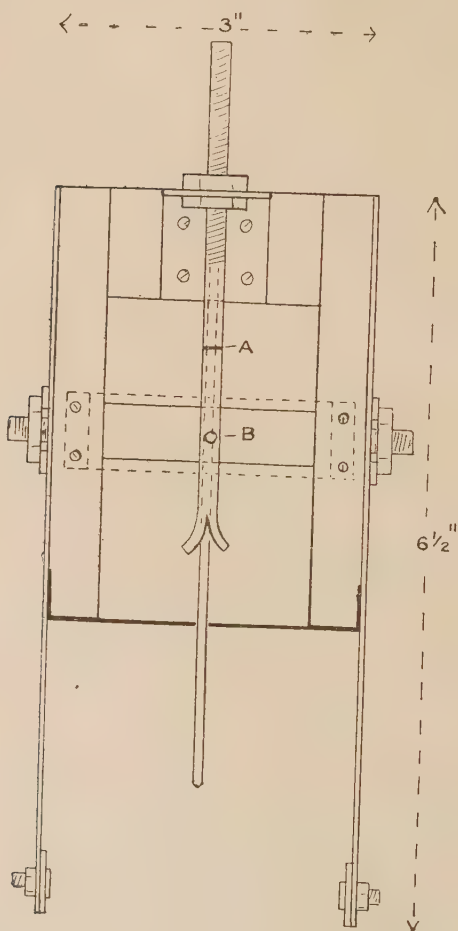
XVIII. *On a Method of Measurement of Newton's Coefficient of Restitution, and the Law of Oblique Impact.* By H. G. GREEN, M.A., *Lecturer in Mathematics, University College, Nottingham**.

THE following research was undertaken in order to find with what degree of accuracy the theoretical equations for the rebound of a sphere from a plane, whether smooth or rough, were obeyed in the case of an oblique impact. For a satisfactory investigation it was clearly essential that angles of impact and rebound could be measured with accuracy, and that during impact the sphere should be free from external restraint. The general disposition of the apparatus designed by the author to fulfil these conditions is shown in fig. 4. The sphere used was a ball of fairly soft wood through which a cylindrical hole ran

* Communicated by Prof. E. H. Barton, F.R.S.

centrally of such radius that it could slide easily on the guiding-rod of the pistol (fig. 1). It was shot obliquely on to a brass plate mounted on an inclined plane, and

Fig. 1.

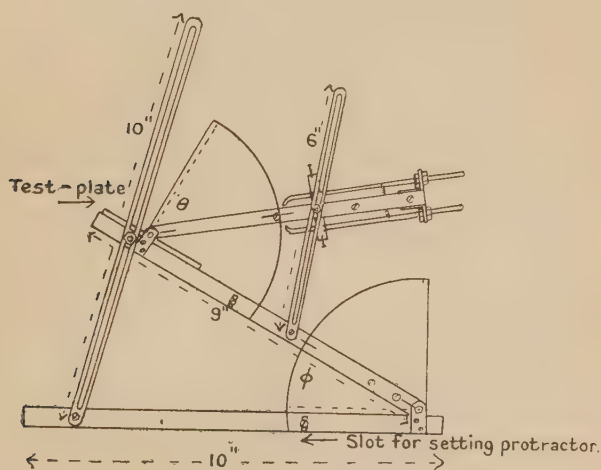


The pistol shown in plan.

the angle of the plane was varied until the direction of rebound was as nearly vertical as could be obtained by the means of adjustment, the ball falling back approximately to the point of impact. The angles of impact

and rebound (directions from the normal), θ , ϕ as marked, were measured by means of four protractors permanently mounted on the apparatus, of which a side view is shown in fig. 2. It was found advisable, in order to obtain accurate angle measurements, to dispense with ordinary hinges at the points of measurement, and to replace them by small tightly-fitting bolts through brass plates attached to the frame of the apparatus, the protractors being carefully centred on these bolts. It was also found, to avoid strain on the guiding-rod and to secure smooth discharge, that the release system of the ball had to be double and of even action on

Fig. 2.



Sectional view of the apparatus.

both sides. The triggers consisted of two rods with curved double prongs at the extremities towards the plane, the rods being in the direction of the guiding rod. The prongs were sheathed in pieces of rubber tube to prevent damage to the ball. In order to mount a trigger, one plate of an ordinary metal hinge was fastened to the pistol frame, and the rod was fitted through a hole in the other plate. The length of the trigger could be varied by means of two nuts, which were screwed up tightly on to the hinge on either side. The two triggers were connected by a spring (A, fig. 1), and provided with screw-stops (B) on bridges over them, by means of which their ranges could be adjusted.

Theory.

The detailed discussion of the mathematical theory for the impact of a sphere against a rough plane will be found in any text-book on Rigid Dynamics (for example, Loney, 'Dynamics of a Particle and of Rigid Bodies,' pp. 274-276).

In the case under discussion the sphere has no initial angular velocity. Let u, v be the components of velocity tangential and normal to the plane on approach, and u', v' the corresponding components after impact, a the radius, and k the radius of gyration about the central axis perpendicular to the plane of motion.

Then

$$v \tan \theta = u, \quad v' \tan \phi = u', \quad v' = ev,$$

where e is the Newton Coefficient of Restitution. For "large" values of θ where sliding takes place

$$u' = u - \mu v(1 + e),$$

or since

$$v' = ev, \quad e \tan \phi = \tan \theta - \mu(1 + e). \quad [\text{Type A.}]$$

For "small" values of θ where there is no sliding

$$\left(1 + \frac{k^2}{a^2}\right) u' = u,$$

or

$$\left(1 + \frac{k^2}{a^2}\right) e \tan \phi = \tan \theta. \quad [\text{Type B.}]$$

The critical angle between the cases is obtained when

$$\tan \theta = \mu(1 + e) \left(1 + \frac{a^2}{k^2}\right),$$

where μ is the coefficient of friction.

Experimental Procedure.

It was found convenient, in making any observation, to appoint first the angle θ and then to find the corresponding ϕ by adjustment of the inclined plane, the greater arc of the ϕ adjustment rendering it the more sensitive one. As the correct setting was approached, a considerable number of trials were made in each position so as to cut out the possibility of a false bounce. In addition, after the best position was obtained and when the readings had been observed, for further check two near settings of the plane, equally spaced from the read one, were made and the resulting ranges of the projectile on the plane noticed:

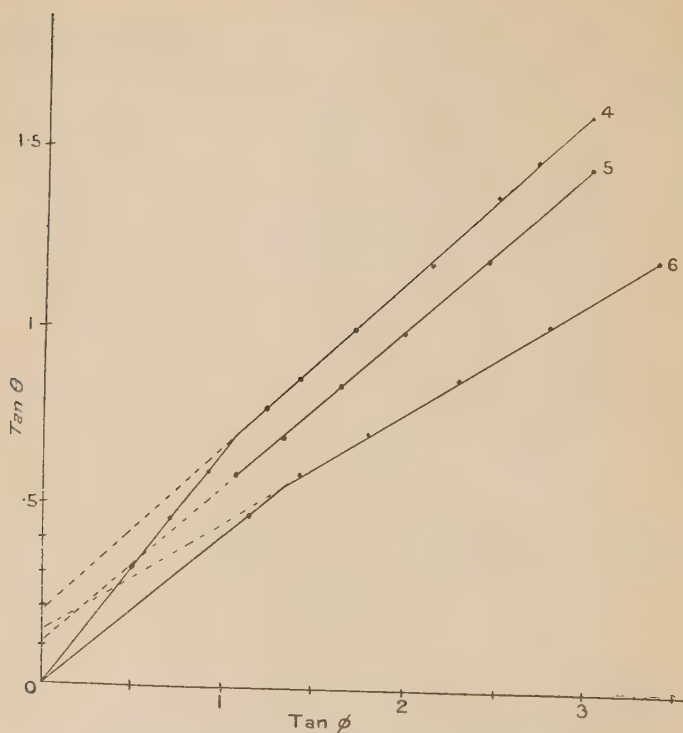
these should be very approximately equal. The angle readings are all direct (θ , not its complement, being observed) since errors in the deduced value of e due to overestimate (or underestimate) of both θ and ϕ tend to cut out. This takes advantage of a psychological phenomenon that, in a short series of readings such as make up an observation in this case, any temporary tendency to read high will probably persist through that series. In the following tables the angle readings are the average ones.

In Experiments 1, 2, 3 (Table I.) the brass plates were very highly polished. The observations were all of type A, but with a μ too small to detect. We have, therefore, for all intents and purposes the case of a ball impinging on a smooth plane and obeying the law $e \tan \phi = \tan \theta$.

In Experiment 4 (Table II.) the brass plate was roughened before being mounted. Experiments 5, 6 were made immediately after 2, 3 respectively, the planes being roughened with sand-paper while still mounted. This course was taken, as it was desired to notice the effect on the Coefficient of Restitution of a slight breaking up of the surface. It was found that the coefficient of the system depended not only on the plate itself, but also on the security of its fastenings, so that in any comparative experiments the fastenings had to be left undisturbed. A considerable decrease in the value of the constant was found. In deducing the numerical results of Experiments 4, 5, 6 the graphs connecting $\tan \theta$, $\tan \phi$ were first plotted (shown in fig. 3) to determine the types of the observations. The numerical values of e , $\mu(1+e)$ for type A were obtained by Gauss's Method of Mean Squares applied to the four best-spaced readings; for type B the value of e for each observation was determined directly; the critical value for θ was obtained by solution of the equations of the two lines and also by theoretical deduction from the value obtained for $\mu(1+e)$. The diameter of the sphere was .86 inch; that of the cylindrical hole .24 inch, leading to $k^2/a^2 = .4078$.

The degree of accuracy obtained in the experiments of Table II. was not as high as that obtained in those of Table I. In the latter case the " ϕ " readings for any setting " θ " were determined by repeated experiment, between each of which the inclined plane was moved and readjusted in the course of the next trial, the relative position of the pistol being undisturbed. This involved a very great number of impacts, and in the experiments of Table II. this number had to be reduced to minimize the wear of the plate with consequent change of μ . The two

Fig. 3.



The results of experiments expressed graphically.

TABLE I.

1.			2.			3.		
θ°	ϕ°	e	θ°	ϕ°	e	θ°	ϕ°	e
61 $\frac{5}{8}$	74	.53085	60	73 $\frac{1}{2}$.49870			
55	69 $\frac{5}{8}$.53022	55	70 $\frac{3}{4}$.49874	55	74 $\frac{1}{4}$.40277
50 $\frac{1}{2}$	66 $\frac{1}{8}$.52983	50 $\frac{5}{16}$	67	.49914	50	71 $\frac{1}{2}$.40165
45 $\frac{1}{4}$	62 $\frac{1}{4}$.53073	45 $\frac{3}{16}$	63 $\frac{1}{2}$.49912	45	68 $\frac{1}{2}$.40149
40	57 $\frac{3}{4}$.52943	40	59 $\frac{1}{4}$.49922	40	64 $\frac{1}{2}$.40233
34 $\frac{3}{8}$	52 $\frac{1}{2}$.53007	35 $\frac{1}{8}$	54 $\frac{1}{2}$.49946	35	60 $\frac{1}{2}$.40224
30	47 $\frac{1}{2}$.52904	30	49 $\frac{1}{2}$.49967	30	55 $\frac{1}{2}$.40239
			25	43 $\frac{3}{8}$.49855	25	49 $\frac{1}{4}$.40180
Average		.5300	Average		.4991	Average		.4021

TABLE II.

	4.		5.		6.	
	θ° .	ϕ° .	θ° .	ϕ° .	θ° .	ϕ° .
Type A	58	$71\frac{1}{2}$	55	$71\frac{3}{4}$		
	56	$69\frac{7}{8}$	50	$67\frac{3}{4}$	$50\frac{1}{8}$	$73\frac{7}{8}$
	54	$68\frac{1}{4}$	45	64	45	$70\frac{1}{8}$
	50	*65	40	$58\frac{3}{4}$	40	$66\frac{1}{8}$
	45	$59\frac{3}{4}$	35	$53\frac{1}{8}$	35	$60\frac{5}{8}$
	$40\frac{7}{8}$	$54\frac{1}{8}$	$30\frac{1}{2}$	$47\frac{1}{2}$	30	54
	38	$51\frac{1}{8}$				
Type B	$30\frac{7}{8}$	$42\frac{1}{2}$		†	25	48
	$25\frac{3}{4}$	$35\frac{7}{8}$				
	$20\frac{1}{8}$	29				
e from Type A.	·470		·437		·299	
e from Type B.	·467				·298	
$\mu(1+e)$	·197		·125		·157	
Critical θ (theory).	$\tan^{-1} \cdot 682$		$\tan^{-1} \cdot 430$		$\tan^{-1} \cdot 543$	
" " (intersect. of lines).	$\tan^{-1} \cdot 693$				$\tan^{-1} \cdot 548$	

* The graph shows this to be a faulty reading.

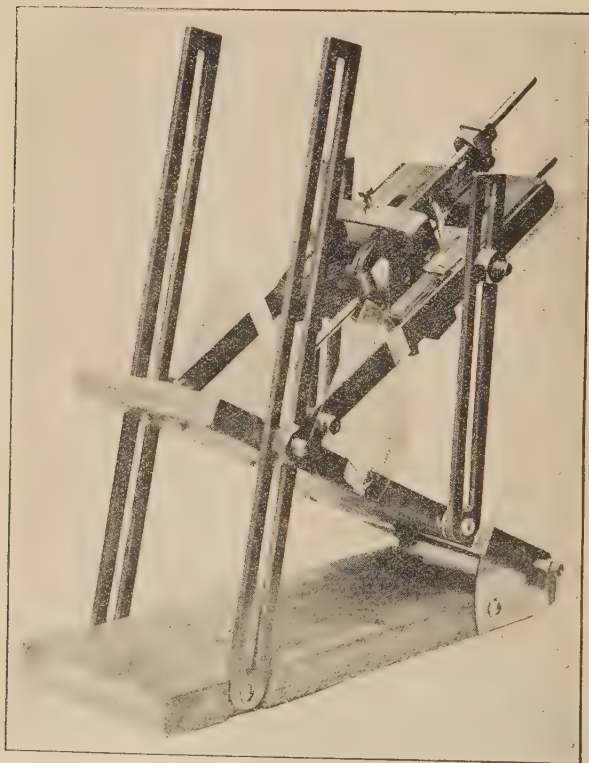
† No readings of Type B were obtainable.

values for the critical angle (Table II.) are not completely independent. The theoretical expression is that which satisfies the theoretical equations, and its numerical result is the one which would be obtained if the Type B value for e were taken as exactly equal to the Type A value; the closeness of these results is a severe test on the accuracy of the method. The same table also illustrates a drawback to the method, which is unsatisfactory for impacts near the normal. The last angles in each set are the least for which satisfactory definition could be obtained.

The close adherence of the results to the two linear laws and the near equality of the values of "Newton's Constant" deduced from these laws justify the assumptions that, within the ranges of tangential and normal velocities employed, μ and e have constant values, and confirms the resulting

dynamical equations for the behaviour of a sphere impinging on a rough plane.

Fig. 4.



General view of the apparatus used for impact experiments.

Summary.

An apparatus is described by which the coefficient of restitution between a plane and a sphere can be obtained to a considerable degree of accuracy. Impacts of a sphere with smooth and rough planes are dealt with, and the theoretical equations are shown to be very closely satisfied.

XIX. *On an Extension of the Negative Band Spectrum of Nitrogen.* By T. R. MERTON, F.R.S., and J. G. PILLEY, B.A.*

WE have recently described (Roy. Soc. Proc. A cvii. p. 411, 1925) observations of the spectrum of Nitrogen which is produced when discharge-tubes containing a very small proportion of nitrogen in helium at comparatively high pressures are excited by condensed discharges of moderate intensity. Under these conditions the arc spectrum is isolated, and it was pointed out that in the presence of helium the negative bands were enhanced at the expense of the positive bands. We have now further investigated the discharge conditions which are most favourable to the isolation of the negative bands. These experiments have not only facilitated a remeasurement of the known band heads, but have also made it possible to observe an extension of the bands into the less refrangible parts of the spectrum. Measurements of the heads of the bands recognized are summarized in Kayser's 'Handbuch der Spectrographie,' vol. v., the most reliable of these being probably those given by Deslandres (*Comptes Rendus*, cxxxix. p. 1174, 1904), who has arranged the heads of the bands into six series. Deslandres' assignment of the different bands into these series seems to have depended to some extent on the general appearance of the bands, for the members of the series do not show constant second differences in the wave-numbers, and his arrangement therefore seems to merit some further consideration. These discrepancies seem to be due in part to a confusion with the bands of the positive system, and many of the bands are so weak under ordinary conditions that their identification is almost impossible.

According to recent developments in the application of the quantum theory to band spectra, the heads of bands are points of no special theoretical significance, but they nevertheless serve in the arrangement of the different bands into series, and a knowledge of their wave-lengths is of importance for purposes of identification in celestial spectra. In particular the negative bands of nitrogen constitute an important part of the spectrum of the aurora. The appearance of the bands in the aurora and under different conditions in the

* Communicated by the Authors.

laboratory has been studied by Rayleigh (Roy. Soc. Proc. A, ci. p. 114, 1922). Rayleigh found that the distribution of intensity in the bands in the auroral spectrum more closely resembled that seen in the positive column in discharge-tubes at low pressures than that seen in the negative glow and first negative layer, though in the latter sources the negative bands were more completely (though not entirely) isolated from the positive system.

The preparation of the discharge-tubes used in the experiments here recorded has been described in a previous investigation (*loc. cit.*). When these tubes, which contained helium at pressures about 30 mm. of mercury and a trace of nitrogen, and which were provided with wide tubes in place of the usual capillary, were excited by uncondensed discharges the negative bands were very much more prominent than in tubes containing pure nitrogen. It is well known that in vacuum-tubes containing pure nitrogen the negative bands are enhanced at very low pressures and appear strongly throughout the tubes. With feebly condensed discharges our tubes show an even greater enhancement of the negative bands, but in the course of a series of experiments to discover the optimum conditions for the isolation of the bands it was found that when the tubes were excited by a high frequency discharge from a small Tesla coil the positive bands very nearly disappeared, and it was moreover evident that further members of the negative band system could be traced into the less refrangible parts of the spectrum. All the negative bands could be seen clearly and distinctly, and these conditions seemed appropriate to a remeasurement of the spectrum. A preliminary examination showed that such a remeasurement was essential to an arrangement of the heads of the bands. The spectrum was photographed with the concave grating instrument and the Littrow glass spectrograph described in the previous investigation (*loc. cit.*), and the iron arc served as a comparison spectrum. It must be borne in mind that a high degree of precision cannot be attained in the measurement of the heads of unresolved bands, and the wave-lengths are accordingly given to the nearest tenth of an ångström. The results are given in Table I., in which the wave-lengths are given in comparison with those of previous investigators. The intensities in the tubes containing helium and nitrogen with the Tesla excitation are also compared with those observed with a wide bore tube containing nitrogen and excited by a discharge of moderate intensity.

TABLE I.

λ (I.A.).	Series.	Intensity.		Des- landres.	Hassel- berg.	^o Ang- ström.	Hem- salech.
		(He+N)	(N)				
5864.7	1	4	0				
5653.1	3	4	1				
5564.1	4	1	0				
5485.5	5	5	0				
5330.4	?	2	0				
5228.3	1	7	2	5227.5	
5148.8	2	4	3	5150.0	
5076.6	3	7	1				
5012.7	4	3	10				
4957.9	5	5	10				
4881.9	?	5	0				
4709.2	1	4	2	...	4708.6	4709.5	
4651.8	2	4	1	...	4651.2	4653.5	
4599.7	3	6	2	...	4599.4	4601.2	
4554.1	4	4	0	...	4553.8	4555.2	
4515.9	5	6	0	...	4515.3	4516.5	
4490.3	6	2	1	...	4484.9		
4278.1	1	8	6	...	4278.0	4281.0	4278.4
4236.5	2	7	5	...	4236.3	4239.0	4236.8
4201.1	?	4	4				
4199.1	3	4	2	...	4198.7	4203.0	4198.8
4166.8	4	3	0	...	4166.4	4175.0	4166.6
4140.5	5	2	—				
3914.4	1	6	6	3914.4	3914.4
3884.3	2	3	1	3883.9	3884.2
3857.9	3	2	2	3857.1	3857.1
3835.4	4	1	1				
3818.1	5	1	0				
3582.1	2	4	3	3581.5			
3563.9	3	4	0	3563.5			
3548.9	4	3	C	3548.2			
3538.3	5	2	C				
3532.6	6	1	0C				
3368.0	3	2	1				
3298.7	4	3	1	3298.5			
3293.4	5	3	0	3296.1			

C denotes a head much confused with other bands.

198 *Extension of the Negative Band Spectrum of Nitrogen.*

In Table II. the assignment of the heads into series is given, the wave-numbers *in vacuo* being arranged in columns and the first and second differences being also given. Our results do not agree well with those of Deslandres, but the constancy of the second differences in our wave-numbers

TABLE II.

Series.	Wave-length in air.	Wave-number <i>in vacuo.</i>	1st diff.	2nd diff.
1	5864.7	17046.5		
	5228.3	19121.6	2075.1	
	4709.2	21229.2	2107.6	32.5
	4278.1	23368.3	2139.1	31.5
	3914.4	25539.5	2171.2	32.1
2	5148.8	19422.0		
	4651.8	21491.1	2069.1	
	4236.5	23597.7	2106.6	37.5
	3884.3	25737.4	2139.7	33.1
	3582.1	27908.8	2171.4	31.7
3	5653.1	17684.4		
	5076.6	19692.8	2008.4	
	4599.7	21734.4	2041.6	33.2
	4199.1	23807.8	2073.4	31.8
	3857.9	25913.5	2105.7	32.3
	3563.9	28051.3	2137.8	32.1
	3308.0	30221.5	2170.2	32.4
4	5564.1	17967.5		
	5012.7	19944.2	1976.7	
	4554.1	21952.0	2007.8	31.1
	4166.8	23992.3	2040.3	32.5
	3835.4	26065.4	2073.1	32.8
	3548.9	28169.8	2104.4	31.3
	3298.7	30306.7	2136.9	32.5
5	5485.5	18224.9		
	4957.9	20164.1	1939.2	
	4515.9	22137.6	1973.5	34.3
	4140.5	24144.7	2007.1	33.6
	3818.1	26183.5	2038.8	31.7
	3538.3	28254.2	2070.7	31.9
	3293.4	30355.5	2101.3	30.6

is much closer than in the case of Deslandres' values, and it may be surmised that the recognition of the true heads of some of the bands is extremely difficult unless a comparison is made of spectra under two different conditions in one of which the negative band system is very strongly accentuated. A word must be said about the nature of the Tesla excitation. It seems possible that the chief virtue of this method lies in providing a condition intermediate between the uncondensed discharge and a condensed discharge with a very small spark-gap, but there are certain changes in spectra which seem to be peculiar to this excitation. Vegard (Phil. Mag. xvi. No. 271, p. 193, 1923) has given a summary of his measurements of the auroral spectrum and has attempted to identify a number of the lines observed with lines of the spark spectrum of nitrogen. These lines have been compared with the extension of the nitrogen bands observed in this investigation, but there appears to be no systematic agreement. At the same time it would appear that Vegard's identification with the spark spectrum seems hardly justified in view of the fact that most of the lines with which they are identified are relatively faint, and do not appear to be selectively enhanced under any known conditions of excitation. It may be mentioned that a comparison has also been made with unidentified radiations observed in the spectrum of Comet Morehouse by de la Baume Pluvinel and Baldet (Astrophys. Journ. vol. xxxiv. p. 88, 1911), but here again there appears to be no correspondence.

We wish to record our thanks to the Department of Scientific and Industrial Research for a grant made to one of us (J. G. P.) during the course of this investigation.

Winforton House, Hereford,
March 10th, 1925.

XX. *The Flow of Water in a Corrugated Pipe.*
By Professor A. H. GIBSON, *D.Sc.**

Introduction.

THE author recently had occasion to measure the loss of head in a copper pipe whose walls were corrugated circumferentially. The results showed that the loss of head was proportional to $v^{2.135}$. The case of non-accelerated flow in which the index of v is greater than two is unusual, and

* Communicated by the Author.

although results of tests on pipes have occasionally been published indicating such an index, no such case has hitherto come before the notice of the author. It is both of practical importance and philosophical interest, since, if the theory of dimensional similarity holds for such a state of flow, the loss of head should be diminished if the viscosity of the fluid is increased. The experiments were therefore extended with a view of investigating this point.

Experiments.

The experimental pipe is of smooth drawn copper. The internal diameter at the bottom of the corrugations is 1·80 in. and at the top 2·0 in. Each corrugation takes approximately the form of a sine curve 0·4 in. pitch from crest to crest. The pressure drop along the pipe was obtained from pressure orifices drilled at the tops and at the bottoms of the corrugations. The difference in pressure between the top and bottom of a corrugation was also measured in a number of tests. All pressure differences were measured on an inverted U-tube water-gauge. The majority of the experiments were carried out with water at 15°·3 C. Two series were afterwards carried out at 51°·7 C. and 73°·3 C.

Tests at Normal Temperature.

The results of the tests are shown in Table I. and in the curve of fig. 1. The velocities (computed on the

TABLE I.
Temp. 15°·3 C.

Expt.		1.	2.	3.	4.	5.	6.	7.	8.	9.
$(p_1 - p_2)$ ft.	at top	·00288	·00630	·00824	·01236	·0222	·0247	·0433	·0610	·0848
	at bottom	·00288	·00630	·00824	·01230	·0220	·0240	·0422	·0595	·0824
v f.s. at enlarged section.		·513	·735	·866	1·066	1·380	1·470	1·862	2·22	2·60
Expt.		10.	11.	12.	13.	14.	15.	16.	17.	
$(p_1 - p_2)$ ft.	at top	·1296	·230	·285	·327	·428	·650	·763	1·000	
	at bottom	·1260	·222	·274	·315	·413	·618	·730	·952	
v f.s. at enlarged section.		3·19	4·16	4·53	4·90	5·52	6·65	7·15	8·12	

TABLE I. (continued).

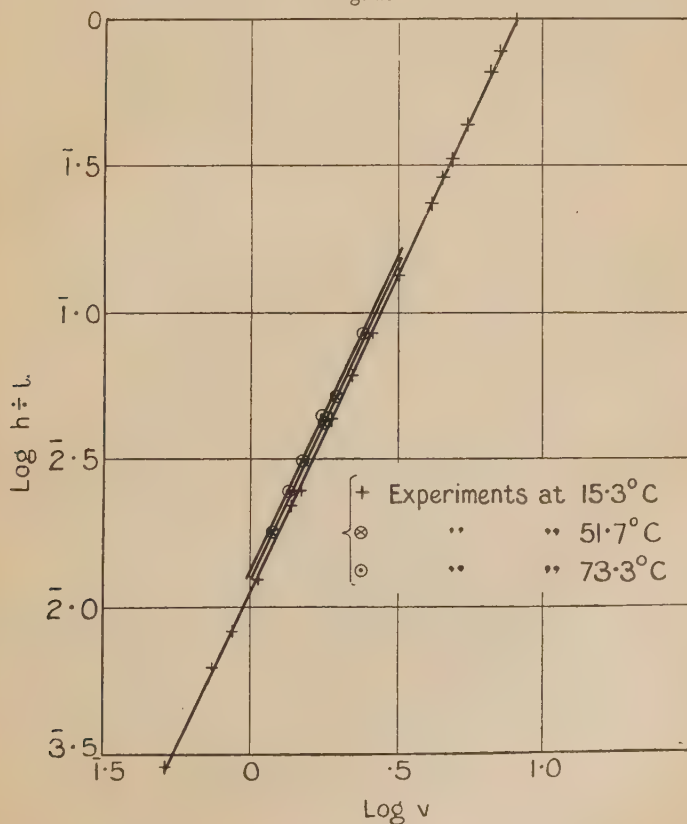
Temp. 51°·7 C.

Expt.	1.	2.	3.
$(p_1 - p_2)$ ft. at enlarged section	·0181	·0429	·0515
v f.s. at enlarged section	1·291	1·800	1·955

Temp. 73°·3 C.

Expt.	1.	2.	3.	4.
$(p_1 - p_2)$ ft. at enlarged section	·02455	·0310	·0439	·0824
v f.s. at enlarged section	1·350	1·505	1·769	2·425

Fig. 1.



diameter of the tube at the top of the corrugations) range from 0.5 f.s. to 8.1 f.s. On plotting the logarithms of log head against log velocity on a large scale, it appears that over this range the loss of head is proportional to $v^{2.135}$, and is given by

$$h = .0113 v^{2.135} \text{ ft. per foot run of pipe}$$

if the pressures are taken at the enlarged sections, and by

$$h = .0113 v^{2.120}$$

if the pressures are taken at the bottom of the corrugations.

For comparison, data were also obtained for plain smooth drawn copper pipes having diameters of 1.8 in. and 2.0 in., or respectively the same as the diameters at the bottom and top of the corrugations in the corrugated pipe. The loss of head in these parallel pipes is given by

$$h = .0030 v^{1.80} \text{ ft. per foot run in the 1.8 inch pipe}$$

and

$$h = .0026 v^{1.80} \text{ ,, ,, ,, 2.0 ,, ,,}$$

The comparative losses of head per foot run at velocities of 1, 2, and 4 f.s. are shown in the following table:—

Pipe.	Velocity f.s.		
	1.0.	2.0.	4.0.
Corrugated pipe (vel. at large section).	.0113	.0496	.218
Ditto (vel. at small section)0074	.0324	.142
2.0 in. parallel pipe0026	.0091	.0317
1.8 ,, ,, ,,0030	.0105	.0366

The results show that the resistance of the corrugated pipe is much greater even than that of a smooth pipe having the same diameter as the contracted section of the corrugations. At 1 f.s. it is 2.5 times as great, and the effect becomes relatively greater at higher velocities.

The loss of head in such a pipe may be looked upon as being mainly due to the shock and eddy formation caused by the enlargements and contractions of section which take place throughout its length. It is known that the loss due to a sudden enlargement is given approximately by

$$\frac{(v_1 - v_2)^2}{2g} \text{ ft.,}$$

where v_1 and v_2 are respectively the higher and lower velocities. There are 30 enlargements per foot run of the pipe, so that with a velocity of 1 f.s. in the larger sections, corresponding to 1.235 f.s. at the bottom of the corrugations, the loss per foot run, if the enlargements were sudden, would be

$$\frac{(1.235-1.00)^2}{2g} \times 30 = .0256 \text{ ft.}$$

The actual loss per foot run (.0113 ft.) is 44 per cent. of this. The corresponding values at 2 f.s. and 4 f.s. are 48.5 per cent. and 53.4 per cent. This would tend to indicate that as the velocity is increased, the type of flow gradually changes, the water in the corrugations taking part to an increasing degree in the general flow.

Confirmation of this is obtained from pressure readings at adjacent points in the crest and trough of a corrugation, for assuming the loss between a trough and the adjacent crest to be due to a reduction in velocity corresponding to the cross section of the pipe, the pressure at the enlarged section should be the greater by an amount theoretically equal to

$$\frac{v_1^2 - v_2^2 - (v_1 - v_2)^2}{2g} \text{ ft.}$$

Thus in experiment 12, $v_1 = 5.60$, $v_2 = 4.53$, so that the theoretical difference in pressure would be

$$\frac{31.4 - 20.5 - (1.14)}{64.4} \text{ ft.} = .151 \text{ ft.}$$

The measured difference is .094 ft., or .625 of its theoretical value. Similarly in experiment 15, with $v_2 = 6.65$ f.s., the measured difference in pressure is .78 of the theoretical, and in experiment 16, when $v_2 = 7.15$ f.s., it is .83 of the theoretical value.

Tests at different Temperatures.

It may readily be shown from the principle of dynamical similarity that the loss of pressure " p " per unit length of a pipe conveying a virtually incompressible fluid should be given by

$$p \propto \rho v^2 \left(\frac{\nu}{vd} \right)^{2-n},$$

where ρ is the density of the fluid,
 ν „ kinematic viscosity.

This indicates that if n is greater than 2 the resistance will diminish if the viscosity is increased, and in order to investigate this point further tests were carried out in which the mean temperature of the water in the pipe was respectively $51^{\circ}7$ C. and $73^{\circ}3$ C.

At these temperatures the following are the values of μ , ρ , and ν :—

Series.	Temp. 0° C.	Coeff. of Viscosity.	ρ .	$\frac{\mu}{\rho} = \nu$.
1	$15^{\circ}3$	$\cdot 0114$	$\cdot 999$	$\cdot 01142$
2	$51^{\circ}7$	$\cdot 0055$	$\cdot 987$	$\cdot 00557$
3	$73^{\circ}3$	$\cdot 0039$	$\cdot 977$	$\cdot 00399$

For the experiments in which the pressure-drop at the tops of the corrugations was taken, $n=2\cdot 135$, so that, at any given velocity, and with different temperatures,

$$\frac{p_2}{p_1} = \frac{\rho_2}{\rho_1} \left(\frac{\nu_1}{\nu_2} \right)^{135}.$$

If $T_2=51^{\circ}7$ and $T_1=15^{\circ}3$:

$$\frac{p_2}{p_1} = \frac{\cdot 987}{\cdot 999} \left(\frac{\cdot 01142}{\cdot 00557} \right)^{135} = 1\cdot 089 ;$$

while if $T_3=73^{\circ}3$ and $T_1=15^{\circ}3$,

$$\frac{p_3}{p_1} = \frac{\cdot 977}{\cdot 999} \left(\frac{\cdot 01142}{\cdot 00557} \right)^{135} = 1\cdot 128.$$

The logs of head and velocity for the experiments at these temperatures (Table I.) have been plotted to a large scale and on the same sheet. From these it appears that the measured loss of head at $51^{\circ}7$ C. is 8.3 per cent. greater, and at $73^{\circ}3$ C. is 12.7 per cent. greater than at $15^{\circ}3$ C.

The experiments thus confirm the fact, indicated by dimensional theory, that in a pipe in which the resistance to flow increases at a greater rate than the square of the velocity, the resistance is diminished if the viscosity of the fluid is increased. The rate of diminution is also in accordance with the dimensional theory.

XXI. *The Determination of the Best Linear Relationship connecting any Number of Variables.* By H. GLAUERT, M.A.*

IF it is anticipated that two observed quantities x and y are connected by a linear relationship, it is customary in the theory of correlation to determine two lines of regression,

$$y = m_1x + c_1,$$

$$x = m_2y + c_2,$$

by the standard methods of the combination of observations. In this process the errors of observation are assumed in turn to be wholly on the variable y and wholly on the variable x . Frequently, however, it is necessary to determine the best linear relationship connecting the observed quantities, and the following method is suggested, which is applicable to any number of variables.

Consider an experiment in which m variables $x, y \dots$ are determined by observation with equal probable error $\pm \epsilon$, in association with n variables $u, v \dots$ whose values are known accurately in each experiment. Let $\xi, \eta \dots$ be the true values of the first set of variables satisfying the linear relationship

$$F = \Sigma a\xi + \Sigma au = a\xi + b\eta + \dots + \alpha u + \beta v + \dots = 0.$$

The probable value of F , when the observed values are inserted, is

$$\begin{aligned} F(x, y \dots u, v \dots) &= \pm \epsilon a \pm \epsilon b \dots \\ &= \pm \epsilon \sqrt{\Sigma a^2}, \end{aligned}$$

where the summation extends over the coefficients $a, b \dots$ but not over the coefficients $\alpha, \beta \dots$. Equations of equal weight are obtained by writing this result in the form

$$\frac{\Sigma ax + \Sigma au}{\sqrt{\Sigma a^2}} = \pm \epsilon,$$

and the sum of the squares of the errors is

$$S = \Sigma \frac{(\Sigma ax + \Sigma au)^2}{\Sigma a^2}.$$

The best linear relationship connecting the variables will be that which makes the sum S a minimum, and so the

* Communicated by Prof. A. S. Eddington, F.R.S.

normal equations for solving the problem are of the form

$$\Sigma(\Sigma ax + \Sigma au)\{x\Sigma a^2 - a(\Sigma ax + \Sigma au)\} = 0$$

and $\Sigma(\Sigma ax + \Sigma au)u = 0.$

Now put

$$X = a[xx] + b[xy] + \dots + \alpha[xu] + \dots,$$

$$U = a[xu] + b[yu] + \dots + \alpha[uu] + \dots,$$

and then

$$S = \frac{\Sigma aX + \Sigma aU}{\Sigma a^2},$$

while the typical normal equations become

$$X - aS = 0$$

and

$$U = 0.$$

There are m normal equations of the first type and n of the second type, so that in all there are $(m+n)$ equations to determine the quantity S and the $(m+n-1)$ ratios of the coefficients of the linear relationship. On eliminating the coefficients from the normal equations, a determinantal equation of degree m is obtained for S , namely

$$\begin{vmatrix} [xx] - S & [xy] & \dots & [xu] \dots \\ [xy] & [yy] - S & \dots & [yu] \dots \\ \cdot & \cdot & \cdot & \cdot \\ [xu] & [yu] & \dots & [uu] \dots \\ \cdot & \cdot & \cdot & \cdot \end{vmatrix} = 0.$$

No ambiguity arises in the solution, since the smallest positive value of S is required, and when this value of S is inserted in the normal equations, the coefficients of the linear relationship are uniquely determined. Since S is a small quantity for good observational data, it is frequently sufficient to retain only the first power of S in expanding the determinant.

It is of interest to note the connexion between the general solution and the lines of regression when there are two variables x and y and one parameter u .

The normal equations in this case are :

$$([xx] - S)a + [xy]b + [xu]\alpha = 0,$$

$$[xy]a + ([yy] - S)b + [yu]\alpha = 0,$$

$$[xu]a + [yu]b + [uu]\alpha = 0,$$

and the two lines of regression correspond exactly to the neglect of S in the first and second of these equations respectively. Geometrically, the lines of regression are derived by measuring the distance of an observed point from the line parallel to one or other of the coordinate axes, while the generalized solution depends on measuring the distance normal to the line.

XXII. *A further Note on the Forsythe Method of comparing Inductance and Capacity* *. By R. L. EDWARDS †.

IN the January Philosophical Magazine, Prof. Ganguli adversely criticised the Forsythe method of comparing inductance and capacity, both from the standpoint of accuracy and sensibility. The objections are not inherent in the method, but arose in Prof. Ganguli's work as a result of his neglecting the ohmic resistance of the coils compared. That is, his $r \neq Q$, which prevented the existence of a null point. His attempt to reduce error due to this source, led him to use very high resistances. Experience in these tests, as well as theory, shows that with high resistances, low sensibility is inevitable, even though a correspondingly high resistance receiver is used. Large values of r necessitate excessively small values of C , as for a given inductance C varies inversely as r^2 for a balance. With $r = Q$, and of suitable magnitude, we obtain a very sharp null point in our work.

Our data, obtained with a thousand-cycle microphone hummer, a Brooks Inductometer, standard mica condensers, and adjustable receivers tuned to 1000 cycles, yield results with an error of less than a fifth of a percent. over the range of the inductometer. Obviously, we are not concerned with what portion of Q is within the inductive coil itself.

The shifting of resistance between s and Q and r is a tedious process, which might be greatly simplified by a potentiometer arrangement. This difficulty is averted, however, by the use of a variable standard of capacity (or inductance).

The State University of Iowa.
April 8, 1925.

* The Physical Review, Second Series, vol. i. p. 463 (1913).

† Communicated by the Author.

XXIII. *The Scattering of Beta-Rays.* By J. CHADWICK, *Ph.D., Fellow of Gonville and Caius College, Cambridge,* and P. H. MERCIER, *D. ès S., Lausanne**.

§ 1.

THE phenomenon of the scattering of charged particles in their passage through matter has been of great importance in the development of atomic physics. As is well known, it was from consideration of the scattering of α -particles through large angles that Rutherford was led to the conception of the nuclear atom and the theory of single scattering. In single scattering the deflexion of a charged particle through a certain angle is due to an encounter with a single atom, the effect of the other atoms in the scattering material being very small compared with this single large deflexion. In compound scattering, on the other hand, the final deflexion of the particle is the resultant of a very large number of small deflexions of the same order of magnitude. Both these types of scattering can be easily realized in the case of α -particles. The phenomena of single scattering are essentially simple, and it is easy to interpret the results of experiment in terms of the structure of the atom. Thus the observations, particularly of Geiger and Marsden†, and also of one of us‡, have given the strongest possible support to the Rutherford conception of the atom and the theory of single scattering. It is not so simple to interpret quantitatively the experiments on compound scattering, and, speaking generally, the best that can be done is to show that the results are in accord with the theory of the nuclear atom. Such deductions have been drawn from measurements of the compound scattering of α -particles both by Geiger§ and by Mayer||.

While the experiments on the scattering of α -particles are of a simple and straightforward character, the corresponding experiments with β -particles are attended by numerous difficulties, some of which arise from the nature of the available sources of β -particles, while others are due to the small energy of the particles. In contrast to the α -radiation the β -radiation emitted by a radioactive source is not homogeneous, but composed of particles of widely differing

* Communicated by the Authors.

† Geiger & Marsden, *Phil. Mag.* xxv. p. 604 (1913).

‡ Chadwick, *Phil. Mag.* xl. p. 734 (1920).

§ Geiger, *Proc. Roy. Soc. A*, lxxxvi. p. 235 (1912).

|| Mayer, *Ann. d. Phys.* xli. p. 931 (1913).

velocities. In order to work with a beam of β -particles of a suitably narrow range of velocity, it is necessary to sort them out in a magnetic field, with the result that the available primary beam of particles is of relatively small intensity. In most experiments, radium B+C has been used as the source of β -rays, and the strong γ -radiation emitted by this source adds a further complication to the experimental problem. The definiteness of the experiments on the scattering of α -particles is largely due to the simplicity and certainty of the scintillation method of counting the particles. For the β -rays no such method is available. Whatever means are used to detect the β -rays, the measurement of the scattered beam of β -rays, which must usually be of very small intensity, in the presence of a strong γ -radiation is a matter of some difficulty. Again, owing to the small energy of the average β -particle, the chance of scattering is so great that there may be some doubt as to whether, under the experimental conditions, the effects observed are to be ascribed to single or to compound scattering, or to an intermediate type.

For these and other reasons, the conclusions which have been derived from the measurements of the scattering of β -particles are not of that definite and clear-cut character shown by the corresponding experiments with α -particles, and, in fact, some observers have found it difficult to reconcile their results with the accepted views of atomic structure.

The early experiments of Crowther* were carried out before Rutherford put forward the theory of the nuclear atom, and were therefore interpreted in terms of the Thomson atom and on the assumption of compound scattering. It was shown later by Rutherford that the observations could also be approximately explained on the nuclear theory of the atom and on the hypothesis of single scattering.

Recently, experiments on the scattering of β -rays have been made by Geiger and Bothe†, by Crowther and Schonland‡, and by Schonland§.

The experiments of Geiger and Bothe dealt mainly with compound scattering, and on the whole their results were in good accord with the corresponding experiments on α -rays. At the smallest thicknesses of scattering material the amount of scattering was decidedly less than that given by theory, indicating that the conditions for the application of the

* Crowther, *Proc. Roy. Soc. A*, lxxxiv. p. 226 (1910).

† Geiger & Bothe, *Zeit. f. Phys.* vi. p. 204 (1921).

‡ Crowther & Schonland, *Proc. Roy. Soc. A*, c. p. 526 (1922).

§ Schonland, *Proc. Roy. Soc. A*, ci. p. 299 (1922).

theory of compound scattering were no longer fulfilled, and that single scattering began to be appreciable. They did not attempt to make observations of single scattering.

Crowther and Schonland carried out a detailed investigation of the scattering of β -rays under conditions in which they considered the theory of single scattering was applicable. Their results showed marked divergences from the Rutherford theory. The amount of scattering by light elements, such as carbon and aluminium, was several times that to be expected theoretically for all angles investigated (4° to 18°). On the other hand, for heavy elements such as gold and platinum, the scattering for small angles agreed fairly well with theory, but increased rapidly with the angle until for an angle of 18° it was in agreement with the scattering shown at all angles by the lighter elements. As a possible explanation of their results, Crowther and Schonland put forward a tentative suggestion that either the law of force close to the nucleus was not that of the inverse square, or that the electron might have a magnetic moment.

Later, Schonland repeated the experiments for larger angles of scattering, and obtained results in fair accord with theory. He endeavoured to explain the previous results by attributing the large scattering shown by the light elements to an effect of the divergence of the primary beam of β -rays, and by ascribing the deficient scattering at small angles by heavy elements to the screening of the nuclear charge by the K and L groups of electrons. His calculation of the influence of the divergence of the primary beam is certainly not correct, and, indeed, Jeans has shown that provided conditions for single scattering are fulfilled, the effect of a small divergence is negligible. Further, it appears to us that far too much weight has been given to the screening effect of the inner electrons in the case of the heavy atoms.

The explanation of the discrepancy between the results of Crowther and Schonland and the predictions of the theory of single scattering lies in the fact that their experiments are mainly concerned not with single scattering, as they supposed, but with compound scattering or with a type of scattering between the two. In their experiments they measured the thickness of material necessary to scatter one-half of the particles incident on it through more than a prescribed angle ϕ . Now, if the probability that a particle should be scattered through an angle ϕ is $1/2$, then the probability that it should be scattered twice through this angle is $1/4$. When we take into account the variation in the scattering with angle, it is clear that the particles scattered through more

than ϕ must consist to a large extent of particles which have suffered more than one deflexion. This explanation of Crowther and Schonland's results has also been given by Bothe*, and he has shown that some of their results are in approximate agreement with those of Geiger and Bothe, and therefore with corresponding experiments on the scattering of α -rays. Detailed investigations, made by H. A. Wilson†, Jeans‡, and Wentzel§, lead to the same conclusion. Jeans showed how difficult it is to disentangle the effect of single scattering from that of compound scattering when both are present, but was able to account in a general way for the results of Crowther and Schonland. Wentzel has developed in detail the theory of scattering for the transition type between the two extremes of simple and compound scattering—that is, for conditions in which the final deflexion of the particle is the result of a few single deflexions through angles of medium size. Scattering of this type may be termed, for want of a better word, “plural” scattering. He has shown that under certain conditions “plural” scattering may be more important than single scattering, or, in other words, that the deflexion of the particle through a certain angle is more likely to occur in a small number of medium steps than in a single large step. The scattering observed under these conditions will therefore be greater than that predicted by the theory of single scattering, in agreement with the observations of Crowther and Schonland. Wentzel has also obtained a criterion for the presence of single scattering. The argument by which he arrives at this is briefly as follows. A particle passing through the scattering foil is at every instant subjected to the influence of the external atomic fields. The very small deflexions of the particle due to these fields must be left out of account, for we are only concerned with the deflexions due to the internal fields of the atoms. As the external field merges continuously into the internal field it is somewhat arbitrary to fix any definite boundary to the atomic field, or a corresponding lower limit for the deflexion of the particle which may be considered in the calculation. For the present purpose, however, we may ascribe a definite radius R to the sphere of influence of the internal atomic field, and regard all particles which do not penetrate within this distance of the centre of an atom as undeflected. A particle which just penetrates into this region will undergo a

* Bothe, *Zeit. f. Phys.* xiii. p. 368 (1923).

† H. A. Wilson, *Proc. Roy. Soc. A*, cii. p. 9 (1923).

‡ Jeans, *Proc. Roy. Soc. A*, cii. p. 437 (1923).

§ Wentzel, *Ann. d. Phys.* lxi. p. 335 (1922).

deflexion ω . Limiting the action of the atomic field in the above way is then equivalent to neglecting all deflexions less than ω . In any investigation of the scattering of particles the conditions of experiment must be so adjusted that the total angle of scattering through which the particles are observed is several times greater than this minimum deflexion ω . Otherwise the possibility arises that the greater part of the particles have attained their final deflexion by a combination of several single deflexions each less than ω . We thus arrive at an upper limit to ω and a corresponding lower limit to R . This, then, gives a lower limit to the number of atomic encounters which the particle makes in passing through the foil. Only if this number is less than 1 can the type of scattering be considered as mainly single scattering. If the scattering foil is of thickness t and contains n atoms per c. c., then the average number of atoms traversed by the particle in passing through the foil is $\pi R^2 nt$. Wentzel shows that the most probable is equal to the whole number between $\pi R^2 nt$ and $\pi R^2 nt - 1$. If this is less than 1, then the scattering consists mainly of single scattering. The criterion for single scattering is thus

$$\pi R^2 nt < 2,$$

or R must not be greater than

$$R_{\max.} = \sqrt{2/\pi nt}.$$

A particle which traverses an atom at this distance $R_{\max.}$ from the nucleus will suffer a deflexion $\omega_{\min.}$ Deflexions less than $\omega_{\min.}$ must occur so seldom that they cannot contribute appreciably to the measured scattering. Wentzel then shows that repeated single deflexions through angles of less than $\omega_{\min.}$ will not contribute markedly to the scattering, provided that the observed angle of scattering ϕ is at least a small multiple of $4\omega_{\min.}$ This is then a sufficient criterion for the presence of single scattering under the given experimental conditions—viz., a thickness t of scattering foil containing n atoms per c. c., and an angle of scattering ϕ .

Applying this criterion to the experiments of Crowther and Schönland, Wentzel found that it was not fulfilled. By a detailed calculation of the effect of "plural" scattering he was able to account for their results on the basis of the accepted theory of atomic structure.

At the time the experiments which follow in this paper were begun, the above calculations of Wentzel had not been published. While we saw no reason to doubt the validity of the general theory of scattering and atomic structure, yet in view of the disagreement between the conclusions of different observers, it appeared to us advisable to conduct, in as simple

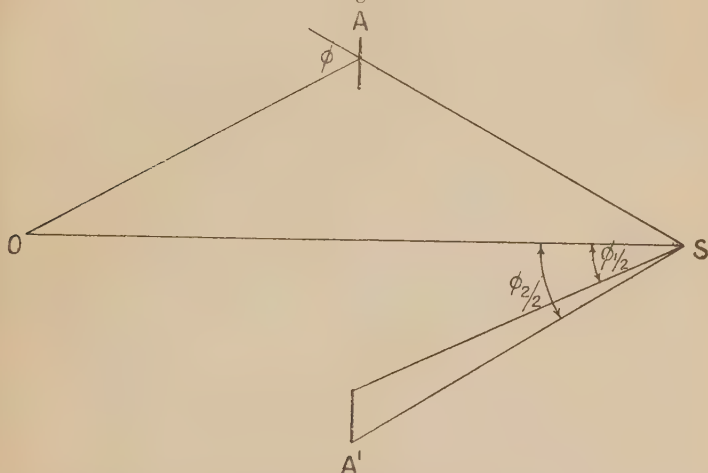
a way as possible, a few experimental tests in which the conditions for single scattering were at least approximately observed. These experiments will now be described.

§ 2. The Method of Measurement.

The method of studying the single scattering of β -rays was similar in principle to that used by one of us* in some measurements of the scattering of α -particles.

The particles from a source S (fig. 1) are scattered by a thin foil AA', in the form of an annular ring, to a point O on the axis of the cone SAA', such that OA=AS. It was shown in the previous paper that on the theory of single

Fig. 1.



scattering the number of particles scattered per second to unit area at O is

$$\frac{Qntb^2}{64r^2} \left[\log \tan \phi_2/4 - \log \tan \phi_1/4 - \cot \phi_1/2 \operatorname{cosec} \phi_1/2 - \cot \phi_2/2 \operatorname{cosec} \phi_2/2 \right]$$

where $\phi_1/2$, $\phi_2/2$ are the angular limits of the foil, and

Q = the number of particles emitted per second by the source,

t = thickness of scattering foil,

n = number of atoms per c.c. in the scattering material,

b = Ne^2/T , where N is the atomic number of the scattering atom and T is the initial kinetic energy of the particle.

* Chadwick, *loc. cit.*

The number of particles falling directly on unit area at O is

$$\frac{Q}{4\pi l^2}, \quad \text{where } l = OS.$$

By allowing the β -rays to enter an ionization chamber provided with a small opening at O we can thus measure in a simple way the fraction of β -particles scattered by a foil between two fixed angles.

This method of measuring the scattering of particles has several obvious advantages. For example, the ratio of the scattered beam of particles to the direct beam is so high that the thinnest sheets of foil can be used. Further, the area of the scattering foil is so large that the error due to lack of uniformity is rendered inappreciable.

Its application to β -ray scattering, however, is attended by one serious disadvantage. As is well known, the β -rays emitted by a radioactive body consist of particles of widely differing velocities, and in order to obtain a homogeneous pencil it is necessary to sort out the rays in a magnetic field. We found it very difficult to devise a suitable combination of the magnetic separation and the above method of observing the scattering, and preferred to use the heterogeneous β -rays emitted by a source of radium E as the primary pencil. This lack of homogeneity of the primary beam is of little moment in the comparison of the scattering by different elements, but becomes very important when we estimate the actual fraction of scattered particles, for the chance of scattering varies inversely as the square of the energy of the particle.

In the above calculation we have assumed that the mass of the β -particle remains constant in the orbit; that is, we have assumed that the increase in kinetic energy of the particle as it approaches the nucleus goes wholly in increasing its speed. Since the mass of the particle increases with the velocity, it will actually move more slowly in the nuclear field than in the case considered in the calculation, and its deflexion will be greater. The orbit of the β -particle when the variation of the mass with speed is taken into account has been calculated by Darwin*, and he has also worked out the correcting factor which must be applied to the simple theory. This correction depends on the angle of scattering and on the velocity of β -rays. It will be introduced when we calculate the fraction of particles scattered by aluminium (§ 6).

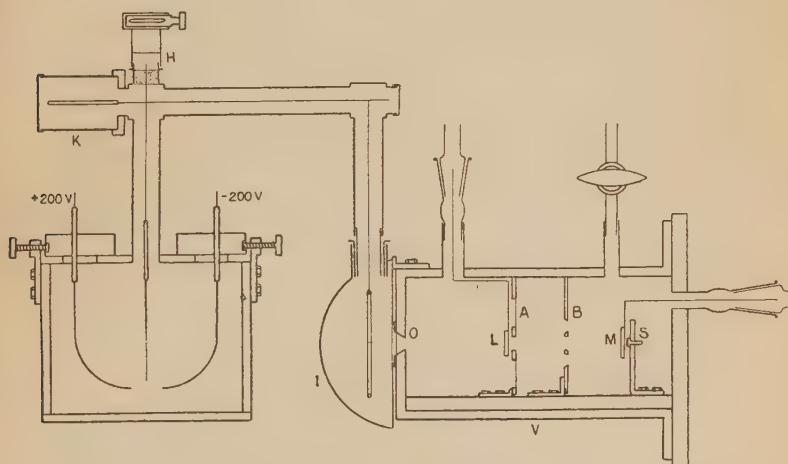
* Darwin, Phil. Mag. xxv, p. 201 (1913).

We have also neglected the effect of encounters of the β -particles with the electrons in the scattering material. On account of the small charge of the electron this effect is relatively small. It is easily seen that the electronic scattering can be included by putting the b in the above expression equal to $\sqrt{(N^2 + N')} \times e^2/T$. The contribution of the electrons to the scattering is thus only appreciable in the case of the lighter elements. For aluminium it is about 7 per cent. of the total scattering, for gold about 1 per cent.

3. The Apparatus.

The apparatus is shown diagrammatically in fig. 2. The diaphragm B served to limit the beam of β -rays from the

Fig. 2.



source S, and consisted of a circular disk of 11.22 mm. diameter suspended in a circular opening of 19.30 mm. diameter. The scattering foil was held on the support A, equidistant from the source S and the opening O, through which the particles entered the measuring apparatus. The distance from the source to the diaphragm B was 26.5 mm. and from the source to the opening O, 100 mm. The source, diaphragm, and foil-holder were mounted on a brass base which fitted into slides in the brass box V, and were adjusted so that their common axis was central to the opening O. The diaphragm and foil-holder were made to fit closely to the sides of the box so as to prevent as far as possible the entrance through O of particles scattered by the walls of

the box. The opening O, of 5 mm. diameter, was covered with a sheet of aluminium of just over 4 cm. stopping-power for α -rays, sufficient to cut out the α -particles from any polonium which might be present on the source.

The direct pencil of β -rays, which came through holes in the central disks of A and B, could be cut off at will by the movable lead screen L, and both direct and scattered pencils could be cut off by bringing the screen M in front of the source.

The brass box was evacuated by means of a Fleuss pump, and then by charcoal cooled in liquid air. It was found that the scattering of the rays by residual air in the box was negligible so long as the pressure was below .5 mm., but the final experiments were all carried out in a charcoal vacuum.

The β -particles passing through the opening O were measured by the ionization they produced in the hemispherical chamber I. Thus the scattered particles and the direct particles had the same length of path in the chamber, and the ratio of the ionization currents gave the ratio of the numbers of particles in the scattered and direct beams. The ionization currents were measured by means of an electrometer of the type devised by Beatty*. This consists of a gold leaf hanging between two oppositely charged plates. The deflexion of the gold leaf was observed by a microscope of 85 \times magnification. The sensitivity was about 300 divisions of the eyepiece scale per volt. A null method was used in which the current in I was compensated by the charge induced on the inner electrode of the small condenser K, the outer case being connected to a sliding contact on a potentiometer.

When no scattering foil was in position, a small current was obtained in I, due to the natural leak and to β -rays scattered from the walls of the box and edges of the diaphragms. This was balanced by a weak ionization produced in the small chamber H.

When measuring the scattered rays the condenser K was charged gradually to two volts, keeping the gold leaf as near as possible to its undeflected position. For measurement of the direct rays, the intensity of which was between 10 and 100 times that of the scattered rays, the potential was increased to ten volts. In some experiments the direct beam was reduced to about the same intensity as the scattered beam by rotating a wheel containing a suitable slit between the hole O and the ionization chamber. The two methods gave concordant results.

The source of β -rays was a disk of 3.8 mm. diameter coated with a deposit of radium E, obtained by electrolysis

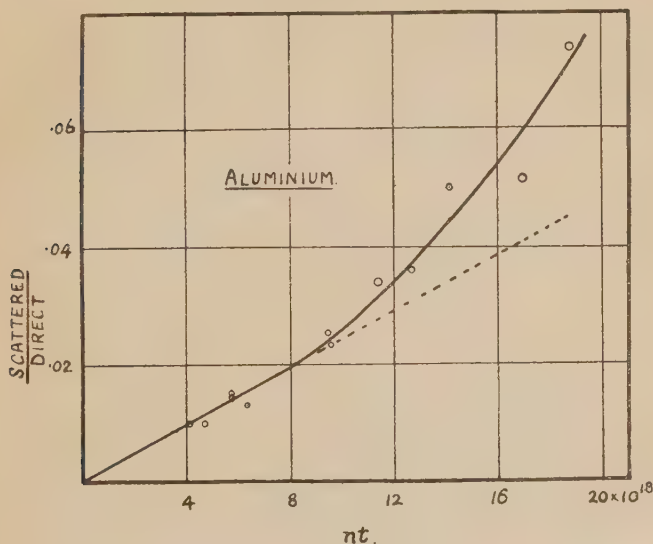
* Beatty, Phil. Mag. xiv. p. 604 (1907).

of a solution of radium D, E, and F. The purity of the radium E was examined by observing the rate of decay of activity of the source. In only one case was the source found to contain a detectable amount of radium D. The initial activity of the source was about equal to that of 1 mg. Ra (B + C) as compared on a β -ray spectroscope.

§ 4. Test for Single Scattering.

At the beginning of an experiment the lead screen L was rotated in the path of the direct rays. The small ionization current in I, due to the natural leak and to particles scattered from the walls of the box, was then balanced by means of the compensation chamber H. On moving L away, the direct beam entered I and was measured. The scattering foil, say one thickness of the thinnest aluminium leaf, was then placed on the support A, and the scattered beam was

Fig. 3.



measured with the screen L in position. Several measurements of the scattered beam alone and of the direct beam together with the scattered beam were made, and then the scattering foil was replaced by a foil of two thicknesses of aluminium, and the process repeated. The sensitivity of the electrometer could be checked at any time on rotating the screen M in front of the source, and so cutting off all β -particles from the ionization chamber.

In this way the results shown in fig. 3 were obtained for

aluminium as scattering material. The ordinates represent the ratio of the scattered rays to the direct rays, and the abscissæ the value of nt for the foil used.

If the conditions for single scattering are fulfilled, the curve obtained should be a straight line passing through the origin. It is seen that this is true only for small values of nt . For larger values the experimental curve is much higher than the straight line passing through the earlier points, indicating that with these thicknesses multiple scattering begins to play an appreciable part. The thinnest foil of aluminium we could obtain had a weight of $\cdot 184$ mg./sq. cm., corresponding to a thickness of $\cdot 68\mu$ and a value of nt of $4\cdot 1 \times 10^{18}$. The results show that even with only four thicknesses of this foil the scattering is not entirely single scattering. These measurements bring out very clearly the difficulty of obtaining conditions under which true single scattering of β -particles takes place, but show at the same time that these conditions are realized in our experiments so long as we use the thinnest scattering foils.

We may here apply Wentzel's criterion for the presence of single scattering which we discussed in § 1—viz., that the angle of scattering ϕ should be a multiple of $4\omega_{\min.}$, where $\omega_{\min.}$ is the deflexion suffered by a particle which passes the scattering nucleus at a distance $R_{\max.} = \sqrt{2/\pi nt}$. In these experiments, the minimum angle of scattering of the particles which were observed in the ionization chamber was 24° . For the thinnest sheets of scattering foil of the different elements examined, the values of $4\omega_{\min.}$ varied from $2^\circ 48'$ to 5° . Thus Wentzel's criterion is fulfilled in all cases.

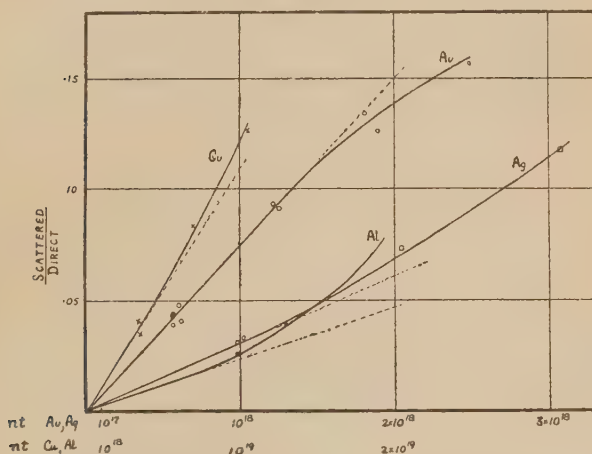
§ 5. *Comparison of Different Scattering Materials.*

Measurements were made of the scattering by four different materials—aluminium, copper, silver, and gold. The results are shown in fig. 4. As in fig. 3, the ordinates give the observed ratio of the ionization due to the scattered rays to that of the direct rays, while the abscissæ give the values of nt for the various scattering foils. In order to obtain all the curves satisfactorily on the same diagram, two scales of nt are used, one for aluminium and copper, and one for silver and gold, as shown in the figure.

It will be seen that for small values of nt the curve for each element is a straight line. This straight line, shown dotted in the diagram, is taken to represent the effect of pure single scattering. Copper and silver behave similarly to aluminium in showing for the thicker foils an excess scattering

due to the appearance of multiple scattering. The curve for gold, on the other hand, is straight for some distance, and then falls slightly below the single scattering value. No weight is attached to this point, as only one observation was made with the greatest thickness of foil; but it is easy to see that multiple scattering should be less noticeable in the case of gold on account of the screening effect of the electrons in the inner orbits, corresponding to a smaller effective nuclear charge. This would make scattering through small angles less probable than we should expect from measurements at larger angles.

Fig. 4.



From these curves the single scattering by the four elements examined can be compared as in the following table, where the ratio of the scattered rays to the direct rays, for a foil for which $nt = 10^{18}$, is given in the second column for the element in the first. Before we compare these ratios, we must apply a correction for the scattering by the electrons in the material. As pointed out in § 2, the electronic scattering is $1/N$ times the nuclear scattering, where N is the atomic number of the element. In this way the corrected ratios of column 3, representing the nuclear scattering, are obtained, the ratio for aluminium being put equal to unity. On the theory of single scattering the ratio for a given element should be proportional to the square of the nuclear charge. Column 4 gives the ratios of the squares of the nuclear charges of Cu, Ag, and Au to that for Al, and comparison of columns 3 and 4 shows that the theory is verified within

the accuracy of experiment in the cases of copper and silver. The discrepancy in the case of gold is explained by a calculation of the orbit of a β -particle scattered by a gold nucleus under the conditions of our experiments, when it appears that the path of the particle lies wholly outside the K-ring of the atom. Thus the effective nuclear charge of gold will be about two units less than the actual charge. On taking this into account, we get a close agreement between experiment and theory in the case of gold as well as with the other elements.

TABLE I.

Element.	Scattered Direct	for $nt=10^{18}$. Corrected.	N^2/N^2_{Al} .
Aluminium	·00234	1	1
Copper	·0113	5·03	4·98
Silver.....	·0302	13·5	13·1
Gold	·075	34·1	37·0

§ 6. *The Amount of Scattering.*

The next test we can apply is to compare the actual amount of the scattering observed experimentally with that to be expected on the theory. This is perhaps best done by using the theory to calculate from the observations the nuclear charge of the scattering elements. This calculation need be performed only for one element, for we have shown in the previous section that the scattering varies for the different elements in the way demanded by theory.

We may write the fraction ρ of β -particles of kinetic energy T which are scattered through a given angle by an element of atomic number N in the form

$$\rho = K \cdot b^2 \cdot f^2(\phi, \beta),$$

where K is a constant involving the geometrical conditions of the experiment, $b = Ne^2/T$, and $f^2(\phi, \beta)$ * is the correction for the change of mass of the particle in its orbit round the scattering nucleus.

In the first place we notice that the chance of scattering is proportional to $1/T^2$, where T is the kinetic energy of the particle. Now the β -rays of radium E, the source used in our experiments, are not homogeneous, but differ rather widely in velocity, so that the estimation of the average value of $1/T^2$ is a somewhat unsatisfactory process. Mr. Madgwick, of this laboratory, has kindly investigated the

* Cf. Crowther & Schonland, and Schonland, *loc. cit.*

distribution of the β -rays in the magnetic spectrum of radium E, measuring the intensity of the rays for different values of $H\rho$ by an ionization method. The curve showing the intensity of the rays against the value of $H\rho$ is similar to a probability curve, and has a pronounced maximum at 2200 $H\rho$. From his results we find an average value of e^2/T^2 of 2.25×10^{-6} e.s. units. This corresponds to an energy of 200,000 volts and a velocity of .70 c. We are also indebted to Dr. Bothe, of the Reichsanstalt, Charlottenburg, for information on this question. Dr. Bothe measured the intensity of the rays of different energies by a photographic method, and, taking into account the different conditions of absorption, his results agree very closely with those of Mr. Madgwick.

In the next place we have to calculate the average value of the relativity correction, $f^2(\phi, \beta)$, for the conditions of our experiments. For a particle of velocity βc scattered through an angle ϕ this correction is

$$f^2(\phi, \beta) = \frac{\operatorname{cosec}^2 \psi}{\left\{ \frac{\beta \cdot \cot \phi / 2}{2(1 - \sqrt{1 - \beta^2})} \right\}^2},$$

where $\beta \cot \psi = \tan \{ \pi - (\cos \psi)^{\frac{1}{2}} (\phi + \pi) \}$.

In our experiments the scattering angle varied from 20° to 40° , but fortunately the correction changes fairly slowly with the angle. The average value was found to be 1.80.

The expression for K has been given in § 2. Putting in the values of $\phi_1/2$ and $\phi_2/2$, $11^\circ 58'$ and $20^\circ 1'$ respectively, and taking a scattering foil for which the value of nt is 10^{18} , we find

$$K = 1.11 \times 10^{19}.$$

Finally, we have for the fraction of particles scattered under the prescribed conditions by a nucleus of charge N ,

$$\begin{aligned} \rho &= 1.11 \times 10^{19} \times (Ne)^2 \times 2.25 \times 10^{-6} \times 1.80 \\ &= (Ne)^2 \times 4.5 \times 10^{13}. \end{aligned}$$

To take the electronic scattering into account, we must write $(N^2 + N)$ for N^2 (§ 2), and we get

$$\rho = (N^2 + N) e^2 \times 4.5 \times 10^{13}.$$

This represents the total scattering under our conditions by a sheet of matter of nuclear charge Ne of thickness corresponding to a value of $nt = 10^{18}$.

We found (§ 5) that the observed fraction of rays scattered by aluminium was equal to $\cdot 00234$.

The atomic number of aluminium is therefore given by

$$\cdot 00234 = (N^2 + N)e^2 \times 4.5 \times 10^{13},$$

whence

$$N = 14.6$$

instead of 13, the true atomic number. The scattering observed is thus greater than that calculated in the above way, and this is the case for all four elements investigated.

§ 7. *Discussion of Results.*

In the previous sections we have shown that it is possible to obtain conditions of experiment in which the single scattering of β -particles can be observed, and we have compared the results of such experiments with the theory of single scattering.

In the first place, it has been shown by comparing the amount of scattering by four elements, viz. aluminium, copper, silver, and gold, that the nuclear scattering is proportional to the square of the atomic number of the element. In this comparison the small amount of scattering due to the electrons in the atom was deducted.

Secondly, the value of the nuclear charge of aluminium has been calculated from the scattering measurements to be 14.6 units, instead of the true value of 13 units, indicating that the scattering is a little greater than that to be expected on the theory. In considering this point, however, we must remember that the β -particles used in the experiments were heterogeneous, and that consequently an average value of $1/T^2$ had to be calculated from measurements of the magnetic spectrum of the particles. This calculation cannot be made with any great accuracy. Further, we have compared the numbers of β -particles in the scattered and direct beams by comparing the ionizations produced by them. This will only be correct when the average particle in each beam has the same ionizing power. This is not the case, for, since the scattering is inversely proportional to the square of the energy of the particle, the scattered beam of β -rays is on the average of lower velocity than the direct beam, and will therefore produce more ionization per particle. On the other hand, the scattered beam will suffer a greater absorption in the aluminium window at O, not only on account of the lower velocity of the rays, but also on account of the obliquity of the beam.

An attempt was made to take these factors into account in the following way. The absorption coefficients of the scattered and direct beams were measured, using an absorbing foil of aluminium of the same thickness as that over the window O. They were found to be 144 cm.^{-1} and 58 cm.^{-1} respectively. It follows at once that to allow for the increased absorption of the scattered beam we must multiply the observed ratio of scattered to direct ionizations by the factor 1.29. In order to determine the correction for the greater efficiency of the scattered particles in the ionization chamber, we need to know how the ionizing power of a β -particle changes with the absorption coefficient. We may assume with Rutherford * that, to a fair approximation, the absorption coefficient of the β -particle is proportional to $T^{-3/2}$, where T is the energy of the particle, and that its ionizing power is proportional to $T^{-1/2}$. The ionizing power is thus proportional to the cube root of the absorption coefficient. In our experiments, therefore, the scattered particle had an ionizing power 1.36 times that of the direct particle, and we must reduce the observed ratio of scattered to direct ionizations by this factor in order to get the ratio of particles in the two beams. Thus the final correcting factor is $1.29/1.36 = .95$. These corrections thus reduce our experimental value for the nuclear charge and bring it nearer to the true value.

Taking the above considerations into account, we conclude that the agreement between theory and experiment is as satisfactory as one could expect. We may at least say that there is no marked discrepancy between theory and experiment. It is, of course, possible that the excess scattering observed may be due to a loss of energy by radiation as the β -particle describes its orbit in the nuclear field. To investigate this question it would be necessary to use a primary pencil of homogeneous β -rays, and for such work our experimental arrangement is not suitable.

There is one further point on which some remarks may be made. In their paper, Crowther and Schonland mentioned that their results were rendered less regular by the introduction of the relativity correction term, $f^2(\phi, \beta)$, and later H. A. Wilson † and Davisson ‡ have suggested that Darwin's method of calculating this correction should be modified.

* Rutherford, 'Radioactive Substances,' p. 238 *et seq.*

† H. A. Wilson, Proc. Roy. Soc. A, cii. p. 9 (1923).

‡ Davisson, Phys. Rev. xxi. p. 637 (1923).

In the first place, it should be pointed out that Crowther and Schonland applied far too large a correction term to their results, because they assumed that they were dealing with single scattering; that is, they put ϕ equal to the total angle of scattering. Actually, their particles were deflected several times in undergoing the total deflexion, and for such small angles the relativity correction is barely appreciable. In the second place it must be remembered that the explanation of the fine structure of the lines of hydrogen and ionized helium depends on an exactly similar application of a relativity correction, and that this has been beautifully confirmed by Paschen's measurements. We have therefore no reason to doubt the validity of Darwin's calculation.

§ 8. *Summary.*

In this paper we have described some experiments on the scattering of β -rays, in which the conditions for single scattering were approximately fulfilled. The scattering angle was between 20° and 40° , and the thinnest obtainable foils of matter were used.

The scattering by four elements, viz. aluminium, copper, silver, and gold, has been compared, and found to vary with the atomic number in the way demanded by the theory of single scattering.

The fraction of particles scattered under definite conditions has been measured. It appears that this fraction is slightly greater than is to be anticipated on the theory. Owing to the use of a heterogeneous beam of β -rays it was not possible to decide whether this discrepancy is genuine, or due to error in estimating the quantities concerned in the calculation of the theoretical fraction.

Our best thanks are due to Sir Ernest Rutherford for his interest in these experiments, and for placing at our disposal the necessary radioactive material.

XXIV. *On the Electrification of Gases by Surface Combustion.*

By J. DICKINSON, M.A., M.Eng., Lecturer in Electrical Engineering in Armstrong College, Newcastle-upon-Tyne.*

1. **T**HIS work was suggested as a possible means of explaining certain phenomena of boilers and boiler furnaces now known to be associated with surface combustion—*e. g.*, the secondary effects accelerating corrosion, and the exceedingly high local temperatures reached.

There is also the question of wider theoretical interest, as to how far the electrical processes, which are now admitted to accompany all forms of chemical activity, can be identified in surface combustion. The study of electrification of gases under the influence of external sources of ionization has been so well worked out that the electrical phenomena of gaseous combustion should be capable of explanation in terms of accepted experimental evidence.

The experiments described have for their object the measurement of the rate of growth of charge gained both by a chamber in which surface combustion is taking place, and by an electrode surrounding the products of combustion after they have passed from this chamber. A measure of the ionization accompanying gaseous combustion of any kind is thus obtained.

The conductivity of the gases in intimate contact with the surfaces upon which the combustion is being accelerated has been examined in the present case, with a view to determining the dependence of the thermionic currents from the heated solid on various percentages of gas and air in the neighbourhood of the mixture which gives, theoretically, complete combustion.

If the extraordinary efficiency of surface combustion is due to the greater ease and completeness with which the gases are prepared for combustion by an intense electrical discharge from the hot surfaces, of the kind investigated by Richardson and Harker, it follows that, by varying the conditions under which surface combustion occurs, there should be a corresponding variation in the electrical phenomena observed, and that it should be possible to identify the state of perfect surface combustion by the electrical equilibrium of the gaseous products.

The phenomena most closely associated with the present investigation are those of the electrification produced by flame, which have been known for 150 years. The most

* Communicated by Prof. W. M. Thornton, O.B.E., D.Sc.

characteristic fact of the electrification of flame is that there are two kinds of ions present. The unburnt gas carries a negative charge, while the burnt or burning gas carries a positive charge (J. J Thomson, 'Conduction of Electricity through Gases,' chapter ix.). It would appear from this, but it has never been previously investigated, that when the mixture is in the proportion for perfect combustion, and when the volume of flame or combustion is confined to a surface layer, so that there is no opportunity for variation of mixture during combustion, there should be no electrification produced. This is now found to be the case.

2. It is well known that solid surfaces provide a suitable field for the modification of mutual gaseous actions in many, if not in all cases, considerably accelerating many gaseous reactions. This attribute of extended solid surfaces is an essential in, and leads to the definition of, surface combustion. Thus surface combustion consists in utilizing the accelerating effect which hot surfaces exert on gaseous combustion (C. D. McCourt, 'Electrician,' lxxi. May 2nd, 1913). In the light of modern work on the electrification of gas near hot bodies, this acceleration can be regarded as activation or ionization of one or of both of the combining gases by the ionic discharge from the hot surface.

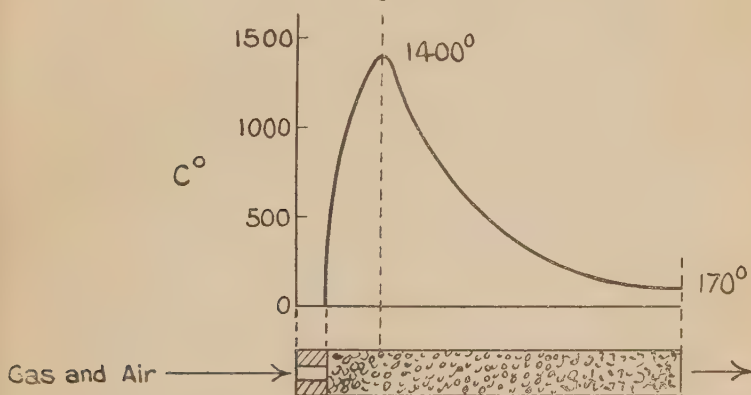
The leading principle of the Boncourt process of surface combustion (*loc. cit.*) is the passage of a mixture of gas and air, adjusted to give complete combustion, through or over porous refractory materials. The theoretical proportions for complete combustion are 16 parts of gas to 84 parts of air by volume. When the refractory material has reached a certain temperature, the combustion takes place on the porous surfaces, all flame disappears, and the resulting radiant heat further increases the temperature of the surface on which it falls.

A tube packed with refractory masses of about one inch in diameter, through which the explosive mixture is drawn, is the method adopted in the following work. In this case the velocity of the mixture at inlet must be greater than the speed of ignition, which for the mixture theoretically giving complete combustion is greater than 16 feet per second. The fragments of refractory material then quickly become incandescent, accelerating combustion and producing high temperature. With a small percentage of air or of gas the mixture is non-explosive. Until the percentage of gas reaches about 16 the speed of ignition increases, the combustion accelerates, and the temperature rises with increased

gas, keeping the air constant ; but beyond this value for the gas there is deceleration both of combustion and of speed of ignition with consequent falling of temperature.

Fig. 1 shows a boiler tube, as used in this research, filled with refractory granules, on whose surface the combustion takes place. At the inlet the tube is fitted with a fire-clay plug having a central opening to admit the explosive mixture. The fragments of ganister or fire-brick touch the plug. After previous heating with flame, the gas is turned off and on again immediately, when it burns within the tube. Incandescence is quickly reached and combustion is complete within the first few inches of the tube, giving rise to a very steep temperature gradient throughout, as

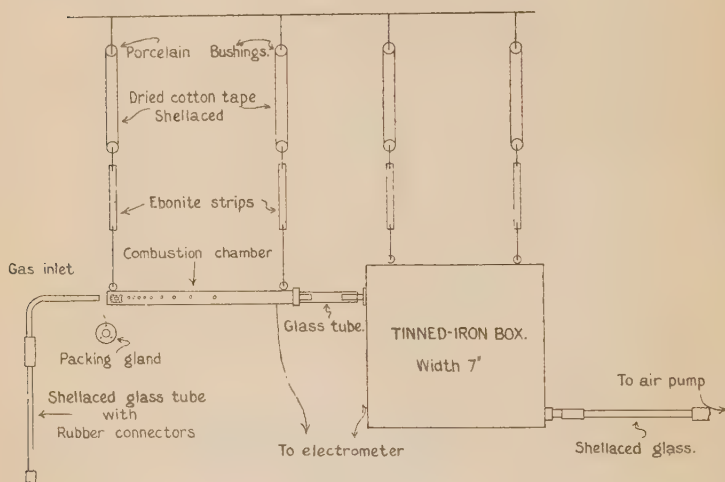
Fig. 1.



shown in the diagram. The granules are also instrumental in withdrawing the heat from the hot gases, which leave the tube, when mounted in a boiler, at approximately 170°C . The difference of pressure between the entrance to the tube and the exit may be produced by direct pressure of about 1 lb. per square inch, or by suction. In the latter case, for a given adjustment of the suction mechanism, the quantity of air drawn through is constant, giving complete regulation by means of the gas cock, and inspection of the glow within the tube gives the correct adjustment. In consequence of this greatly increased heat of combustion at the critical value of the mixture which yields complete combustion, the present work has been undertaken to determine whether there is intense electrical activity which can be identified, and even whether there are currents in the metal tube which help the heat of combustion.

3. The apparatus consists of a 2-in. wrought-iron steam tube, packed with fire-brick granules of about 1 in. in diam., on the surface of which combustion is developed, and of a tinned-iron box into which the total products of combustion are drawn by a rotary suction pump, belt-connected and well earthed. The combustion chamber and box are suspended by means of ebonite strips and cotton tape impregnated with shellac, joined together by copper wire and porcelain bushings, and an air-tight joint of $1\frac{1}{2}$ in. glass tube connects them. The glass tube fits closely over asbestos-lagged adaptors.

Fig. 2.



Apparatus used.

Diagonally opposite to the inlet of the box is the outlet, by way of a 1-in. tube to the suction-pump. A glass insulating tube covered within and without with shellac connects the box to the pump through 1-in. rubber tubing. This arrangement gives the best possible circulation within the box, and affords the products of combustion opportunity of coming into contact with the walls of the vessel to impart to it any free charge they may be carrying. Thus both the combustion chamber and the box, or metal electrode, surrounding the products of combustion, are insulated from earth and from each other. The gas is controlled by a cock, and measured by a Griffin meter of the water type, calibrated to read $1/1200$ cubic foot, and the jet is insulated as shown in the diagram (fig. 2).

A Negretti & Zambra anemometer, reading to 5000 feet per minute, connected to the inlet by an air-tight paper cone, gave the number of feet of air passing per minute for those speeds at which the pump was driven. This was checked several times, giving only negligible differences in readings. From these results, by measuring the net area of the orifice at the anemometer, the volume of air passing per minute was calculated.

When the gas was turned on, the total volume of gas and air entering the combustion chamber was assumed to be that corresponding to the calibrated speed of the pump. In this way the gas percentage was derived by volume.

The combustion chamber has a small mica window a few inches from the inlet, enabling inspection of the interior to observe the maximum glow corresponding to perfect surface combustion. There are also a number of equispaced $\frac{1}{4}$ -in. holes, bushed with clay-pipe stems, along the side of the combustion chamber, through which platinum electrodes may be inserted for examination of the electrification in intimate contact with the refractory surfaces. These tubules are sealed with fire-clay. A packing gland closes the entrance to the tube except for a central aperture 1-in. in diameter. This consists of an outer ring of diameter greater than that of the combustion chamber, and a stout iron ring which will move freely within the chamber. The equidistant set-screws serve both to hold the asbestos packing in position, and to swell out the asbestos packing when placed in the chamber and screwed up. The function of the central aperture is to increase the velocity of the mixture entering the chamber to a value greater than the speed of ignition in open tubes, otherwise combustion solely in the the chamber is impossible.

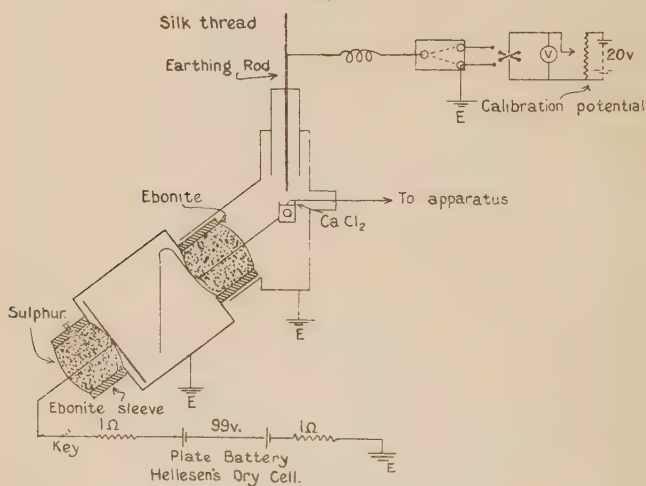
Electrometer Connections.

The C. T. R. Wilson tilted gold-leaf electrometer used is shown diagrammatically (fig. 3), and was constructed, with slight modifications, according to the specifications in the Proc. Camb. Phil. Soc. xii. p. 135 (1903), and of Dr. G. W. C. Kaye in the Proc. Phys. Soc. 1901 and 'Electrician,' March 24, 1911.

It was found that ability to adjust the plate was advantageous, consequently the sulphur insulating the plate was moulded in an ebonite sleeve, which could be moved inwards or outwards. The make-and-break cup contained a strong

solution of calcium chloride, since mercury produced appreciable electrification by "splashing." A Reichert Wien micro-eyepiece and Number (1a) objective, with requisite adjustments, enabled the leaf to be followed and focussed. The maximum sensitivity used gave a deflexion of 200 eyepiece divisions per volt over the working range. The plate was connected to the positive pole of a dry battery of approximately 100 volts, well insulated on a slab of paraffin wax 3-in. thick. It was found that the leaf returned to its zero position correctly, on earthing, after each set of readings

Fig. 3.



Electrometer and Connexions.

taken, showing that the high-tension battery was adequately insulated, since this controls the zero position of the leaf. The light illuminating the eyepiece scale was more than ten feet away from the electrometer.

The earths were all combined in one node and joined to a water main.

An earthed wire gauze of less than $\frac{1}{2}$ -in. mesh completely enveloped the combustion chamber and box, and a lead-covered lead with sheath earthed, having sulphur bushings at each end, was used to connect the apparatus to the electrometer.

After many modifications of the system of insulation and protection, this final method ensured that the whole apparatus would retain a charge giving full-scale deflexion on the

electrometer for sixteen hours with only the loss corresponding to less than five small-scale divisions, and that disturbances due to induction would be deleted.

The above precautions have been taken in order to eliminate the effects of capacity of the surrounding walls and bodies, and of local fields; otherwise, when working with such a sensitive instrument, the results are affected and are entirely spurious. To effect complete insulation of the whole apparatus was a difficult and lengthy operation, but without such insulation it was not possible faithfully to repeat the results.

Experimental Details.

The readings given by the gold-leaf electrometer are interpreted in terms of volts by means of calibration curves taken at the end of each series of experiments, and the points thus obtained are directly assembled in the figures shown. The points, therefore, are not the means of a number of determinations, but give the observed values in any particular case. Each particular case has been many times repeated, and the subsequent determinations have been correct within five per cent. The variations in the state of the combustible mixture and the temperature of air and objects surrounding the combustion chamber do not admit of closer approximation. The derived curves also are constructed from observed values in each particular case.

4. The first series of experiments is described to identify the sign of the electrification produced by surface combustion as distinct from that produced by flame.

Evidence of the sign of the charge acquired by the tinned-iron box surrounding the products of combustion was obtained directly, by means of the gold-leaf electrometer, for various percentages of gas. The results, when the deflexions of the gold-leaf are interpreted in terms of volts, form a family of curves having the characteristics shown in fig. 4.

Fig. 4 shows the effect obtained under steady temperature conditions.

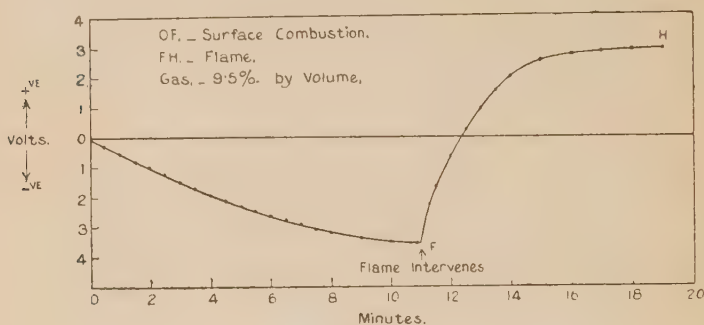
The curve is divided into two parts to illustrate the electrical effect of :—

- (a) Surface Combustion—OF on curve.
- (b) Flame—FH on curve.

In the latter case the gas is lit back to the feed-pipe by a wax taper.

In the first part (OF) the gold leaf of the electrometer moves towards the positively-charged plate, showing that the sign of the electrification produced in the flue gases by surface combustion alone is negative. Thus there are negative ions present in the products of surface combustion with air in excess.

Fig. 4.



Electrification of the Tinned-iron Box.

The second part of the curve, or the portion onwards from the point F, illustrates the electrical condition of the flue gases after the intervention of flame. There is an immediate change of sign, and the direction of the deflexion shows, in accordance with modern experiment, a surplus of positively-charged ions.

This is a striking illustration of the opposite effects produced in the flue gases by surface combustion on the one hand and by flame on the other.

In fig. 5 the signs of the charges acquired by the *combustion chamber itself* in the two cases, for surface combustion and flame, are compared for the same gas percentage as in fig. 4.

During surface combustion the charge is wholly positive, while in the case of flame there is a short period when the charge is negative before changing to positive permanently.

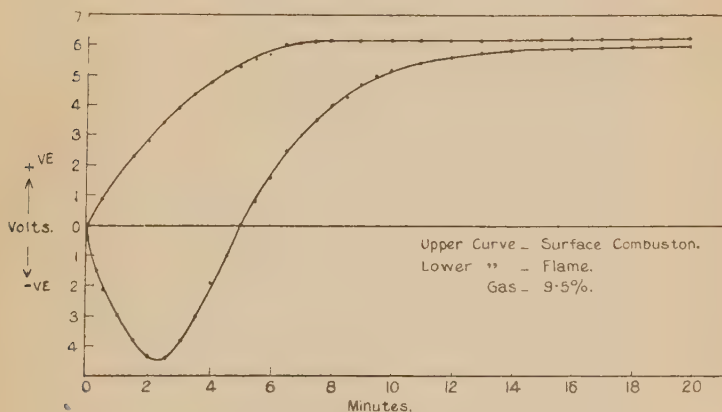
The chamber is heated more slowly in the case of flame, but a larger amount of the tube forming the chamber is heated to redness than in the case of surface combustion. In surface combustion, however, the heat is much more intense and more localized towards the inlet.

In the curve representing the effects due to surface combustion the chamber is clearly positive, emitting electrons profusely when steady conditions producing bright redness have been reached. The well-known positive

emission from the tube at low temperatures probably accounts for the departure of the initial portion from a straight line. On the other hand, the charging up of the chamber gives rise to a back E.M.F. which tends to stop the current. A limiting potential is reached which is sufficient to arrest further action. This is shown by the curve reaching a steady or saturation value in each case.

The negative portion of the flame curve shows the conditions within the combustion chamber prior to the activation by discharge of negative ions from the refractory fragments, and not until a certain temperature is reached, shown by the minimum point on the curve, is this activation by negative discharge from the refractory masses possible.

Fig. 5.



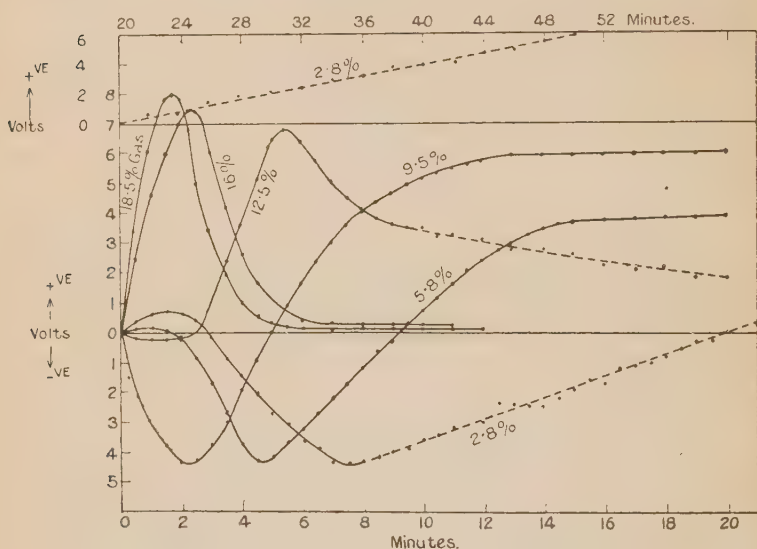
Combustion Chamber.

Thus, comparing the effects displayed by the combustion chamber and the tinned-iron box, the electrification produced by surface combustion is positive in the former and negative in the latter, showing that the ionic or electronic attack upon the combustible is vigorous, surplus negative ions being carried over in the gaseous products to the tinned-iron box. However, in the case of flame, the available electrons are insufficient for the combining gases, and excess positive ions are carried over in the products of combustion. The result of this scarcity of activation is slower combination of the gases forming the combustible, and consequently less intense radiation, although the total heated surface within the combustion chamber is appreciably greater than that during surface combustion, as shown by the region of redness of the tube.

5. Examination of the electrical conditions in the combustion chamber and in the products of combustion for various mixtures, with a view to identifying perfect combustion by electrical means.

Fig. 6 is a family of curves showing the growth and decay of charge acquired by the combustion chamber with combustible of various percentages, including and exceeding that percentage which gives, theoretically, perfect combustion. The combustion here is by flame alone, and each curve is taken with the combustion chamber cold at the start.

Fig. 6.



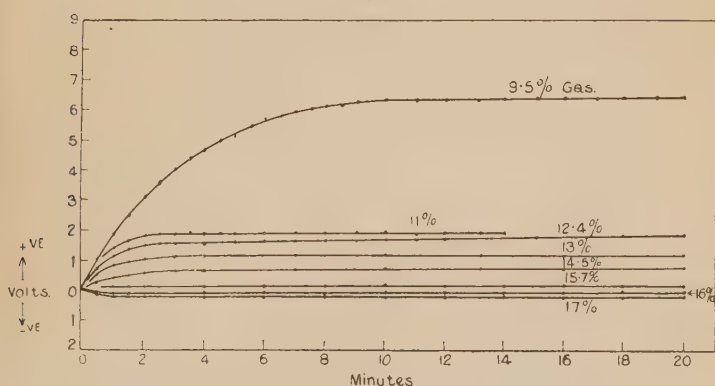
Combustion Chamber—Flame.

Beginning with the least percentage of gas, the first portion is positive, such as would be produced by positive ions crossing from the hot granular packing, as one electrode, to the cold tube as the other. The effect is transitory, and depends for its detection on the rate of heating of the tube. The slower the tube is heated, the more readily is this observed. It is possibly an example of the Thomson effect for a vapour, as suggested by Harker under similar conditions *in vacuo* (Proc. Roy. Soc. Ser. A, April 25, 1912). The second and third portions of this curve are analogous to the third curve, which is the lower curve of fig. 5.

With larger percentages of gas, the negative portion decreases rapidly, the rate of charging, positively, increases, and the heat of the tube becomes more intense, producing an increasingly profuse negative emission from the granules, which reduces the positive charge on the tube, but does not entirely neutralize it. This emission, increasing with temperature, accelerates the combination of the gases, but does not reach a sufficiently high value to effect a change of sign. Further attempts to increase the gas percentage resulted in a violent explosion in the tinned-iron box.

Fig. 7 is a similar family of curves showing the effects of percentage mixture upon the charge acquired by

Fig. 7.



Combustion Chamber—Surface Combustion.

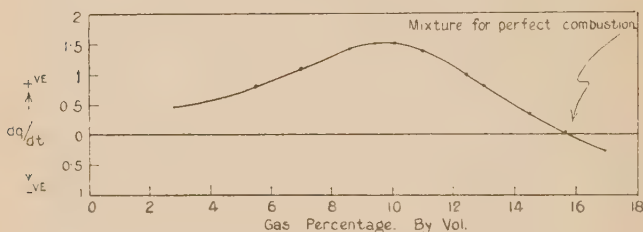
the combustion chamber when surface combustion is being developed within it, for percentages of 9.5 and above. The curves for percentages below this value occurred in the reverse order, but were of the same sign, and, being similar, are omitted for clearness.

The electrification is positive, and decreases rapidly for percentages between 12 per cent. and 16 per cent. At 15.8 per cent. there is no evidence of electrification on the combustion chamber, but for values above 15.8 per cent. the sign of the charge produced by the products of combustion is changed. This suggests that it might conceivably be possible to determine when perfect combustion is obtained in a boiler furnace by sampling the flue gases and testing the sign of their electrification.

Rates of Growth of Charge.

6. Fig. 8 is a derived curve for the combustion chamber. Since the capacity of the system has been maintained constant, the rate of change of volts will give a measure of the growth of charge. Consequently for this curve the rate of increase of volts during the early stages of the curves in fig. 7 is a measure of dq/dt or the conduction current produced by the passage of electrons or ions. This "Conduction Current" is plotted against per cent. of gas, and is a maximum for a combustible mixture of 9.5 per cent. gas. The curves for percentages less than 9.5 per

Fig. 8.



Combustion Chamber—Surface Combustion.

cent. have the same form as those above 9.5 per cent. These latter are assembled in fig. 7.

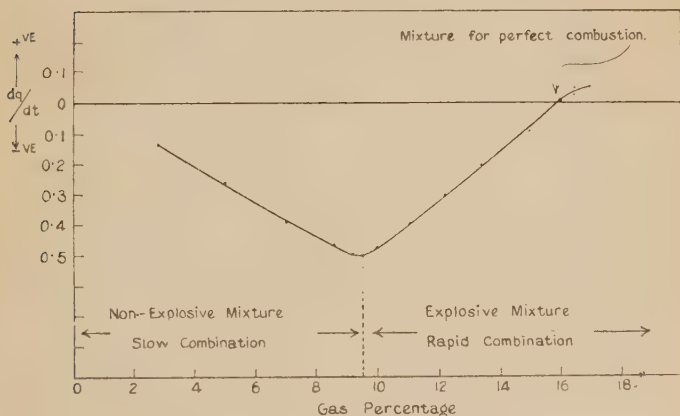
It was not possible to maintain surface combustion below 2.5 per cent., the cooling effect of the air-stream upon the granules being too great.

From this curve it appears that the number of negative ions discharged into the combustible mixture by the red-hot material increases up to 9.5 per cent. of gas, and then falls, until at 15.8 per cent. the electrical discharge is zero. This means that, when the mixture is reached in which inflammable gas and air are in the proportions for perfect combustion, the electrification given out by the red-hot material is completely utilized in the activation of the combining gases. At this point, as will be seen in the next figure, 9, there is no electrification of the products of combustion. Figs. 8 and 9 show conclusively that perfect surface combustion is a state of electrical equilibrium, all the surplus electrical discharge being completely taken up by the gases in the combustion chamber, so that there are no ions in the products of combustion.

The function of the heated granules is seen to be the production of electrons or ions in increasing numbers until the percentage of 15·8 per cent. is reached, when the combustion is perfect and the activation of the combining gases is the greatest possible. At this point, the point of perfect surface combustion, the electrical system seems totally self-contained, and neither the combustion chamber nor the tinned-iron box surrounding the products of combustion gives evidence of the slightest electrification. This outstanding phenomenon is also shown in the next figure.

Fig. 9.—The tinned-iron box, when surface combustion is taking place in the combustion chamber, receives negative charge at an increasing rate for percentages up to 9·5 per cent., and then the rate decreases until at 15·8 per cent.,

Fig. 9.



Tinned-iron Box—Surface Combustion.

approximately, there is no evidence of electrification. This process is the reverse of that occurring in the combustion chamber, as might be expected, and shows that electrons or negatively charged ions are swept over into the flue gases. The capacity of the combustion chamber is less than that of the tinned-iron box, and this is shown in the different charging rates.

The straight-line slopes of the curves of figs. 8 and 9 are similar to those of the velocities of explosion waves in open tubes*.

* R. V. Wheeler, Journ. Chem. Soc. Trans. p. 2608 (1914).

Below 9.5 per cent. the lower limit of inflammability, the mixture cannot support self-ignition, or, in other words, is non-explosive. This is an indication of rapidity of combination, for the difference between mixtures just below and just above the lower limit is entirely one of rapidity of combination. The more rapid the combination the greater the drain or utilization of the electrification supplied by the hot material.

Examination of Modifying Causes.

7 (a). In order to eliminate the effects arising from suspected ionic currents within the combustion chamber, which may help the heat of combustion, a series of experiments was undertaken.

Platinum exploring wires 2 mm. apart were inserted to a depth of 3 cm. along the tube forming the combustion chamber, and a reversible potential of 2 volts was impressed upon them. The low voltage was used in order that ionization by collision in the gases might be negligible. A sensitive tangent galvanometer detected the currents.

The maximum current for surface combustion at 9.5 per cent. gas was 50 micro-amperes, and this rapidly diminished as the gaseous mixture approached that for theoretical perfect combustion. At 15.8 per cent. the galvanometer reading was approximately one micro-ampere. Above and below this percentage the current increased. Whereas for flame, *ceteris paribus*, the current was 205 micro-amperes for 18.5 per cent. gas; diminishing to 195 micro-amperes for 13 per cent. gas.

The maximum current due to temperature alone both for surface combustion and flame was approximately 3 micro-amperes, obtained by completely sealing similar electrodes in the fire-clay plugs in the same exploring holes. Thus, as might be expected, the conductivity of the fire-clay, at these temperatures, had little influence upon the currents determined. The tubule situated four inches from the inlet to the combustion chamber gave the maximum effects in all cases, the current density falling off on either side of the tubule.

From these results it appears, as might be expected, that the zone of the greatest ionic activity is the tract surrounding the refractory fragments in which the combination of the gases is most active and the temperature of surface combustion highest. Further, the difference between the flame and surface combustion curves may arise from the

fact that it is extremely difficult to get contact with the surfaces on which surface combustion is being developed. Certainly the gas beyond the surfaces in the space usually occupied by flame, when there is flame combustion, is not so electrically active as when there is surface combustion. This shows that the region of electrical activation of the combining gases is strictly confined to a region of little more than molecular thickness on the porous surfaces of the heated refractory material.

8. The influence of thermionic discharge alone—no inflammable gas present.

As a control experiment the combustion chamber was heated both by surface combustion and by flame up to various temperatures, and when the conditions had become steady, the gas was turned off and air alone was drawn through the apparatus.

In all cases, both the combustion chamber and the tinned-iron box gave evidence of very slight negative electrification. The maximum effect occurred on the tube.

Thus, since the most important effects were of positive electrification on the tube, it is possible to neglect this slight modification due to thermionic discharge. If the effects of thermionic discharge were at all comparable with those due to combustion, the observed loss of charge of the tube, when the gas is cut off and air alone drawn over the heated surface, should be of the same order as that due to combustion. But this is not the case. There is a scarcely perceptible fall of voltage after the gas is cut off. The vessels are so well insulated that the constancy of the charge is a certain indication of the relative importance of direct transfer of negative ions from the heated material to the tube when there is only air present.

Summary of Experimental Results.

1. Sign of electrification of surface combustion alone as distinct from flame.

(a) *Flue Gases*.—Negative for gas percentages less than about 16 per cent., when all trace of electrification disappears. For percentages higher than 16 per cent. the sign is positive. Air is in excess below 16 per cent., gas is in excess above 16 per cent.

(b) *Combustion Chamber*.—The above electrification is reversed. The sign is positive for percentages less than 16 per cent. approximate, owing to the burning gases

carrying a positive charge, as quoted above. The burning gases impinge upon the walls of the chamber, thereby imparting to it their positive charge; while for percentages above approximately 16 per cent. it appears that the *unburnt* gas predominates, imparting a negative charge. When there is perfect combustion there is *no electrification on either*, showing definitely that there is then complete electrical equilibrium between gases and heated surfaces. Thermionic discharge from the combustion tube is negligible.

2. Electrification produced by flame.

(a) *Flue Gases*.—Wholly positive between 2·6 per cent. and 18·5 per cent. gas.

(b) *Combustion Chamber*.—The sign appears to depend on the temperature. Until a certain low temperature is reached (the chamber tube is red hot), the electrification is negative; beyond this it remains positive for the percentages examined.

3. Items 1 and 2, *supra*, stated otherwise:—

The identification of perfect combustion by electrical means is possible.

(a) The *Flue Gases* display increasing electrification from 2·8 per cent. to 9·5 per cent. gas, from which point to 15·8 per cent. the electrification decreases. At 15·8 per cent. gas, the mixture for perfect surface combustion, *no electrification is detectable*. Beyond this value electrification is again apparent, but is of opposite sign.

(b) The *Combustion Chamber* gives evidence of the same series of phenomena, but of opposite sign.

Thus perfect surface combustion may be detected electrically, but the exact conditions are difficult to determine owing to the flatness of the curve connecting rate of charge with percentage. Moreover, elaborate precautions are essential regarding the careful insulation from all metallic contacts and inductive effects of the electrometer used to detect the electrical conditions.

4. If the conductivity of the gases within the combustion chamber during perfect combustion be represented by unity, then the conductivity during flame combustion is found to be approximately 70. This is strong evidence that the added heat of combustion during surface combustion is not due to currents in the metal tube.

5. Thermionic discharge has negligible influence upon the results.

During surface combustion alone the region of most

intense radiation is appreciably more concentrated towards the combustion chamber inlet than during flame combustion.

The increase of gas from 2·8 per cent. to 16 per cent. produces, in the case of surface combustion, increasing temperature in a small and well-defined region, whereas such an increase in flame combustion results in an appreciably extended region within which combustion is developed.

The author is indebted to Professor Thornton for his active interest in this research.

Bibliography.

Harker, J. A.—“Very High Temperatures,” *Proc. Roy. Soc.* Feb. 9, 1912.

Harker, J. A., & Kaye, G. W. C.—“Emission of Electricity from Carbon at High Temperatures,” *Proc. Roy. Soc. A*, lxxvi. pp. 379-396, April 1912.

——— “Thermionics—Electrical Emission and Disintegration of Metals.” *Proc. Roy. Soc. A*, lxxxviii. pp. 522-538, July 1913.

McCourt.—“Electrician,” lxxi. May 2, 1913.

Pring & Parker.—*Phil. Mag.* pp. 192-200, Jan. 1912.

Richardson, O. W.—“Emission of Electricity from Hot Bodies.”

Thornton, W. M.—“The Reaction between Gas and Pole in the Electrical Ignition of Gaseous Mixtures.”

——— “Some Researches into the safe use of Electricity in Coal Mines.”

Report of the Brit. Assoc., Proceedings, 1910.—“Gaseous Explosions.”

Thomson, J. J.—“Conduction of Electricity through Gases.”

Townsend, J. S.—“Electricity in Gases.”

Wilson, H. A.—“Electrical Properties of Flames and of Incandescent Solids.”

Wheeler, R. V.—*Journ. Chem. Soc. Trans.* p. 2603 onwards (1914).

XXV. *X-Ray Terms and Intensities.* By H. R. ROBINSON, *Ph.D., DSc., University of Edinburgh*.*

[Plate V.]

I RECENTLY published the results of a series of measurements on the groups of electrons ejected by homogeneous X-rays from a number of elements†. The elements under examination were exposed to an intense beam of copper $K\alpha_1$ X-rays, and the energies of the expelled electrons were deduced from measurements of their trajectories in a uniform magnetic field. Each element gives a characteristic “spectrum” made up of a number

* Communicated by Professor C. G. Barkla, F.R.S.

† Robinson, “The Secondary Corpuscular Rays produced by Homogeneous X Rays,” *Proc. Roy. Soc. A*, civ. p. 455 (1923). For brevity, this paper will be referred to as “R.S.1.”

of groups of practically homogeneous cathode rays, each group corresponding to one of the "X-ray absorption levels" of the element—*i. e.*, to a term in its X-ray spectrum.

Measurements of these corpuscular spectra provide therefore an independent method of measuring X-ray absorption limits, and I have shown that the method can be successfully applied to regions in which the ordinary methods of X-ray spectrometry break down. Further—which is of greater immediate importance in the theory of atomic structure—the experiments yield fairly precise data as to the relative amounts of absorption of X-rays by the electrons in the different Bohr levels of the atom*.

The experiments to be discussed here are a continuation of those described in R.S. 1, where full experimental details may be found. For a number of reasons the progress of the work has been interrupted, and the results given below refer to experiments which have been carried out at irregular intervals during the past year. The apparatus has been entirely rebuilt, with but slight modification in detail. The Helmholtz-Gauguin double coil has again been used for producing the magnetic field: it has been necessary to use slightly smaller coils—37.5 instead of 39.6 cm. diameter. This change involves a rather greater departure from uniformity of the magnetic field, especially when weaker fields are used to secure greater dispersion. The corrections for inhomogeneity of field and for the stray effect of the compensating coils have, however, been very carefully investigated, and satisfactory consistency has been obtained in the measurements for the same lines in different fields. The mounting of the coils has been improved, and the absolute values of the currents have been measured with greater accuracy. On the whole, therefore, the accuracy of the measurements has been slightly increased, in spite of the use of smaller coils. The construction of new coils has made it possible to re-determine the absolute values of the magnetic fields, and naturally some of the experiments made with the original apparatus have been repeated for comparison. It appears probable that the values of rH given in R.S. 1 were on the average too low by about 1 part in 1000. There were also slight errors in some of the old results for the lines with relatively large rH , in cases where these were not measured in strong fields, on account of insufficient allowance being made for lack of uniformity of field.

* See in this connexion a very interesting paper by E. C. Stoner, *Phil. Mag.* xlviii. p. 719 (1924).

The Müller water-cooled X-ray tube* has again been used, with a crude form of mercury vapour pump. The tube has been driven by an induction coil with mercury-gas break and mechanical or point-and-plate rectifier; in a few cases an electrolytic break has been used with good results. It has been found that the ordinary medical type of induction coil is inadequate for the continuous high output required, and the latest experiments have been carried out with a home-made—or rather re-built—induction coil immersed in engine-oil for more efficient cooling.

The following are the additional results obtained with copper $K\alpha_1$ as primary X radiation. The notation is the same as in R.S.1. r =radius of the path of an electron in a field of H gauss. The kinetic energy of the electron is calculated from the formulæ:—

$$\frac{mv}{e} = rH,$$

where v =velocity and m =mass of electron,
 e =charge in E.M.U.

If $\beta = \frac{v}{c}$, where c is the velocity of light,

$$\beta^2 = \frac{(mv/e)^2 \times (e/m_0)^2}{c^2 + (mv/e)^2 (e/m_0)^2}$$

where m_0 is the mass of an electron at rest.

$$\text{Energy of electron } W = m_0 c^2 \left(\frac{1}{\sqrt{1 - \beta^2}} - 1 \right).$$

The energies are expressed in terms of the equivalent frequency divided by the Rydberg frequency, *i. e.*

$$\frac{W}{h \times R} = \nu/R,$$

where h =Planck's constant and $R=109737 \times c$.

The following are the values adopted for the various constants:—

$$e/m_0 = 1.7686 \times 10^7 \text{ E.M.U./gramme,}$$

$$e = \frac{4.774 \times 10^{-10}}{c} \text{ E.M.U.,}$$

$$h = 6.545 \times 10^{-27} \text{ erg. sec.,}$$

$$c = 3 \times 10^{10} \text{ cm./sec.,}$$

$$\text{Copper } K\alpha_1 \nu/R = 592.8.$$

* A. Müller, Phil. Mag. xlii. p. 419 (1921).

92. URANIUM (Oxide).

Remarks	Intensity.	rH.	r R.	5928-r R.	Origin.	Other values of Uranium
	3	206.3	276.9	315.9	M _{III}	M _{III} = 87
	4	221.4	318.8	274.0	M _{IV}	M _{IV} = 218
	5	226.1	332.4	260.4	M _V	M _V = 200
	2	273.9	486.8	106.0	N _I	N _I = 106
	3	277.7	500.3	92.5	N _{II}	N _{II} = 92
	5	282.4	517.3	75.5	N _{III}	N _{III} = 75
Double; not quite separated * ...	6	288.7	540.4	52.4	{ N _{IV} N _V	{ N _{IV} = 52 N _V = 48
	2-3	292.8	555.5	47.3	Oxygen K?	Oxygen K = 47
Head of a narrow band	3	295.7	566.8	26.0	{ N _{VI} , N _{VII} C _I	{ N _{VI} = 26 N _{VII} = 26 C _I = 26
	2	298.4	577.1	15.7	O _{II} , O _{III}	C _{III} = 15
Head of a narrow band	2-3	301.7	589.9	2.9	O _{IV} , O _V P	F = 2

* When the lines are too close to be separated only the one with larger rH can be measured—i. e. the one corresponding to the smaller term in the X-ray spectrum.

+ Mean of values: Kurth, Mohler and Foote.

90. THORIUM (Nitrate).

Remarks	Intensity.	rH.	r R.	5928-r R.	Origin.	Other values of Thorium
	1	181.0	213.3	379.5	M _I	M _I = 381
	1	191.1	237.7	355.1	M _{II}	M _{II} = 355
	3	213.2	295.8	297.0	M _{III}	M _{III} = 298
	4-5	226.8	324.5	258.3	M _{IV}	M _{IV} = 258
	5-6	231.5	345.3	244.5	M _V	M _V = 244
	2	276.1	494.6	98.2	N _I	N _I = 97
	2-3	279.5	506.8	86.0	N _{II}	N _{II} = 86
	3-4	284.2	523.8	69.0	N _{III}	N _{III} = 71
Double; not quite separated	5	289.8	544.4	48.4	{ N _{IV} N _V	{ N _{IV} = 51 N _V = 48
	3	293.0	556.4	36.4	Oxygen K	Oxygen K = 36
Narrow band.....	2-3	296.1	568.4	24.4	{ N _{VI} , N _{VII} Nitrogen K	{ N _{VI} = 24 N _{VII} = 24
	2	298.2	576.5	16.3	O _I ?	—
	3	301.7	590.1	2.7	P	F _I = 2

79. GOLD (Leaf).

Remarks.	Intensity.	ν H.	ν R.	$562.8-\nu$ R.	Origin.	Other values of ν R.
						Gold
	2	228.6	339.8	253.0	M_I	$M_I = 252.9$
	3	235.8	361.4	231.4	M_{II}	$M_{II} = 235.1$
	6	245.6	391.9	200.9	M_{III}	$M_{III} = 202.8$
	6	255.8	425.1	167.7	M_{IV}	$M_{IV} = 169.3$
	6	257.8	431.6	161.2	M_V	$M_V = 163.0$
	3	287.7	536.7	56.1	N_I	$N_I = 58.0$
	4	290.1	545.7	47.1	N_{II}	$N_{II} = 49.1$
	4	292.3	553.9	38.9	N_{III}	$N_{III} = 42.8$
arrow band (double).	5	296.2	568.6	24.2	N_{IV}, N_V	$N_V = 25.0$
arrow band.....	3	301.6	589.5	3.3	N_{VI}, N_{VII}, O	$O_V = 0.8$

33. ARSENIC (Oxide).

Remarks.	Intensity.	ν H.	ν R.	$562.8-\nu$ R.	Origin.	Other values of ν R.
						Arsenic
	6	272.2	480.8	112.0	L_I	—
accurate: not ade resolved. }	6?	275.2	491.4	101.4	L_{II}	$L_{II} = 100.7^*$
	6	276.5	496.0	96.8	L_{III}	$L_{III} = 98.4^*$
accurate: edge diffuse..... }	2	292.8	555.8	37.0	Oxygen K	Oxygen K = 36.8
arrow band: diffuse edge ... }	3-4	299.8	582.5	10.3	M	$M_{III} = 11.2^*$

* Interpolated from Walter, *loc. cit.*

25. MANGANESE (Oxide).

Remarks.	Intensity.	ν H.	ν R.	$562.8-\nu$ R.	Origin.	Other values of ν R.
						Manganese
accurate: on two plates only. Doubtful line. }	1	131.4	112.7	480.1	K	$K = 482.4$
end of a broad band..... }	6	243.2	384.3	—	Fluorescent K-L etc.	$384.3 = MnK\alpha_1^*$ —51.1
end of a band: diffuse..... }	3	258.4	433.6	—	Fluorescent K-L etc.	$433.6 = MnK\beta_1^*$ —45.5
accurate: barely resolved..... }	4	287.9	537.5	55.3	L_I	—
	2	289.9	544.9	47.9	L_{II} L_{III}	$L_{II} = 48.7$ $L_{III} = 47.9$
	2	292.9	556.1	36.7	Oxygen K	Oxygen K = 36.8
arrow band: diffuse..... }	2	301.6	589.5	3.3	M	—

* Manganese $K\alpha_1$, $\nu/R = 435.4$; $K\beta_1$, $\nu/R = 479.1$.

22. TITANIUM (Oxide).

Remarks.	Intensity.	ν H.	ν /R.	592.8— ν /R.	Origin.	Other values of ν /R Titanium
	3	187.2	228.3	364.5	K	K=365.4
Head of a band.....	4-5	213.9	297.5	—	{ Fluorescent K-L etc.	297.5=TiK α_1 * —34.8
Band	2	226.3	333.0	—	{ Fluorescent K-L etc.	333.0=TiK β_1 * =30.2
Band	3	251.8	411.8	—		
Band	2-3	266.4	460.6	—		
Band	4	202.8	555.8	37.0	{ TiL Oxygen K }	L _{III} =32.2

* Titanium K α_1 , ν /R=332.3: K β_1 , ν /R=363.2.

The values of ν /R given for comparison have generally been taken from the tables of Bohr and Coster †. Other tables of X-ray terms have appeared more recently—*e.g.* those given by Hjalmar ‡, Walter §, and Nishina ||; these do not, however, differ very greatly from the tables of Bohr and Coster, even for terms which in the earlier tables had to be obtained by interpolation. In any case the Bohr and Coster values are sufficiently accurate for the present purpose.

The “intensities” are again estimated on a 1-6 scale, 6 being the strongest.

It will be seen that the general nature of the distribution of intensity among the sub-groups follows closely the lines indicated in R.S. 1; taken in conjunction with the older experiments, the present set show quite clearly that so long as the critical absorption frequency of a group is not too far removed from the frequency of the incident radiation, most of the secondary electrons emitted come from the “softer” sub-groups (*i.e.* those with higher suffixes in Bohr’s notation). Taking, however, groups with smaller and smaller critical absorption frequencies, a progressive change is observed in the distribution among the sub-groups; this consists in a gradual transference of the maximum intensity from the “softer” to the “harder” members of the group. There is now no doubt that this holds generally in the M and N as well as in the L sub-groups. Similar effects are cited

† Bohr & Coster, *Zeitsch. f. Physik*, xii. p. 342 (1923).

‡ E. Hjalmar, *ibid.* xv. p. 65 (1923).

§ B. Walter, *ibid.* xxx. p. 357 (1924).

|| Y. Nishina, *Phil. Mag.* xlix. p. 521 (1925).

by Ellis and Skinner* in the case of the β rays excited by γ rays. The same effect is also shown in a rather different way in some other experiments by Skinner†. In these experiments Skinner photographed the fluorescent L-spectrum of cerium when excited by primary X-rays varying in wavelength from approximately 0.6–1.5 Å.U. He found that as the wave-length of the exciting radiation was diminished, the cerium emission lines belonging to the L_I sub-group gradually increased in intensity relatively to those of the L_{II} and L_{III} sub-groups. These results completely confirm the view expressed in R.S. 1, p. 475, that the probability of the ejection of an electron from a given sub-group is governed by other factors than the simple number of electrons in that subgroup. This is clearly a point of great intrinsic interest: it seriously complicates, however, the problem of obtaining evidence from the corpuscular spectra about the distribution of electrons among the subgroups (*cf.* Stoner, *loc. cit.* p. 732). The experiments in which only copper K rays are used are necessarily restricted in range, and in order to extend this range experiments have been begun with molybdenum K rays; it is hoped that the results of these will soon be available for publication. Another experimental disadvantage which accompanies the use of a soft primary radiation like copper K has been brought out clearly in the present experiments. The photographic plates employed show a marked diminution in sensitivity for electrons with energies corresponding to ν/R less than about 200. Thus the calcium and sulphur K levels appear very readily on the plates, about equal in intensity (using a CaSO_4 target). Titanium K is appreciably less intense, and vanadium K very faint. Manganese K has been identified on two plates only, and that with no great certainty, in spite of some very prolonged exposures. The manganese K level would be expected to be a very efficient absorber of copper K radiation, and there is in fact ample evidence of this on the plates; by far the strongest line observed here is a "fluorescent" line due to the fluorescent K rays excited in the target itself (see table of results). Of course slow electrons are in any case at a disadvantage as compared with faster ones, as they can only escape from very small depths in the target, but the photographic plate is also responsible for the feebleness of these lines. The effect cannot be due to scattering by residual gas in the

* C. D. Ellis and H. W. B. Skinner, Proc. Roy. Soc. A, cv. p. 186 (1924).

† H. W. B. Skinner, Proc. Camb. Phil. Soc. xxii. p. 379 (1924).

camera, as such low-velocity lines as have been obtained are equally sharp whether recorded in strong or in weak magnetic fields: *i. e.* the sharpness of the lines is independent of the length of the path travelled in the camera.

The same reason probably accounts for the complete failure to observe the M_I and M_{II} lines of uranium. In any case these lines would be expected to be very faint, but they should be detectable. I have searched for these on a large number of plates, without getting sufficiently definite evidence. There are always a number of slight gradations of intensity in the plates, which might possibly be interpreted as spectral lines,—and some of them undoubtedly correspond to faint lines in the fluorescent corpuscular spectra, or possibly to electrons extracted from multiply-ionized atoms, as suggested by Wentzel*. I have felt it safer to ignore “lines” of this type. With thorium, I have fortunately two plates in which M_I and M_{II} stand out fairly clearly, so have been able to include these lines, though without much confidence as to their accuracy. It seems likely that better results would be obtained with Schumann plates in the region of low-velocity electrons†.

There are a few points to be mentioned in connexion with the estimates of intensity, though a detailed discussion is best postponed until the completion of the work with molybdenum rays, in which the complication of variation in photographic sensitivity should be less troublesome. In the present work, the visual estimates of intensity have been supplemented by photometric records. These records were taken with the photoelectric cell photometer used by Professor R. A. Sampson in his work on stellar spectra‡, and I am deeply indebted to Professor Sampson for permission to use the instrument, and to Mr. E. A. Baker for making the records. The comparison of the visual estimate with the photometer records has been most interesting. The most obvious difference is that the eye seems rather more impressed than the photometer by differences in intensity. Thus, compared with the photometer, the visual estimates somewhat exaggerate the differences in intensity. It must of course be remembered that the photometer is just as arbitrary in its judgments as the human eye, though it may be more consistent.

Records of two plates taken under identical conditions with a gold target are reproduced in Plate V. fig. 1, the

* G. Wentzel, *Ann. d. Phys.* lxi. p. 437 (1921).

† Cf. J. A. Becker, *Phys. Rev.* xxiv. p. 478 (1924).

‡ R. A. Sampson, *Monthly Notices R. A. S.* lxxxiii. p. 174 (1923).

two records being placed together for comparison. The high-velocity end of the spectrum is on the left, and the extreme sharpness of the high-velocity edges of the lines is well brought out in the records. (The slight deviation of the trace from the vertical is partially attributable to the finite width of the photometer slit.) The small serrations in the trace are due to the granulations in the photographic emulsion (both plates were over-developed almost to the commencement of chemical fog). Considering the lower record, which is the clearer of the two, reading from right to left, we have M_I and M_{II} appearing as two small humps, then M_{III} as a very well-marked hump. M_{IV} and M_V are clearly separated, though not very far apart: the distance between the two high-velocity edges in the original negative is 0.85 mm. Following M , after a space N_I, N_{II}, N_{III} appear together in a broad hump (one of the four "notches" shown in the group is accidental, and does not appear on other records), N_{IV} and N_V incompletely separated in a narrower hump, and finally the N_{VI}, N_{VII} , and O lines all together. The same lines can be seen less clearly in the upper record.

A comparison of the two records shows the different characteristics of the two kinds of plate used. The lower one is from an Ilford Process Plate, the upper an Ilford X-ray Plate—the latter possibly over-exposed. Although the lower plate gives a much clearer record, there is very little to choose between them for measurements under the micrometer.

The photometer curves bring out very clearly the diffuse nature of the low-velocity sides of the lines—partly due to the geometry of the apparatus, but mainly to the "straggling" of the electrons from the deeper layers of the target. Visually, the lines of the corpuscular spectrum appear well under 1 mm. in width, except in the case of very strong lines; the diffuseness of the low-velocity edges is obvious, but not very obvious to casual inspection. The photometer shows the effect stretching for several centimetres along the plate (this is more clearly shown in other records, where the lines are fewer and more widely spaced, as in the case of a calcium-sulphate target). The low-velocity end of the plates is thus always more or less fogged by straggled electrons belonging to the groups at the high-velocity end. This feature of the photographs was recognized from the first*, but, as Stoner points out (*loc. cit.* p. 733), it may not have been sufficiently emphasized.

* Robinson and Rawlinson, *Phil. Mag.* xxviii. p. 280 (1914).

The actual photographs, though very clear, are not in general suitable for reproduction. The lower plate of fig. 1 has, however, been reproduced in fig. 2. My friend Mr. Drummond Young very kindly placed his considerable skill in photographic work at my disposal, and obtained this print after intensifying the original plate with mercuric chloride*. The prints in my possession are extremely beautiful, and show all the detail given in the table of results, including the separation of N_I , N_{II} , and N_{III} ; they may, in the nature of things, lose some detail in a further reproduction. As in the case of the photometer curves, the high-velocity edge is to the left. This reproduction is from an original negative on a "Process" plate. It is worthy of note that a reproduction from a similar photograph on an X-ray plate (corresponding to the upper photometer curve) shows the strong lines of the N group about equally intense with M_{IV} and M_V (cf. R.S. 1, p. 474).

I wish to express my thanks to Professor Barkla for providing facilities for this work and for his interest in its progress; also to the Committee of the Moray Research Fund for a grant towards the purchase of apparatus and materials.

University of Edinburgh,
March 31, 1925.

XXVI. *On the Statistical Theory of Emission of Electrons from Hot Bodies.* By S. C. ROY, M.Sc., Ghose Research Scholar in Physics, University College of Science, Calcutta †.

§ 1. Introduction.

IT is well known that the classical electron theory of metallic conduction, as developed by Drude, Lorentz, Thomson, and others, is inadequate to give a satisfactory and consistent account of the various outstanding physical properties of metals such as their specific heats, their optical properties, and supraconductivity. In fact, the difficulty of working out a correct law of radiation on the basis of the law of equipartition for the motion of the metallic electrons compels us to abandon the classical theory.

On the other hand, there is an impression that the facts of the thermionic emission of electrons from hot bodies favour

* The photometer record was made before the intensification.

† Communicated by Mr. R. H. Fowler, M.A.

FIG. 1.

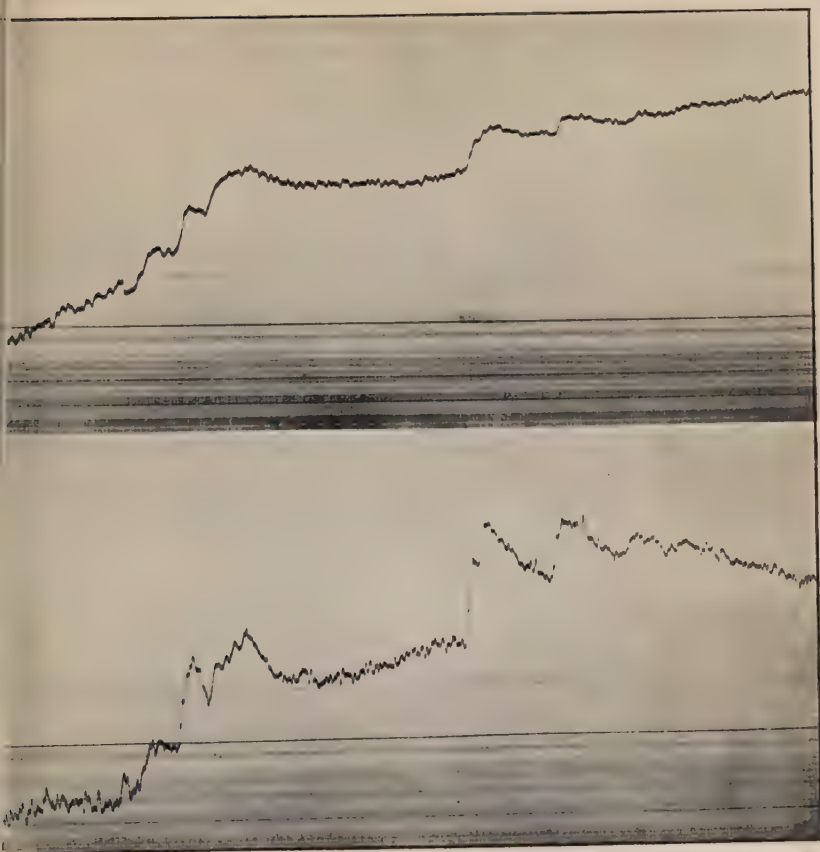
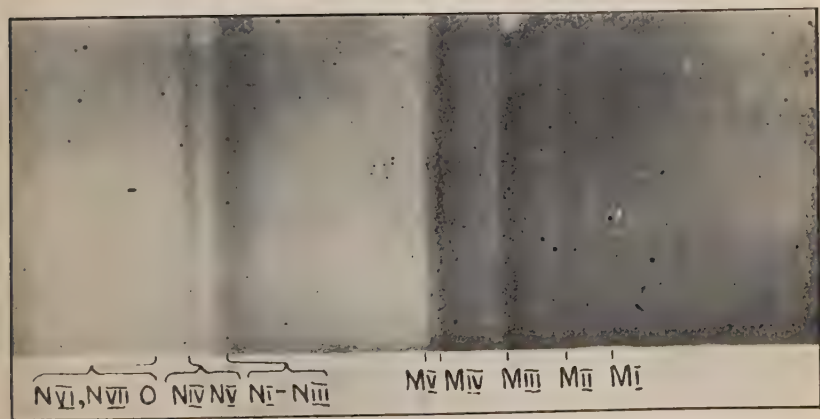


FIG. 2.



GOLD TARGET. 49.4 Gauss.

the kinetic electron theory. This impression is probably due to the fact that a fairly satisfactory representation of the phenomenon is given by the law of emission,

$$I = A \cdot T^{1/2} \cdot e^{-b/T},$$

as originally deduced by Richardson* on the supposition that the electrons both inside and outside a hot body are governed by the same laws of classical dynamics. This fact, however, cannot be accepted as proving the validity of the classical electron theory of metals. As a matter of fact, the experimental results of Davisson† and Germer on the latent heat of electron emission, as measured by the cooling effect, are definitely against the classical theory of metallic conduction. Their measurements lead to the conclusion that electrons inside the metals possess zero or negligible kinetic energy. We are thus forced to abandon the law of equipartition for the motions of the metallic electrons and to adopt Planck's law of quanta as governing their energy-content. We therefore suppose that the metallic electrons, instead of forming an ideal gas, constitute a condensed solid and are distributed in space-lattices like the atoms in a crystal. In a previous paper‡ I pointed out that one can use these ideas in deriving a law of emission of the form

$$I = AT^2 e^{-b/T},$$

where A is a universal constant equal to $2\pi me k^2 / h^3$, provided the electron frequencies be so large as to make $h\nu$ large compared to kT .

In the course of this paper, I propose to present this law as a theorem in statistical mechanics modified to include the modern quantum theory and to show that the law takes the same form if the mechanism of emission be supposed to be radiative. The machinery required for the statistical calculations has been completely set up by Darwin and Fowler in a series of papers§. One has simply to transcribe their results in terms of electrons to obtain the thermionic law of emission. The application of this new method of statistical mechanics to the present problem brings out into clearer view all the assumptions involved.

* Camb. Phil. Proc. ii. p. 286 (1901).

† Phys. Rev. xx. (1922).

‡ Phil. Mag. xlvii. p. 261 (March 1924).

§ Darwin & Fowler, Phil. Mag. xlv. pp. 450, 823 (1922), papers 1 and 2; Proc. Camb. Phil. Soc. xxi. p. 262 (1922), paper 3; p. 392 (1923), paper 6; Fowler, Phil. Mag. xlv. pp. 1, 497 (1923).

In the next paragraph, therefore, I shall give an account of the new method and the principal results in as much detail as is necessary to understand their salient features, and then adopting some of the results proceed directly to the deductions of the law of emission.

§ 2. *Summary of the New Method of Statistical Mechanics and its Principal Results.*

In a series of papers * Fowler and Darwin have discussed at length the general distribution laws of an assembly of various systems by a special method. The essential feature of the new method is the calculation of Averages by means of Integrals whose Integrands are simply expressed in terms of certain functions which they call partition-functions, equivalent to the "Zustand-Summe" of Planck.

For every type of systems in an assembly, quantized or classical, there exists a partition function which depends on the motion of that system alone so long as it is not too frequently interfered with. Such an assumption of limited interference is fundamental in all statistical calculations. This function is originally defined for quantized systems, and is then extended by a limiting process to systems obeying classical laws. All the physically possible states of the system are enumerated. These form a series of discrete states for a quantized system with energies $\epsilon_0, \epsilon_1, \epsilon_2 \dots$ etc., having weights (*a priori* possibilities) $p_0, p_1, p_2 \dots$ etc., and the partition-function is defined as a function of a complex variable Z by the equation

$$f(Z) = \sum_r p_r Z^{\epsilon_r}, \quad . \quad . \quad . \quad . \quad . \quad (1)$$

summed over all permissible states.

The partition-function for a group of N such systems is $[f(Z)]^N$. For the classical systems obeying Hamiltonian equations, the available phase-space is divided into cells whose dimensions are ultimately made to tend to zero, the weight attached to any cell being proportional to its extension. The summation (1) is replaced by an integral, and it is shown that this limit can be used in all formulæ without any restriction.

It is next shown that, for every group of systems in an assembly in statistical equilibrium, the parameter Z must have a unique real value ϑ , which is the temperature of the assembly measured on a special scale, and is related to

* *Loc. cit.*

the absolute temperature of the second law of thermodynamics as follows :

$$\mathfrak{S} = e^{-1/kT}. \quad . \quad . \quad . \quad . \quad . \quad (2)$$

The mathematical principles employed for obtaining adequate approximations are the Multinomial theorem, and the method of Asymptotic expansion by steepest descents. The conditions and the range of applicability of these theorems to statistical calculations have been fully discussed by the two authors.

I will relate here some of the typical results which apply directly to the deduction of the thermionic law of emission. The partition function for a Planck's line vibrator, which takes energy in multiples of quanta $\epsilon = h\nu$, is

$$f(\mathfrak{S}) = \frac{1}{1 - \mathfrak{S}\epsilon}. \quad . \quad . \quad . \quad . \quad . \quad (3)$$

The partition-function for a free monatomic molecule of mass m confined in a volume V is,

$$H(\mathfrak{S}) = \frac{(2\pi m)^{3/2} \cdot V}{h^3 [\log 1/\mathfrak{S}]^{3/2}}. \quad . \quad . \quad . \quad . \quad . \quad (4)$$

The partition-function for temperature radiation has also been constructed. The radiant energy is regarded as the energy of a single system, æther, which is in general heavily degenerate ; but for purposes of statistical calculations all questions of degeneracy are ignored on reasonable grounds, and the partition-function for the radiant energy contained in a volume V takes the form

$$R(\mathfrak{S}) = \exp. \frac{8\pi^5 \cdot V}{45c^3 h^3 (\log 1/\mathfrak{S})^3}. \quad . \quad . \quad . \quad . \quad (5)$$

The same method has enabled the authors to translate Born's results on the mean energy of a crystal into results of partition-functions $K_1(\mathfrak{S})$. Setting aside the higher frequencies due to the motions of the electrons as distinct from the complete atoms,

$$\begin{aligned} \log K_1(\mathfrak{S}) = & -\frac{3}{\log (1/\mathfrak{S})^3} \cdot \sum_{j=1}^3 \frac{1}{k^3 \Theta_j^3} \int_0^{k\Theta_j \log 1/\mathfrak{S}} \frac{x^2 \log (1 - e^{-x})}{x^2} dx \\ & - \sum_{j=4}^{3(S-1)} \log (1 - \mathfrak{S}^{h\nu_j}), \end{aligned} \quad (6)$$

where S is the number of atoms in the elementary cell of the atomic space-lattices of the crystal, and Θ_j and ν_j are constants characteristic of the crystal.

In any discussion in which the atoms are considered to be the only structural units, one can legitimately ignore the electrons, but if one imagines the solid to be constituted of independent atomic and electronic space-lattices, one cannot afford to leave the electron frequencies out of consideration. The partition-function of the electronic lattices, however, is easily constructed in the form

$$\log K_2(\mathfrak{S}) = - \sum_{j=1}^{3n} \log (1 - \mathfrak{S}^{h_{vj}}), \quad . \quad . \quad . \quad (7)$$

where n is the number of electrons contained in each lattice.

§ 3. *Application of this Method to the Phenomenon of Electron Emission from Hot Bodies.*

In the present problem, we have to consider the temperature equilibrium of a hot metal crystal with the radiant energy of the æther and with an atmosphere of gaseous free electrons confined in an enclosure of volume V . The metal crystal is itself constituted of two different systems—atomic (ionic) lattices and electronic lattices ; so that the assembly for our statistical calculations embraces four different types of systems—æther, free electrons, electronic lattices, and atomic space-lattices. To ensure no loss of generality we should formally include all the four systems in our statistical considerations. It is, however, implied that in the specified assembly the atomic lattices preserve their individualities.

Let us suppose that in any example of the assembly we have N free gaseous electrons, genuinely non-atomic, and M electronic lattices each containing n electrons and a number S of the atomic lattices which remains constant in all such examples. We have first to determine the total number of essentially different ways in which such examples of the assembly may be built up out of a total of X equal to $(N + M \cdot n)$ electrons, the other systems—atomic lattices and æther—remaining undisturbed. Each time we choose a group of N electrons out of the total number X for the vapour-phase, we are left with $M \cdot n = (X - N)$ electrons to be arranged in lattices inside the metal crystal. The total number of different ways in which the X electrons can be divided into two groups of N and $(X - N)$ is equal to

$$\overset{X}{C}_N = \frac{X!}{N!(X-N)!} \cdot . \quad . \quad . \quad . \quad . \quad (8)$$

Now, since the present method * of calculation of the partition-function for the translational motion of the gaseous electrons allows for all possible interchange of positions amongst them, any one group of N electrons in the vapour phase cannot be permuted over again to yield more than one distinct mode of forming the assembly. But any group of $(X - N)$ electrons in the condensed phase can be arranged in lattices in $(X - N)!$ ways, and each of these arrangements corresponds to an essentially different mode of building the metal crystal. Hence the total number of essentially different ways of forming the specified assembly is proportional to

$$\sum_{N=0}^X \frac{P^{(X-N)}}{(X-N)!} = \frac{X!}{N!}, \quad (9)$$

where $X = N + M \cdot n = \text{constant}$.

Next, let us define the state of zero energy of the assembly to be that in which all the free electrons have zero kinetic energy and all other systems of the assembly are in their lowest quantum state. Let χ be the work necessary to remove one electron out of the crystal to the free state with zero kinetic energy, the assembly being in zero state of energy as defined above. χ in fact corresponds to what may be called the latent heat of evaporation of an electron at the absolute zero of temperature. If E be the total energy for any example of the assembly relative to the conventional zero, then the energy available for distribution among the partition-functions with N free gaseous electrons is given by

$$F = E - N\chi. \quad (10)$$

But the number of weighted complexions c for any example of the assembly of S atomic lattices, M electronic lattices, N free electrons, and æther in a volume V with energy F available for distribution is given by

$$\begin{aligned} c &= \frac{1}{2\pi i} \int_{\gamma} \frac{dZ}{Z^{F+1}} \cdot R(Z) \cdot [K_1(Z)]^S \cdot [K_2(Z)]^M \cdot [H(Z)]^N \\ &= \frac{1}{2\pi i} \int_{\gamma} \frac{dZ}{Z^{E+1}} \cdot R(Z) \cdot [K_1(Z)]^S \cdot [K_2(Z)]^M \cdot [H(Z) \cdot Z^{\chi}]^N; \\ &\quad (11) \end{aligned}$$

the contour γ is any circle round the origin of radius less than unity. The number of such examples of the assembly

* Cf. footnote, p. 743, of Darwin and Fowler's paper on "Some Refinements of the Theory of Dissociation Equilibria," Proc. Camb. Phil. Soc. xxi. part 6 (1923).

being proportional to $1/N!$, the total number of weighted complexions is proportional to C , where

$$C = \frac{c}{N!} = \frac{1}{2\pi i} \int_{\gamma} \frac{dZ}{Z^{E+1}} \cdot R(Z) \cdot [K_1(Z)]^s \cdot [K_2(Z)]^{x/n} \sum_{N=0}^{N=X} \frac{\beta^N}{N!}, \quad (12)$$

$$\beta = \frac{H(Z) \cdot Z^x}{[K_1(Z)]^{1/n}} \quad (13)$$

If X and E be taken sufficiently large and n a small integer, all the conditions laid down by Fowler and Darwin for the evaluation of such integrals are satisfied. The asymptotic expansion of $\sum_{N=0}^{N=X} \frac{\beta^N}{N!}$ is $\exp. \beta$.

Also we have

$$\begin{aligned} C\bar{N} &= \frac{1}{2\pi i} \int_{\gamma} \frac{dZ}{Z^{E+1}} \cdot R(Z) \cdot [K_1(Z)]^s \cdot [K_2(Z)]^{x/n} \cdot \sum_{N=0}^{N=X} \frac{N\beta^N}{N!} \\ &= \frac{1}{2\pi i} \int_{\gamma} \frac{dZ}{Z^{E+1}} \cdot R(Z) \cdot [K_1(Z)]^s \cdot [K_2(Z)]^{x/n} \cdot \beta \cdot \exp. \beta. \end{aligned} \quad (14)$$

It now easily follows that

$$\bar{N} = \beta(\vartheta) = \frac{H(\vartheta) \cdot \vartheta^x}{[K_1(\vartheta)]^{1/n}}, \quad (15)$$

wherein ϑ and E are related by the equation

$$\begin{aligned} E &= s \frac{\partial}{\partial \vartheta} \log R(\vartheta) + Ss \frac{\partial}{\partial \vartheta} \log K_1(\vartheta) + Ms \frac{\partial}{\partial \vartheta} \log K_2(\vartheta) \\ &\quad + \bar{N}s \frac{\partial}{\partial \vartheta} \log H(\vartheta) + \bar{N}\chi. \end{aligned} \quad (16)$$

The relation (15) on substitution gives

$$\bar{n} = \frac{\bar{N}}{V} = \frac{(2\pi mkT)^{3/2}}{h^3 K_2(T)} \cdot e^{-\chi/kT}, \quad (17)$$

where n is the average number of free electrons per unit volume in the temperature equilibrium with the hot metal. The thermionic current* per second per unit area is therefore

* If allowance is to be made for the reflexion of electrons from metals, the expression for I has to be multiplied by $(1-r)$, where r is the fraction of the incident electrons sent back by reflexion. For most metals r has the value near .5 (Gehrts, *Ann. der Phys.* xxxvi. p. 995, 1911). This fact, if taken into account, would reduce the universal constant to half its value.

equal to

$$I = \bar{n} \cdot e \left(\frac{kT}{2\pi m} \right)^{1/2} = \frac{2\pi m e k^2}{h^3 K_2(T)} \cdot T^2 \cdot \epsilon^{-\chi/kT}. \quad (18)$$

On *à priori* ground, we cannot, probably, neglect the energy-content of the electron-lattices at all temperatures and put function $K_2(T)=1$. According to Haber's law, electronic and atomic frequencies are related to one another by the equation

$$\frac{\nu_e}{\nu_a} = \left(\frac{m_a}{m_e} \right)^{1/2}.$$

The general space-lattice theory of Born also confirms this law. One cannot, however, deny the approximate nature of this law. But in any case this relation points out that the electronic frequencies are much higher than the atomic frequencies. One can also gather some idea of the electronic frequencies from another consideration. It is well known that the specific heats of metals exceed the Dulong-Petit's limit $3R$ at high temperatures. For example, the specific heat* at constant volume for potassium at 300°A . is about 0.56 calorie above Dulong-Petit's value $3R$. This excess must, then, represent the thermal energy of the electrons. One can therefore roughly estimate the order of the electronic frequencies on the supposition that the excess of specific heats of metals at high temperatures over Dulong-Petit's value is contributed by the vibrating electrons according to Planck's quantum law, and can use as a first approximation Einstein's simple expression

$$C_{v \text{ elec.}} = 3R \cdot \frac{x \cdot \epsilon^x}{(\epsilon^x - 1)^2},$$

where

$$x = \frac{h\nu}{kT}.$$

Below are given the values of electronic frequencies of some metals roughly estimated from specific heat data † :—

Metals.	Electronic Frequency.
K	$2 \cdot 10^{13}$
Na	$3 \cdot 10^{13}$
Al	$1.5 \cdot 10^{14}$
Ni	$1.7 \cdot 10^{14}$
Cu	$2.0 \cdot 10^{14}$
Ag	$2.2 \cdot 10^{14}$

* Lewis & Adams, Phys. Rev. iv. p. 331 (1914). Latimer, Phys. Rev. xliii. p. 818 (1921).

† Koenigsberger, *Zeitsch. Electrochem.* xvii. p. 289 (1911). Lewis, Adams, & Latimer, *loc. cit.*

No reliance can, probably, be laid upon the actual numerical figures quoted above. But they show that the function $K_2(T)$ cannot differ much from unity even up to the melting-point of these metals. So that for all practical purposes we can regard $K_2(T)$ as equal to unity in the equation (18).

§ 4. Photo-electric Theory of Emission.

It is of considerable interest to look at the problem from another point of view. For a statistical theory of emission it is immaterial whether the mechanism of emission be radiative or a collision one. It is, however, very probable, as Wilson* pointed out, that the thermionic emission of electrons is really due to the radiation of the hot body itself. The argument against this view is that the magnitude of the auto-photo-electric currents determined experimentally is much lower than the thermionic currents. This is to be expected, for by impinging radiation from outside on metals we do not really attain to the condition of radiation due to the hot body itself.

If the emission of the electrons be supposed to be due to radiation in equilibrium with the hot body, then one† can show, on the basis of the theory of unit mechanism, $\frac{1}{2}mv^2 + \chi = h\nu$, as developed by Kramers‡ and Milne§ that the law of thermionic emission is the same as given by the equation (18).

To adapt Kramer's reasoning to the present problem, it is necessary to modify our idea of the metallic electrons. We have to suppose that they exist in some modified quantized orbits, and constitute Bohr vibrators instead of Planck's line-vibrators.

We start by supposing that the hot body is in a field of "black radiation" at temperatures $T^\circ \text{A.}$, and that there exists inside the hot body a state of dynamical equilibrium of radiation such that the amount of energy gained at any

* *Ann. der Phys.* xlii. p. 1154 (1913); *Roy. Soc. Proc. A*, xciii. p. 359 (1917).

† Since this paper was written, Prof. O. W. Richardson has given a very interesting and illuminating discussion on the Photo-electric Theory of Emission, essentially on the same line (*Proc. Phys. Soc. Lond.* xxxvi. August 1924), and has considered emission from systems with multiple thresholds. His assumptions regarding the chance of capture of an electron by the atom are, however, different from the simple one adopted here. So he obtains an expression for emission of electrons slightly different from the one considered here [equation (47), p. 394]. His expression, however, agrees in form with the one deduced here.

‡ *Phil. Mag.* xlv. p. 840 (1923).

§ *Phil. Mag.* xlvii. p. 209 (1924).

instant by any portion of the hot body by absorption of radiation is exactly balanced by the amount lost by it by emission of radiation. We next adopt the supposition that the absorption or emission of radiation by matter takes place in quanta, and is an additive effect of the actions of individual atoms. The absorption by an atom of a radiation quantum (if large enough to provide for energy necessary to release an electron from the restraining forces) results in the expulsion of an electron from the atom, while the emission of the radiation-quantum is attended by the binding of an electron to the atom. If these two processes of energy-exchange be completely reversible, then, in the steady state of radiation, the rate of photo-electric captures of electrons in any volume V inside the hot body must be exactly equal to the rate of photo-electric ejections of electrons.

The unpolarized radiation between the stretch of frequencies ν and $\nu + d\nu$ emitted through a surface element $d\sigma$ of the hot body in time dt in the cone of solid angle $d\omega$ is equal to

$$2 \cdot dt \cdot d\sigma \cdot \cos \theta \cdot d\omega \cdot K_\nu \cdot d\nu, \quad . \quad . \quad . \quad (1')$$

where θ is the angle between the normal to $d\sigma$ and the axis of the cone, and K_ν is defined by Planck * as the specific intensity of radiation of frequency ν .

In the same way we can write for the number of electrons emitted in time dt through $d\sigma$ in the cone $d\omega$ in the direction θ by the stretch of radiation between ν and $\nu + d\nu$ the expression

$$dt \cdot d\sigma \cdot \cos \theta \cdot d\omega \cdot F_\nu \cdot d\nu, \quad . \quad . \quad . \quad (2')$$

where F_ν may be defined as the specific intensity of photo-electric ejection of electrons.

In the steady state the radiant energy emitted or absorbed in volume V of the hot body in time dt between the frequency range ν and $\nu + d\nu$ is

$$dt \cdot V \cdot N \alpha_\nu \cdot 8\pi \cdot K_\nu \cdot d\nu, \quad . \quad . \quad . \quad (3')$$

where N is the number of atoms per unit volume and α_ν is the atomic absorption-coefficient of radiation. The coefficient α_ν needs a word of explanation. It has the dimensions of an area, and may be interpreted as the "effective cross-section" of the atom which absorbs all the radiation of frequency ν impinging on its surface, so that $V \cdot N \cdot \alpha_\nu$ represents the total effective area presented by all the atoms in volume V to the absorption of radiation of the same frequency.

* Planck, 'Warme Strahlung.'

The total number of quanta absorbed in the specified volume in time dt is equal to

$$\frac{dt \cdot V \cdot \alpha_\nu \cdot 8\pi \cdot K_\nu \cdot d\nu}{h\nu} \quad \dots \quad (4')$$

The expression (4') represents the number of photo-electric ejections of electrons in volume V in time dt by the absorption of radiation between the frequency range ν and $\nu + d\nu$. This number is also given by the expression,

$$dt \cdot V \cdot N \cdot \beta_\nu \cdot 4\pi \cdot F_\nu d\nu, \quad \dots \quad (5')$$

where β_ν is the atomic absorption-coefficient of electrons. This coefficient β_ν may be interpreted as follows:—Each atom acts as a sphere of cross-section β_ν such that a free electron is bound to the atom with the emission of radiation only if it strikes this area.

Equating (4') and (5') we get a relation between K_ν and F_ν as follows :

$$F_\nu = 2 \cdot \frac{\alpha_\nu}{\beta_\nu} \cdot \frac{K_\nu}{h\nu} \quad \dots \quad (6')$$

The physical meaning of relation (6') is that the number of electrons emitted by radiation ν is directly proportional to the intensity of radiation K_ν and inversely proportional to the size of the quantum if α_ν/β_ν were constant.

The quantum theory tells us nothing about the mechanism of absorption or emission of radiation, so that we cannot calculate the coefficients α_ν and β_ν directly. But the process of absorption of radiation by the atoms with the consequent ejection of electrons, and the reverse process of binding of electrons in an atom with the simultaneous emission of radiation, must be governed by the laws of probability in the same manner as absorption and emission of radiation are treated in Einstein's theory of temperature-radiation. On the basis of such probability considerations Kramers has, in developing a theory of absorption of X-rays, obtained a relation between α_ν and β_ν in the form*

$$\frac{\alpha_\nu}{\beta_\nu} = \frac{mc^2}{ah^2\nu^2} \cdot \frac{1}{2}mv^2 = \frac{mc^2}{ah^2\nu^2} \cdot (h\nu - \chi), \quad \dots \quad (7')$$

where a is a numerical constant†. Using the above expression

* Kramers, *loc. cit.* equation (17), p. 843.

† The numerical factor a is determined by the "a priori probability" of an electron remaining bound to the atom.

for α_ν/β_ν in relation (6'),

$$F_\nu = \frac{2mc^2}{ah^3\nu^3} \cdot K_\nu \cdot (h\nu - \chi). \quad . \quad . \quad . \quad (8')$$

Now, in the high-frequency region

$$K_\nu = \frac{h\nu^3}{c^2} \cdot e^{-h\nu/kT}. \quad . \quad . \quad . \quad . \quad (9')$$

Hence we have

$$F_\nu = \frac{2m}{ah^2} \cdot (h\nu - \chi) \cdot e^{-h\nu/kT}. \quad . \quad . \quad . \quad (10')$$

Substituting this expression for F_ν in (2') and integrating, we obtain for the number of electrons emitted from unit area in unit time by radiation of frequency range ν and $\nu + d\nu$,

$$\begin{aligned} dn &= \frac{2m}{ah^2} (h\nu - \chi) \cdot e^{-h\nu/kT} d\nu \cdot \int_0^1 dt \int_0^1 d\sigma \int_0^{2\pi} d\phi \int_0^{\pi/2} \cos \theta \cdot \sin \theta d\theta \\ &= \frac{2\pi m}{ah^2} \cdot (h\nu - \chi) \cdot e^{-h\nu/kT} d\nu. \quad . \quad . \quad . \quad . \quad (11') \end{aligned}$$

Hence the number of electrons emitted per second per unit area by all frequencies of radiation higher than the threshold frequency $\nu_0 = \chi/h$ is

$$\begin{aligned} n &= \frac{2\pi m}{ah^2} \cdot \int_{\chi/h}^{\infty} (h\nu - \chi) e^{-h\nu/kT} d\nu \\ &= \frac{2\pi m}{ah^3} k^2 T^2 \int_{\chi/h}^{\infty} \left(\frac{h\nu - \chi}{kT} \right) \cdot e^{-h\nu/kT} \cdot \frac{h d\nu}{kT} \\ &= \frac{2\pi m k^2}{ah^3} T^2 \cdot e^{-\chi/kT}. \quad . \quad . \quad . \quad . \quad (12') \end{aligned}$$

Thus we arrive at practically the same law of thermionic emission as given in equation (18).

§ 5. Summary and Discussion.

In this paper the law of thermionic emission, in the form

$$I = \frac{2\pi m e k^2}{h^3 K_2(T)} \cdot T^2 \cdot e^{-\chi/kT},$$

has been presented as a theorem in statistical mechanics. The function $K_2(T)$, which depends on the frequencies of metallic electrons, appears, from evidences of excess specific heat of metals over Dulong-Petit's value $3R$, not to differ

much from unity up to the melting-point of metals. It has next been shown on the basis of the theory of complete reversibility of physical processes that the emission law is the same if the mechanism be supposed to be radiative.

The arguments advanced in the deduction of this law are of quite general character. The apparatus of chemical constants and Nernst's Heat Theorem, by which one can get at this law on thermo-dynamic reasoning, is quite uncalled for in the present method. The assumptions adopted are:—

(1) The electrons inside the metals form space-lattices like the atoms in a crystal, and share in heat energy according to Planck's law of quanta.

(2) The external electrons are regarded as constituting an ideal monatomic gas, and are supposed to be emitted with Maxwell's law of distribution of velocities.

The idea of electronic lattices is not new. Such and similar ideas have already been adopted by Lindemann*, Haber †, Borelius ‡, and recently by Thomson § to explain electric and thermal conduction of metals and other metallic properties on the electron theory. The assumption with regard to the external electrons has been widely accepted. The recent experiments of Jones || have proved conclusively that electrons are emitted from hot bodies with Maxwell's distribution of velocities.

It must, however, be noted that the law of emission considered here applies only to low concentrations of electrons emitted inside an ideal vacuum. In cases where the emission is profusely dense, the space-charge effect has got to be taken into consideration.

I have said nothing here about the nature of the work function χ , for I have discussed this point at some length in a previous paper ¶. There I have pointed out that it is possible to evaluate χ from the constants of atomic space-lattices. The question of identity of photo-electric and thermionic work functions is probably uncertain. But the close correspondence between the two is unmistakable. Both are functions of the atomic volumes, and are much smaller than the ionization potentials of the elements in the vapour-phase. This shows that the closeness of atoms in the condensed state releases the force of restraint on the superficial

* Phil. Mag. xxix. p. 127 (1915).

† Berl. Akad. Ber. 1919, pp. 506, 990.

‡ Ann. der Phys. lvii. p. 278 (1918).

§ Phil. Mag. xlv. p. 657 (Oct. 1922).

|| Proc. Roy. Soc. cii. pp. 734-751.

¶ Proc. Ind. Ass. Cult. Sc. ix. part 1, p. 4 (1924).

electrons, so that the ionization potentials of the atoms in the condensed phase are lower than those of atoms in the vapour-phase.

In conclusion, I wish to thank Mr. R. H. Fowler for looking into the manuscript and for advancing helpful criticisms.

Note added in proof, June 11.—J. J. Weigle (Phys. Rev., Feb. 1925, p. 187) has recently presented us with very interesting calculations of the heat of evaporation of electrons from (1) the space-lattice constants and the coefficient of compressibility, and also from (2) the heat of evaporation of the metal, its ionizing energy, and the radii of the ions. The values so calculated agree well with each other and also with these determined from the thermionic emission data. This agreement is in further support of the idea of electron space-lattices in metal crystals.

XXVII. *The Laboratory Construction of Nernst Filaments.*

By HARRY D GRIFFITH, *B.A., Carnegie Teaching Fellow in the University of Aberdeen* *.

THE author has been put to great inconvenience while conducting an investigation on short Infra-Red radiation through inability to obtain Nernst filaments. There is no source available as effective as these are in the region of the spectrum to be studied (up to 5μ), but they are not now obtainable commercially. No information on the old manufacturing process seems to have been published except for patent specifications which do not deal with the main difficulties. The working out of a method for making the filaments was a matter of some difficulty, and this paper is published in the hope that it may be of service to other investigators faced with a similar problem.

The construction of the filament itself is quite a different problem from the subsequent sealing-in of the electrodes, and is a far simpler matter. For the filament, the following mixture is suitable :—

Zirconium Oxide	80 per cent.
Thorium Oxide	10 „
Lime	5 „
Magnesium Oxide	5 „
Boric Acid	a trace

* Communicated by Prof. G. P. Thomson, M.A.

This is ground very fine in an agate mortar, with glycerine or a solution of sugar, so as to yield a thick, creamy paste, which is then extruded into threads with a simple extrusion press with nozzle diameter 1.3 mm. and piston diameter 3 mm. The ratio between piston diameter and nozzle diameter should not be greater than this, and the paste must be worked until it is of a suitable consistency before extrusion. The threads are extruded onto a sheet-iron plate covered with a thin layer of magnesium oxide, and then left to dry. They are then heated slowly until the sugar chars, when they will be strong enough to be handled, and are cut into lengths of about 3 cm. These lengths are then passed through a small carbon arc taking about 3 amperes, after which they will be quite white, hard, and of the consistency of china.

Sealing-in the Electrodes.

The attachment of the negative electrode offers no difficulty. A fine platinum wire (diam. .1 mm.) is bent into a loop, and slipped over one end of a piece of filament. The point of attachment is moistened with thorium nitrate solution, and covered with a layer of filament paste, diluted somewhat with thorium nitrate solution. The seal is slowly dried off in air till it is hard.

The positive seal gives more trouble, since during the running of the filament oxygen is evolved there, and this tends to force the platinum away from the paste, starting an arc which soon destroys the seal. The oxygen can be got away harmlessly through the presence in the seal of iron, manganese, or best yttrium. It is also necessary to have a considerable active area of platinum.

Five or six platinum wires diam. .1 mm. are twisted together, and their ends arranged to clasp the filament as a jewel is held in its setting. The filament is inserted, the clasp damped with thorium nitrate solution, and then covered with a layer of a paste composed of equal parts of

Yttrium Oxide,
Thorium Oxide,
Cerium Oxide,
Zirconium Oxide,

made pasty with thorium nitrate solution.

The whole is dried out slowly in hot air, then ignited strongly to convert the nitrate to thoria, and is then ready for mounting. If both seals are made in this way, the

filament would, presumably, work properly on alternating current. One end of the filament may be rigidly clamped, but the other should be attached only to a bent flexible wire (copper 40 S.W.G.), or the filament will be broken through expansion and contraction.

The Series Resistance.

Since the resistance of the filament decreases if the current through it increases, the circuit will be unstable without a suitable balancing resistance, which may consist of tungsten lamps. For a filament of diam. 1.3 mm., length 20 mm., two 60 watt 220 volt lamps in parallel are satisfactory. The current passing is then .24 amp., and the pressure drop across the filament 96 volts.

The first time the filament is used it will be necessary to heat it and the seals red hot before it will conduct, but afterwards a much lower temperature suffices. Filaments made as described give a somewhat yellower light than the old commercial article, but if a whiter light is required it is probable that slight changes in the filament paste, such as the inclusion of cerium oxide, would have the desired effect.

Dept. of Natural Philosophy,
University of Aberdeen.

XXVIII. *The Theory of Molecular Interaction in the Liquid State.* By G. N. ANTONOFF, D.Sc. (Manch.) *.

Introduction.

WHEN I began to work 25 years ago on liquid systems, the only theory that was then generally accepted was that of van der Waals, which can be described as a purely physical theory. There existed also the theory of De Heen, a kind of a chemical theory, but it did not receive general recognition, and can be regarded as practically abandoned. The same may be said about the theories of solutions. The predominant view ignored any interaction between either homogeneous or heterogeneous molecules. This view had many supporters and an extensive literature, together with a fair amount of quantitative relations which seemed to support the theory. On the other hand, the "chemical theory" (that of Mendeleieff and others) was

* Communicated by the Author.

regarded for a long time merely as a suggestion having few followers and little or no quantitative relations capable of supporting it. However, in the course of time, a number of investigators* showed that the van der Waals theory, although giving a general picture fairly satisfactorily at first sight, did not show a sufficient agreement with the experimental data, and in this sense, in spite of its apparent success, the van der Waals formula cannot be regarded as an expression of a true law.

Although I was never a follower of either of these theories, I realized long ago that any theory which ignores altogether the interaction between the molecules cannot be of a comprehensive character.

In this paper I publish some evidence which enables one to formulate certain general laws which take into account the molecular state of the liquids. The theory here set forth formed itself in my mind as a result of my own experimental work, but at the present time advantage can be taken of quite different methods to corroborate my view.

In the first place such methods as the X-ray analysis throw light on the intimate structure of liquids; and particularly the statement made by Sir William H. Bragg in his lecture to the Chemical Society on "The Significance of Crystalline Structure" to the effect that "the ultimate unit of crystal structure or elementary parallelepiped is not the chemical molecule, but is a complex formed by the union of two, three, or four molecules"†.

The question arises whether the above unit remains the same when a crystal is melted and becomes a liquid, or whether it disintegrates into individual molecules. An attempt to answer this question can be found in the works of C. V. Raman (see 'Nature,' *ibid.*), who worked out special optical methods with the object of studying the intimate structure of liquids. The question cannot perhaps be regarded as definitely settled, but his evidence is in favour of the view that the above unit preserves its structure in the liquid state.

According to my theory it is necessary to assume that in some liquids, especially the associated liquids, the number of units in the molecule is sometimes more than four.

On the above assumption it becomes clear that the process of molecular disintegration between the melting-point and the critical point when the molecules become gaseous will be discontinuous, and will take place in several stages, for

* Young, Proc. Roy. Dublin Soc. xii. p. 374 (1910).

† See 'Nature,' cxi. p. 428.

example, as follows:—



This scheme is in agreement with the facts described in the following pages.

The Theory.

The outlines of the theory described in my paper (Phil. Mag. xxxvi. p. 377, 1918) were originally applied to the systems liquid-liquid. In the above paper I have shown that the law connecting the surface tensions of the two liquid layers in equilibrium with the interfacial tension,

$$\alpha_{12} = \alpha_1 - \alpha_2,$$

where α_{12} is the interfacial tension and α_1 and α_2 are the surface tensions of both layers, implies the equality of molecular concentration of the two layers. This is a condition of equilibrium, and is supported not only by reasons purely mathematical, but also by the physico-chemical evidence.

As, however, the concentrations of the two layers are very different from one another, it is obvious that the liquids must consist of different kinds of molecules. The fact that the two layers have the same vapour-pressure and the same composition of vapour (Konovalov's law), I can only explain by assuming that the molecules forming the gaseous phase are uniformly distributed throughout the system. They thus have the same concentration in both liquid layers, and this concentration must be substantially identical with that of the gaseous phase. This is the only possible condition under which the so-called Konovalov's law can be interpreted physically.

Having observed during a long period the properties of the systems liquid-liquid*, I have always held the view that they are not only in many ways analogous to the systems liquid-gas, but that they are governed by similar physical laws.

I therefore apply without hesitation the just-exposed view to the systems liquid-gas. I assume that the process of formation of liquids is due to the formation of associated molecules, and that the molecules forming the gaseous phase penetrate the liquid phase without suffering any substantial change in concentration. In my recent paper

* I. e. systems consisting of two liquid layers.

(published in *Zeit. Ph. Ch.* Bd. cxii. Heft 5/6, p. 461) I deduced an empirical law for the variation of δ with the temperature. It should be remembered that

$$\delta = \delta_l - \delta_v,$$

where δ_l = the density of the liquid,
 δ_v = „ „ „ vapour.

From the above point of view the quantity δ has a definite physical meaning, and represents the concentration of the associated molecules. I assume that if there were no changes in the molecular state of liquids with change of temperature, a linear law ought to be expected as in gases.

$$\frac{d\delta}{dT} = K,$$

where T is the temperature reckoned from the critical point downwards. However, owing to the molecular association,

$$\frac{d\delta}{dT} = \frac{K \cdot dn}{dT},$$

where n is the number of associated molecules per unit volume. The law connecting n with the temperature must be of the form

$$\frac{dn}{dT} = \frac{K}{T+B}.$$

Thus

$$\begin{aligned} d\delta &= \frac{K \cdot dT}{T+B} \\ &= K \cdot d \ln (T+B), \\ \delta + c &= K \cdot \ln (T+B), \end{aligned}$$

which expression, by putting $K = \frac{1}{\lambda}$, can be represented in the form

$$Ae^{\lambda\delta} = T+B. \quad . \quad . \quad . \quad . \quad . \quad (1)$$

In the critical region it is essential that $A=B$; the equation then satisfies the condition $\delta=0$ when $T=0$. The expression (1), deduced on the above theory, is identical with the empirical expression on p. 462 of my previous paper (*loc. cit.*).

The experimental data show that the δ curve (see fig. 1, on which the figures for ethyl acetate are plotted) is discontinuous in its character, as will be shown later on, and

consists of portions, each satisfying the equation (1), with different constants for every subsequent portion. Thus, from the critical point downwards, the whole curve can be represented by a series of equations :

$$Ae^{\lambda\delta} = T + A,$$

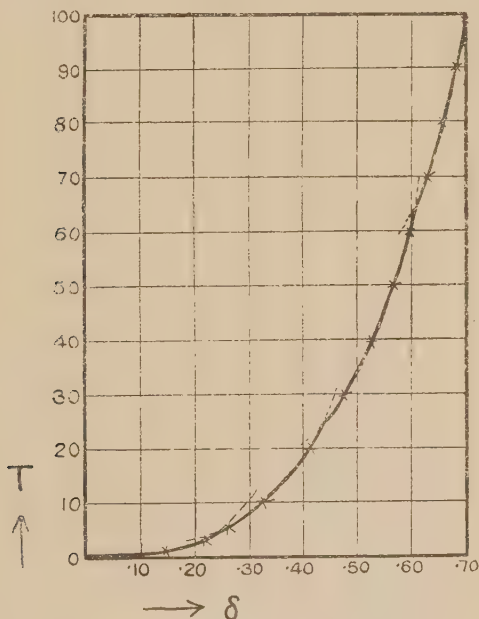
$$A_1e^{\lambda_1\delta} = T + B_1,$$

$$A_2e^{\lambda_2\delta} = T + B_2,$$

and so on.

And this is a general law for all liquids.

Fig. 1.



It will be shown later on that a law of the same form holds true for the latent heats of evaporation, L :

$$Ce^{\mu L} = T + C,$$

$$C_1e^{\mu_1 L} = T + D_1,$$

$$C_2e^{\mu_2 L} = T + D_2, \text{ etc.,}$$

where C , D , and μ are constants for a limited part of the curve between two kinks.

It has been suggested before that some sort of molecular clustering must take place in the liquid state (see Jeans, 'Dynamical Theory of Gases,' p. 203. The fact that the

curve is discontinuous suggests the idea that the clustering or molecular association takes place according to Dalton's law of multiple proportions.

According to this theory all liquids must be regarded as associated, but they may differ in the nature and degree of association.

I am not in a position yet to formulate the difference between the normal and associated liquid exhaustively, but I think I am justified in making the following statement:—*Some liquids undergo between their melting-point and the critical temperature a greater number of the above changes than other liquids.* In other words, the continuous portions of the δ curve are shorter and more numerous. It may be that the corresponding states are connected with the number of the above changes.

Experimental Evidence.

In my previous paper I plotted δ 's against the surface tension for benzene, and the curve obtained was distinctly discontinuous. I therefore assumed that it must be probably due, at least partially, to the discontinuity in the δ curve itself*. However, the discontinuity of the δ curve is not so obvious at first sight, even if the curve is drawn on a large scale, but the mathematical treatment which I have given is much more sensitive and demonstrates it quite clearly. Each portion of the δ curve can be represented in terms of an exponential function with a remarkable accuracy. If two exponential curves with different constants intersect in a given point, the discontinuity is beyond any doubt.

It is therefore necessary to consider whether the existing data are accurate enough to support my theory. This question, of course, is not easy to answer. As all my conclusions were based not on my own, but on other people's experiments, I felt that I was not myself in a position to form an opinion as to their accuracy. In the first instance I consulted on this subject Prof. J. Timmermans, of Brussels, as one experienced in carrying out precision measurements. As the question is a very delicate one, he advised me to write about it to Prof. Sydney Young, of Dublin, on whose experimental figures all my results are substantially based. Prof. Young was kind enough to give to this subject a very careful consideration, and I take the opportunity to express my best thanks to him. The nature of his answer is such that I could not form a definite opinion as to the accuracy of the results, the question being a very complicated one.

However, he indicates which figures he regards as most

* See also Dr. J. Geissler, *Zeit. f. Electrochemie*, Bd. xxiv. p. 101 (1918).

reliable, and if I can prove the discontinuity for them I shall be on safer ground.

Thus he does not recommend me to rely on figures for benzene which were obtained nearly 30 years ago. With increased experience and improved methods the data for the paraffins, hexamethylene, and the esters, also acetic acid, are more accurate than the earlier data.

In view of the above, I had at first some difficulty in working out the experimental data.

However, in the course of time I found that some other properties also show discontinuity, confirming the existence of the kinks, always in the same ranges of temperature.

This enabled me to work out a number of cases from 0°C . up to the critical point, and to establish the number of changes within the above limits.

In the following section, evidence will be brought forward indicating that, apart from δ 's, several other properties are discontinuous : viz.,

- Densities of liquids (δ_l),
- Densities of vapours (δ_v),
- Latent heats of evaporation (L),
- Viscosity (η),
- Surface tensions (α).

On the Discontinuity of some Properties of Liquids.

It is very easy to show that the latent heats of evaporation, L, traced against the temperatures, show a marked discontinuity. The most sceptical mind cannot help noticing it simply by looking at the drawing, especially near the critical point. At low temperatures the curve sometimes flattens out and begins to approach a straight line, but on the whole the discontinuous character of the curve cannot inspire any doubts.

It is not so with densities. One can draw the densities on a large scale, and yet the discontinuity does not appear to be so obvious, especially at first sight.

It is easier to notice the same on δ curves than on either δ_l or δ_v curves, for reasons which will become clear later on.

I generally draw the δ curve against the temperature on a sufficiently large scale. By using a flexible steel curve I can detect the kinks in the regions of low temperatures with extreme ease. The curved part between two kinks can be fitted very easily and accurately into an exponential expression as (1).

At higher temperatures difficulties arise because of a greater curvature, owing to which interpolation becomes difficult, and sometimes involves much labour. This work can

be greatly facilitated by observing the corresponding L curve (latent heat of evaporation), as both methods indicate, as a rule, the existence of kinks in the same intervals of temperature.

The following tables give the results obtained for three substances of a different chemical nature: viz., a hydrocarbon, an ester, and an alcohol, the figures being taken from the work of Prof. Young*.

In these tables T is the temperature reckoned from the critical point, t is the temperature from 0° C. In the column L the brackets show the position of kinks as indicated by the L (latent heat of evaporation) curve.

In these tables I give the values for δ , experimental and calculated by the exponential expression, which is generally given above each table in logarithmic form so as to enable the calculation of δ with the least expenditure of energy. In each table I extend the calculation on either side beyond the boundary within which the given law is valid. By two horizontal lines I separate the region within which the differences between the experimental and the calculated values are negligible. Outside it the differences begin to grow systematically as a rule, and their magnitude is often such that it is beyond the limits of experimental errors. Near the kinks the figures will be found sometimes between two horizontal lines. This indicates that the given point either fits into both intersecting curves, or its position is doubtful.

For each substance I also give the exponential equations, as such, tabulated together.

TABLE I.
Hexamethylene.

(1)

$\log \delta = \log \{ \log (T + 1000 \cdot 1) - 2 \cdot 82141 \} - 1 \cdot 55470.$					
T.	t .	δ exp.	δ calc.	Diff.	L.
280	0	·7966	·7967	+ ·0001	
270	10	·7872	·7872		
260	20	·7776	·7777	+ ·0001	
250	30	·7680	·7680		
240	40	·7584	·7583	- ·0001	
230	50	·7485	·7485		
220	60	·7384	·7388	+ ·0004	
210	70	·7284	·7288	+ ·0004	
200	80	·7177	·7188	+ ·0011	
190	90	·7068	·7086	+ ·0018	

* *Loc. cit.*

TABLE I. (*continued*).

(2)

$\log \delta = \log\{\log(T+77.31)-1.39840\} - \bar{1}.63000.$					
T.	t.	δ exp.	δ calc.	Diff.	L.
260	20	.7776	.7761	- .0015	
250	30	.7680	.7672	- .0008	
240	40	.7584	.7579	- .0005	
230	50	.7485	.7483	- .0002	
220	60	.7384	.7384		
210	70	.7284	.7283	- .0001	
200	80	.7177	.7177		
190	90	.7068	.7067	- .0001	
180	100	.6954	.6954		
170	110	.6835	.6835		
160	120	.6711	.6712	+ .0001	
150	130	.65805	.6584	+ .0004	
140	140	.6442	.6449	+ .0007	
130	150	.62975	.6308	+ .0010	

(3)

$\log \delta = \log\{\log(T+52.93)-1.25990\} - .20190.$					
200	80	.7177	.7181	+ .0004	
190	90	.7068	.7071	+ .0003	
180	100	.6954	.6955	+ .0001	
170	110	.6835	.6836	+ .0001	
160	120	.6711	.6711		
150	130	.65805	.6581		
140	140	.6442	.6442		
130	150	.62975	.6297		
120	160	.6143	.6143		
110	170	.5981	.5981		
100	180	.5805	.5809	+ .0004	
90	190	.5612	.5623	+ .0011	
80	200	.5406	.5426	+ .0020	
70	210	.5183	.5213	+ .0030	
60	220	.4931	.4981	+ .0050	
50	230	.4646	.4728	+ .0082	

TABLE I. (*continued*).

(4)

$\log \delta = \log \{ \log (T + 18.71) - .88034 \} - .31381.$					
T.	<i>t.</i>	δ exp.	δ calc.	Diff.	L.
130	150	.6297	.6273	- .0020	}
120	160	.6143	.6126	- .0017	
110	170	.5981	.5969	- .0012	
100	180	.5805	.5498	- .0007	
90	190	.5612	.5612	+ .0001	
80	200	.5406	.5407		
70	210	.5183	.5183	- .0001	
60	220	.4931	.4931		
50	230	.4646	.4645		
40	240	.4313	.4313		
30	250	.3914	.3919	+ .0005	}
20	260	.3422	.3435	+ .0013	
15	265	.3106	.3144	+ .0038	
10	270	.2692	.2805	+ .0113	
6	274	.2257	.2489	+ .0232	

(5)

$\log \delta = \log \{ \log (T + 5.20) - .3670 \} - .4804.$					
40	240	.4313	.4261	— .0052	}
30	250	.3914	.3904	— .0010	
20	260	.3422	.3422	— .0001	
15	265	.3106	.3105		
10	270	.2692	.2695	+ .0003	
6	274	.2257	.2257		
3	277	.1787	.1809	+ .0022	
1	279	.1288	.1407	+ .0119	

(6)

$\log \delta = \log \{ \log (T + .0727) - \bar{2}.8615 \} - .9590.$					
6	274	.2257	.2113	— .0144	}
3	277	.1787	.1787	— .0003	
1	279	.1288	.1285		
0	280	0	0		

Formulae.

- | | |
|-----------------------------------------------------|-----------------------------------------------------|
| (1) $66\cdot30e^{8258\delta} = T + 1000\cdot1.$ | (4) $7\cdot591e^{4\cdot743\delta} = T + 18\cdot71.$ |
| (2) $25\cdot03e^{3\cdot351\delta} = T + 77\cdot31.$ | (5) $2\cdot328e^{6\cdot961\delta} = T + 5\cdot20.$ |
| (3) $18\cdot20e^{3\cdot655\delta} = T + 52\cdot93.$ | (6) $\cdot0727e^{20\cdot97\delta} = T + \cdot0727.$ |

TABLE II.

Ethyl acetate.

(1)

$$\log \delta = \log \{ \log (T + 459\cdot65) - 2\cdot37501 \} - \bar{1}\cdot71189.$$

T.	t.	δ exp.	δ calc.	Diff.	L.
250·1	0	·9243	·9243		
240·1	10	·9125	·9123	—·0002	
230·1	20	·9002	·9003	+·0001	
220·1	30	·8880	·8880		
210·1	40	·8754	·8754		
200·1	50	·8624	·8627	+·0003	
190·1	60	·8490	·8498	+·0008	
180·1	70	·8350	·8367	+·0017	
170·1	80	·8210	·8234	+·0024	

(2)

$$\log \delta = \log \{ \log (T + 228\cdot31) - 1\cdot87511 \} - \bar{1}\cdot88169.$$

250·1	0	·9243	·9253	+·0010	
240·1	10	·9125	·9133	+·0008	
230·1	20	·9002	·9010	+·0008	
220·1	30	·8880	·8884	+·0004	
210·1	40	·8754	·8756	+·0002	
200·1	50	·8624	·8624		
190·1	60	·8490	·8489	—·0001	
180·1	70	·8350	·8352	+·0002	
170·1	80	·8210	·8210		
160·1	90	·8065	·8065		
150·1	100	·7910	·7916	—·0006	
140·1	110	·7751	·7763	+·0010	
130·1	120	·7580	·7607	+·0027	
120·1	130	·7402	·7445	+·0043	

TABLE II. (*continued*).

(3)

$$\log \delta = \log \{ \log (T + 62.72) - 1.30211 \} - .11289.$$

T.	<i>t.</i>	δ exp.	δ calc.	Diff.	L.
200.1	50	·8624	·8618	—·0006	}
190.1	60	·8490	·8487	—·0003	
180.1	70	·8350	·8352	+·0002	
170.1	80	·8210 ₄	·8211	+·0001	
160.1	90	·8065	·8065		
150.1	100	·7910	·7910	—·0001	
140.1	110	·7751	·7750		
130.1	120	·7580	·7580		
120.1	130	·7402	·7402		
110.1	140	·7213	·7213		
100.1	150	·7003	·7014	+·0011	
90.1	160	·6775	·6802	+·0027	
80.1	170	·6531	·6575	+·0044	
70.1	180	·6265	6332	+·0067	

(4)

$$\log \delta = \log \{ \log (T + 37.64) - 1.12678 \} - .16002.$$

140·1	110	·7751	·7770	+·0019	}
130·1	120	·7580	·7595	+·0015	
120·1	130	·7402	·7410	+·0008	
110·1	140	·7213	·7213		
100·1	150	·7003	·7003	+·0001	
90·1	160	·6775	·6776		
80·1	170	·6531	·6531		
70·1	180	·6265	·6265		
60·1	190	·5966	·5972	+·0006	
50·1	200	·5630	·5648	+·0018	
40·1	210	·5231	·5284	+·0052	
30·1	220	·4757	·4871	+·0114	

TABLE II. (continued).

(5)

$$\log \delta = \log \{ \log (T + 12.80) - .7329 \} - .2773.$$

T.	<i>t.</i>	δ exp.	δ calc.	Diff.	L.
90.1	160	.6775	.6756	-.0019	}
80.1	170	.6531	.6522	-.0009	
70.1	180	.6265	.6266	+.0001	
60.1	190	.5966	.5966		
50.1	200	.5630	.5628	-.0002	
40.1	210	.5231	.5231		
30.1	220	.4757	.4750	-.0007	
20.1	230	.4150	.4142	-.0008	
10.1	240	.3279	.3311	+.0032	

(6)

$$\log \delta = \log \{ \log (T + 5.60) - .3915 \} - .3898.$$

40.1	210	.5231	.5170	-.0061	}
30.1	220	.4757	.4733	-.0024	
20.1	230	.4150	.4150		
10.1	240	.3279	.3279		
5.1	246	.2599	.2599		
3.1	247	.2199	.2234	+.0035	
1.1	249	.1551	.1771	+.0220	

(7)

$$\log \delta = \log \{ \log (T + .120) - \bar{1}.0792 \} - .8127.$$

10.1	240	.3279	.2971	-.0308	}
5.1	245	.2599	.2522	-.0077	
3.1	247	.2199	.2199		
1.1	249	.1551	.1550	-.0001	
0	250.1	0	0		

Formulae :

- | | |
|------------------------------------------|-----------------------------------------|
| (1) $237.1e^{1.186\delta} = T + 459.65.$ | (5) $5.406e^{4.360\delta} = T + 12.80.$ |
| (2) $94.43e^{1.754\delta} = T + 228.31.$ | (6) $2.463e^{5.649\delta} = T + 5.60.$ |
| (3) $20.05e^{2.986\delta} = T + 62.72.$ | (7) $.120e^{14.96\delta} = T + .120.$ |
| (4) $13.39e^{3.328\delta} = T + 37.64.$ | |

TABLE III.

Propyl alcohol.

(1)

$\log \delta = \log \{ \log (T - 99.60) - 2.96080 \} - .39980.$					
T.	t.	δ exp.	δ calc.	Diff.	L.
263.7	0	.8193	.8179	-.0014	
253.7	10	.8110	.8110		
243.7	20	.8034	.8037	+.0003	
233.7	30	.7959	.7959		
223.7	40	.7873	.7874	-.0001	
213.7	50	.7782	.7782		
203.7	60	.7696	.7574	-.0122	
193.7	70	.7604	.7449	-.0155	
183.7	80	.7510	.7310	-.0200	
173.7	90	.7409	.7152	-.0257	

(2)

$\log \delta = \log \{ \log (T - 1.30) - .43840 \} - .38505.$					
243.7	20	.8034	.8019	-.0015	
233.7	30	.7959	.7943	-.0016	
223.7	40	.7873	.7865	-.0008	
213.7	50	.7782	.7782		
203.7	60	.7696	.7696		
193.7	70	.7604	.7605	+.0001	
183.7	80	.7510	.7510		
173.7	90	.7409	.7410	+.0001	
163.7	100	.7302	.7302		
153.7	110	.7188	.71885		
143.7	120	.7066	.7067	+.0001	
133.7	130	.6934	.6937	+.0003	
123.7	140	.6794	.6796	+.0002	
113.7	150	.6634	.6644	+.0010	

TABLE III. (*continued.*)

(3)

$\log \delta = \log \{ \log (T - 47.40) - \bar{1}.2893 \} - .5817.$					
T.	<i>t.</i>	δ exp.	δ calc.	Diff.	L.
163.7	100	.7302	.7275	-.0027	
153.7	110	.7188	.7171	-.0017	
143.7	120	.7066	.7060	-.0006	
133.7	130	.6934	.6934		}
123.7	140	.6794	.6794		
113.7	150	.6634	.6634		
107.7	160	.6462	.6449	-.0013	
93.7	170	.6273	.6226	-.0047	
83.7	180	.6060	.5948	-.0112	

(4)

$\log \delta = \log \{ \log (T + 34.30) - 1.0763 \} - .2157.$					
123.7	140	.6794	.6830	+.0036	
113.7	150	.6634	.6657	+.0023	
103.7	160	.6462	.6473	+.0011	}
93.7	170	.6273	.6273		
83.7	180	.6060	.6059	-.0001	
73.7	190	.6828	.5825	-.0003	
63.7	200	.6567	.5568	+.0001	
53.7	210	.527	.5283	+.0010	
43.7	220	.492	.4965	+.0036	

(5)

$\log \delta = \log \{ \log (T + 12.33) - .7126 \} - .3225.$					
73.7	190	.5828	.5806	-.0022	
63.7	200	.5567	.5551	-.0016	
53.7	210	.5273	.5269	-.0004	}
43.7	220	.4929	.4929		
33.7	230	.4526	.4523	-.0003	
23.7	240	.4016	.4017	+.0001	
13.7	250	.3345	.3345		
3.7	260	.2295	.2348	+.0053	

TABLE III. (continued).

(6) Figures not available.

Formulæ.

(1) $0.09137e^{9.162\delta} = T - 99.60.$	(4) $11.90e^{3.787\delta} = T + 34.30.$
(2) $2.744e^{5.588\delta} = T - 1.30.$	(5) $5.160e^{4.838\delta} = T + 12.33.$
(3) $0.1947e^{8.788\delta} = T - 47.40.$	(6) $Ae^{\lambda\delta} = T + A.$

A look at these equations, as well as at the above tables, indicates that these kinks are general for all regions. Although in some individual cases the figures may be doubtful, I think the number of cases where there can be no doubt at all is sufficiently large to allow us to regard the fact as established.

It should be added that I have had experience with a large number of liquids, using figures of different authors, and everywhere the result is the same.

I shall now proceed to show that the δ_l and δ_v curves are discontinuous as well. This is not so easy to show, because in this case the discontinuity is not quite so pronounced as in the case of δ curves.

However, it can be shown by the following method :—

To solve the equation

$$\delta = \delta_l - \delta_v = \frac{\log \left(\frac{T+B}{A} \right)}{.4343 \lambda} \quad . \quad . \quad . \quad . \quad (2)$$

for δ_l and δ_v respectively it is necessary to have another equation connecting the above quantities with the T . To this end, advantage can be taken of the Cailletet-Mathias law of rectilinear diameter in the cases where this law is valid.

According to this law

$$\frac{\delta_l + \delta_v}{2} = \frac{T+b}{a}, \quad . \quad . \quad . \quad . \quad . \quad (3)$$

where a and b are constants, *i. e.* it is a rectilinear function of temperature.

Or using for the sake of simplicity the symbol Δ for $\frac{\delta_l - \delta_v}{2}$,

$$\Delta = \frac{T+b}{a} \quad . \quad . \quad . \quad . \quad . \quad (4)$$

The question is whether this law is general and accurate enough. A more close examination shows that probably it is not. But for the purposes of this investigation it can easily be assumed that a and b remain constant within a given portion of the curve for which A , B , and λ are constant. I thus assume that a and b also undergo sudden

changes from time to time, although their change is minute compared with the corresponding change in A , B , and λ .

Thus for a given interval δ_l and δ_v can be evaluated from the equations (2) and (3) or (4):

$$\delta_l = \Delta + \frac{1}{2} \frac{\log \left(\frac{T+B}{A} \right)}{.4343 \lambda}, \quad (5)$$

$$\delta_v = \Delta - \frac{1}{2} \frac{\log \left(\frac{T+B}{A} \right)}{.4343 \lambda}. \quad (6)$$

The two expressions differ only in so far as the logarithmic term containing A , B , and λ comes in with the opposite sign. As these constants undergo sudden changes at regular intervals, the discontinuity of both curves is thereby accounted for.

In the expression $\delta_l + \delta_v$ the discontinuity is substantially compensated, at least the part of it due to the change in the constants A , B , and λ , because the logarithmic term disappears.

On the other hand, in the expression $\delta_l - \delta_v$ the two halves of the logarithmic expression add up, and the discontinuity is of a much more pronounced character.

For example, I calculated $\Delta \pm \frac{1}{2} \delta$, which is the accurate expression for δ_l and δ_v respectively, for two different intervals of temperature, using the following expressions:

For 220—170 T

$$\frac{T+594.91}{2197.7} \pm \frac{1}{2} \frac{\log (T+77.31)-1.39840}{1.45546}, \quad . (7)$$

and for 160—110 T

$$\frac{T+603.35}{2222.3} \pm \frac{1}{2} \frac{\log (T+52.93)-1.25988}{1.59191}. \quad . (8)$$

The results are given in Table IV.

By prolonging the calculations by the above formulæ, one can also observe a systematic deviation. In cases represented in Tables I., II., and III. the differences are magnified owing to the addition of two effects, *i. e.* of two logarithmic terms.

In the curves δ_l and δ_v the same deviations ought to be about half as big, if the effect were due to the half-logarithmic term with constants A , B , and λ only.

It appears, however, that there is also a small change in constants a and b ; at least it seems to be so in the case of hexamethylene.

TABLE IV.

T.	Δ exp.	Δ calc.	$\frac{1}{2}\delta$ calc.	δ_l exp.	δ_l calc.	δ_v exp.	δ_v calc.
220	·3708	·3708	·3692	·7400	·7400	·0016	·0016
210	·3664	·3663	·3642	·7306	·7305	·0022	·0021
200	·3617	·3617	·35885	·7205	·7206	·0029	·0028
190	·3572	·3571	·3534	·7106	·7105	·0038	·0037
180	·3526	·3526	·3477	·7003	·7003	·0049	·0049
170	·3481	·3480	·34175	·6898	·6898	·0063	·0062
160	·3435	·3435	·33555	·6791	·67905	·00796	·00795
150	·3390	·3390	·32905	·6680	·66805	·00995	·00995
140	·3344	·3345	·3221	·6565	·6566	·01227	·01210
130	·3299	·3300	·31485	·6448	·64485	·01505	·01515
120	·3254	·3255	·30715	·6325	·63265	·01818	·01835
110	·3210	·3210	·29905	·6200	·62005	·02193	·02195

The above relations assume the validity of Mathias-Cailletet's law. In cases when it is not valid, it is sometimes possible to see the discontinuity of the δ_l and δ_v curves simply by drawing the curves on a sufficiently large scale: for example, for propyl alcohol the law of rectilinear diameter does not hold true. However, the discontinuity of the densities is so sharp in the region between 60° and 50° C. that it cannot remain unnoticed.

Latent Heats of Evaporation.

The discontinuous character of the mechanism of disaggregation of liquids is particularly well demonstrated by the latent heats of evaporation (L).

Plotting the L's against the temperature T, one can see that the curve consists of curved portions intersecting with each other within the same ranges of temperature as in the δ curves. The bits of the curve are generally strongly curved at higher temperatures, especially near the critical point. Although the work near the critical point may be difficult, and involve considerable experimental errors, the angle at which the curves intersect with one another is such that the existence of the kinks is beyond any doubt.

The variation of L with temperature can be expressed fairly well by the expression of the same type as (1), viz.

$$Ce^{\mu L} = T + D,$$

where C, μ , and D are constants for the given interval of the curve.

At lower temperatures the curves often flatten out, and sometimes begin to approach a straight line.

In the following table the results are given for propyl alcohol.

TABLE V.
Propyl alcohol.

L Curves.

(2)

$\log L = \log \{ \log (T - 62.70) - .5785 \} - \bar{3}.9393.$				
T.	t.	L exp.	L calc.	Diff.
183.7	80	173	173	
173.7	90	169	168.7	-0.3
163.7	100	164	164	
153.7	110	159	158.8	-0.2
143.7	120	153	153	

(3)

$\log L = \log \{ \log (T - 100.2) - \bar{4}.5659 \} - \bar{2}.5281.$				
133.7	130	147	147	
123.7	140	142.4	142.4	
113.7	150	135.3	135.3	

(4)

$\log L = \log \{ \log (T + 156.05) - 2.0601 \} - \bar{3}.4390.$				
103.7	160	129	129	
93.7	170	122.8	122.7	-0.1
83.7	180	116.3	116.3	
73.7	190	109.6	109.6	
63.7	200	102.2	102.5	+0.3

(5)

$\log L = \log \{ (\log T + 58.04) - 1.6353 \} - \bar{3}.6401.$				
53.7	210	94.5	94.56	+0.06
43.7	220	85.3	85.25	-0.05
33.7	230	75.0	74.97	-0.03
23.7	240	63.4	63.46	+0.06
13.7	250	50.6	50.50	-0.10

Formulae :

$$\begin{aligned}
 (2) \quad & 3.789e^{.02007L} = T - 62.70. & (4) \quad & 114.2e^{.00633L} = T + 155.04. \\
 (3) \quad & .00037e^{.07787L} = T - 100.2. & (5) \quad & 43.22e^{.01005L} = T + 58.04.
 \end{aligned}$$

Surface Tensions.

The discontinuity is still more pronounced if the δ 's are plotted against the surface tensions; but nothing more definite can be said about it until the true law connecting the surface tensions and the densities is known.

Apart from the above, I have also come to the conclusion that the surface tensions plotted against the temperature show also signs of discontinuity. Although at first sight it appears to be a linear function of temperature, a more close examination shows that this is not the case at all. From a logarithmic plot it may appear that an expression may hold true of the type—

$$\alpha = (kT)_n,$$

where α is the surface tension and k and n constants.

However, the examination of errors makes me believe that such a law can be only regarded as a rough approximation, and it certainly is not the true law.

I have come to the conclusion that an accurate law can only be found for a limited part of the curve. The experimental data show that also in this case the law can be expressed by means of an exponential formula. If we plot the surface tensions (α) as abscissæ, and the temperatures (T) as ordinates, the relation will be of the form

$$\alpha + B = Ae^{\lambda T}.$$

Thus for ethyl acetate in the interval of temperatures 150.1—110.1 T the above formula acquires the form

$$\alpha + 33.62 = 33.19e^{.0024T},$$

and in the interval 100.1—70.1 T

$$\alpha + 21.32 = 20.93e^{.0035T}.$$

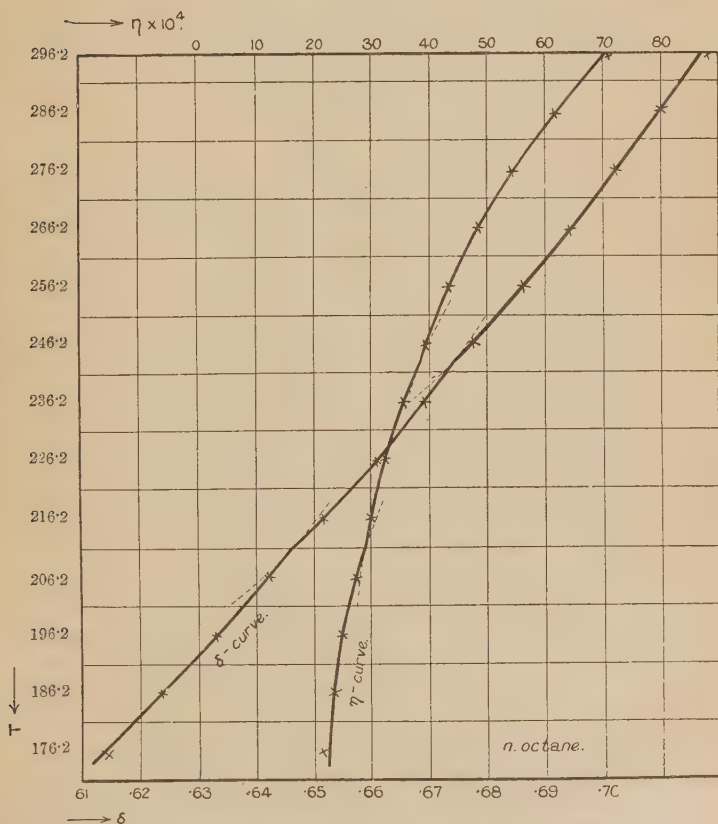
The figures for the above expressions are taken from the work of Ramsay and Shields (Phil. Trans. clxxxiv. I, p. 647, 1893). They indicate the presence of kinks in the same interval of temperatures as other properties do. They also indicate that near the critical point the surface tension will follow very closely the vertical axis, *i. e.* the increase of α with temperature will be only minute at first.

Viscosities.

It is generally assumed that the association of liquids must be intimately connected with their viscosities. It is therefore probable that if the association takes place in stages,

as indicated above, the viscosity-temperature curve will be also discontinuous. The existing data, although not very complete, throw enough light on the subject to make it clear that such is actually the case. Fig. 2 represents a δ curve, together with a corresponding viscosity curve (η curve) plotted against temperatures T (vertical axis

Fig. 2.



common to both curves) for n -octane. The viscosities ($\eta \times 10^4$) are plotted on the upper horizontal axis. On the lower axis the values of δ are plotted. The values of δ are taken from Sydney Young (*loc. cit.*) and the viscosities from the Landolt-Börnstein Tables. The figure shows that both curves are discontinuous, and the kinks on both curves correspond to more or less the same intervals of temperature.

It can also be observed from fig. 2 that the form of law will be the same as for surface tensions, viz.

$$\eta + C = De^{uT}.$$

In fig. 2 the viscosities of a liquid were plotted against the temperature. More strictly one ought to plot

$$\eta = \eta_l - \eta_v,$$

where η_l is the viscosity of the liquid and η_v that of its vapour. However, at low temperatures η_v is small, and η_l can be readily used as a good approximation for η . One can thus find that the law is of the form as indicated.

Conclusion.

The view that liquids contain more than one kind of molecules is not novel. Such a view has already been expressed in a paper by C. Drucker*, and also in the works of A. Smits†, although the latter author chiefly deals with such substances as sulphur and phosphorus, which liquids may not be regarded as typical (see also Cohen‡ and others).

This paper is intended to demonstrate the discontinuity of certain properties of liquids—viz., of the densities of the vapour, the densities of the liquid, of the latent heats of evaporation, the surface tensions, and viscosities.

The observation of the results tabulated in the accompanying tables shows that the mechanism of disintegration of the liquids proceeds always according to a definite and general law. In this sense there is no difference in the behaviour of the so-called "associated" and "normal" liquids. However, the examination of the constants of the exponential equations reveals some peculiarity in the case of an "associated" liquid, propyl alcohol. Whereas in the case of ethyl acetate and hexamethylene the numerical values of the constants vary in a certain more or less regular manner (for example, the constant B increases as we proceed from the critical point, and the constant λ on the contrary diminishes), their variation is most peculiar in the case of propyl alcohol. So the constant B increases at first as in the case of "normal" liquids, and then even changes sign. Also the constants λ and A show a peculiar behaviour.

It is noteworthy that the equations for the latent heat of evaporation (L) are not only of the same form, but they show

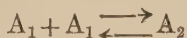
* *Zeit. Phys. Ch.* lxxviii, p. 616 (1909).

† *Zeit. Phys. Ch.* lxxvi, p. 421 (1911); lxxvii, p. 367 (1911).

‡ See numerous papers in *Zeit. Phys. Ch.* and elsewhere.

the same peculiarities, viz. the constants B also increase at first, change sign, and so on.

Thus it looks as if L was intimately related to δ . Both properties are discontinuous and show kinks in the same places, and they both become =0 at the critical point. All this can receive a reasonable explanation if the association of molecules takes place according to the law of multiple proportion. It would then be quite natural to expect a more radical change near the critical point. For example, if a change



is taking place, and is succeeded by a change, say



the kinks will be well pronounced. On the other hand, in a change, say



the addition of A_1 to an already complicated molecule will produce an effect which may be hardly noticeable at all.

The examples worked out in this paper indicate on the whole that such is actually the case, and the kinks, being well pronounced near the critical point, become less and less noticeable at lower temperatures (see fig. 1). It can be seen that the increase of δ per change diminishes as we proceed from the critical point, viz. its values are .25, .20, .15, .10, etc.

However, in some cases at low temperatures the kinks may become of such a nature as to indicate a deeper change.

In this paper I regard the vapour as the dissociation product, and in the above schemes it figures as one of the reacting bodies. Such a view accounts for the discontinuity of the density of the vapour.

However, at lower temperatures the vapour becomes negligible, and yet the δ curve may sometimes indicate a substantial change.

Considerations of that kind make me believe that at lower temperatures some other change may take place. For example, it seems natural to conclude that only the first three changes from the critical point in the case of propyl alcohol proceed "normally," as I may call it. The other three changes suggest something different, and particularly the last one (numbered (1) in the tables). In the latter case

a more substantial change suggests itself. For example,



or something of that kind.

The fact that in the latter case the curve can be expressed by a formula of the same form as above makes me believe that in this case also a chemical change must be at the bottom of it.

Apart from the scheme just indicated, I can also think of such a change as will consist in an intermolecular re-grouping, in which case the form of the δ curve may remain substantially the same.

However, I can quite believe that in the vicinity of the melting-point the above relations may cease to hold true. Such is, for example, the case with water at about 4° C.

The explanation of this case can be found in Tyndall's work, 'Heat a Mode of Motion,' 1908, p. 108, where a model is given explaining the behaviour of water at about 4° C. In such a case the molecules are assumed to be in such a proximity to one another that the friction becomes an important factor in accounting for the above phenomenon.

It was mentioned in the Introduction that there is some evidence of association in the liquid state (Sir Wm. Bragg, C. V. Raman), suggesting that near the melting-point the molecular unit consists of 2, 3, 4, or more molecules.

On the other hand, in a gaseous state the molecular weight is known to correspond to a simple molecule (at least in cases dealt with in this paper).

The question arises, where does the association take place? It is highly improbable that it should take place directly below the critical point, or that it should take place suddenly somewhere else between the critical point and the melting-point.

However, the facts set out in this paper suggest that it takes place in several stages, and I do not think the kinks here described can have any other interpretation than that it takes place in accordance with the law of multiple proportions.

Summary.

1. In this paper evidence has been collected to show that the temperature changes in the liquid state take place in a discontinuous manner.

2. Four properties have been investigated in this paper—viz. densities, latent heats of evaporation, surface tensions, and viscosities.

3. They all show kinks at the same temperatures.

4. The densities (δ) and latent heats of evaporation (L) vary with temperature according to a definite exponential law which is general for both normal and associated liquids and practically for all ranges of temperature, viz.

$$Ae^{\lambda\delta} = T + B \quad \text{and} \quad Ce^{\mu L} = T + D,$$

where T is the temperature reckoned from the critical point. These formulæ are valid for an interval between two kinks with given constants. For each interval the constants are different, but the form of law remains the same. The curve, plotted as in fig. 1, is convex towards the horizontal axis.

5. The surface tensions (α) and viscosities (η) similarly follow a simple and also an exponential law, viz.

$$\alpha + B = Ae^{\lambda T} \quad \text{and} \quad \eta + C = De^{\mu T}.$$

Both expressions are such that not the properties (α , η) but T is in the exponential. The curve is concave towards the horizontal axis.

6. The above evidence indicates that the discontinuity is an intrinsic property of liquids, and is interpreted as an indication of definite molecular changes in given intervals of temperature.

XXIX. *The Atomic Structure Factor in the Intensity of Reflexion of X-Rays by Crystals.* By D. R. HARTREE, M.A., Fellow of St. John's College, Cambridge*.

§ 1. Introduction.

THE intensity of reflexion of X-rays by a crystal depends on several variables, one of which is the nature of the atoms composing it; the effect of this variable is represented in the formula for the intensity of reflexion† by the introduction of the number F for each atom, which represents the ratio of the amplitude of the wave scattered by this atom to the amplitude of the wave scattered by an electron. Adopting the classical theory, which at least gives results

* Communicated by Prof. W. L. Bragg, F.R.S.

† See W. H. and W. L. Bragg, 'X-Rays and Crystal Structure,' 4th edition, p. 203 *et seqq.*, where references to the original theoretical work of C. G. Darwin and A. H. Compton are given. See also W. L. Bragg, R. W. James, and C. H. Bosanquet, *Phil. Mag.* xli. p. 309; xlii. p. 1 (1921); xliv. p. 433 (1922).

of the right order of magnitude*, it is clear that F must depend not only on the atom, but also on the angle of scattering, *i.e.* on the glancing angle, and on the wave-length of the incident radiation; for, if the wavelets scattered by all the electrons were in phase, F would be equal to the number of electrons concerned in the scattering, but if the differences of phase between the wavelets scattered by different electrons were appreciable, the amplitude of the wave scattered by the atom as a whole would be less than it would be if the wavelets were in phase, so that F is less than the number of electrons concerned in the scattering; these phase differences vary, and so F varies, with the glancing angle and wave-length.

The dependence of F on glancing angle and wave-length depends on the dimensions of the atomic orbits, and on the distribution of electrons in them. Approximate dimensions of the core orbits of some atoms can be found from the results of a numerical analysis of the terms of the optical and X-ray spectra, and the dimensions of orbits of other atoms interpolated from them, so that it is possible to calculate approximate values of F as a function of the glancing angle for any atom; these values can be represented by a graph which may be called an "F-curve." These F-curves may be of value in the analysis of crystal structure by X-rays, as will be explained shortly; the object of this paper is to give data from which the approximate F-curve for any ion may be constructed very simply, and to give F-curves for some interesting ions.

The importance of F-curves for the X-ray analysis of crystal structure can be explained shortly as follows.

For the simplest crystal structures (*e.g.* the elements crystallizing in the cubic system, or salts of the NaCl type), in which the positions of all atoms are given by considerations of symmetry once the general scheme or space group of the arrangement is known from X-ray results, the analysis does not depend on the F-curves for the atoms of the crystal; and for structures in which the positions of most of the atoms can be determined from considerations of symmetry alone, but which involve one parameter (*e.g.* the calcite series), or perhaps two, the values of these parameters can often be determined very closely from the abnormally low or high intensities of a few orders of reflexion from a small number of faces, without reference to the relative scattering powers of different atoms. But for more complicated structures, in

* Cf. W. L. Bragg, R. W. James, and C. H. Bosanquet, *loc. cit.* (3rd paper, p. 446).

which the positions of few or none of the atoms are given by considerations of symmetry and the number of parameters is large, it becomes necessary to make more use of the intensities of reflexion of different orders and from different faces, and in order to do this fully it is necessary to know something about the relative amplitudes of the waves scattered by different atoms at different glancing angles*.

Though the method of calculating F-curves given in this paper involves some approximation and doubtful assumptions, it is hoped that the results obtained may form a better basis for X-ray analysis than the assumption usually, if not always, made hitherto, that the amplitude of the wave scattered by an atom is proportional to its atomic number.

§ 2. *General Theory of the Method.*

It will be assumed that, for the purpose of calculating the intensity of reflexion from a crystal as a whole, the total effect of all the atoms of one kind, situated at corresponding points of different elementary cells of the space-lattice, can be treated as if each atom consisted of a spherically symmetrical distribution of scattering material†.

For reflexion of X-rays of wave-length λ at glancing angle β , the contribution to the value of F from an electron in a circular core orbit‡ of radius r is $\xi^{-1} \sin \xi$, where

$$\xi = (4\pi r \sin \beta) / \lambda. \quad . \quad . \quad . \quad (2.1)$$

If the electron in a non-circular core orbit spends a fraction df of a radial period between radii r and $r + dr$, the contribution from this orbit to F is $\oint \xi^{-1} \sin \xi df$, so that the total value of F is

$$F = \Sigma \oint \xi^{-1} \sin \xi df, \quad . \quad . \quad . \quad (2.2)$$

the summation being taken over all core orbits.

Thus if df/dr is known as a function of r for the core orbits of an atom, F can be calculated. For approximate evaluation of F the work can be much simplified; the results

* A further discussion and illustration of the use of F-curves in crystal analysis is given in a note by Prof. W. L. Bragg accompanying this paper.

† For a further discussion of this assumption, see a previous paper by the present writer, *Phil. Mag.* xlv. p. 1091 (1923), especially § 4.

‡ See Bragg, James, and Bosanquet, *loc. cit.* (3rd paper, p. 439), and D. R. Hartree, *Phil. Mag.* (*loc. cit.* § 2).

of numerical calculation of core orbits show that the progress of time in all non-circular core orbits is very similar; more precisely, the fraction of a radial period which an electron spends between any given fractions of the maximum radius of the orbit is very nearly the same for all such orbits, so that if r_0 is the maximum radius and $r/r_0 = r'$, df/dr' is very nearly the same function of r' for them all (see § 3). If we neglect the small differences of df/dr' as a function of r' for different orbits, and write

$$\xi_0 = (4\pi r_0 \sin \beta)/\lambda, \quad . \quad . \quad . \quad (2.3)$$

we can write the contribution to F from a non-circular orbit as

$$C_2(\xi_0) = \oint \frac{\sin \xi_0 r'}{\xi_0 r'} \frac{df}{dr'} dr', \quad . \quad . \quad . \quad (2.4)$$

a function of ξ_0 only, *i. e.* a function of the maximum radius r_0 only, for a given value of $(\sin \beta)/\lambda$. Thus if $C_2(\xi_0)$ is evaluated once for all by integration for some values of ξ_0 , and interpolation for other values, and tabulated, then for any particular non-circular orbit of a particular atom it is only necessary to know the maximum radius r_0 and to evaluate ξ_0 and look up $C_2(\xi_0)$ from the table; it is not

necessary to carry out the integration $\oint \xi^{-1} \sin \xi df$ for each separate orbit at each glancing angle. The saving of numerical work hereby is very considerable.

Certainly on account of the different ratios of minimum radius to maximum radius of different orbits, the values of df/dr' for different orbits differ most for small values of r' , for which the value of $\xi^{-1} \sin \xi$ is greatest, but the fraction of a radial period spent in this part of the orbit is always small, and numerical investigation shows that the error involved in assuming the same $(df/dr' r')$ curve for all orbits is not serious.

If, corresponding to the contribution $C_2(\xi_0)$ to F from a non-circular orbit, we write the contribution from a circular orbit (for which $\xi = \xi_0$),

$$C_1(\xi_0) = \xi_0^{-1} \sin \xi_0, \quad . \quad . \quad . \quad (2.5)$$

then (2.2) becomes

$$F = \Sigma_1 C_1(\xi_0) + \Sigma_2 C_2(\xi_0), \quad . \quad . \quad . \quad (2.6)$$

suffixes 1 and 2 referring to circular and non-circular orbits respectively.

§ 3. Numerical Data on Dimensions of Core Orbits.

By numerical analysis of the terms of the optical and X-ray spectra, it is possible to obtain a rough idea of the field of an atom, and from this field the dimensions of and progress of time in the core orbit can be calculated. The general lines of this analysis and preliminary results for Na, K, and Ca^+ have been given by the writer in an earlier paper*: the numerical work has since been revised, and similar work carried out for Cl^- (roughly), Cu, Rb, Cs, and Tl. The results must be considered as still subject to revision, but so long as the general ideas on which this work is based are retained, it does not seem probable that any modifications will seriously affect the calculated dimensions of the core orbits, which are the quantities required for the purposes of this paper.

There are two main results of this calculation of core orbits:—

- (a) The determination of df/dr' as a function of r' for non-circular orbits.
- (b) The values of the maximum radii of the different core orbits.

The first is only concerned with relative times and dimensions of different orbits, the second with absolute values of the dimensions.

The great similarity of the $(df/dr', r')$ curves for different non-circular core orbits is shown by fig. 1, in which points on the curves for various orbits of various atoms are plotted (the diagram would be too confused if the whole curve for each orbit were drawn). The curve drawn is an average one†, which has been used in the evaluation of the function C_2 .

As to the actual dimensions of orbits of the core electrons, one result of the numerical analysis is that the maximum radii of all non-circular core orbits with the same

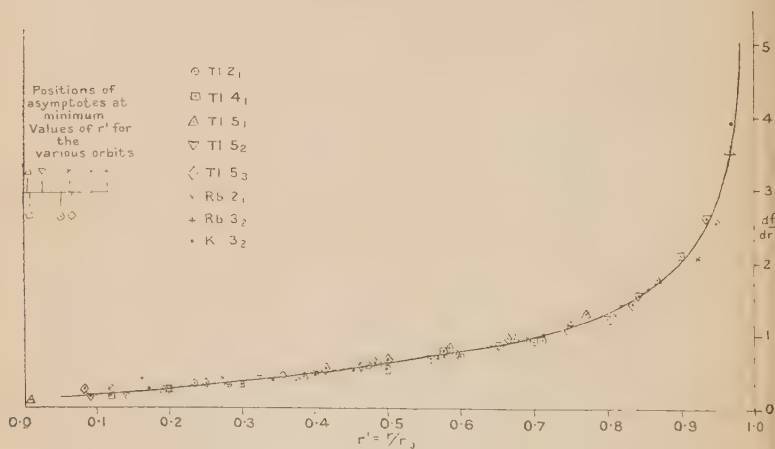
* D. R. Hartree, *Proc. Camb. Phil. Soc.* xxi. p. 625 (1923).

† The curve for any actual orbit has a vertical asymptote at the minimum value of r' , which is different for different orbits; the average curve has been drawn to stop at $r' = 0.05$, without a vertical asymptote. The curves for the actual orbits differ little for $r' > 0.2$, and the maximum fraction of a radial period spent within this radius is about 0.06; this is also the maximum possible error in C_2 due to the assumption that (df/dr') is the same function of r' for all core orbits; actually it seems unlikely that the error will ever be greater than 0.03.

principal quantum number n are very nearly the same*. This again shortens the numerical work of calculating F for any given atom, since—taken in conjunction with the result that the contribution to F from a non-circular orbit is a function of the maximum radius of the orbit only—it means that all non-circular core orbits with the same value of n can be treated as equivalent, so far as their contributions to F are concerned; it is not necessary to consider orbits with different values of k separately. This is not exact, but the error is less than the probable error of determination of the maximum radii of the separate core orbits from the numerical analysis.

Fig. 1.

Showing similar progress of time in all non-circular core orbits.



The vertical lines in Scale A show the positions of the vertical at the minimum radii of the various orbits.

df = fraction of a radial period spent between fractions r' and $r' + dr'$ of the maximum radius r_0 .

$\frac{df}{dr'}$ is plotted against r' for various core orbits of various atoms, and a mean curve is drawn.

For different atoms, it seems probable that r_k , the radius of the circular k -quantum core orbit, should vary with

* For example, for Tl the calculated maximum radii of the 4_1 , 4_2 , and 4_3 core orbits are 0.50, 0.53, and 0.52 times the radius of the 1_1 orbit of hydrogen; the differences between these values are less than the amounts by which they may be in error. It may perhaps be mentioned that the calculations for different values of k are carried out almost entirely independently of one another.

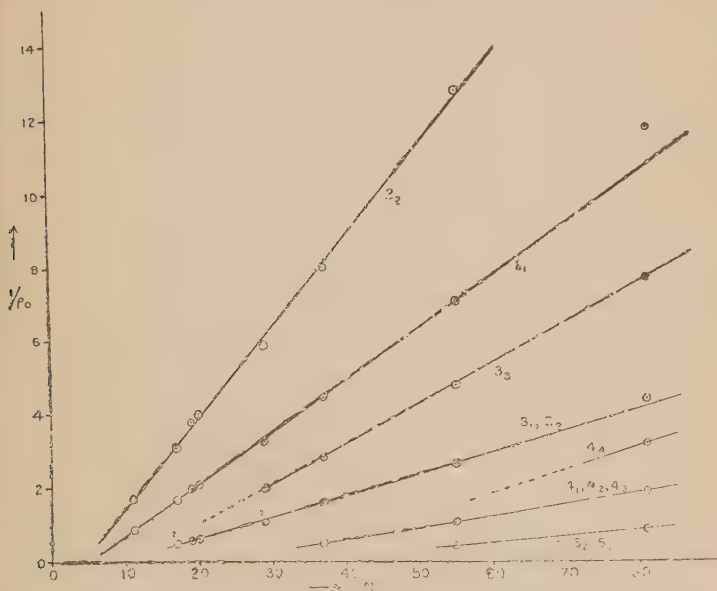
atomic number N approximately according to the relation *

$$r_k (N - \gamma_k) = \text{const.}, \quad . \quad . \quad . \quad (3.1)$$

where γ_k is independent of N , so that $1/r_k$ should be linear in the atomic number N ; and it might be expected that a similar relation would hold for the maximum radius of the non-circular orbit with given quantum numbers n_k , except perhaps in that part of the periodic table where the group of principal number n is being built up—more strictly, where the number of electrons in the group of principal quantum number n varies with the atomic number.

Fig. 2.

Showing relation between maximum radii of core orbits and atomic number.



ρ_0 = maximum radius of orbit as multiple of radius of 1_1 orbit of H atom.
Calculated values of $1/\rho_0$ plotted against atomic number N .

Writing a for the radius of the 1_1 orbit of the H atom (0.532 \AA.U.), and $r = a\rho$, the calculated values of $1/\rho$ for the radii of the circular core orbits and the maximum radii of the non-circular core orbits, of all atoms for which a numerical analysis of the spectra have been made by the writer, are plotted against the atomic number N in fig. 2.

* See D. R. Hartree, Proc. Roy. Soc. cvi. p. 552 (1924).

TABLE II.

Values of $C_2(\xi_0)$ for contributions to F from
Non-circular Orbits.

$$\xi_0 = (4\pi r_0 \sin \beta)/\lambda. \quad \beta = \text{glancing angle,}$$

$$C_2(\xi_0) = \oint \frac{\sin \xi_0 r'}{\xi_0 r'} \frac{df}{dr'} dr'. \quad = \text{half angle of scattering.}$$

ξ_0	·0	·1	·2	·3	·4	·5	·6	·7	·8	·9
0	1·00	1·00	0·99	0·99	0·98	0·97	0·96	0·95	0·93	0·92
1	0·90	0·88	0·86	0·83	0·81	0·78	0·75	0·72	0·69	0·66
2	0·63	0·60	0·57	0·54	0·51	0·48	0·44	0·41	0·38	0·35
3	0·32	0·29	0·27	0·24	0·21	0·19	0·17	0·14	0·12	0·10
4	0·08	0·06	0·04	0·03	0·02	0·01	0·00	-0·01	-0·02	-0·03
5	-0·03	-0·03	-0·04	-0·04	-0·04	-0·04	-0·04	-0·04	-0·03	-0·03
6	-0·03	-0·02	-0·02	-0·01	-0·01	0·00	0·00	0·01	0·02	0·02
7	0·03	0·03	0·04	0·04	0·05	0·05	0·06	0·06	0·06	0·06
8	0·07	0·07	0·07	0·07	0·07	0·07	0·07	0·07	0·07	0·06
9	0·06	0·06	0·06	0·05	0·05	0·05	0·04	0·04	0·03	0·03
10	0·03	0·02	0·02	0·02	0·01	0·01	0·00	0·00	0·00	-0·01
11	-0·01	-0·01	-0·01	-0·01	-0·01	-0·02	-0·02	-0·02	-0·02	-0·02
12	-0·01	-0·01	-0·01	-0·01	-0·01	-0·01	-0·01	0·00	0·00	0·00
13	0·00	0·01	0·01	0·01	0·01	0·01	0·01	0·02	0·02	0·02
14	0·02	0·02	0·02	0·03	0·03	0·03	0·03	0·03	0·03	0·03
15	0·03	0·02	0·02	0·02	0·02	0·02	0·02	0·02	0·02	0·01
16	0·01	0·01	0·01	0·01	0·00	0·00	0·00	0·00	0·00	0·00
17	-0·01	-0·01	-0·01	-0·01	-0·01	-0·01	-0·01	-0·01	-0·01	-0·01
18	-0·01	-0·01	-0·01	-0·01	-0·01	-0·01	-0·01	-0·01	0·00	0·00
19	0·00	0·00	0·00	0·00	0·00	0·00	0·01	0·01	0·01	0·01
20	0·01	0·01	0·01	0·02	0·02	0·02	0·02	0·02	0·02	0·02

First, in Tables I. and II. are tabulated the values of $C_1(\xi_0)$ and $C_2(\xi_0)$, the contributions to F from a circular and non-circular orbit respectively ; they are given by

$$C_1(\xi_0) = \xi_0^{-1} \sin \xi_0, \quad . \quad . \quad . \quad . \quad . \quad (2\cdot5)$$

$$C_2(\xi_0) = \oint \frac{\sin \xi_0 r'}{\xi_0 r'} \frac{df}{dr'} dr'. \quad . \quad . \quad . \quad . \quad (2\cdot4)$$

In evaluating C_2 , the function df/dr' given by the curve in fig. 1 has been used. C_1 and C_2 are tabulated to two decimal

places, so the numerical error in F is of the order of 1 per cent. of the total number of electrons in the scattering atom; this is less than the possible error due to the approximations made in treating df/dr' as the same for all non-circular core orbits, and in estimating the actual dimensions of the orbits.

If ρ_0 is the maximum value of ρ for any orbit (i. e. $r_0 = a\rho_0$), then for reflexion of X-rays of wave-length λ at glancing angle β the argument ξ_0 of the function C_1 or C_2 giving the contribution to F from the orbit is, from (2.3),

$$\begin{aligned}\xi_0 &= (4\pi a\rho_0 \sin \beta)/\lambda, \\ &= (6.68\rho_0 \sin \beta)/\lambda, \quad . \quad . \quad . \quad (4.1)\end{aligned}$$

if λ is measured in Å.U.

It will be noticed that in so far as ξ_0 , and therefore F , is a function of the wave-length λ and the glancing angle β , it depends only on the value of $(\sin \beta)/\lambda$, so that if F is plotted as a function of $\sin \beta$ for any wave-length, the curve for any other wave-length will be found by a simple change of scale of $\sin \beta$. It would, of course, be possible to plot F as a function of $(\sin \beta)/\lambda$, but it will probably be found most convenient in practice to calculate and plot F as a function of $\sin \beta$ for some standard λ (e. g. Rh or Mo $K\alpha$).

In order to have enough points on the F -curve, it is advisable to calculate F for a set of values of $\sin \beta$ such that successive values of $(\sin \beta)/\lambda$ do not differ by much more than 0.1, if λ is measured in Å.U. For example, for Rh $K\alpha$ X-rays ($\lambda = 0.615$ Å.U.) it is best to calculate F for values of $\sin \beta$ which are multiples of 0.05; if it is only calculated for $\sin \beta = 0.1, 0.2, 0.3 \dots$, the points are too far apart to define an F -curve properly.

The values of ρ_0 for the various orbits could be found by reading off values of $1/\rho_0$ from fig. 2, but on account of the rather small scale of the diagram it is probably more satisfactory to use formulæ deduced by fitting linear relations between $1/\rho_0$ and N , using a larger scale diagram. If we write

$$\rho_0 = K/(N - \gamma),$$

then K and γ are functions of the quantum numbers n_k ; values of K and γ for the straight lines drawn in fig. 2 are given in Table III. For circular orbits in a central field we must have $K = k^2$. This has been kept in mind in drawing the lines in fig. 2.

TABLE III.

Data for the Approximate Calculation of Maximum Radii of Core Orbits.

Max. radius $r_0 = a\rho_0$, where a is radius of 1_1 orbit of hydrogen atom.

$\rho_0 = K/(N-\gamma)$, where K and γ are approximately the same for core orbits of the same quantum numbers in different atoms.

Table gives values of K and γ .

Orbit.	K .	γ .
1_1	1.0	1.0
2_1	7.0	5.2
2_2	4.0	4.2
$3_1, 3_2$	17.0	9.5
3_3	9.0	12.0
$4_1, 4_2, 4_3$	32	20.5
4_4	16	30
$5_1, 5_2$	54	32

The only other question we have to consider is the distribution of electrons among the different n_k orbits; and since, so far as their contribution to F is concerned, all the non-circular orbits with the same principal quantum number are equivalent to the order of accuracy required, all we need to know is the distribution of electrons in the circular and non-circular orbits.

Two general arrangements of electrons have been suggested—one by Bohr*, based chiefly on arguments as to symmetry, and concerned with the distribution of electrons among groups characterized by the two quantum numbers n_k ; and one recently by Stoner†, from considerations of inner quantum numbers and from experimental evidence, in which the distribution of electrons among groups characterized by the three quantum numbers $n_{k,j}$ is considered. The interpretation of the quantum numbers—especially the inner quantum number j —cannot be taken as yet certain, but assuming that for both distributions the quantum numbers n_k can be correlated with the ordinary principal and azimuthal quantum numbers of an orbit in a central field, the circular orbits are given by $n=k$ and the non-circular by $n \neq k$.

On this assumption the distribution of electrons between the circular and non-circular orbits according to the two schemes is given in Table IV. for the inert gases (and ions of the alkali metals) and for the ions Cu^+ , Ag^+ , and Au^+ , which represent important stages in the building-up of atoms.

* N. Bohr, *Zeit. f. Phys.* ix. p. 1 (1922), or 'The Theory of Spectra and Atomic Constitution,' Third Essay.

† E. C. Stoner, *Phil. Mag.* xlviii. p. 719 (1924).

TABLE IV.

Distribution of Electrons in Circular and Non-Circular Orbits in Various Atoms and Ions.

Atom or Ion.	Number of Elec- trons.	According to Bohr.						According to Stoner.					
		$n=1,$ $k=1.$	2	3	4	5	6	1	2	3	4	5	6
He, Li ⁺ ...	2												
Ne, Na ⁺ ...	10	2	4 4					2	2				
A, K ⁺ ...	18	2	4 4					2	2				
Cu ⁺ ...	28	2	4 4	8				2	2	8			
Kr, Rb ⁺ ...	36	2	4 4	12 6				2	2	8 10			
Ag ⁺ ...	46	2	4 4	12 6	8			2	2	8 10	8		
Xe, Cs ⁺ ...	54	2	4 4	12 6	18			2	2	8 10	18		
Au ⁺ ...	78	2	4 4	12 6	18	8		2	2	8 10	18	8	
Nt, 87 ⁺ ...	86	2	4 4	12 6	24 8	18	8	2	2	8 10	18 14	18	8

TABLE V.
Calculated Values for F for Various Ions as Functions of the Glancing Angle
for Mo K α X-Rays ($\lambda=0.71$ Å.U.).

Ion.	$\sin \beta$ for Mo K α .														
	0.00	0.05	0.10	0.15	0.20	0.25	0.30	0.35	0.40	0.45	0.50	0.55	0.60	0.65	0.70
C ⁺²	2.0	2.0	2.0	2.0	2.0	1.9	1.9	1.9	1.8	1.8	1.7	1.7	1.6	1.6	1.5
O ⁻²	10.0	9.4	8.2	6.4	4.8	3.5	2.4	1.5	0.9	0.6	0.6	1.0	1.4	1.8	2.1
Na ⁺	10.0	9.8	9.4	8.7	8.0	7.0	6.0	5.1	4.1	3.3	2.6	2.1	1.6	1.3	1.0
Si ⁺⁴	10.0	9.9	9.7	9.5	9.1	8.5	7.9	7.3	6.5	5.9	5.1	4.5	3.9	3.3	2.9
S ⁺⁶	10.0	9.9	9.8	9.6	9.3	8.9	8.5	8.0	7.5	6.9	6.3	5.7	5.1	4.6	4.1
S ⁻²	18.0	16.7	13.7	10.7	9.1	8.7	8.8	8.6	7.7	6.8	6.2	5.8	5.3	4.7	4.0
Cl ⁻	18.0	17.0	14.5	11.8	9.7	8.8	8.7	8.7	8.4	7.7	6.8	6.2	5.9	5.4	4.9
K ⁺	18.0	17.3	15.6	13.5	11.3	9.6	8.7	8.4	8.4	8.3	8.0	7.5	6.8	6.1	5.3
Ca ⁺²	18.0	17.5	16.0	14.1	12.0	10.4	9.2	8.5	8.4	8.4	8.3	7.9	7.5	6.9	6.0
Cu ⁺	28.0	27.7	27.0	25.8	24.1	22.2	20.2	18.1	16.1	14.0	12.0	10.3	9.0	7.9	6.9
Sr ⁺²	36.0	35.2	33.2	30.6	27.8	25.5	23.8	22.6	21.8	20.6	19.3	17.7	16.0	14.4	13.1
Ba ⁺²	54.0	52.6	49.1	44.8	40.7	37.4	34.8	32.5	29.9	27.4	24.6	23.1	21.9	21.1	20.4
Tl ⁺³	78.0	77.1	75.2	72.0	68.1	63.4	58.8	54.4	50.3	46.8	43.7	40.9	38.8	37.0	34.7

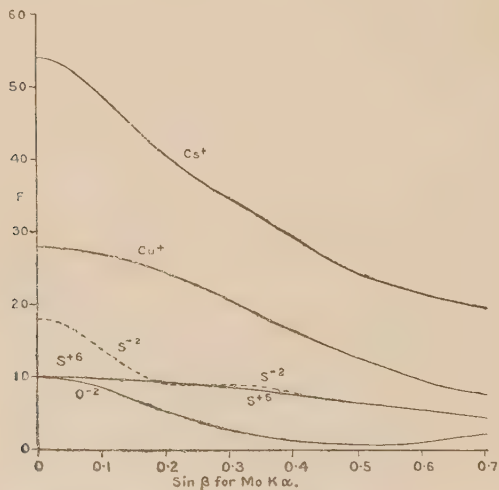
Stoner's distribution of electrons in core orbits has been assumed in calculating the above figures.
F for zero glancing angle is equal to the number of electrons in the ion.

The differences between the values of F calculated from the two distributions are not usually very large; expressed as a fraction of the whole value of F they are most important for the lighter atoms, and particularly for the negative ions with the neon structure (*e.g.* O^{--}). For the numerical examples of F -curves given in this paper, Stoner's distribution will be used unless the contrary is specified.

§ 5. Some Numerical Results.

Values of F as a function of the glancing angle β for Mo $K\alpha$ radiation, calculated from the data of § 4, are given

Fig. 3.



F -curves for various ions. Calculated values of F are plotted against the sine of the glancing angle β for Mo $K\alpha$ X-rays.

for various ions in Table V.*, and F -curves for some of these ions are shown in fig. 3. The F -curves show two striking features: firstly there is the slow initial decrease of F with increasing glancing angle for the compact ions (such as Cu^+ , S^{+6}), compared with that for the ions of greater size (*e.g.* Cs^+ , O^{-2}); and secondly there is the very small difference between the values of F for the same element in different

* The differences between the values for both Na^+ and Cl^- and the values given by the writer in a previous paper (*Phil. Mag. loc. cit.*) are due partly to a revision of orbital dimensions and partly to the adoption of Stoner's distribution of electrons in core orbits.

states of ionization, except for small glancing angles. These features could both have been predicted from considerations of the general form of the contributions to F from the outer orbits of the atom.

Apart from these it does not seem possible to draw any quantitative generalization from these curves, and for practical application it seems best to calculate the F -curve for each ion as it is required.

§ 6. *Discussion.*

It has been assumed in the above method of calculating F -curves that the electrons in an atom scatter X-rays like free electrons in their instantaneous positions would do on the classical theory.

Two doubts arise in connexion with this assumption: firstly, are we justified in applying classical laws to the scattering of X-rays at all; and secondly, even if the scattering by the loosely-bound electrons can be treated as classical, is classical scattering applicable to electrons bound in orbits of energy of the order of (or greater than) the quantum energy of the incident X-rays?

As to the second of these points, if it is assumed that some electrons (*e.g.* those in K orbits) do not contribute to the radiation scattered (as it seems) classically by the atom as a whole, it is probably best to omit their contributions entirely in evaluating F . For the ordinary X-rays used in crystal analysis, only the K electrons of the heavier elements and perhaps the L electrons of the heaviest would have to be neglected for this reason; as the values for F for these atoms is always considerable, the proportional change in F is not very important.

The question whether even the loosely-bound electrons can be taken as scattering classically is more fundamental and more difficult. All the evidence from the consistent results of X-ray analysis of crystals suggests that each atom scatters a wavelet which interferes classically with those scattered by other atoms; a striking example is the absence of the first-order (111) reflexion from KCl. Further, if we assume classical scattering by an atom as a whole, and assign to each atom a number F representing the ratio of the amplitude of the wave scattered by the atom to that of the wave scattered classically by a free electron, the experimental work of Bragg, James, and Bosanquet* on NaCl shows that F varies with the glancing angle in at any rate the same sort of way

* *Loc. cit.*

as would be calculated by the methods of § 4 of this paper, assuming classical scattering by the individual electrons in each atom.

Certainly there is a considerable difference between the observed and calculated values of F for both Na^+ and Cl^- , the observed values being smaller than the calculated ones whether Bohr's or Stoner's distribution of electrons is assumed, as is shown in Table VI.; for O^{-2} the observed

TABLE VI.

Comparison of Observed and Calculated Values of F for O^{-2} , Na^+ , and Cl^- .

$\sin \beta$ (for Mo $K\alpha$)	0.15	0.2	0.25	0.3	
$F(\text{O}^{-2})$ { obs.	5.6	3.9	2.6	1.5	
calc. (S)	6.4	4.8	3.5	2.4	
calc. (B)	5.5	3.9	3.0	2.3	
$\sin \beta$ (for Rh $K\alpha$)	0.1	0.2	0.3	0.4	0.5
$F(\text{Na}^+)$ { obs.	8.3	5.4	3.4	2.0	0.8
calc. (S)	9.4	7.6	5.6	3.7	2.4
calc. (B)	9.1	6.9	4.7	3.1	2.2
$F(\text{Cl}^-)$ { obs.	12.7	7.9	5.8	4.4	3.2
calc. (S)	13.8	9.1	8.6	7.5	5.9
calc. (B)	13.7	8.8	8.2	7.0	5.3

(S)=Stoner's distribution of electrons assumed.

(B)=Bohr's " " " "

values* of F are smaller than the values calculated with Stoner's distribution of electrons, in very much the same way as the values for Na^+ and Cl^- ; for small glancing angles the observed values agree with those calculated on Bohr's

* In a recent paper (Phil. Mag. xlix, p. 1225 (1925) A. J. Bradley has given some figures for the scattering power of O^{-2} , relative to $\text{K}^+ + \text{S}^{+6} = 28$; I have taken these figures, interpolated for exact values of $\sin \beta$ for the Mo $K\alpha$ radiation used, and multiplied by the ratio of the sum of the calculated values of F for K^+ and S^{+6} (Table V.) to 28, to obtain the values of F for O^{-2} given in Table VI. The actual values of F for K^+ and S^{+6} are probably smaller than the calculated values, so that the actual values for O^{-2} are probably smaller than the "observed" values.

distribution of electrons *, but for larger glancing angles the observed values are smaller, as for the other ions. But the effects of some of the other variables which affect the intensity of reflexion are not yet properly known (the effect of primary extinction † is the most important at small glancing angles, and the effect of the heat-motion the most important at large glancing angles), and possibly have not been properly allowed for in reducing the experimental results to obtain values of F . It is also possible, however, and such evidence as there is at present seems to point to the conclusion, that for some reason at present unexplained the actual values of F are smaller than those calculated on the assumption of classical scattering by the individual electrons; but if such scattering is not assumed, it is difficult to see how a variation of F with glancing angle is to be explained, and it is also not clear why the values of F for small glancing angles should agree at least approximately with those calculated, assuming classical scattering.

For the analysis of crystal structure it is at present impracticable to correct the measured intensities of reflexion for the effects of heat-motion or of primary or secondary extinction; and any difference between actual and calculated values of F will simply give rise to another factor in that part of the variation of intensity of reflexion with glancing angle which it is not practicable to evaluate for each particular case in the determination of crystal structure. For clearness let us consider the intensity of reflexion written in the form of a product of two functions, ϕ_1 and ϕ_2 , of the variables on which it depends, the function ϕ_1 being one which it is practicable to evaluate for given values of its arguments in practical crystal analysis, and the function ϕ_2 being one which depends on the variables in such a way that it is not practicable to evaluate it. The effects of heat-motion and extinction have at present to be taken into account by the second function ϕ_2 , and so far the same is true of the variation of F with glancing angle. It is hoped that the use of calculated values of F will make it possible to take into account at least part of the variation of F with glancing angle in ϕ_1 , leaving only the difference between actual and calculated values of F

* This agreement must not be taken as significant, as the "observed" values of F for O^{-2} are based on values of F for K^{+} and S^{+6} calculated using Stoner's distribution of electrons, and are probably too large (see previous footnote).

† See C. G. Darwin, *Phil. Mag.* xliii. p. 800 (1922), or Bragg, James, and Bosanquet (*loc. cit.* 3rd paper, p. 446) for explanation of primary and secondary extinction.

to be taken care of by ϕ_2 , and so reducing the range of variation of this function.

§ 7. *Summary.*

In the analysis of the more complicated crystal structures by means of X-rays, it is important to know the F-curves of the atoms concerned, *i. e.* the relations between the scattering power F of an atom, defined as the ratio of the amplitude of the wavelet scattered by the atom to that scattered by an electron, and the glancing angle. Assuming that the individual electrons of the atoms in a crystal scatter classically, the F-curve for any given atom can be calculated from the dimensions of and progress of time in the core orbits; for some atoms the atomic field can be found approximately by numerical analysis of the optical and X-ray spectra, and the core orbits can then be calculated; it is possible to generalize the results and put them in such a form that an approximate F-curve for any atom (or rather ion) can be calculated very simply. Numerical results for some ions are given.

XXX. *The Interpretation of Intensity Measurements in X-Ray Analysis of Crystal Structure.* [A Note on the paper "The Atomic Structure Factor in the Intensity of Reflexion of X-Rays by Crystals." by D. R. Hartree.]
By W. LAWRENCE BRAGG, M.A., *Langworthy Professor of Physics, The University of Manchester*.*

1. **I**N all methods of crystal analysis by means of X-rays, the final test of the structure which is assigned to the crystal as a result of the X-ray measurements consists in a comparison of the observed intensities of X-ray reflexion by different planes of the crystal structure with intensities which have been calculated for the proposed atomic arrangement. The structure which leads to the best agreement between calculated and observed values is chosen as the closest approximation to the truth. Anyone who is familiar with X-ray analysis will realize the unsatisfactory nature of the assumptions usually made in calculating the intensity of reflexion to be expected from a given atomic arrangement, and the uncertainty of the results due to an ignorance of the laws governing the intensity. Experimental observations can be made with a high order of accuracy, but their interpretation is extremely difficult. One

* Communicated by the Author.

factor which is highly important takes account of the amount of X-radiation scattered by the atoms through different angles. The assumption is generally made that the relative scattering powers of the atoms are simply proportional to their atomic numbers, but this approximation to the truth is only made in the lack of a more complete knowledge. The paper on the Atomic Structure Factor by Mr. Hartree is extremely interesting, because it gives estimates of the relative scattering power of the atoms based on calculation of orbit-dimensions. Although these estimates may need modification, and other factors which will be referred to below must be taken into consideration in using Mr. Hartree's results, they represent a great advance on the simple assumption of proportionality between scattering power and atomic number. They are extremely interesting in showing, for instance, how fast the effect of negative ions of low atomic weight falls off with increase in glancing angle, when they are compared with atoms of higher atomic weight.

2. The factors which govern the intensity of X-ray reflexion may for convenience be divided into two types. In the first of these must be classed all those factors which cause a general falling away of intensity as the angle of incidence increases. The exact forms which these factors assume depend on the method of analysis which is employed (spectrometer, Debye powder-photograph, rotating crystal method), as these different methods present different geometrical problems. They also depend on the shape of the crystal sample. For the spectrometer method this may be an extended crystal face, or a very small crystal which is bathed in the X-rays. In the powder method a fine column or an extended surface of powder may be employed. A factor must be introduced to represent the allowance for polarization of the scattered radiation. These factors are functions of the glancing angle θ .

In addition to this the intensity is governed by the structure factor S . This is generally defined as the ratio of the wave amplitude due to a complex plane of atoms when the phase difference introduced by atomic position has been taken into account, to the ideal amplitude which would exist were all the atoms centred exactly on the successive planes. It may perhaps be more conveniently defined as the ratio of the actual amplitude to that which would exist if all the electrons of all the atoms were arranged exactly on successive planes, since we are now allowing for electronic as well as for atomic configuration.

Any expression for the relationship between incident and diffracted radiation depends also on the wave-length of the X-rays employed, on the number of molecules per cubic centimetre, and the number of electrons in the molecule (if this be not already included in the structure factor S). In certain cases it depends on the absorption coefficient of the crystal, and this in its turn is a most complex function, being the sum of the true absorption coefficient μ and an extinction coefficient ϵ which varies with the state of perfection of the crystal structure and with the intensity of reflexion itself.

The Debye effect, or weakening of the spectra due to the heat-motion of the atoms, may perhaps be most conveniently considered as being included in the structure factor S , since its effect on the amplitude may be calculated by the laws of interference which govern the structure factor.

3. The two points about which most uncertainty exists are: (*a*) the correct method of calculating the structure factor S for any given atomic arrangement, (*b*) the relation of the intensity to the structure factor S . In certain cases it is possible to determine atomic positions accurately without making any precise assumptions about scattering power, and with the most approximate experimental determinations of intensity. This is the case for simple structures containing two or three parameters, which can often be evaluated one at a time by considering certain groups of planes, and it is also the case for structures of the elements where the atoms are all alike so that at any given angle they scatter equally. In more complex crystals it is absolutely necessary to make some assumptions in order to fix the atomic positions.

The following point must be emphasized in this connexion. Even though the dependence of intensity on structure factor is so very obscure, an accurate method of calculating the structure factor furnishes by itself a sufficient guide to the analysis of a structure. If the observed intensities show a parallelism to the calculated structure factors when both are arranged in order of increasing glancing angle, the assigned structure must be right. In comparing each plane with the next at a higher angle, a rise in structure factor should correspond to increased intensity, and a fall in structure factor to a decreased intensity. The absence of certain reflexions, which must be accounted for by a very small factor, is in particular a most important indication of

atomic position. The structure factor depends both on the positions of the atoms and on their scattering powers. Since it is so necessary to know this factor, Mr. Hartree's figures should prove most useful.

In the earlier work on X-ray analysis it was assumed that the intensity of reflexion varied as the square of the structure factor, other factors being equal. This assumption is still made in the analysis of the powder-photographs and of the Laue photographs, and it is probably justifiable in these cases. However, it has long been known as an empirical law that strong reflexions from faces of highly perfect crystals measured by the X-ray spectrometer were more nearly proportional to the structure factor itself*. The law seems to change from one expressed by " $I \propto S$ " to one expressed by " $I \propto S^2$," as one passes from the strong spectra of low order to the weak spectra of high order. Discussions of the intensity of reflexion by Darwin† and Ewald‡ suggest reasons for this. Both these authors agree in attributing a departure from the law " $I \propto S^2$ " to the fact that regions of the crystal are very highly perfect, so that there are sufficient planes in perfectly regular array to give complete reflexion of the X-rays over a short range of glancing angles. Darwin regards the existence of these small blocks of perfect crystal as giving rise to a high extinction coefficient, the underlying positions of the crystal not having an opportunity of playing their part in reflexion because the absorption of X-rays at the reflecting angle is abnormally large and the upper layers shield those beneath. Some experimental work on rock-salt§ made an estimate of the extinction coefficient ϵ possible, and it was found that

$$I \propto \frac{S^2}{\mu + \epsilon}$$

for this crystal, where the extinction factor ϵ is proportional to the intensity of reflexion I . In the case of rock-salt, which is a highly distorted crystal, ϵ was only about one-half the absorption coefficient μ for the strongest reflexion. In a more perfect crystal ϵ might be much larger than μ . In

* W. H. Bragg, *Phil. Trans. Roy. Soc.* See also 'X-Rays and Crystal Structure.'

† C. G. Darwin, *Phil. Mag.* xliii. (May 1922).

‡ P. P. Ewald, *Phys. Zeit.* xxvi. pp. 29-32 (1925).

§ Bragg, James, and Bosanquet, *Phil. Mag.* xlii. (July 1921).

this case the law

$$“I \propto \frac{S^2}{\mu + \epsilon}” \text{ may be written } “I \propto \frac{S^2}{\mu + \alpha I}”$$

where α is a constant. When I is large this becomes a law “ $I^2 \propto S^2$ ” or “ $I \propto S$.” When I is small it assumes the normal form “ $I \propto S^2$.”

Ewald shows that, when perfect reflexion of X-rays takes place over a short range, this range is proportional to the structure factor S , so that a highly perfect crystal should give rise to a law

$$I \propto S.$$

The number of perfectly-arranged planes which are necessary to give complete reflexion increases as I diminishes, so that a crystal which obeys Ewald's law for low orders might obey the law “ $I \propto S^2$ ” for the weaker reflexions of high order. This is again in agreement with experience.

These examples show how much caution must be exercised in comparing calculated and observed intensities of reflexion. One is on far surer ground in correlating structure factor and intensity by tabulating both in order of increasing glancing angle and seeing whether they rise and fall together. The necessary data for such a comparison are provided by any means of observing the intensity of reflexion by all planes of the crystal under equal conditions. With the spectrometer this is done, for instance, by comparing them all with some common standard.

5. In testing the figures for the scattering coefficient given in Hartree's paper, there are indications that the actual coefficients fall away rather more rapidly with increasing glancing angle than those which he gives. This may be partly or wholly due to the heat-motions of the atoms, for which no allowance has been made. Figures for sodium, chlorine, and oxygen given in the paper illustrate this point. Nevertheless, the author is convinced that these F -curves are a closer approximation to the truth than the assumption of a scattering power proportional to atomic number, and that with their help more reliable estimates of atomic configuration can be made.

XXXI. *X-Ray Analysis of Copper-Zinc, Silver-Zinc, and Gold-Zinc Alloys.* By ARNE WESTGREN and GÖSTA PHRAGMÉN*.

[Plates VI.-XI.]

1. THE CHEMICAL NATURE OF METALLIC PHASES.

INVESTIGATIONS on metallographic equilibrium diagrams are usually not considered to be complete if they do not result in stating which chemical compounds the phases found represent. This endeavour to label metallic phases by chemical formulæ has probably its root in the idea that it would be possible in this way to obtain a general survey of intermetallic reactions in the same way as order has been brought into other domains of chemistry by the use of chemical notation. As is well known, this attempt has led to little success, nothing except some rather vague rules concerning the intermetallic reactivity having been derived in this way †.

There are many causes for this failure. One of the most important is evidently that methods hitherto used to determine the chemical nature of metallic phases are inadequate, which is most clearly illustrated by the fact that different investigators examining the same system usually differ widely as to the statement of formulæ for the chemical compounds found. To quote an example, some authors have supposed γ -brass to be CuZn_{23} , while others believe that it is a solid solution of zinc in Cu_2Zn_3 ‡. To the γ -phases of the Ag-Zn and Au-Zn systems have been ascribed the formulæ Ag_2Zn_3 and Au_3Zn_5 . As will be seen in the following, all these formulæ are incorrect, as none of them is compatible with the fact that the elementary parallelepiped of the phases mentioned contains 52 atoms.

The difficulty in arriving at correct definitions of intermetallic compounds is evidently due to the fact that metal atoms may easily substitute each other in many lattices—*i. e.*, the solubility of the components in many metallic compounds is comparatively high. The domains of homogeneous phases are thus usually extended to relatively wide ranges of

* Communicated by the Authors.

† G. Tammann, *Lehrbuch der Metallographie*, 3. Aufl. Leipzig, 1923, p. 255.

‡ Unlike most investigators of the Cu-Zn system, S. Shepherd has restrained himself from proposing any formulæ for the Cu-Zn phases. He has taken the scientifically more valid standpoint of regarding all the Cu-Zn phases as solid solutions. *Journ. Phys. Chem.* viii. p. 421 (1904).

composition. In the case of an intermetallic compound dissolving very little or practically nothing of its components, its chemical formula is of course found as soon as its composition is established, but cases of this kind are so rare that they may be regarded almost as exceptional*.

As it might thus rightly be presumed that a great number, if not the majority, of the formulæ hitherto assigned to intermetallic compounds are wrong, it is no wonder that the attempt to find any laws governing intermetallic reactivity on the basis of these chemical symbols has met with little success.

In the following the authors will try to elucidate the question to what extent X-ray analysis may contribute to a deeper insight into the chemical nature of metallic phases. But before that topic is treated, it is necessary to discuss the fundamental question of the differences between solutions and chemical compounds in solid systems.

Different opinions have of late been expressed on this matter. It has been suggested that the term chemical compound loses its physical meaning in ranges of low temperatures, where no diffusion in solid systems is possible, and where thus the only movement of the atoms consists in vibrations about the points of the lattice†. This conception is evidently absurd as, according to this view, substances such as for instance aluminium oxide and sodium chloride would cease to be chemical compounds when cooled down to a sufficiently low temperature. It is highly improbable that at any temperature diffusion would take place within a NaCl-crystal in such a manner that a Na-atom would always move together with a Cl-atom, and yet solid sodium chloride is certainly a chemical compound. A definition of what is essential in solid chemical compounds is evidently not to be based on any assumptions concerning the mobility of their atoms.

W. Rosenhain‡ has recently put forth the hypothesis of the atoms being more intimately combined in intermetallic compounds than in solid solutions, which would bring about that the interatomic distances in the first-mentioned substances would differ markedly from the normal ones.

* During the examination of ten binary systems by means of X-rays the authors have met with few phases of this kind. The translation group has been determined for three of them, viz. FeSi_2 , CuAl_2 , and Fe_3C , the first two of these being tetragonal and the last one orthorhombic.

† G. Tammann, *loc. cit.* p. 832 (1923).

‡ 'Nature,' cxii. p. 832 (1923).

Confronted with reliable experimental facts, this view has, however, already turned out to be untenable. The distances between the atomic centres in intermetallic compounds do not seem to differ perceptibly from those in other crystals. Rosenhain's supposition has evidently its origin in the very common idea that the forces holding together atoms in an intermetallic compound are of another kind, or at least stronger than those acting between atoms in a pure metal or in a solid solution. The validity of this view has, however, never been proved. The bonds probably being non-polar in all cases, there seems to be no reason not to believe that the interatomic forces should be essentially the same in a solid solution as in a compound. They are certainly as "chemical" in the one case as in the other.

According to the authors' opinion, the fundamental difference between solid chemical compounds and solid solutions lies in their structure. *In an ideal chemical compound structurally equivalent atoms are chemically identical. In an ideal solid solution all atoms are structurally equivalent.* In the latter case some of the atoms of the solvent are replaced by atoms of another kind, which take the place of the former, and which are distributed quite irregularly in the parent lattice*.

Of these two extreme types of structures the first one seems to occur comparatively seldom in metallic phases, while the second one is met with frequently. A multitude of metallic phases seem, however, to represent an intermediate stage between these two extreme cases, forming what might be characterized as solid solutions in chemical compounds.

Comprehensive investigations on the corrodibility of binary solid solutions have led Tammann† to conclude that in the case of simple proportions between the atomic concentrations of the solute and the solvent the atoms of the former have a tendency to arrange themselves in a regular manner in the parent lattice of the solvent. This adjustment in the structure of solid solutions may, however, be expected to take place only if the alloys are annealed for a considerable time at a temperature just below the melting-point, where the mobility of the atoms is great enough to allow of their changing place.

* In exceptional cases this substitution may be of a *complex* nature (comp. Journ. Inst. Metals, xxxi. p. 204, 1924, and Journ. Iron & Steel Inst. cix. p. 171, 1924).

† G. Tammann, 'Mischkristallreihen und ihre Atomverteilung,' Leipzig, 1919

The X-ray testing of this hypothesis has led to contradictory results. Several investigators have failed to confirm it*. Bain† has, however, reported the discovery of some supernumerary interferences in the photograms of annealed gold-copper alloys containing 25 atomic per cent. gold or copper, and he thinks these might be explained according to the view of Tammann. Quite recently one of the present authors has also found that in a solid solution of 25 atomic per cent. of silicon in iron the silicon atoms are orientated in a face-centred cubic lattice of a parameter twice that of the body-centred α -iron lattice‡. At this composition the substituting silicon atoms are thus arranged in a regular manner, and the solid solution is transformed into the chemical compound Fe_3Si .

So far, it has not yet been made out how complete this rearrangement of the dissolved atoms in solid solutions may be, and it is still unknown whether its occurrence is confined only to some very narrow ranges of composition. Of course, it seems most probable, however, that, sometimes at least, the readjustment of the atoms may be only partial, and it takes place even if the composition differs a little from the values where it sets in most easily. This grouping of the atoms would thus also give rise to systems of a kind which, like so many other metallic phases, might be considered to form an intermediate stage between the two ideal structures defined above. A complete readjustment of the atoms causes the formation of an ideal chemical compound.

2. ANALOGIES BETWEEN DIFFERENT METALLIC SYSTEMS.

While examining alloys by means of X-rays§, the authors accidentally came across a very strange resemblance between a Cu-Al phase containing 31 atomic per cent. of aluminium and a Cu-Zn alloy holding about the same atomic percentage of copper||. The X-ray photograms, which were very

* P. Scherrer, *Compt. rend. Soc. suisse de Physique*, Schaffhausen, Aug. 27th, 1921. F. Kirchner, *Ann. d. Physik*, [4] lxii. p. 59 (1922). F. Wever, according to G. Tammann, *Ann. d. Physik*, [4] lxxv. p. 214 (1924). A. E. van Arkel, *Physica*, iv. p. 33 (1924).

† Chem. & Met. Eng. xxviii. p. 68 (1923).

‡ G. Phragmén, 'Stahl u. Eisen,' xlv. p. 299 (1925).

§ E. R. Jette, G. Phragmén, and A. F. Westgren, *Journ. Inst. Metals*, xxxi. p. 193 (1924).

|| Comp. 'Nature,' cxiii. p. 123 (1924), where X-ray photograms of these alloys are reproduced.

similar, proved that in both cases the substances were cubic and contained 52 atoms per elementary cube. One of the compounds thus corresponded to Cu_3Al_4 and the other to Zn_3Cu_4 .

Such analogies in structure between metallic phases of different composition are evidently common. Already the shape of the equilibrium diagrams gives in some cases evidence of a close relationship between different systems. H. C. H. Carpenter * has thus pointed out how similar the diagrams of the Cu-Zn, Ag-Zn, and Ag-Cd alloys are, and he has suggested an explanation of this fact by assuming an analogous formation of the different phases of these systems.

Problems of this kind might, of course, advantageously be penetrated by means of modern X-ray methods, and the authors have, therefore, in this way investigated the systems Cu-Zn, Ag-Zn, and Au-Zn, which could be supposed to show far-reaching analogies in structure. The melting-point curves and the state of these alloys at ordinary temperature as derived from microscopical examination and from X-ray analysis are schematically demonstrated in fig. 1.

The Cu-Zn diagram in that figure is in entire agreement with that given by S. Shepherd †. The investigation of Ag-Zn has confirmed the results of Carpenter ‡ with the exception that the decomposition of the β -phase into α and γ at about 260°C ., stated by him, has not been verified. The Cu-Zn and Ag-Zn systems have been found to be completely analogous; each phase found in one of them has been met with also in the other. All these phases with their different characteristic grouping of atoms recur also in the Au-Zn alloys, but in addition to these there have been found two more phases in the latter system. This is therefore a little more complicated than the other ones, which is in agreement with the Au-Zn diagram recently suggested by P. Saldau §. His diagram has not, however, as will be seen in the following, been verified in all respects.

The Cu-Zn and Ag-Zn alloys have already previously been the subject of some X-ray investigations. E. C. Bain || has determined the lattice dimensions of their α -phases, and

* *Intern. Zeitschr. f. Metallographie*, iii. p. 170 (1913).

† *Loc. cit.*

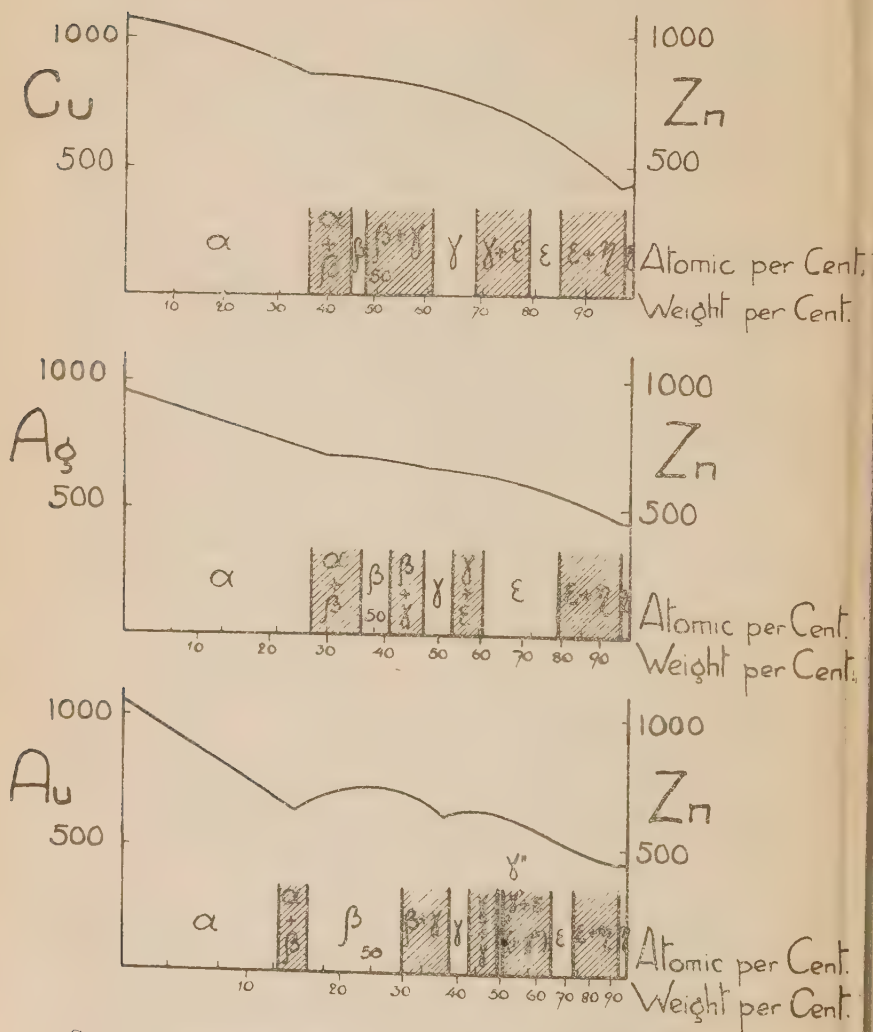
‡ *Intern. Zeitschr. f. Metallographie*, iii. p. 175 (1913).

§ *Journ. Inst. Metals*, xxx. p. 351 (1923).

|| *Chem. & Met. Eng.* xxviii. pp. 21, 65 (1923).

M. R. Andrews *, as well as E. A. Owen and G. D. Preston †, have analysed the Cu-Zn systems throughout its whole

Fig. 1.



Survey of the phases in the Cu-Zn, Ag-Zn, and Au-Zn systems.

* Phys. Rev. xxi. p. 245 (1921).

† Proc. Phys. Soc. Lond. xxxvi. p. 49 (1923). When the work of Owen and Preston was published, the authors had nearly finished their X-ray analysis of the Cu-Zn alloys.

range. The latter investigations are, however, incomplete as to the γ -brass, as Andrews has totally overlooked this phase, while Owen and Preston have not succeeded in determining its crystal form.

3. PREPARATION OF THE ALLOYS.

The metals used in the investigation were silver and gold containing more than 99.98 per cent. of the pure metal, electrolytic copper, and zinc from Kahlbaum. The meltings were made in porcelain crucibles in a carbon resistance furnace.

Because of their relative expensiveness, the gold alloy specimens could not be made larger than a few grammes. It was, however, found to be quite easy to get even those small meltings sound without using any protecting slag. The zinc mixed with gold was molten very cautiously, after which it dissolved the gold rapidly. At a certain state of dissolution a reaction suddenly occurred, through which an amount of heat was liberated, just sufficient to raise the temperature to a point where all the gold was solved. This practice made the loss of zinc through evaporation very small.

When a melting was finished, the crucible with its content was left to cool in the air. It is thus possible that the decrease in temperature in some cases was too rapid to give a state of the alloy corresponding to true equilibrium at ordinary temperature. As the chief purpose of the investigation was not, however, to control the boundary lines of the equilibrium diagrams but to make an examination of the crystal structure of the different phases of the systems, it was nevertheless considered that the alloys in most cases could be used without any further heat treatment.

The composition of the alloys was controlled by chemical determination of the copper, silver, or gold content. It differed only a few tenths of one per cent. from the percentages aimed at in the weighing together of the metals before melting.

4. EXPERIMENTAL ARRANGEMENTS.

The X-ray apparatus and most of the instruments used have been described in previous papers*. Some new cameras have, however, also been employed which were constructed on the basis of the focussing principle, introduced by H. Bohlin†. His camera type has the

* Journ. Iron & Steel Inst. cvi. p. 241 (1922); cix. p. 159 (1924). Journ. Inst. Metals, xxxi. p. 193 (1924).

† *Ann. d. Physik*, [4] lxi. p. 421 (1920).

advantage, over the ordinary arrangement for taking powder photograms, that it makes use of the radiation from a larger part of the focus on the target. A considerable increase in dispersion may thus be attained without lengthening the time of the exposure. Some Au-Zn photograms taken in one of these new cameras covering the diffraction range $33-62^\circ$ are reproduced in fig. 5 (Pl. IX.), and may there be compared with the corresponding photograms obtained in the ordinary camera. The dispersion in the former is about seven times as great as in the latter. Besides this precision camera, another new one of a similar kind has been used photographing the interferences in the range $59-113^\circ$. These Bohlén cameras have been calibrated empirically, whereby the fundamental spacing of rock-salt, $d = 5.628 \text{ \AA.}$, has been used as a basis*.

The mean error of the $\sin^2 \frac{\theta}{2}$ values (θ being the diffraction angle), derived from the precision photograms, might be estimated at ± 0.001 in the ranges $0.070-0.259$ and $0.636-0.987$, while it might be considered to be ± 0.002 in the range $0.259-0.636$. Being somewhat more uncertain, the $\sin^2 \frac{\theta}{2}$ values obtained from the ordinary powder photograms will be marked off by smaller types in the following.

All photograms except the Laue patterns have been taken with iron radiation ($\lambda K_{\alpha 1} = 1.932 \text{ \AA.}$; $\lambda K_{\alpha 2} = 1.934 \text{ \AA.}$; $\lambda K_{\beta} = 1.753 \text{ \AA.}$).

5. RESULTS OF THE X-RAY ANALYSIS.

The analogy between the three systems displays itself already at a glance at the series of photograms given in figs. 2-4 (Pls. VI.-VIII.). Every kind of diffraction pattern occurring in the Cu-Zn series is met with also in the other ones. Phases denoted in the same way must thus have an analogous structure.

A. The α -Phases.

The diffraction patterns of the α -alloys are all of the copper, silver, or gold type, and thus confirm that these phases represent solid solutions of zinc in these metals.

* M. Siegbahn, 'Spektroskopie der Röntgenstrahlen,' Berlin, 1924, p. 20.

Precision photograms of pure copper and of α -brass containing 32.2 per cent. zinc have been taken beside each other on one and the same plate * (Pl. X. fig. 6, I.). The displacement of the interferences caused by the larger volume of the substituting zinc atoms stands out very distinctly on this plate. The X-ray data obtained from this plate, together with those derived from precision photograms of pure gold and of pure silver, are given in Table I. h_1, h_2 , and h_3 denote the Miller indices, d_{100} the edge of the elementary cube, and I the relative intensity of the interferences. The latter is indicated with v.w.=very weak ; w.=weak ; m.=of medium strength ; st.=strong.

TABLE I.

Precision Photogram of Copper, α -Brass (32.2 per cent. Zn), Silver and Gold.

Substance.	I.	$\sin^2 \frac{\theta}{2}$.	Radiation.	$h_1 h_2 h_3$.	$\sin \frac{\theta}{2}$ $\sqrt{h_1^2 + h_2^2 + h_3^2}$.	d_{100} in Å.
Copper.	m.	0.6485	$K\beta$	311	0.05895	3.610
	v.w.	0.7075	$K\beta$	222	0.05896	
	st.	0.789	$K\alpha$	311	0.07173	
	m.	0.861	$K\alpha$	222	0.07175	
α -Brass containing 32.2 % Zn.	st.	0.7575	$K\alpha$	311	0.06868	3.688
	m.	0.826	$K\alpha$	222	0.06883	
Silver.	st.	0.6745	$K\alpha$	222	0.05621	4.080
	m.	0.8765	$K\beta$	331	0.04613	
	m.	0.8985	$K\alpha$	400	0.05615	
	m.	0.923	$K\beta$	420	0.04615	
Gold.	st.	0.678	$K\alpha$	222	0.05633	4.073
	m.	0.8805	$K\beta$	331	0.04634	
	m.	0.902	$K\alpha$	400	0.05638	
	m.	0.9255	$K\beta$	420	0.04628	

The average weight of the atoms constituting the α -brass investigated is $64.14 \cdot 1.650 \cdot 10^{-24}$ g. ($1.650 \cdot 10^{-24}$ g. being the weight of an atom with the atomic weight 1); the density of the alloy determined by weighing in the air and in water has been found to be 8.45, and its lattice parameter is 3.688 Å. (Å.= 10^{-8} cm.). If the number of atoms per elementary cube is calculated on the basis of these data, the number 4.009 is obtained, *i. e.* four within the limits of error. The statement of previous investigators is thus

* Comp. Journ. Inst. Metals, xxxi. p. 202 (1924).

confirmed that α -brass is formed by a simple substitution of copper by zinc atoms.

The dissolving of 32 per cent. zinc into copper causes an increase in the lattice parameter from 3.610 Å. to 3.688 Å., *i.e.* about 2 per cent. The powder photograms of the corresponding Ag-Zn and Au-Zn phases indicate that the lattices of these alloys are somewhat smaller than the lattices of silver and gold. The zinc atoms are evidently considerably "larger" than the copper atoms, but slightly "smaller" than the gold and silver atoms.

It was considered useless to take precision photograms of the α -Ag-Zn and α -Au-Zn alloys, as their interferences were found to be very cloudy. The real cause of this diffuseness of the lines still remains to be unravelled. Attention might also be drawn to the fact that not even the pure metals—copper, silver, or gold—have given precision photograms of the same distinctness as other substances, such as, for instance, iron or aluminium*. The most deviated K_{α} -interferences of the latter metals are easily resolved into distinct doublets, but in the precision photograms of Cu, Ag, and Au the $K_{\alpha 1}$ and $K_{\alpha 2}$ lines flow together.

Saldau has found a maximum in the electrical conductivity of the Au-Zn alloys at a composition of 25 atomic per cent. Zn, and from the fact that this maximum shifts at 250° C., he concludes that a transformation takes place at this temperature giving rise to a phase corresponding to the compound Au_3Zn . In order to produce this phase, an alloy having the composition of Au_3Zn was annealed during 10 hours at 250° C.

The powder photogram of the annealed specimen turned out to be exactly identical with that of the unannealed α -phase, and thus did not indicate the existence of any compound Au_3Zn †.

According to previous determinations, the lattice of gold should be somewhat larger than that of silver. Already the ordinary powder photograms indicate, however, and comparative precision photograms have proved conclusively, that the contrary is right. Wh. P. Davey‡ has recently stated that the lattice parameters of silver and gold are 4.058 ± 0.004 and 4.076 ± 0.004 Å. respectively. The values found by the authors are, however, for silver 4.080 Å., and

* See Jette, Phragmén, and Westgren, *loc. cit.* p. 200, pl. xviii. V.

† *Note to the proof.*—The authors have later found that an Au-Zn alloy containing about 25 atomic per cent. zinc undergoes a phase change when annealed in a *cold-worked* state.

‡ Phys. Rev. [2] xxiii. p. 292 (1924).

for gold 4.073 \AA . Their mean error might be estimated at $0 \pm 0.003 \text{ \AA}$. It seems probable that the silver investigated by Davey has not been quite free from copper.

B. The β -Phases.

Andrews, as well as Owen and Preston, have stated that β -brass has a body-centred cubic structure. The powder photogram of this phase obtained by the authors is in fair agreement with that statement. A thin plate was, however, also cut out of a coarse-grained β -brass sample and examined according to the Laue method. When the incident rays were parallel to $[100]$, a Laue pattern (Pl. XI. fig. 7, I.) was produced showing tetragonal symmetry, and when the primary X-ray beam was parallel to $[111]$ a photogram of trigonal symmetry was obtained. As the Cu- and Zn-atoms differ very little in diffractive power, it cannot be settled from the X-ray data if β -brass is to be regarded as an ideal solid solution or not. The powder photograms of β -Ag-Zn and β -Au-Zn prove, however, that the elementary cube in this case is primitive. The relative intensity of the interferences agrees with that calculated on the assumption that the lattice is built up of two simple cubic lattices centring each other (CsCl-structure). It is thus constituted of two groups of atoms, structurally inequivalent, and the β -phases might accordingly be considered to form solid solutions having the compounds CuZn, AgZn, and AuZn for bases.

As to β -brass, this conclusion may, of course, be drawn only if it is presumed that its structure is analogous to that of β -Ag-Zn and β -Au-Zn, but there is no reason to believe anything else. There is thus very little reason for the opinion recently expressed by Rosenhain* that β -brass might be regarded as a solid solution of zinc in a body-centred cubic modification of copper. It is very improbable that β -brass is an ideal solid solution.

Though it might thus be taken almost for granted that β -brass has the compound CuZn as a basis, an alloy of this composition is not homogeneous at ordinary temperature, but consists of a mixture of γ -brass and a phase, corresponding to CuZn, where about 5 per cent. of the zinc atoms are substituted by copper atoms. To form a β -brass that is homogeneous and stable at ordinary temperatures it is thus necessary that a few per cent. of copper are dissolved into CuZn.

* Journ. Inst. Metals, xxx. p. 23 (1923).

TABLE II.—Powder Photographs of the β -Phases.

Alloy.	I.	$\sin^2 \frac{\theta}{2}$.	Radiation.	$h_1 h_2 h_3$.	$\frac{\sin^2 \frac{\theta}{2}}{h_1^2 + h_2^2 + h_3^2}$.	d_{100} in Å.	Density.	Average Atomic Weight.	Number of Atoms per Elementary Cube.
Cu-Zn 46.9 per cent. Zn.	m.	0.174	K_β	110	0.087	2.945	8.32	64.40	2.000
	st.	0.214	K_α	110	0.107				
	w.	0.355	K_β	200	0.0888				
	st.	0.4305	K_α	200	0.1076				
	m.	0.534	K_β	211	0.0890				
	st.	0.6435	K_α	211	0.1073				
	w.	0.704	K_β	220	0.088				
	st.	0.858	K_α	220	0.107				
	v.w.	0.093	K_α	100	0.093				
	w.	0.154	K_β	110	0.077				
Ag-Zn 38.25 per cent. Zn.	st.	0.187	K_α	110	0.093	3.156	9.10	86.39	2.007
	v.w.	0.202	K_β	111	0.077				
	w.	0.281	K_α	111	0.0937				
	m.	0.310	K_β	200	0.0775				
	st.	0.375	K_α	200	0.0938				
	m.	0.463	K_β	211	0.0772				
	w.	0.470	K_α	210	0.0740				

Au-Zn 30.2 per cent. Zn.	st.	0.5635	K_{α}	211	0.0939	3.146 13.12 123.73 2.001	
	v.w.	0.622	K_{β}	220	0.078		
	st.	0.754	K_{α}	220	0.094		
	w.	0.777	K_{β}	310	0.078		
	w.	0.848	K_{α}	$\left\{ \begin{smallmatrix} 300 \\ 221 \end{smallmatrix} \right\}$	0.094		
	v.w.	0.931	K_{β}	222	0.078		
	st.	0.945	K_{α}	310	0.094		
	v.w.	0.077	K_{β}	100	0.077		
	m.	0.093	K_{α}	100	0.093		
	m.	0.155	K_{β}	110	0.078		
st.	0.189	K_{α}	110	0.095			
w.	0.2835	K_{α}	111	0.0945			
v.w.	0.313	K_{β}	200	0.078			
st.	0.3795	K_{α}	200	0.0949			
st.	0.470	K_{α}	210	0.0940			
st.	0.568	K_{α}	211	0.0947			
w.	0.624	K_{β}	220	0.078			
st.	0.758	K_{α}	220	0.094			
st.	0.850	K_{α}	$\left\{ \begin{smallmatrix} 300 \\ 221 \end{smallmatrix} \right\}$	0.094			
st.	0.945	K_{α}	310	0.095			

The Laue investigation of the large β -brass grains has proved that they are real crystal individuals. As already stated by H. Imai *, as well as by Owen and Preston, it is therefore very improbable that the thermal effect observed in β -brass at about 470°C. † should be caused by any polymorphic change. The same seems to be the case as to the analogous phenomenon in $\beta\text{-Ag-Zn}$ observed by Carpenter ‡. In any case, the thermal effect in this phase at 260°C. can hardly be explained in the way suggested by him—*i. e.*, by a splitting-up of β into α and γ at this temperature. An AgZn alloy of a composition corresponding to AgZn (41 per cent. Zn) was annealed for 10 hours at 250°C. The powder photogram of this specimen was, however, quite like the photogram of the same alloy quenched in water from the liquid state, and it is thus proved that no crystallographic change had taken place at annealing.

The compound AuZn has a greater capacity than AgZn and CuZn of keeping either of its components in solution at ordinary temperature; for instance, an alloy containing 30.2 per cent. Zn has a homogeneous β -structure. This alloy may thus be considered to be AuZn (25 per cent. Zn), in which every fifth gold atom is replaced by a zinc atom. In spite of the very considerable divergence from the ideal CsCl-structure, the interferences in the powder photogram of this alloy (Pl. VIII. fig. 4, V.) are quite distinct; even those fainter K_{α} -lines which are caused by the difference in reflective power between the gold and the zinc atoms are plainly visible.

X-ray data of the β -phases are given in Table II.

C. The γ -Phases.

A sliver, cut out of a coarse-grained γ -brass specimen (65 per cent. Zn) was investigated according to the Laue method. One of the photograms obtained showed tetragonal (Pl. XI. fig. 7, II.) and another one trigonal symmetry. They both proved that γ -brass is cubic (T_d , O_c , or O_h) and has a lattice parameter of about 9\AA .

The sliver was also mounted in a camera for taking rotation photograms§, and while rotating round one of its

* Science Reports, Tohoku Imp. Univ. xi. no. 5, p. 313 (1922).

† Carpenter & Edwards, Journ. Inst. Metals, v. p. 127 (1911). O. F. Hudson, Journ. Inst. Metals, xii. p. 89 (1914).

‡ *Loc. cit.* p. 159.

§ Journ. Iron & Steel Inst. cix. p. 161 (1924).

tetragonal axes, it was illuminated by a narrow beam of iron radiation. The diffraction pattern obtained (Pl. XI. fig. 7, III.) contains 81 interference spots (K_α - and K_β -interferences), all in perfect agreement with the equations:

$$\sin^2 \frac{\theta}{2} = 0.0119 (h_1^2 + h_2^2 + h_3^2) \dots (K_\alpha),$$

$$\sin^2 \frac{\theta}{2} = 0.0098 (h_1^2 + h_2^2 + h_3^2) \dots (K_\beta).$$

The relative intensity and the indices of the interferences observed in the rotation photograph are given in Table III.

TABLE III.

Photogram of a γ -Brass Crystal rotating about [001].

I.	$h_1 h_2 h_3$.	I.	$h_1 h_2 h_3$.	I.	$h_1 h_2 h_3$.	I.	$h_1 h_2 h_3$.	I.	$h_1 h_2 h_3$.
st.	330	w.	321	st.	222	w.	123	w.	224
w.	420	st.	411	w.	312	st.	303	st.	424
m.	510	w.	501	v.w.	402	st.	323	st.	444
v.w.	440	w.	521	m.	332	v.w.	433	w.	534
st.	600	m.	611	m.	422	v.w.	523	w.	604
st.	550	m.	631	w.	512	st.	613	w.	624
m.	640	st.	721	m.	442	w.	543	st.	{ 554 ?
m.	730	w.	651	v.w.	532	st.	633		{ 714
m.	800	st.	{ 811 ?	st.	712	w.	703		
st.	820	w.	831	w.	642	m.	733		
st.	660	st.	841	m.	732	m.	653		
w.	750	st.	941	m.	802	m.	813		
m.	840			st.	822	st.	843		
st.	910			st.	662				
				st.	752				

The γ -phases of the three zinc alloys resemble each other strikingly, and are also very like the phase occurring in the range 16 to 25 per cent. aluminium in the copper-aluminium alloys. All these substances are extremely brittle and have a vitreous and lustrous fracture. This likeness is evidently due to a similar grouping of their atoms. The X-ray data, obtained from the powder photographs of γ -brass, γ -Ag-Zn, and γ -Au-Zn are set out in Tables IV. and V.

TABLE IV.—Powder Photographs of γ -Brass.

I.	$h_1 h_2 h_3$	61.7 per cent. Zn.		64.7 per cent. Zn.		67.7 per cent. Zn.	
		$\sin^2 \frac{\theta}{2}$	$\frac{\sin^2 \frac{\theta}{2}}{h_1^2 + h_2^2 + h_3^2}$	$\sin^2 \frac{\theta}{2}$	$\frac{\sin^2 \frac{\theta}{2}}{h_1^2 + h_2^2 + h_3^2}$	$\sin^2 \frac{\theta}{2}$	$\frac{\sin^2 \frac{\theta}{2}}{h_1^2 + h_2^2 + h_3^2}$
w.	222 K_β	0.114	0.0095	0.117	0.0093	0.116	0.0097
w.	222	0.142	0.0118	0.142	0.0118	0.144	0.0120
w.	321	0.164	0.0117	0.164	0.0117	0.166	0.0119
st.	{ 411 K_β	0.173	0.0096	0.173	0.0096	0.177	0.0098
	{ 330						
st.	{ 411	0.211	0.0117	0.212	0.0118	0.214	0.0119
	{ 330						
v.w.	420	0.230	0.0115	0.236	0.0118	0.233	0.0117
m.	332	0.264	0.01200	0.263	0.01195	0.261	0.0119
w.	422	0.2865	0.01194	0.285	0.01187	0.284	0.0118
w.	510	0.310	0.01192	0.310	0.01192	0.309	0.0119
	{ 442 K_β	0.3545	0.00985	0.353	0.00981	0.352	0.0098
w.	{ 600						
st.	{ 442	0.4315	0.01199	0.4305	0.01196	0.426	0.0118
	{ 600						
w.	{ 532	0.453	0.01192	0.453	0.01192	0.452	0.0119
	{ 611						

v.w.	444 K β	0.473	0.00985	0.473	0.00985	0.471	0.0118
w.	{ 633 K β	0.5315	0.00984	0.5295	0.00980	0.524	0.0097
w.	721	0.548	0.01191	0.547	0.01189	0.550	0.0120
m.	631	0.5735	0.01195	0.570	0.01187	0.572	0.0119
w.	444	0.5965	0.01193	0.5955	0.01191	0.596	0.0119
st.	550	0.6455	0.01195	0.6435	0.01192	0.642	0.0119
v.w.	{ 633	0.670	0.01195	0.669	0.0119	0.6625	0.01183
v.w.	721	0.707	0.01198	0.704	0.0119	0.734	0.01184
w.	642	0.739	0.01192	0.741	0.0120	0.781	0.01183
st.	{ 822 K β	0.788	0.01192	0.789	0.0120	0.8055	0.01185
w.	660	0.811	0.01193	0.809	0.0119	0.8285	0.01184
v.w.	{ 651	0.834	0.01192	0.834	0.0119	0.851	0.01182
st.	732	0.8595	0.01194	0.859	0.0120	0.8765	0.01184
w.	{ 554 ?	0.8835	0.01194	0.882	0.0119	0.902	0.01187
v.w.	741	0.906	0.01192	0.909	0.0120	0.9255	0.01187
st.	{ 811 ?	0.9305	0.01193	0.930	0.0119		
w.	{ 644 ?						
v.w.	820						
st.	{ 653						
w.	822						
v.w.	{ 660						
st.	750						
w.	{ 831						
v.w.	662						
v.w.	752						

TABLE V.—Powder Photographs of γ -Ag-Zn and γ -Au-Zn.

Ag-Zn. 50.3 per cent. Zn.			Au-Zn. 41.1 per cent. Zn.			
I.	$h_1 h_2 h_3$.	$\sin^2 \frac{\theta}{2}$.	$\sin^2 \frac{\theta}{2}$.	$\frac{\sin^2 \frac{\theta}{2}}{h_1^2 + h_2^2 + h_3^2}$.	$\sin^2 \frac{\theta}{2}$.	$\frac{\sin^2 \frac{\theta}{2}}{h_1^2 + h_2^2 + h_3^2}$.
v.w.	$\begin{Bmatrix} 211 \\ 210? \end{Bmatrix}$	0.056	0.065	0.0108	0.066	0.0110
v.w.	211	0.067			0.088	0.0110
w.	222	0.131	0.160	0.0089	0.164	0.0091
m.	$\begin{Bmatrix} 411 \\ 330 \end{Bmatrix}$	0.160	0.194	0.0108	0.200	0.0111
st.	$\begin{Bmatrix} 411 \\ 330 \end{Bmatrix}$	0.195			0.221	0.0111
w.	332	0.239	0.236	0.0107	0.241	0.0109
w.	422	0.259	0.2615	0.01090	0.265	0.01103
v.w.	510	0.2785	0.2835	0.01090	0.285	0.01094
w.	$\begin{Bmatrix} 442 \\ 600 \end{Bmatrix}$	0.3175	0.323	0.00897	0.326	0.00906
w.	440	0.342	0.3395	0.00894	0.342	0.00901
st.	$\begin{Bmatrix} 442 \\ 600 \end{Bmatrix}$	0.389			0.354	0.01103
w.	$\begin{Bmatrix} 532 \\ 611 \end{Bmatrix}$	0.4095	0.3915	0.01088	0.374	0.01100
					0.3975	0.01102

v.w.	444 K_{β}	0.424	0.00883	st.	{ 532 611	0.414	0.01090	0.420	0.1103
v.w.	{ 621 540 ?	0.4415	0.01077	w.	444 K_{β}	0.4295	0.00895	0.433	0.0903
v.w.	541	0.453	0.01078	v.w.	541			0.463	0.01101
v.w.	533	0.464	0.01079	m.	{ 633 K_{β} 721	0.482	0.00893	0.487	0.0902
m.	{ 633 K_{β} 721	0.476	0.00881	w.	631			0.505	0.01098
w.	631	0.4935	0.01073	st.	444	0.5215	0.01086	0.527	0.01097
m.	444	0.515	0.01073	m.	{ 710 ? 550	0.543	0.01086	0.550	0.01100
w.	{ 710 550 ?	0.537	0.01074	st.	{ 633 721	0.5875	0.01088	0.595	0.01101
v.w.	{ 641 720 ?	0.569	0.01074	w.	642			0.618	0.01102
st.	{ 633 721	0.580	0.01074	st.	{ 554 ? 741 811 ?	0.718	0.01088	0.726	0.0110
st.	{ 554 ? 741 811 ?	0.709	0.01074	st.	{ 644 ? 820	0.738	0.0108	0.750	0.0110
w.	{ 644 ? 820	0.736	0.0108	m.	{ 822 660	0.782	0.0109	0.792	0.0110
st.	{ 822 660	0.745	0.01076	m.	662			0.835	0.0110
w.	662	0.819	0.0107	m.	752			0.858	0.0110
				w.	840			0.884	0.0110
				m.	744 ?			0.893	0.0110
				m.	?			0.945	

The values of the lattice parameters derived from the precision photograms are given in Table VI., together with the data necessary for determining the number of atoms per elementary cube.

TABLE VI.

Lattice Dimensions and Number of Atoms per Elementary Cube in the γ -Phases.

Alloy.	Per cent. Zn.	Average Atomic weight.	Density.	d_{100} in A.	Number of Atoms per elementary cube.
Cu-Zn ...	61.7	64.67	8.04	8.850	52.22
Cu-Zn ...	64.7	64.72	7.99	8.861	52.05
Cu-Zn ...	67.7	64.78	7.92	8.887	52.02
Ag-Zn ...	50.3	81.29	8.66	9.327	52.37
Au-Zn ...	36.9	113.07	12.25	9.268	52.27
Au-Zn ...	41.1	107.71	11.76	9.223	51.96

As might be gathered from the table, and also from the comparative precision photograms reproduced in fig. 6, II. (Pl. X.), the lattice dimensions of γ -brass increase in size with rising content of zinc. The lattice of γ -Au-Zn, however, becomes smaller the more zinc it contains. The lattice dimensions of the γ -phases change in the same way as they do in the α -phases, and corresponding to what might be expected if copper and gold atoms are replaced by zinc atoms one by one. The substitution seems to be *simple*. This is conclusively proved by the fact that exactly the same number of atoms per elementary cube, viz. 52, has been found in all the γ -phases investigated.

These 52 atoms cannot be structurally equivalent, and accordingly the γ -phase must be regarded as a solid solution in a chemical compound. It is impossible, however, to state definitely what formula this compound has, as long as nothing is known concerning the function of the atoms in the lattice. The only way of dividing the 52 atoms into two groups of structurally equivalent atoms is obviously in the proportion of 4 to 48. That leads up to formulæ of the types AB_{12} and $A_{12}B$, but such compounds can hardly be the bases of the γ -phases, as they fall far out of the composition range of the phases. The atoms within the elementary cube must thus be composed of at least three

groups of structurally equivalent individuals. As there is a great number of combinations of that kind possible, and as it is unknown which of them corresponds to reality, it is impossible as the case now stands to find out the bases of the γ -phases.

By way of conjecture, the formulæ Cu_4Zn_9 , Ag_4Zn_9 , and Au_4Zn_9 may, however, possibly be suggested, as they correspond to compositions coinciding with one of the homogeneous γ -phase ranges*.

D. The ϵ - and η -Phases.

As all attempts to obtain a single crystal of any of the ϵ -phases failed, the determination of their structure had to be carried out by means of powder photograms only. Generally this procedure is not as reliable as the investigation of crystal individuals, but in this case there are very good reasons to believe that the results obtained are trustworthy.

The photograms were all very simple, and compared with the graphs of A. W. Hull and Wh. P. Davey †, they proved to be of the type corresponding to a close-packed hexagonal lattice, having an axial ratio of about 1.6. This confirms the statement of Owen and Preston concerning the structure of ϵ -brass. But as zinc and copper atoms differ very little in diffractive power, Owen and Preston were not able to decide if the two kinds of atoms in ϵ -brass were orientated in lattices of their own or if they were irregularly mixed in a common lattice; they considered it possible that the elementary parallelepiped of ϵ -brass actually was larger than indicated by the photogram. As, however, diffraction patterns of the ϵ -phases of the Ag-Zn and Au-Zn systems are quite like that of ϵ -brass, being both of the type corresponding to an element of close-packed hexagonal structure, it can hardly be doubted that the ϵ -phases are to be regarded as ideal solid solutions.

As might be expected, the η -phases were found to have the structure of zinc, being close-packed hexagonal with an axial ratio of about 1.9. These phases must be considered to be solid solutions of copper, silver, and gold in zinc.

The lattice of the ϵ - and η -phases would thus be of the same kind, only differing as to their axial ratios. As is well known, the close-packed hexagonal elements may be divided into two groups, one having the axial ratio of about 1.9

* This is also the case with the γ' -phase of the Cu-Al systems, which accordingly would represent a solid solution in the compound Cu_3Al_4 . Comp. Jette, Phragmén, and Westgren, *loc. cit.* p. 204.

† Phys. Rev. xvii. p. 549 (1921).

(the Zn-type), and the other an axial ratio of about 1.6 (the Mg-type). When the atoms of a zinc lattice are substituted by copper, silver, or gold atoms to a sufficient extent, the lattice is thus changed from the first of these types to the other. As pointed out by Hull, the first of these lattices may be considered to be built up of atoms having the form of prolate spheroids and the other one may be regarded as formed of spheres or slightly flattened spheroids.

The $\sin^2 \frac{\theta}{2}$ values obtained from precision photograms of the ϵ - and η -phases are given in Tables VII.-X. The

TABLE VII.

Precision Photograms of ϵ -Ag-Zn.

I obs.	I comp.	Radiation.	$h_1 h_2 h_3 h_4$.	60.5 per cent. Zn.		78.1 per cent. Zn.	
				$\sin^2 \frac{\theta}{2}$ obs.	$\sin^2 \frac{\theta}{2}$ comp.	$\sin^2 \frac{\theta}{2}$ obs.	$\sin^2 \frac{\theta}{2}$ comp.
w.	...	K_β	10 $\bar{1}0$	0.130	0.129	0.130	0.129
m.	...	K_β	0002	0.155	0.155	0.159	0.160
m.	3	K_α	1010	0.157	0.157	0.1565	0.157
m.	...	K_β	10 $\bar{1}1$	0.168	0.168	0.169	0.169
st.	4	K_α	0002	0.189	0.188	0.194	0.195
st.	18	K_α	10 $\bar{1}1$	0.204	0.204	0.206	0.206
w.	...	K_β	10 $\bar{1}2$	0.2835	0.284	0.289	0.289
st.	6	K_α	10 $\bar{1}2$	0.346	0.345	0.351	0.352
w.	...	K_β	11 $\bar{2}0$	0.3865	0.387	0.388	0.388
st.	12	K_α	11 $\bar{2}0$	0.470	0.471	0.471	0.472
m.	...	K_β	10 $\bar{1}3$	0.477	0.477	0.488	0.489
w.	...	K_β	11 $\bar{2}2$	0.541	0.542	0.546	0.548
v.w.	...	K_β	20 $\bar{2}1$	0.554	0.555	0.5575	0.557
st.	18	K_α	10 $\bar{1}3$	0.580	0.581	0.595	0.596
w.	3	K_α	20 $\bar{2}0$	0.630	0.629	0.629	0.629
st.	24	K_α	11 $\bar{2}2$	0.6595	0.659	0.6675	0.667
st.	18	K_α	20 $\bar{2}1$	0.675	0.675	0.678	0.678
m.	4	K_α	0004	0.754	0.754	0.779	0.779
m.	6	K_α	20 $\bar{2}2$	0.817	0.816	0.824	0.824
w.	...	K_β	20 $\bar{2}3$	0.864	0.864	0.877	0.877
m.	6	K_α	10 $\bar{1}4$	0.910	0.911	0.9365	0.937

TABLE VIII.

Precision Photograms of ϵ -Brass.

I obs.	Radiation.	$h_1 h_2 h_3 h_4$.	80.3 per cent. Zn.		86.1 per cent. Zn.	
			$\sin^2 \frac{\theta}{2}_{\text{obs.}}$	$\sin^2 \frac{\theta}{2}_{\text{comp.}}$	$\sin^2 \frac{\theta}{2}_{\text{obs.}}$	$\sin^2 \frac{\theta}{2}_{\text{comp.}}$
m.	K_{β}	10 $\bar{1}$ 2	0.302	0.303	0.301	0.301
st.	K_{α}	10 $\bar{1}$ 2	0.368	0.368	0.367	0.367
w.	K_{β}	11 $\bar{2}$ 0	0.408	0.408	0.4025	0.403
st.	K_{α}	11 $\bar{2}$ 0	0.4955	0.496	0.491	0.491
m.	K_{β}	10 $\bar{1}$ 3	0.511	0.511	0.5105	0.510
w.	K_{β}	11 $\bar{2}$ 2	0.576	0.575	0.570	0.570
v.w.	K_{β}	20 $\bar{2}$ 1	0.5855	0.586	0.579	0.579
st.	K_{α}	10 $\bar{1}$ 3	0.6215	0.622	0.6215	0.622
w.	K_{α}	20 $\bar{2}$ 0	0.662	0.661	0.6555	0.655

TABLE IX.

Precision Photograms of ϵ -Au-Zn.

I obs.	Radiation.	$h_1 h_2 h_3 h_4$.	67.5 per cent. Zn.		72.3 per cent. Zn.	
			$\sin^2 \frac{\theta}{2}_{\text{obs.}}$	$\sin^2 \frac{\theta}{2}_{\text{comp.}}$	$\sin^2 \frac{\theta}{2}_{\text{obs.}}$	$\sin^2 \frac{\theta}{2}_{\text{comp.}}$
m.	K_{β}	10 $\bar{1}$ 2	0.289	0.290	0.290	0.291
st.	K_{α}	10 $\bar{1}$ 2	0.353	0.353	0.353	0.354
w.	K_{β}	11 $\bar{2}$ 0	0.389	0.389	0.389	0.389
st.	K_{α}	11 $\bar{2}$ 0	0.474	0.474	0.474	0.474
w.	K_{β}	10 $\bar{1}$ 3	0.490	0.490	0.4915	0.492
w.	K_{β}	11 $\bar{2}$ 2	0.5495	0.549	0.5495	0.550
v.w.	K_{β}	20 $\bar{2}$ 1	0.559	0.559	0.5585	0.559
st.	K_{α}	10 $\bar{1}$ 3	0.5975	0.597	0.599	0.599
w.	K_{α}	20 $\bar{2}$ 0	0.632	0.632	0.632	0.632
st.	K_{α}	11 $\bar{2}$ 2	0.6695	0.669	0.6695	0.670
w.	K_{α}	20 $\bar{2}$ 1	0.680	0.681	0.6805	0.681
	K_{β}	20 $\bar{2}$ 2		0.679		0.680

TABLE X.

Precision Photographs of Zinc, η -Brass, and η -Au-Zn.

I.	Radiation.	$h_1h_2h_3h_4$.	Zinc.		Au-Zn, 95.0% Zn.		Cu-Zn, 96.5% Zn.	
			$\sin^2 \frac{\theta}{2}_{\text{obs.}}$	$\sin^2 \frac{\theta}{2}_{\text{comp.}}$	$\sin^2 \frac{\theta}{2}_{\text{obs.}}$	$\sin^2 \frac{\theta}{2}_{\text{comp.}}$	$\sin^2 \frac{\theta}{2}_{\text{obs.}}$	$\sin^2 \frac{\theta}{2}_{\text{comp.}}$
m.	K_β	10 $\bar{1}2$	0.271	0.271	0.273	0.273		
st.	K_α	10 $\bar{1}2$	0.329	0.329	0.331	0.331		
w.	K_β	10 $\bar{1}3$	0.428	0.428		0.430		
					0.432			
w.	K_β	11 $\bar{2}0$	0.434	0.434		0.433		
st.	K_α	10 $\bar{1}3$	0.520	0.521		0.523		
					0.525			
st.	K_α	11 $\bar{2}0$	0.528	0.528		0.526		
w.	K_β	11 $\bar{2}2$	0.560	0.560	0.559	0.559		
v.w.	K_β	20 $\bar{2}0$	0.578	0.578				
w.	K_β	20 $\bar{2}1$	0.610	0.610	0.606	0.605		
st.	K_α	11 $\bar{2}2$	0.681	0.681	0.680	0.680	0.6815	0.681
w.	K_α	20 $\bar{2}0$	0.704	0.704	0.697	0.697	0.7015	0.702
st.	K_α	20 $\bar{2}1$	0.742	0.742	0.737	0.736	0.740	0.740
w.	K_α	10 $\bar{1}4$	0.789	0.789	0.801	0.802		
st.	K_α	20 $\bar{2}2$	0.858	0.858	0.854	0.854	0.856	0.856

values of the intensity $I_{\text{comp.}}$, given in Table VII., are deduced from the product of the relative occurrence of the reflecting planes and the factor of structure.

In fig. 6, III. (Pl. X.) comparative photographs are reproduced of two Ag-Zn alloys, one containing 60.5 per cent. Zn, and the other 78.1 per cent. Zn. It may be seen in this figure how the interferences of these hexagonal substances are displaced unequally when the composition of the phase is changed.

The lattice dimensions vary as the zinc is substituted by silver, but the two parameters of the lattice are not altered in the same proportion. In spite of this considerable and unequal change in the $\sin^2 \frac{\theta}{2}$ values with varying composition, the diffraction angles of the different ϵ -phases always satisfy

an equation of the type corresponding to a hexagonal lattice :

$$\sin^2 \frac{\theta}{2} = \frac{\lambda^2}{3a_1^2}(h_1^2 + h_1h_2 + h_2^2) + \frac{\lambda^2}{4a_4^2}h_4^2.$$

where λ is the wave-length, and a_1 and a_4 are the side and height respectively of the elementary prism.

This perfect agreement forms the most important support for the conception that the ϵ -phases have a hexagonal structure.

The intensity values observed agree with those computed for a close-packed hexagonal lattice, with the exception that for some of the alloys the reflexions against the basal planes show up a little stronger than expected. This is probably due to the fact that the grains of the alloys at the powdering have been pressed into thin lamellæ, the largest faces of which are parallel to the basal planes. Thus the crystal individuals have not been orientated completely at haphazard in the specimens investigated, but a disproportional number of them have got an orientation parallel to the axis of the rod, or to the surface illuminated.

The density values and the final X-ray data of the ϵ - and η -phases are included in Table XI. In the close-packed hexagonal lattice there should be two atoms in the elementary parallelepiped, and within the limits of error this number has in fact been obtained for all the phases investigated. It may be noted in the table mentioned that in all the phases the axial ratio $\frac{a_4}{a_1}$ is approaching towards 1.63 with increasing content of copper, silver, or gold—*i. e.*, the more atoms of the latter kind the lattice contains, the more it gets the shape of one built up of spherical atoms.

E. The γ' - and γ'' -Phases of the Au-Zn System.

From powder photographs of the Au-Zn alloys in the range 49–55 per cent. zinc it could be concluded that two phases existed in that range to which no analogies were found in the Cu-Zn and Ag-Zn systems. One of these phases, called γ' , is stable at ordinary temperature, and is homogeneous within a composition range of only 1 per cent. at about 50 per cent. zinc. The other, γ'' , was found to be stable only at higher temperatures. Alloys containing 53 to 55 per cent. zinc consisted of the three phases γ' , γ'' , and ϵ . A gold-zinc melting with 53.5 per cent. zinc quenched in water from the liquid state gave a photogram (Pl. IX. fig. 5, VI.) where the γ'' -interferences predominate.

TABLE XI.

Lattice Dimensions and Number of Atoms per Elementary Parallelepiped in the ϵ - and η -Phases.

Phase.	Per cent. Zn.	Average Atomic Weight.	Density.	$\frac{\lambda^2}{3a_1^2}$.		$\frac{\lambda^2}{4a_4^2}$.		$\frac{a_1}{a_0}$ in Å.	$\frac{a_1}{a_0}$ in Å.	$\frac{a_1}{a_1}$.	V in Å ³ .	Number of Atoms per Elementary Parallelepiped.
				K α .	K β .	K α .	K β .					
Cu-Zn	80.3	65.01	7.71	0.1652	0.1360	0.0507	0.0417	2.746	4.294	1.564	28.04	2.01
Cu-Zn	86.1	65.11	7.51	0.1637	0.1342	0.0509	0.0418	2.761	4.286	1.552	28.30	1.98
Ag-Zn	60.5	77.42	8.35	0.1570	0.1290	0.0471	0.0387	2.818	4.456	1.581	30.64	2.00
Ag-Zn	78.1	71.54	7.77	0.1573	0.1292	0.0487	0.0400	2.815	4.382	1.557	30.07	1.98
Au-Zn	67.5	83.52	9.34	0.1580	0.1297	0.0488	0.0400	2.809	4.377	1.558	29.91	2.03
Au-Zn	72.3	80.23	8.67	0.1580	0.1297	0.0490	0.0402	2.809	4.369	1.555	29.86	1.96
Cu-Zn	96.5	65.31	7.26	0.1754	...	0.0387	...	2.666	4.916	1.844	30.26	2.04 †
Au-Zn	95.0	67.63	7.40	0.1743	0.1432	0.0392	0.0322	2.674	4.887	1.828	30.27	2.01
Zn	100.0	65.37	7.14 *	0.1760	0.1446	0.0383	0.0315	2.662	4.941	1.856	30.31	2.01

* A. C. Egerton and W. B. Lee, Proc. Roy. Soc. A, ciii, p. 499 (1923).

† The divergence of this value from 2.00, the one expected, is probably due to the fact that this alloy does not consist of pure η but also contains some ϵ .

When the same specimen was investigated only one day after quenching, the interferences corresponding to γ' and ϵ had already become considerably more distinct, which may be seen in the precision photograms VIII. to X. in fig. 5 (Pl. IX.). It is thus evident that γ'' splits up spontaneously into γ' and ϵ at the ordinary temperature.

The γ'' -phase could never be obtained quite free from the adjacent phases, and, unfortunately, all attempts failed to get a single crystal of γ' . The investigation had thus to be confined to the powder method only. Some of the photograms obtained are shown in fig. 5 (Pl. IX.).

As may be seen in Table XII., the γ' -interferences are in accordance with the formulæ :

$$\sin^2 \frac{\theta}{2} = 0.01506 (h_1^2 + h_2^2 + h_3^2) \dots (K_\alpha),$$

$$\sin^2 \frac{\theta}{2} = 0.01238 (h_1^2 + h_2^2 + h_3^2)^r \dots (K_\beta).$$

As every line of the photogram agrees perfectly with these formulæ, it is highly probable that they really represent the correct quadratic forms of the γ' -phase. The γ' -crystals would thus be cubic with a parameter of 7.880 Å.

Density measurements on three γ' -alloys containing 48.3, 50.2, and 50.5 per cent. zinc gave the values 10.88, 10.63, and 10.56 respectively. Of these specimens the one containing 50.2 per cent. zinc consisted of only γ' , while the first was a mixture of γ' with some γ , and the third contained some γ'' beside γ' . The average weight of the atoms in the homogeneous γ' -specimen was calculated to $98.1 \cdot 1.650 \times 10^{-24}$ gm., and consequently the number of atoms per elementary cube in that phase would be 32.17, *i. e.* 32 within the limit of error. As the homogeneous γ' -phase contains 75 atomic per cent. zinc, its elementary cube would thus be occupied by 8 gold and 24 zinc atoms, and there is accordingly nothing contradicting the statement of Saldau, that the phase consists of AuZn_3 .

As may be seen in fig. 5 (Pl. IX.), the photograms of the quenched alloy containing 53.5 per cent. zinc (VI. and VIII.) are not quite free from interferences corresponding to the γ' -phase (V. and X.). Yet a striking resemblance between photogram VI. and the γ -photogram (VII.) may be noted. In fact, at a hasty glance these diffraction patterns seem to be identical. A closer inspection shows, however, that there is a distinct difference between them. The $\sin^2 \frac{\theta}{2}$ values of the five strongest interferences are in both photograms in the

I.	Radiation.	$h_1^2 + h_2^2 + h_3^2$	$\sin^2 \frac{\theta}{2}$	$\frac{\sin^2 \frac{\theta}{2}}{h_1^2 + h_2^2 + h_3^2}$	I.	Radiation.	$h_1^2 + h_2^2 + h_3^2$	$\sin^2 \frac{\theta}{2}$	$\frac{\sin^2 \frac{\theta}{2}}{h_1^2 + h_2^2 + h_3^2}$
v.w.	K_{β}	4	0.050	0.0125	v.w.	K_{β}	34	0.4215	0.01240
w.	K_{α}	4	0.060	0.0150	st.	K_{α}	29	0.437	0.01507
m.	K_{α}	5	0.075	0.0150	w.	K_{α}	30	0.451	0.01503
m.	K_{α}	6	0.0905	0.01503	v.w.	K_{β}	38	0.471	0.01239
w.	K_{α}	8	0.1205	0.01506	m.	K_{α}	32	0.483	0.01509
w.	K_{β}	13	0.160	0.01231	m.	K_{α}	34	0.512	0.01506
w.	K_{β}	14	0.173	0.01236	v.w.	K_{α}	35	0.528	0.01508
st.	K_{α}	13	0.1955	0.01504	m.	K_{α}	36	0.542	0.01506
st.	K_{α}	14	0.211	0.01507	w.	K_{α}	37	0.558	0.01505
m.	K_{α}	16	0.241	0.01506	st.	K_{α}	38	0.573	0.01505
w.	K_{α}	17	0.2565	0.01509	w.	K_{α}	41	0.6175	0.01506
v.w.	K_{β}	21	0.259	0.01233	w.	K_{α}	42	0.645	0.01504
w.	K_{α}	18	0.2715	0.01508	m.	K_{α}	44	0.664	0.01509
v.w.	K_{α}	19	0.286	0.01505	m.	K_{α}	45	0.6775	0.01506
w.	K_{α}	20	0.301	0.01505	m.	K_{α}	46	0.692	0.01504
m.	K_{α}	21	0.3165	0.01507	w.	K_{α}	49	0.737	0.01504
m.	K_{α}	22	0.332	0.01509	m.	K_{α}	52	0.782	0.01504
m.	K_{β}	29	0.361	0.01241	st.	K_{α}	53	0.797	0.01504
v.w.	K_{α}	25	0.377	0.01508	m.	K_{α}	54	0.814	0.01508
w.	K_{β}	32	0.396	0.01237	st.	K_{α}	61	0.918	0.01505

proportion 3, 6, 9, 11, and 12; but there are some lines corresponding to the γ'' -phase which are incompatible with the quadratic formula of the γ -phase. Among these are the least deviated interferences, which give the $\sin^2 \frac{\theta}{2}$ values 0.068 and 0.083. If the γ'' -phase is cubic, which seems most probable in view of the simple relation between the $\sin^2 \frac{\theta}{2}$ values of its strongest lines, the constant of its quadratic form must thus be equal to or less than 0.083-0.068, *i. e.* 0.015. In fact, half of this value, *i. e.* 0.0075, gives a suitable constant. Every K_{α} -interference of γ'' can be explained by the formula:

$$\sin^2 \frac{\theta}{2} = 0.0075 (h_1^2 + h_2^2 + h_3^2).$$

The $(h_1^2 + h_2^2 + h_3^2)$ values of the five strongest lines would accordingly be 27, 54, 81, 99, and 108. The formula gives a lattice parameter of 11.17 Å.; and, as the density of the alloy was found to be 10.2, there would thus be about 90 atoms in its elementary cube. As the specimen investigated was not homogeneous, the results of the X-ray investigation must, however, in this case be considered to be somewhat uncertain*.

According to Saldau†, AuZn_3 should be subjected to transformations in the solid state. An attempt was made to test if an alloy of that composition really solidifies in some other form than γ' . For this purpose it was quenched in water from a temperature above its melting-point, by which procedure at least some part of the phases stable at higher temperatures might be expected to be retained. The photograph of this product was, however, completely identical with a γ' -photogram; no new interferences whatever appeared. The negative result of this experiment cannot, however, be considered to settle the question, as eventual transformations may very well be complete, even at a most rapid quenching‡.

* The authors have recently commenced an analysis of the Au-Cd system, and have found that an Au-Cd alloy containing somewhat more than 75 atomic per cent. Cd gives a powder photogram which is similar to that of γ'' -Au-Zn. It seems, thus, as if the Au-Cd system should have a phase that is analogous to γ'' -Au-Zn, but stable at ordinary temperature. A closer investigation of this phase will, perhaps, throw some light also upon γ'' -Au-Zn.

† *Loc. cit.*

‡ Comp. note on p. 320.

6. CONCLUDING REMARKS.

At a general survey of the results of the X-ray analysis, it might seem as if in some cases the chemical characterization of metallic phases could not be performed much more definitely by this new procedure than has been possible by previous methods. When it cannot be settled if chemically identical atoms of a metallic phase are structurally equivalent or not, a chemical formula can at the utmost be suggested with a certain degree of probability; its validity is not to be conclusively proved.

From the fact that the ordinary valency rules do not hold for intermetallic compounds, it follows, however, that the chemical constitution of these substances is not defined by their chemical formulæ to the same extent as is, for instance, the case with electrolytes or gaseous compounds. Even if it were possible to find out the correct formulæ for the bases of metallic phases, it would certainly not bring about any deeper insight into the question of intermetallic reactivity.

The X-ray analysis makes, however, a penetration of this problem possible. Chemically related phases give photograms of a similar type; and even if these photograms sometimes cannot be completely unravelled, they prove in an incontrovertible way the relationship between different phases and display analogies between different metallic systems.

What, however, makes this X-ray research of alloys seem most promising is the fact that some types of structure seem to recur frequently in the metallic systems. Thus the atomic arrangements of the β - and γ -phases, described above, seem to be common; and in a preliminary investigation of the Ag-Cd, Ag-Al, Cu-Sn, and Ag-Sn systems the authors have got photograms indicating that in all these alloys a phase is present which has the same structure as the ϵ -phase of the Cu-Zn, Ag-Zn, and Au-Zn alloys*.

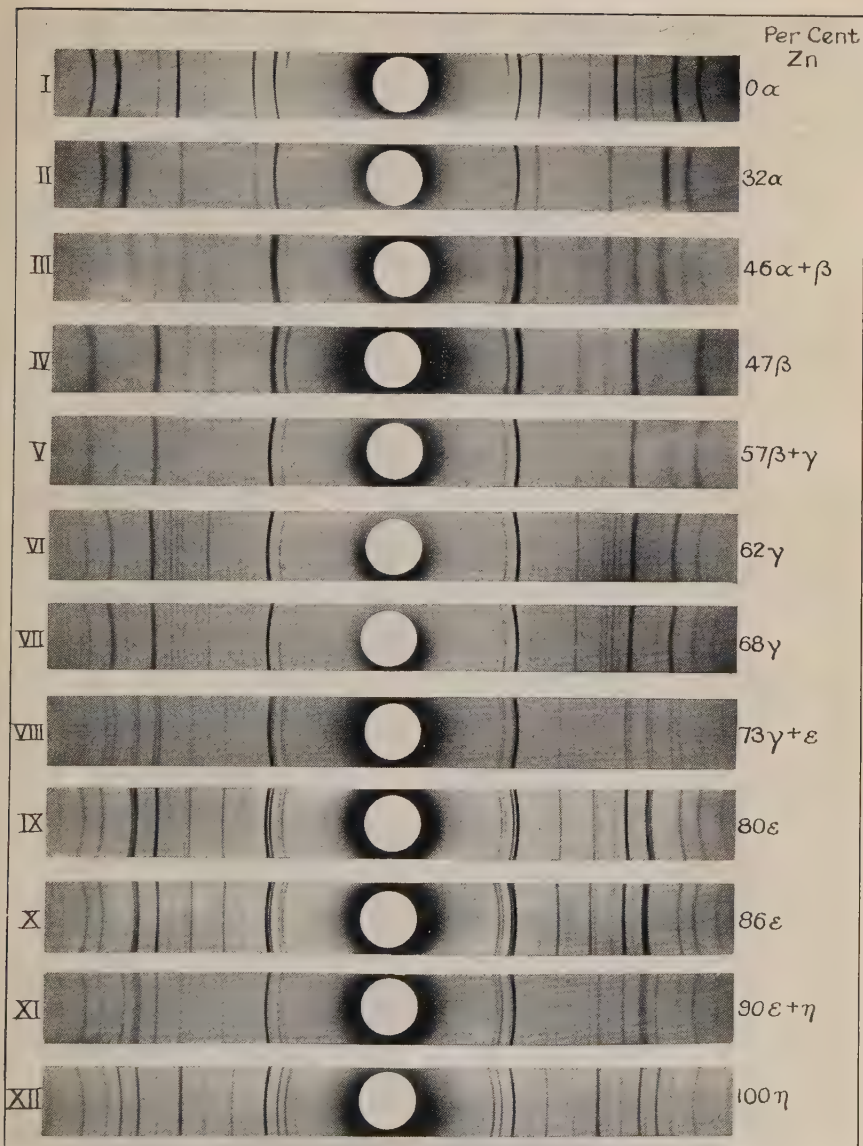
X-ray research will therefore undoubtedly, to a very high degree, contribute to the unveiling of the laws governing the combination of the atoms in composite metallic phases.

7. SUMMARY.

1. According to the authors' opinion, the difference between solid chemical compounds and solid solutions lies in their structure. The terms *ideal solid chemical compound* and *ideal solid solution* are defined, and it is pointed out that most of the metallic phases represent intermediate stages between these two extreme types of structure.

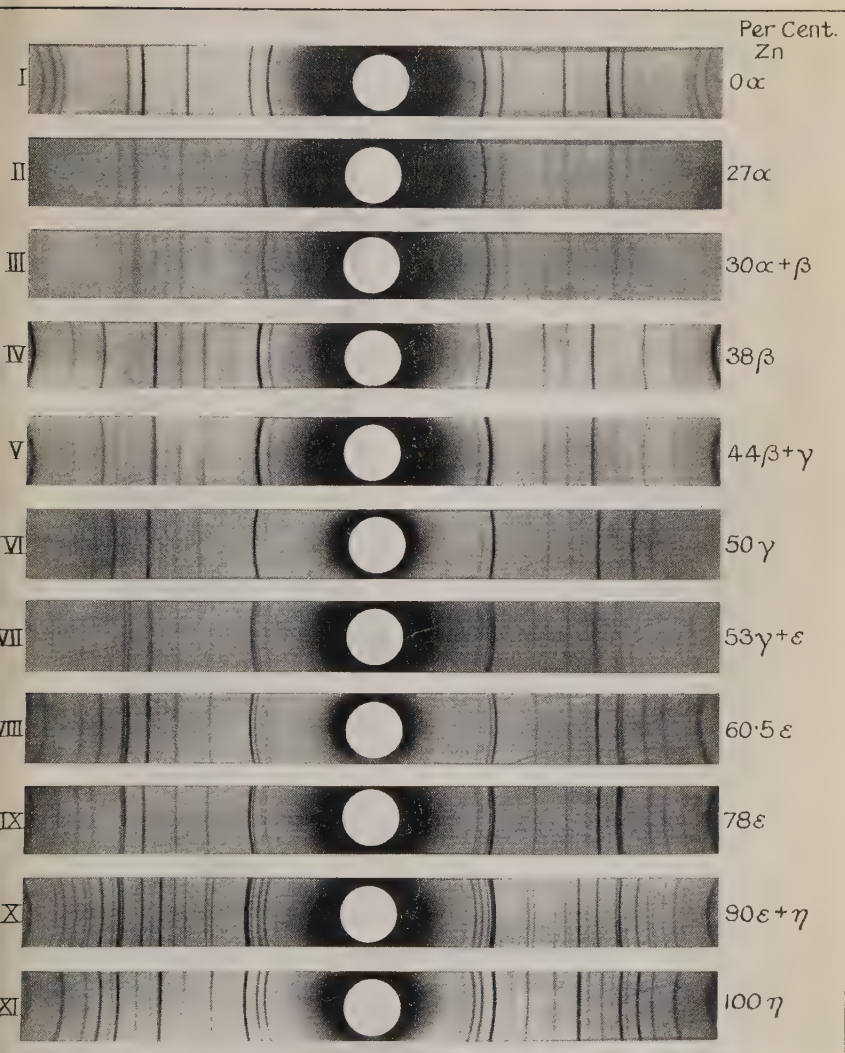
* Comp. Zsigmondy-Festschrift, *Erg.-Band der Kolloid-Zeitschr.* xxxvi. p. 86 (1925).

FIG. 2.



POWDER PHOTOGRAMS OF COPPER-ZINC ALLOYS.

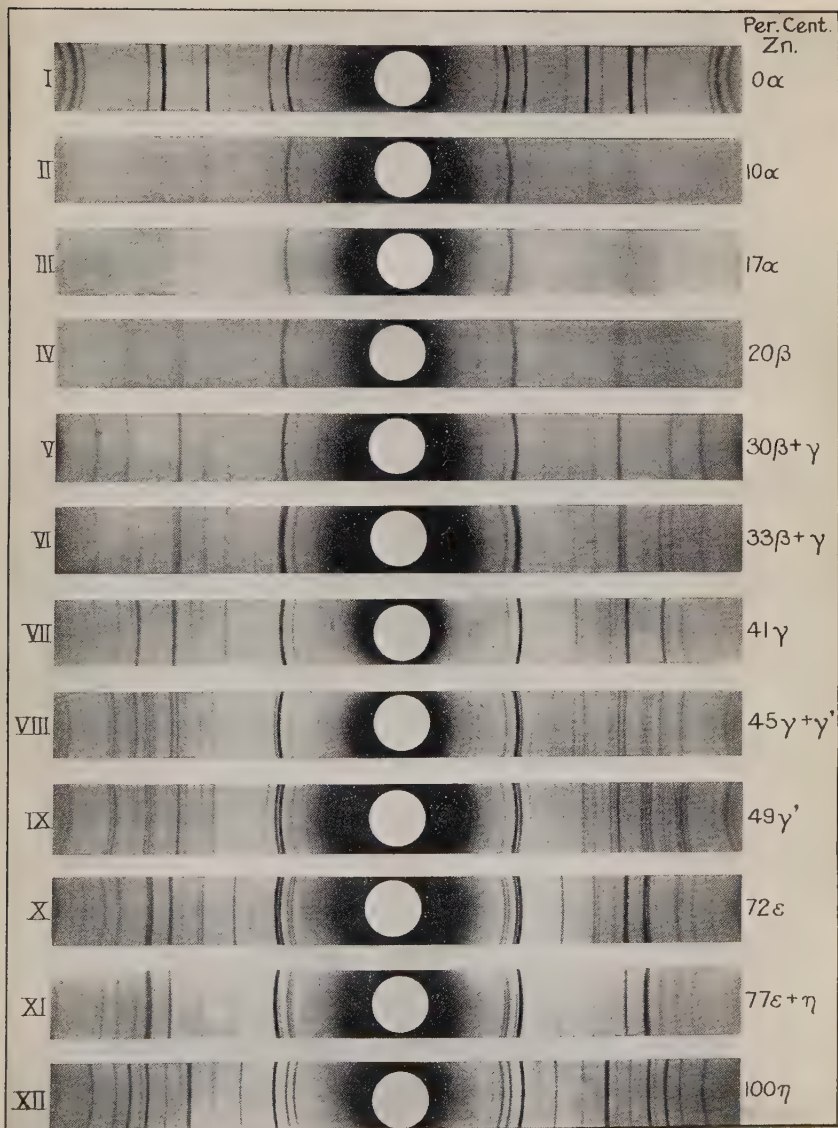
FIG. 3.



POWDER PHOTOGRAMS OF SILVER-ZINC ALLOYS.



FIG. 4.



POWDER PHOTOGRAMS OF GOLD-ZINC ALLOYS.

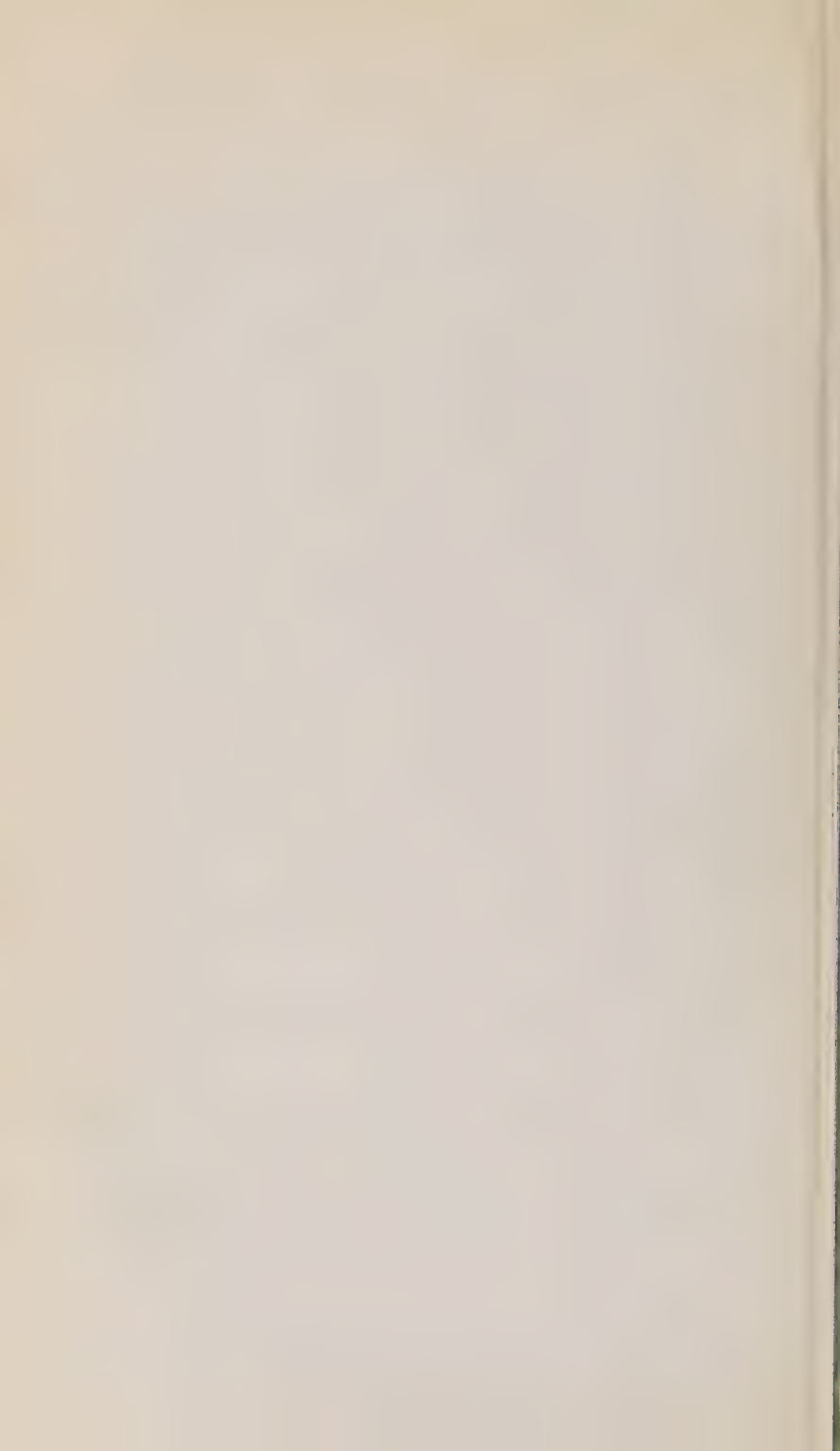
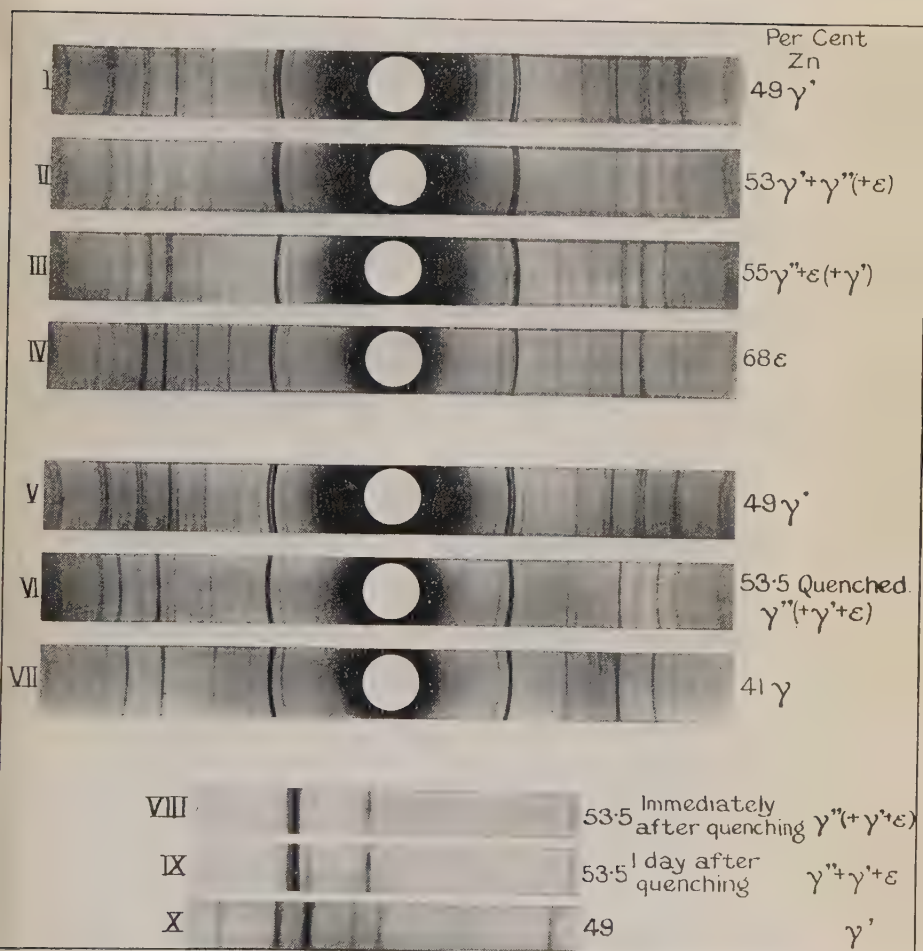


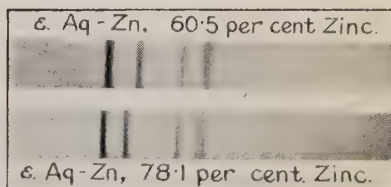
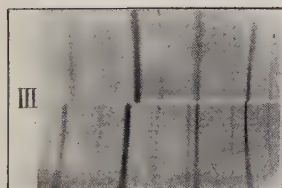
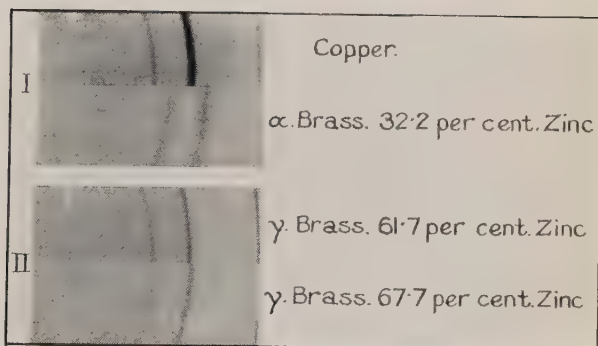
FIG. 5.



POWDER PHOTOGRAMS OF GOLD-ZINC ALLOYS (41-68 per cent. Zn).



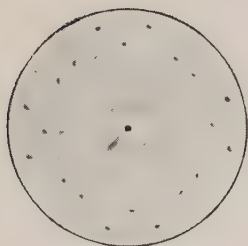
FIG. 6.



COMPARATIVE PRECISION PHOTOGRAMS.



FIG. 7.

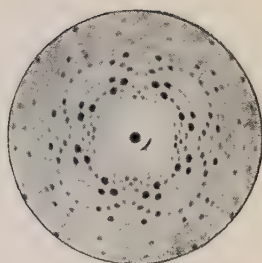


I. Laue Photogram of β -Brass.

Projection Distance 4.33 centimetres.

$$\lambda > 0.16 \text{ \AA.}$$

Reduced 3 : 5.

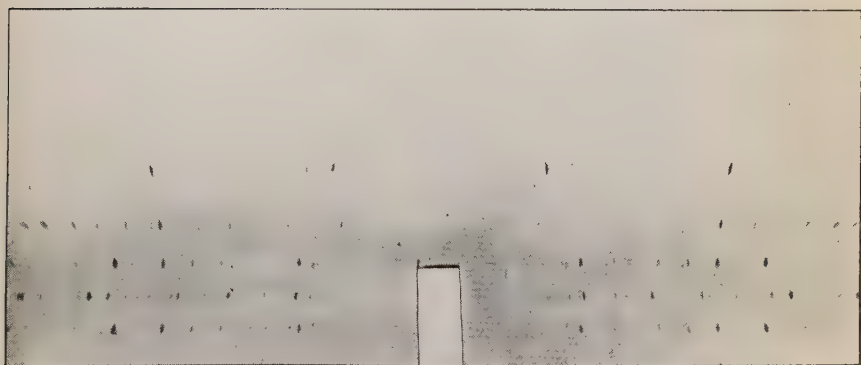


II. Laue Photogram of γ -Brass.

Projection Distance 4.45 centimetres.

$$\lambda > 0.16 \text{ \AA.}$$

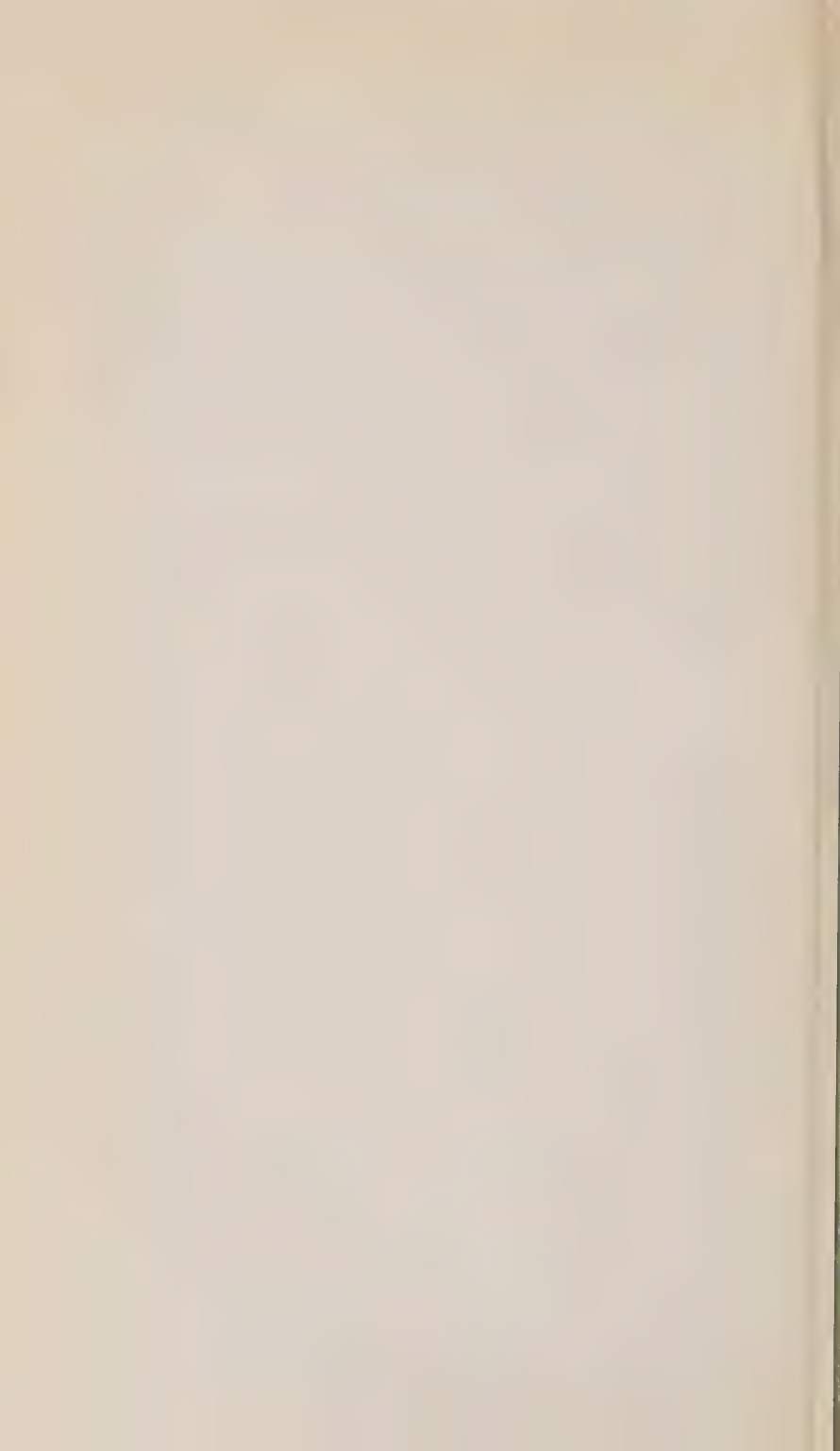
Reduced 3 : 5.



III. Photogram of a γ -Brass Crystal rotating around [100].

Diameter of Film Cylinder 6.3 centimetres.

Reduced 3 : 5.



2. X-ray analysis of the Cu-Zn, Ag-Zn, and Au-Zn systems has proved that the five different types of structure occurring in the first-mentioned of these systems are met with also in the other ones. In addition to them there are two more phases found in the Au-Zn-system.

The β - and γ -phases of the Cu-Zn system have been investigated in the form of single crystals; in other cases the analyses have been performed by means of the powder method only. Arranged according to rising content of zinc, the structures common to the three systems have turned out to be the following:— α , face-centred cubic; β , cubic of CsCl-type; γ , cubic with 52 atoms in the elementary cube; ϵ , close-packed hexagonal with an axial ratio of 1.55–1.60; and η , close-packed hexagonal with an axial ratio of 1.80–1.90. An Au-Zn phase (γ') containing about 50 per cent. Zn was found to be cubic, very likely with an elementary cube occupied by 32 atoms; another phase (γ''), obtained by quenching Au-Zn alloys containing 53–54 per cent. Zn, seemed also to be cubic, with about 90 atoms in its elementary cube. The powder photogram of the γ' -phase has a peculiar similarity to those of the γ -phases.

3. In accordance with the definitions made, the α -, η -, and, with great probability, also the ϵ -phases represent ideal solid solutions, the first one having Cu, Ag, or Au, and the last two Zn, as solvent. The other phases may be regarded as solid solutions in chemical compounds. The solvents of the β -phases are CuZn, AgZn and AuZn. By way of conjecture the formulæ Cu_4Zn_9 , Ag_4Zn_9 , and Au_4Zn_9 are proposed for the bases of the γ -phases, and it is most likely that the γ -phase of the Au-Zn system corresponds to AuZn_3 .

The Metallographic Institute, Stockholm,
February 1925.

XXXII. *Optical Interference Experiments with Multiple Sources.* By JOHN J. DOWLING, M.A., F.Inst.P., M.R.I.A., and J. A. C. TEEGAN, M.Sc.*

[Plate XII.]

WITH the possible exception of the Lummer parallel plate interferometer, there does not appear to have been any attempt made to extend the investigation of the class of interference phenomena associated with the names of Young, Fresnel, and Lloyd to the cases where there are more than two sources. The ordinary diffraction grating may be considered as equivalent to a large number of equally-spaced

* Communicated by the Authors.

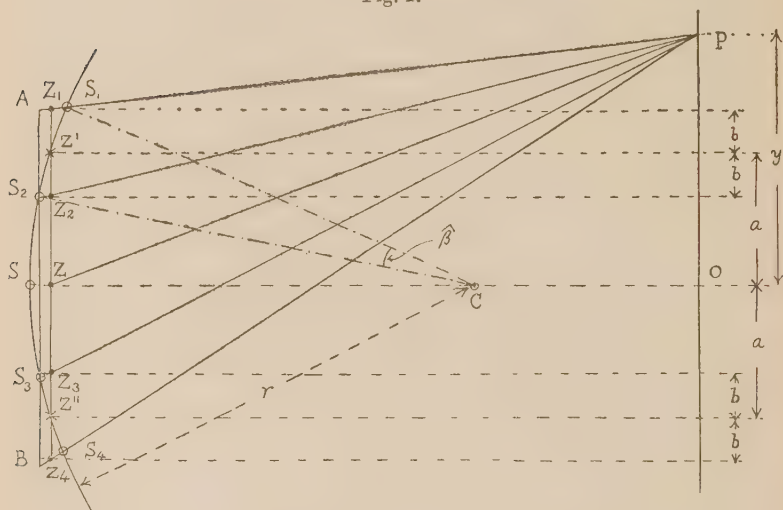
sources; but it seems of interest to describe briefly some results we have been able to obtain with an arrangement giving four (and eight) coherent sources grouped in any desired symmetrical arrangement.

A brief statement of the theory may be stated thus:—

The light proceeding from a source Z (fig. 1) arriving at P yields a vibration

$$z = A \sin \frac{2\pi}{\lambda} \left[Vt - x - \frac{y^2}{2x} \right] \dots \dots \dots (I.)$$

Fig. 1.



If Z be divided (*e.g.* by a biprism) into two coherent sources Z' and Z'' ($2a$ apart),

$$\begin{aligned} z &= \frac{A}{2} \sin \frac{2\pi}{\lambda} \left[Vt - x - \frac{(y+a)^2}{2x} \right] \\ &\quad + \frac{A}{2} \sin \frac{2\pi}{\lambda} \left[Vt - x - \frac{(y-a)^2}{2x} \right] \\ &\doteq A \cos \frac{2\pi}{\lambda} \left[\frac{ay}{x} \right] \cdot \sin \frac{2\pi}{\lambda} [Vt - x] \dots \dots \dots (II.) \end{aligned}$$

A further division of Z' and Z'' each into two sources ($2b$ apart) yields four sources, Z_1, Z_2, Z_3, Z_4 , arranged along the line Z_1, Z, Z_4 at $a+b; a-b; -a+b; -a-b$. The vibration at P is

$$\begin{aligned} z &= \Sigma \frac{A}{4} \sin \frac{2\pi}{\lambda} \left[Vt - x - \frac{(y \pm a \pm b)^2}{2x} \right] \\ &\doteq A \cos \left(\frac{2\pi}{\lambda} \cdot \frac{ay}{x} \right) \cdot \cos \left(\frac{2\pi}{\lambda} \cdot \frac{by}{x} \right) \cdot \sin \frac{2\pi}{\lambda} (Vt - x). \quad (III.) \end{aligned}$$

The separations a and b are effected by two biprisms, one mounted behind the other in front of the slit. If α, β are the acute angles of these biprisms, and R and r their respective distances from the slit,

$$a \doteq (\mu - 1)\alpha R, \quad \text{and} \quad b \doteq (\mu - 1)\beta r. \quad (\text{IV.})$$

The grouping is symmetrical, but the most interesting case is when $b = 2a$ (or $a = 2b$), the four sources being then equally spaced. Here

$$z = \left\{ \frac{A \sin 4 \left(\frac{2\pi}{\lambda} \cdot \frac{ay}{x} \right)}{4 \sin \left(\frac{2\pi}{\lambda} \cdot \frac{ay}{x} \right)} \right\} \sin \frac{2\pi}{\lambda} (Vt - x). \quad (\text{V.})$$

The illumination distribution, proportional to the square of the term in chain brackets, corresponds to that of a grating having four openings.

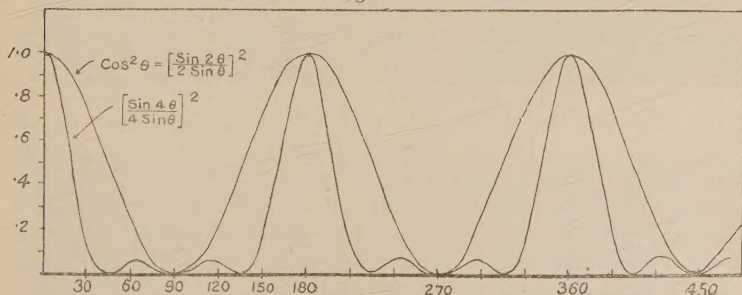
A further subdivision may now be carried out, using a third biprism; and if the spacing constant $2c = 4b = 8a$, we again arrive at the corresponding grating distribution.

The illumination, as a function of

$$\theta = \frac{2\pi}{\lambda} \cdot \frac{ay}{x},$$

is shown in fig. 2. The upper curve shows the illumination

Fig. 2.



of the fringes due to two sources (Fresnel's experiment): the lower curve with subsidiary maxima that due to four equally-spaced sources (two biprisms). In Pl. XII. enlarged photographs of the fringes are given: A, with the first biprism alone; B, with the second; C, with both biprisms in position. The characteristic narrowing and intensification of the principal maxima are clearly observable in the part of the field indicated by the arrow.

It was found extremely difficult to locate the fringe

systems when three biprisms were installed, so much so that we were unable to get a good photograph. The following considerations afford a clue to why this should be.

Reverting to fig. 1, it will be observed that the four sources, S_1, S_2, S_3, S_4 , are actually situated around a circle of radius r , the distance of the second biprism from the slit S . Let us reconsider the formula for four equispaced sources in this connexion. Let x be now measured from the plane AS_2S_3B a little in front of S . It will be readily found that, since $b=2a$,

$$\xi = Z_1S_1 + Z_2S_2 \doteq \frac{4a^2}{r} \dots \dots \dots (VI.)$$

We must now write, instead of equations (III.),

$$\begin{aligned} z = & \Sigma_2 \frac{A}{4} \sin \frac{2\pi}{\lambda} \left\{ Vt - x - \frac{[y \pm (a-b)]^2}{2x} \right\} \\ & + \Sigma_2 \frac{A}{4} \sin \frac{2\pi}{\lambda} \left\{ Vt - x - \xi - \frac{[y \pm (a+b)]^2}{2x} \right\} \\ \doteq & \frac{A}{2} \cos \frac{2\pi}{\lambda} \frac{y(a-b)}{x} \sin \frac{2\pi}{\lambda} (Vt - x) \\ & + \frac{A}{2} \cos \frac{2\pi}{\lambda} \frac{y(a+b)}{x} \cdot \sin \frac{2\pi}{\lambda} (Vt - x - \xi). \end{aligned} \dots \dots \dots (VII.)$$

This will only reduce to the final form of (III.) when $\xi = \frac{n\lambda}{2}$, and we may regard ξ as affecting the "visibility" of the fringes. The value of ξ^* depends on the position of the second biprism, and we found that the "visibility" underwent rapid variations with small displacements of that biprism in the neighbourhood of the position which made $b=2a$. It was indeed possible, but by no means easy, to obtain visual fringes of the proper type, using three biprisms; but we were unable to obtain a photograph, for the reason that the fringes were localized in a very restricted space, rendering very accurate registration of the photographic plate essential.

* Numerical data:—

Angular separation by second biprism

$$= 30' = \frac{\pi}{360}, \quad r = 32.3 \text{ cms.} \quad 4a = 2b = \frac{\pi r}{360} \doteq .3 \text{ cm.}$$

$$\xi = \frac{4a^2}{r} \doteq 70 \times 10^{-5}, \quad \lambda \doteq 5000 \times 10^{-8} \text{ cm.}$$

Hence $n \doteq 28$.

[The Editors do not hold themselves responsible for the views expressed by their correspondents.]

